THE

LONDON, EDINBURGH, AND DUBLIN

PHILOSOPHICAL MAGAZINE

AND

JOURNAL OF SCIENCE.

[SEVENTH SERIES.]

MARCH 1934.

XLIV. *On the Hertzian Impact of an Elastic Hammer on a Damped Pianoforte String.* *By* M. GHOSH, *M.Sc., A.Inst.P.**

SOME twelve years ago Raman and Banerjee [1], in a paper that appeared in the Proc. Roy. Soc. A, tried to develop a theory of the pianoforte from the standpoint of a loaded string. Later on Kar [2] modified it, by pointing out the mathematical error that crept in, in taking the solution in the form of a series. Among the other workers in the subject may be mentioned the names of Helmholtz [3], Kaufmann [4], Delemer [5], Lamb [6], Bhargava-Ghosh [7], and Das [8], each of whom has built up a theory apparently different from the other. Recently, in a number of papers that have appeared elsewhere, Kar and the present writer [9], and the present writer alone [10], have built up a generalized theory of the pianoforte, taking into consideration the damping of the string, and considering the hammer to be slightly elastic. It has also been shown by the writer that some of the previous theories are only special cases of theirs. Unfortunately none of the theories mentioned above can explain the variation of the duration of contact between the felt hammer and the string, as noticed by Weak [11] and Kaufmann [4] during their

* Communicated by Prof. K. C. Kar, D.Sc.

experiments. It may be remarked that this effect Kaufmann pointed out only as a deviation from his theory without explaining it Furthermore, the recent experiment of the writer [16] confirms the above fact beyond doubt, which therefore necessitates further generalization of the author's theory.

In this paper we shall extend the previous theory for all elastic values of the hammer in the direction of Hertz's theory of impact. This explains the above experimental fact remarkably well. It may be noted that recently Andrews [12] also adopted a similar procedure in solving the problem of collision of two soft and plastic spheres.

The equation of motion of a string with damping is

$$\frac{\partial^2 Y}{\partial t^2} + k\frac{\partial Y}{\partial t} - c^2\frac{\partial^2 Y}{\partial x^2} = 0. \quad . \quad . \quad . \quad . \quad (1)$$

The equation of motion of the hammer striking the string at a distance (a) from one of the fixed ends of the string, the other end being supposed to be at infinity, is

$$T_1 \Delta\left(\frac{\partial Y}{\partial x}\right)_{x=a} + Fe^{-qt} + Ge^{-pt} = P_0 \quad . \quad . \quad . \quad (2)$$

and

$$T_1 \Delta\left(\frac{\partial Y}{\partial x}\right)_{x=a} = -E(u-u_0). \quad . \quad . \quad . \quad . \quad . \quad (3)$$

where Y is the displacement of the string at any point x, t is the variable time, k the damping coefficient, T_1 the tension of the string of line density ρ, c the velocity of the wave propagation along the string; q, p, F, and G are constant, being independent of x and t, E the elastic constant given by Hooke's law, u the compression of the hammer at any instant t, and P_0 is the pressure attained by the hammer before the string is appreciably displaced, the compression at this instant being u_0.

In the case of a felt hammer which is soft and plastic the compression of the hammer-felt obeys Hertz's law on coming in contact with the string until the string is appreciably disturbed. Thus after the compression has reached a certain value the Hertz's law ceases to hold and the string begins to be displaced. During this time the compression obeys Hooke's law and the motion is

given by equations (2) and (3). During the period Hertz's law is obeyed the pressure exerted by the hammer varies as $u^{3/2}$. In passing we may remark that Hertz's law, $P=-\epsilon u^{3/2}$, may be taken in Hooke's form, $P=-Eu$, provided we suppose that E, instead of being a constant, varies as $u^{1/2}$. The equation of motion of the hammer during the period the Hertz's law is valid is

$$m\ddot{z}=m\ddot{Y}_{x=a}+m\ddot{u}=-\epsilon u^{3/2}, \quad . \quad . \quad . \quad (4a)$$

where z is the displacement of the centre of gravity of the hammer and is given by

$$z=Y_{x=a}+u. \quad . \quad . \quad . \quad . \quad . \quad (4b)$$

As the string is not appreciably disturbed at this stage we may assume $Y_{x=a}=0$ approximately, so equation (4a) becomes

$$\ddot{u}+\frac{\epsilon}{m}u^{3/2}=0. \quad . \quad . \quad . \quad . \quad . \quad . \quad (5)$$

On integrating equation (5), and evaluating the constant of integration from the condition that at $t=0$, $\dot{u}=v_0$ (velocity before impact), we get

$$v_0^2-\dot{u}^2=nu^{5/2}, \quad . \quad . \quad . \quad . \quad . \quad (6a)$$

where

$$n=4\epsilon/5m. \quad . \quad . \quad . \quad . \quad . \quad . \quad (6b)$$

Now suppose that the limiting values of u and $\dot{u}$ at the end of Hertz's period are u_0 and v_1 respectively; so we have from the meaning of P_0, explained before, $P_0=-\epsilon u_0^{3/2}$. At this instant (6a) becomes

$$u_0=\left(\frac{v_0^2-v_1^2}{n}\right)^{2/5} \quad . \quad . \quad . \quad . \quad . \quad . \quad (7)$$

From (6a) we have for the time (τ) taken to produce the compression (u_0):

$$\tau=\frac{1}{v_0}\int_0^{u_0}\frac{du}{\sqrt{1-nu^{5/2}/v_0^2}}=\frac{1}{n^{2/5}v_0^{1/5}}\int_0^{x_0}\frac{dx}{\sqrt{1-x^{5/2}}}, \quad (8)$$

where

$$x_0=n^{2/5}.u_0/v_0^{4/5}. \quad . \quad . \quad . \quad . \quad . \quad . \quad . \quad . \quad . \quad (9)$$

As v_1 is always less than v_0, x_0 is less than unity (see equations (7) and (9)). Hence the integration in equation (8) may be performed after expanding the expression

$(1-x^{5/2})^{-1/2}$. It may, however, otherwise be solved graphically for different value of v_0.

From equation (8) we have, after integrating term by term,

$$\tau=\frac{u_0}{v_0}\left(1+\frac{nu_0^{5/2}}{7v_0^2}+\frac{n^2u_0^5}{16v_0^4}+\frac{5n^3u_0^{15/2}}{136v_0^6}+\frac{35n^4u_0^{10}}{704v_0^8}+\ldots\right). \quad \ldots \quad (10)$$

After the time (τ) given by equation (10) Hertz's law of pressure is over and Hooke's law is called into play; at the same time the string begins to move appreciably, as stated before. During this period the motion of the hammer, as already remarked, is given by equations (2) and (3). It is evident [13] from (2) that the displacement of the string at the point of contact is of the form

$$(Y_1)_{x=a}=\gamma_1e^{-qt}+\gamma_2e^{-pt}+\gamma_3. \quad \ldots \quad (11)$$

Thus in general at any point (x) we may take

$$(Y_1)_x=(\gamma_1)_xe^{-qt}+(\gamma_2)_xe^{-pt}+\gamma_3, \quad \ldots \quad (12)$$

where $(\gamma_1)_x$ and $(\gamma_2)_x$ are functions of x only, such that at the point $x=a$

$$(\gamma_1)_a=\gamma_1$$

and

$$(\gamma_2)_a=\gamma_2.$$

From (12) equation (1) becomes, by putting the values of $\ddot{Y}$ and $\dot{Y}$,

$$e^{-qt}.\frac{\partial^2(\gamma_1)_x}{\partial x^2}+e^{-pt}.\frac{\partial^2(\gamma_2)_x}{\partial x^2}+\lambda_1^2(\gamma_1)_xe^{-qt}+\lambda_2^2(\gamma_2)_xe^{-pt}=0,$$

where $\quad \ldots \quad (13)$

$$\lambda_1=\frac{q}{c}\sqrt{1-k/q}, \quad \ldots \quad (14a)$$

$$\lambda_2=\frac{p}{c}\sqrt{1-k/p}. \quad \ldots \quad (14b)$$

It is evident from equation (13) that the coefficients of e^{-qt} and e^{-pt} must separately vanish; so we have

$$\frac{\partial^2(\gamma_1)_x}{\partial x^2}+\lambda_1^2(\gamma_1)_x=0 \quad \ldots \quad (15a)$$

and

$$\frac{\partial^2(\gamma_2)_x}{\partial x^2}+\lambda_2^2(\gamma_2)_x=0, \quad \ldots \quad (15b)$$

whence we get

$$(\gamma_1)_x = C_1 e^{-\lambda_1 x}, \quad . \quad . \quad . \quad . \quad . \quad . \quad (16a)$$

$$(\gamma_2)_x = C_2 e^{-\lambda_2 x}. \quad . \quad . \quad . \quad . \quad . \quad . \quad (16b)$$

Equation (12), with the help of (16 *a*) and (16 *b*), can be written as

$$(Y_1)_x = C_1 e^{-\lambda_1 x}.e^{-qt} + C_2 e^{-\lambda_2 x}.e^{-pt} + \gamma_3. \quad . \quad . \quad (17)$$

At $x=a$ equation (17) becomes identical with equation (11), giving the relation

$$\left.\begin{aligned} C_1 e^{-\lambda_1 a} &= \gamma_1, \\ C_2 e^{-\lambda_2 a} &= \gamma_2. \end{aligned}\right\} \quad . \quad . \quad . \quad . \quad . \quad . \quad . \quad (18)$$

Now, putting these values of C_1 and C_2 in (17), we get the solution for the first part of the string from $x=0$ to $x=a$,

$$(Y_1)_{x_1<0} = \gamma_1 e^{-(qt+\lambda_1 x_1)} + \gamma_2 e^{-(pt+\lambda_2 x_1)} + \gamma_3. \quad . \quad (19a)$$

In like manner it is evident that for the second part of the string we have

$$(Y_1)_{x_1>0} = \gamma_1 e^{-(qt-\lambda_1 x_1)} + \gamma_2 e^{-(pt-\lambda_2 x_1)} + \gamma_3, \quad . \quad (19b)$$

where

$$x_1 = x - a. \quad . \quad . \quad . \quad . \quad . \quad . \quad . \quad (20)$$

Now the pressure exerted by the hammer of mass (m) is $m(\ddot{Y}+\ddot{u})$, so from equations (2) and (3)

$$(P-P_0) = m(\ddot{Y}+\ddot{u}) = -(Fe^{-qt}+Ge^{-pt}) \quad . \quad . \quad (21a)$$

$$= T_1 \Delta \left(\frac{\partial Y}{\partial x}\right)_{x=a} \quad . \quad . \quad . \quad (21b)$$

$$= -E(u-u_0). \quad . \quad . \quad . \quad (21c)$$

Equation (21 *b*) gives, with the help of equations (11), (19), and (21 *c*),

$$\gamma_1 m q^2 \left(1 - \frac{2T_1\lambda_1}{E}\right) e^{-qt} + \gamma_2 m p^2 \left(1 - \frac{2T_1\lambda_2}{E}\right) e^{-pt}$$

$$= 2T_1(\lambda_1\gamma_1 e^{-qt} + \gamma_2\lambda_2 e^{-pt}). \quad (22)$$

Now equating the coefficients of e^{-qt} and e^{-pt} on both sides, and putting the value of λ_1 and λ_2 from equation (14), we have

$$\left.\begin{aligned} &\sqrt{1-k/q}\,(1+mq^2/E) = mcq/2T_1 \\ \text{and} \quad &\sqrt{1-k/p}\,(1+mp^2/E) = mcp/2T_1. \end{aligned}\right\} \quad . \quad . \quad (23)$$

These two equations are identical, so that q and p are the roots of the equation

$$(1-k/x)^{1/2}(1+mx^2/\mathrm{E})=mcx/2\mathrm{T}_1. \quad . \quad . \quad . \quad (24)$$

Taking k to be small, q and p are given by

$$[q,\ p]=\frac{1}{2}\left[\frac{\mathrm{E}c}{2\mathrm{T}_1}\mp\sqrt{\left\{\left(\frac{\mathrm{E}c}{2\mathrm{T}_1}\right)^2-\frac{4\mathrm{E}c}{2\mathrm{T}_1}\left(\frac{2\mathrm{T}_1}{mc}-\frac{k}{2}\right)\right\}}\right]. \quad (25)$$

Now at $t=\tau$, where τ is given by equation (10), we have

$$(\mathrm{Y}_1)_{x=a}=0,$$

which gives, from equation (11),

$$\gamma_1 e^{-q\tau}+\gamma_2 e^{-p\tau}=-\gamma_3. \quad . \quad . \quad . \quad . \quad (26)$$

So equation (11) becomes

$$(\mathrm{Y}_1)_{x=a}=\gamma_1 e^{-q\tau}(e^{-qt_1}-1)+\gamma_2 e^{-p\tau}(e^{-pt_1}-1), \quad . \quad (27\,a)$$

where

$$t_1=t-\tau. \quad . \quad . \quad . \quad . \quad . \quad . \quad (27\,b)$$

At $t=\tau$, i. e., $t_1=0$, z is continuous; but as Y is zero, u is also continuous. From $u=u_0$ at $t=\tau$, which gives, with the help of equations (19), (21 *b*), and (21 *c*),

$$2\mathrm{T}_1(\lambda_1\gamma_1 e^{-q\tau}+\lambda_2\gamma_2 e^{-p\tau})=0. \quad . \quad . \quad . \quad (28)$$

Again, from the continuity of $\dot{z}$ at $t_1=0$, and from the fact that $\dot{\mathrm{Y}}=0$ just before and after the instant, we find that $(\dot{u})$ is continuous; so at this instant

$$2\mathrm{T}_1(\lambda_1 q\gamma_1 e^{-q\tau}-\lambda_2 p\gamma_2 e^{-p\tau})=\mathrm{E}v_1, \quad . \quad . \quad . \quad (29)$$

where v_1 is given by (7).

From equations (28) and (29) one can easily get, remembering the values of λ_1 and λ_2 given in (14),

$$\gamma_1 e^{-q\tau}=\frac{\mathrm{E}v_1 c}{2\mathrm{T}_1(q-p)}\cdot\frac{1}{q}, \quad . \quad . \quad . \quad . \quad . \quad (30)$$

neglecting k in the denominator, which is a small quantity, and

$$\overline{\gamma_2 e^{-p\tau}}=-\frac{\mathrm{E}v_1 c}{2\mathrm{T}_1(q-p)}\cdot\frac{1}{p}. \quad . \quad . \quad . \quad . \quad . \quad (31)$$

Substituting (30) and (31) in equation (27), we get

$$(\mathrm{Y}_1)_{z_1=0}=y_1(t_1)_{t_1=0}=\mathrm{A}v_1\{(1-e^{-qt_1})/q-(1-e^{-pt_1})/p\}. \quad (32\,a)$$

In similar manner,

$$(Y_1)_{x_1<0}=Av_1\{(1-e^{-(qt_1+\lambda_1 x_1)})/q-(1-e^{-(pt_1+\lambda_2 x_1)})/p\}, \quad (32\,b)$$

$$(Y_1)_{x_1>0}=Av_1\{(1-e^{-(qt_1-\lambda_1 x_1)})/q-(1-e^{-(pt_1-\lambda_2 x_1)})/p\}, \quad (32\,c)$$

where t_1 is given by (27 *b*) and x_1 by (20), and A is given by

$$A=-Ec/2T_1(q-p). \quad . \quad . \quad . \quad . \quad . \quad (33)$$

Second Epoch.

At $t_1=0$ the two waves represented by equations (32 *b*) and (32 *c*) originate at the struck point and travel in the opposite direction. The former, after being reflected from the nearest end, $x=0$, reaches the hammer at the instant $t_1=2a/c$, i. e., $t=\tau+\frac{2a}{c}$ as $-y_1(t_2)_{x_1>0}$, where

$$-y_1(t_2)_{x_1>0}=Av_1[(1-e^{-(qt_2-\lambda_1 x_1)})/q-(1-e^{-(pt_1-\lambda_2 x_1)})/p]$$

and $\quad . \quad . \quad . \quad (34\,a)$

$$t_2=t_1-\frac{2a}{c}=t-\tau-\frac{2a}{c}. \quad . \quad . \quad . \quad . \quad . \quad (34\,b)$$

The wave in the larger segment, which is supposed to be extended up to infinity, travels out. Now after reaching the hammer the reflected wave $-y_1(t_2)_{x_1>0}$ is transmitted through the struck point. Denoting the disturbance during the time $t_1<\frac{2a}{c}$ by (y_2), we have

$$(y_2)_{x_1=0}=y_1(t_1)_{x_1=0}-y_1(t_2)_{x_1=0}, \quad . \quad . \quad . \quad (35\,a)$$

$$(y_2)_{x_1<0}=y_1(t_1)_{x_1<0}-y_1(t_2)_{x_1>0}, \quad . \quad . \quad . \quad (35\,b)$$

$$(y_2)_{x_1>0}=y_1(t_1)_{x_1>0}-y_1(t_2)_{x_1>0}. \quad . \quad . \quad . \quad (35\,c)$$

Now during transmission the reflected wave $-y_1(t_2)_{x_1=0}$ exerts pressure on the hammer, which, in return, gives an equal and opposite impulse, generating two new waves which travel in two opposite directions along the string; this impulsive pressure acts on the dynamical system.

Thus the pressure is obtained by differentiating equation (34) twice with respect to time for the struck point

$x_1=0$ (its sign being reversed); the value of this impulsive pressure at any instant is

$$-\mathrm{A}v_1(qe^{-qt_2}-pe^{-pt_2}). \quad . \quad . \quad . \quad . \quad . \quad (36)$$

If this pressure acts on the dynamical system at $t_2=t$ for a short time dt, it will impart to it a velocity

$$-\mathrm{A}v_1(qe^{-qt}-pe^{-pt})\,dt. \quad . \quad . \quad . \quad . \quad . \quad (37)$$

Substituting the value of velocity in the dynamical system ($32\,a$), and integrating, we get for the displacement $y_2(t_2)$ at any time t_2 measured from beginning of the second epoch, after adding the natural vibration $(\gamma_1 e^{-qt_2}+\gamma_2 e^{-pt_2}+\gamma_3)$ of the system during the epoch, or we have

$$y_2(t_2)_{x_1=0}=-\mathrm{A}^2v_1\int_0^{t_2}(qe^{-qt}-pe^{-pt})\left\{\frac{1-e^{-qt}}{q}-\frac{1-e^{-pt}}{p}\right\}dt$$
$$+\gamma_1 e^{-qt_2}+\gamma_2 e^{-pt_2}+\gamma_3.$$

Integrating the above, we have

$$y_2(t_2)_{x_1=0}=\mathrm{A}^2v_1\left[\frac{e^{-qt_2}}{q}(1+qt_2)-\frac{1}{q}+\frac{e^{-pt_2}}{p}(1+pt_2)-\frac{1}{p}\right]$$
$$+\mathrm{C}_1e^{-qt_2}+\mathrm{C}_2e^{-pt_2}+\mathrm{C}_3. \quad . \quad . \quad . \quad . \quad (38\,a)$$

So

$$y_2(t_2)_{x_1<0}=\mathrm{A}^2v_1\left[\frac{e^{-(qt_2+\lambda_1x_1)}}{q}(1+qt_2+\lambda_1x_1)-\frac{1}{q}\right.$$
$$\left.+\frac{e^{-(pt_2+\lambda_2x_1)}}{p}(1+pt_2+\lambda_2x_1)-\frac{1}{p}\right]$$
$$+\mathrm{C}_1e^{-(qt_2+\lambda_1x_1)}+\mathrm{C}_2e^{-(pt_2+\lambda_2x_1)}+\mathrm{C}_3 \quad . \quad (38\,b)$$

and

$$y_2(t_2)_{x>0}=\mathrm{A}^2v_1\left[\frac{e^{-(qt_2-\lambda_1x_1)}}{q}(1+qt_2-\lambda_1x_1)-\frac{1}{q}\right.$$
$$\left.+\frac{e^{-(pt_2-\lambda_2x_2)}}{p}(1+pt_2-\lambda_2x_1)-\frac{1}{p}\right]$$
$$+\mathrm{C}_1e^{-(qt_2-\lambda_1x_1)}+\mathrm{C}_2e^{-(pt_2-\lambda_2x_1)}+\mathrm{C}_3, \quad . \quad (38\,c)$$

where t_2 is given by ($34\,a$) and x_1 by (18) and C_1, C_2, and C_3 are constants (different from γ_1, γ_2, and γ_3) to be determined.

Now the total displacement (Y_2) during the second epoch is obtained by adding the expressions (35) and (38), or we have

$$(Y_2)_{x_1}=(y_2)_{x_1}-y_2(t_2)_{x_1}, \quad . \quad . \quad . \quad . \quad (39)$$

giving the displacement of any point of the string.

In order to evaluate the constants C_1, C_2, and C_3 appearing in equation (38) we shall use, as before, the conditions of continuity of $(Y)_{x_1=0}$ and u, $\dot{u}$ at $t_2=0$. The first condition gives, with the help of (32a) and (39),

$$C_1+C_2=-C_3. \quad . \quad . \quad . \quad . \quad . \quad (40)$$

The continuity of u is the same as the continuity of $A\left(\frac{\partial Y}{\partial x}\right)_{x=a}$, which gives from (32$a$, b) and (38)

$$C_1\lambda_1+C_2\lambda_2=0. \quad . \quad . \quad . \quad . \quad . \quad (41)$$

In like manner the continuity of $\dot{u}$, which is equivalent to the continuity of $\frac{\partial}{\partial t}\left\{A\left(\frac{\partial Y}{\partial x}\right)_{x=a}\right\}$, gives

$$C_1\lambda_1 q+C_2\lambda_2 p=A^2v_1(\lambda_1+\lambda_2). \quad . \quad . \quad . \quad (42)$$

On solving equations (41) and (42) for C_1 and C_2, and as $\lambda_1+\lambda_2=\frac{E}{2T_1}$ when k is small (from (14) and (25)), we have

$$C_1=\frac{A^2v_1(\lambda_1+\lambda_2)}{(q-p)\lambda_1}=-\frac{A^3v_1}{q}, \quad . \quad . \quad . \quad (43)$$

$$C_2=-\frac{A^2v(\lambda_1+\lambda_2)}{(q-p)\lambda_2}=\frac{A^3v_1}{p}. \quad . \quad . \quad . \quad . \quad (44)$$

Now, putting the values of these constants in (38), expression (39) (with the help of (32) and (34)) becomes

$$(Y_2)_{x_1=0}=y_1(t_1)_{x_1=0}-y_1(t_2)_{x_1=0}+A^2v_1\left[\frac{e^{-qt_2}}{q}(1-A+qt_2)\right.$$

$$\left.-\frac{1-A}{q}+\frac{e^{-pt_2}}{p}(1+A+pt_2)-\frac{1+A}{p}\right], \quad . \quad (45a)$$

$$(Y_2)_{x_1<0}=y_1(t_1)_{x_1<0}-y_1(t_2)_{x_1>0}$$

$$+A^2v_1\left[\frac{e^{-(qt_2+\lambda_1x_1)}}{q}(1 \quad A+qt_2+\lambda_1x_1)-\frac{1-A}{q}\right.$$

$$\left.+\frac{e^{-(pt_2+\lambda_2x_1)}}{p}(1+A+pt_2+\lambda_2x_1)-\frac{1+A}{p}\right], \quad (45b)$$

$$(Y_2)_{x_1>0}=y_1(t_1)_{x_1>0}-y_1(t_2)_{x_1>0}$$
$$+A^2v_1\left[\frac{e^{-(qt_2-\lambda_1x_1)}}{q}(1-A+qt_2-\lambda_1x_1)-\frac{1-A}{q}\right.$$
$$\left.+\frac{e^{-pt_2}}{p}(1+A+pt_2-\lambda_2-x_1)-\frac{1+A}{p}\right]. \quad . \quad (45c)$$

These are the displacements during the second epoch.

Third Epoch.

Proceeding in the same manner as in the second epoch we find that the two waves (38 *b*) and (38 *c*) originate at $x_1=0$ at the beginning of the second epoch, and travel along the string in opposite directions, while the wave (38 *b*) is reflected from $x=0$ as

$$-y_2(t_3)_{x_1>0}=-A^2v_1\left[\frac{e^{-(qt_3-\lambda_1x_1)}}{q}(1-A+qt_3-\lambda_1x_1)-\frac{1-A}{q}\right.$$
$$\left.+\frac{e^{-(pt_3-\lambda_2x_1)}}{p}(1+A+pt_3-\lambda_2x_1)-\frac{1+A}{p}\right], \quad (46)$$

where

$$t_3=t_2-\frac{2a}{c}=t-\tau-\frac{4a}{c} \quad . \quad . \quad . \quad . \quad . \quad (47)$$

This wave crosses the hammer at $x_1=0$, i. e., $x=a$, while that in the longer segment continues to travel outward.

Thus the displacement $(y_3)_{x_1}$ becomes, after reflexion,

$$\left.\begin{aligned}(y_3)_{x_1=0}&=(Y_2)_{x_1=0}-y_2(t_3)_{x_1=0},\\(y_3)_{x_1<0}&=(Y_2)_{x_1<0}-y_2(t_3)_{x_1>0},\\(y_3)_{x_1>0}&=(Y_2)_{x_1>0}-y_2(t_3)_{x_1>0}.\end{aligned}\right\} \quad . \quad . \quad (48)$$

The reflected wave while crossing the hammer produces two new waves which travel in opposite directions along with waves produced by the natural vibration of the system. The pressure obtained as before from (46), is

$$-A^2v_1[qe^{-qt_3})1+A-qt_3)+pe^{-pt_3}(1-A-pt_3)]. \quad (49)$$

If this pressure acts on the dynamical system at $t_3=t$ for a short time, dt, it will impart to it a velocity

$$-A^2v_1[qe^{-qt}(1+A-qt)+pe^{-pt}(1-A-pt)]dt.$$

Substituting this value of the velocity in the dynamical system, and then integrating and adding the natural vibration $\gamma_1 e^{-qt_3} + \gamma_2 e^{-pt_3} + \gamma_3$, we get for the displacement $y_3(t_3)_{x_1=0}$ at any time t_3 measured from the beginning of the third epoch

$$y_3(t_3)_{x_1=0} = -A^3 v_1 \int_0^{t_3} [qe^{-qt}(1-qt+A) + pe^{-pt}(1-pt-A)] \left\{ \frac{1-e^{-qt}}{q} - \frac{1-e^{-pt}}{p} \right\} dt + \gamma_1 e^{-qt_3} + \gamma_2 e^{-pt_3} + \gamma_3.$$

On integrating we get

$$y_3(t_3)_{x_1=0} = A^3 v_1 \left[\frac{e^{-qt_3}}{q} \left\{ A(1+qt_3) - \frac{q^2 t_3^2}{2} \right\} - \frac{A}{q} + \frac{e^{-pt_3}}{p} \left\{ A(1+pt_3) + \frac{p^2 t_3^2}{2} \right\} - \frac{A}{p} - \frac{1}{q-p} \{ e^{-qt_3} . qt_3 + e^{-pt_3} . pt_3 \} \right] + C_1 e^{-qt_3} + C_2 e^{-pt_3} + C_3 ; \quad . \quad . \quad . \quad . \quad . \quad (50\,a)$$

so

$$y_3(t_3)_{x_1<0} = A^3 v_1 \left[\frac{e^{-(qt_3+\lambda_1 x_1)}}{q} \left\{ A(1+qt_3+\lambda_1 x_1) - \frac{(qt_3+\lambda_1 x_1)^2}{2} \right\} - \frac{A}{q} + \frac{e^{-(pt_3+\lambda_2 x_1)}}{p} \left\{ A(1+pt_3+\lambda_2 x_1) + \frac{(pt_3+\lambda_2 x_1)}{2} \right\} - \frac{A}{p} - \frac{1}{q-p} \{ e^{-(qt_3+\lambda_1 x_1)} . (qt_3+\lambda_1 x_1) + e^{-(pt_3+\lambda_2 x_1)} . (pt_3+\lambda_2 x_1) \} \right] + C_1 e^{-(qt_3+\lambda_1 x_1)} + C_2 e^{-(pt_3+\lambda_2 x_1)} + C_3, \quad . \quad . \quad . \quad . \quad . \quad (50\,b)$$

$$y_3(t_3)_{x_1>0} = A^3 v_1 \left[\frac{e^{-(qt_3-\lambda_1 x_1)}}{q} \left\{ A(1+qt_3-\lambda_1 x_1) - \frac{(qt_3-\lambda_1 x_1)^2}{2} \right\} - \frac{A}{q} + \frac{e^{-(pt_3-\lambda_2 x_1)}}{p} \left\{ A(1+pt_3-\lambda_2 x_1) + \frac{(pt_3-\lambda_2 x_1)^2}{2} \right\} - \frac{1}{q-p} \{ e^{-(qt_3-\lambda_1 x_1)} . (qt_3-\lambda_1 x_1) + e^{-(pt_3-\lambda_2 x_1)} . (pt_3-\lambda_2 x_1) \} \right] + C_1 e^{-(qt_3-\lambda_1 x_1)} + C_2 e^{-(pt_3-\lambda_2 x_1)} + C_3, \quad . \quad . \quad . \quad . \quad . \quad (50\,c)$$

where C_1, C_2, and C_3 are to be determined. Now the total displacement during the third epoch is obtained by adding (48) and (50), or we have

$$(Y_3)_x=(y_3)_x+y_3(t_3)_x$$
$$=(Y_2)_x-y_2(t_3)_x+y_3(t_3)_x. \quad . \quad . \quad . \quad (51)$$

From the continuity of Y, u, and $\dot{u}$ at $t_3=0$ we have

$$y_3(t_3)=\dot{y}_3(t_3)=\ddot{y}_3(t_3)=0.$$

These give

$$C_1+C_2+C_3=0, \quad . \quad . \quad . \quad . \quad . \quad . \quad (52)$$

$$C_1q+C_2p=A^4v_1, \quad . \quad . \quad . \quad . \quad (53)$$

and

$$C_1q^2+C_2p^2=A^3v_1(q-p)+A^4v_1(q+p)-2A^3v_1\left(\frac{q^2+p^2}{q-p}\right).$$
$$. \quad . \quad . \quad (54)$$

On solving equations (53) and (54) for C_1 and C_2 we get

$$C_1=-\frac{A^5v_1}{q}\left(2-\frac{p}{q+p}\right). \quad . \quad . \quad . \quad . \quad (55a)$$

and

$$C_2=\frac{A^5v}{p}\left(2-\frac{q}{q+p}\right). \quad . \quad . \quad . \quad . \quad (55b)$$

Now putting these values of C_1, C_2, C_3 from (52) and (55) in the expression (51), we have

$$(Y_3)_{x_1=0}$$
$$=(Y_2)_{x_1=0}-y_2(t_3)_{x_1=0}+A^3v_1\left[\frac{e^{-qt_3}}{q}\left\{A(1+qt_3)-\frac{q^2t_3^2}{2}\right\}\right.$$
$$-\frac{A}{q}+\frac{e^{-pt_3}}{p}\left\{A(1+pt_3)+\frac{p^2t_3^2}{2}\right\}-\frac{A}{p}$$
$$\left.-\frac{1}{q-p}\{e^{-qt_3}.qt_3+e^{-pt_3}.pt_3\}\right]$$
$$+A^5v_1\left[\left(2-\frac{p}{q+p}\right)\frac{1-e^{-qt_3}}{q}-\left(2-\frac{q}{q+p}\right)\frac{1-e^{-pt_3}}{p}\right],$$
$$. \quad . \quad . \quad (56a)$$

$$(Y_3)_{x_1<0}$$

$$=(Y_2)_{x_1<0}-y_2(t_3)_{x_1>0}$$

$$+A^3v_1\left[\frac{e^{-(qt_3+\lambda_1x_1)}}{q}\left\{A(1+qt_3+\lambda_1x_1)-\frac{(qt_3+\lambda_1x_1)^2}{2}\right\}\right.$$

$$-\frac{A}{q}+\frac{e^{-(pt_3+\lambda_2x_1)}}{p}\left\{A(1+pt_3+\lambda_2x_1)+\frac{(pt_3+\lambda_2x_1)^2}{2}\right\}$$

$$-\frac{A}{p}-\frac{1}{q-p}\left\{e^{-(qt_3+\lambda_1x_1)}.(qt_3+\lambda_1x_1)\right.$$

$$\left.\left.+e^{-(pt_3+\lambda_2x_1)}.(pt_3+\lambda_2x_1)\right\}\right]$$

$$+A^5v_1\left[\left(2-\frac{p}{q+p}\right)\frac{1-e^{-(qt_3+\lambda_1x_1)}}{q}\right.$$

$$\left.-\left(2-\frac{q}{q+p}\right)\frac{1-e^{-(pt_3+\lambda_2x_1)}}{p}\right], \quad \ldots\ldots\ldots (56\,b)$$

$$(Y_3)_{x_1>0}$$

$$=(Y_2)_{x_1>0}-y_2(t_3)_{x_1>0}$$

$$+A^3v_1\left[\frac{e^{-(qt_3-\lambda_1x_1)}}{q}\left\{A(1+qt_3-\lambda_1x_1)-\frac{(qt_3-\lambda_1x_1)^2}{2}\right\}\right.$$

$$-\frac{A}{q}+\frac{e^{-(pt_3-\lambda_2x_1)}}{q}\left\{A(1+pt_3-\lambda_2x_1)+\frac{(pt_3-\lambda_2x_1)^2}{2}\right\}$$

$$-\frac{A}{p}-\frac{1}{q-p}\left\{e^{-(qt_3-\lambda_1x_1)}.(qt_3-\lambda_1x_1)\right.$$

$$\left.\left.+e^{-(pt_3-\lambda_2x_1)}.(pt_3-\lambda_2x_1)\right\}\right]$$

$$+A^5v_1\left[\left(2-\frac{p}{q+p}\right)\frac{1-e^{-(qt_3-\lambda_1x_1)}}{q}\right.$$

$$\left.-\left(2-\frac{q}{q+p}\right)\frac{1-e^{-(pt_3-\lambda_2x_1)}}{p}\right]. \quad \ldots\ldots\ldots (56\,c)$$

These are the displacements during the third epoch where $(Y_2)_{x_1}$ and $y_2(t_3)_{x_1}$ are given by (45) and (46) respectively.

Proceeding in a similar manner one can easily find the displacements at any epoch higher than the third.

Pressure exerted by the Hammer.

From equation (21 *b*) we find that the pressure P exerted by the hammer is given by

$$P - P_0 = m\ddot{z} = T_1 \Delta \left(\frac{\partial Y}{\partial x}\right)_{x=a}, \quad . \quad . \quad . \quad (57)$$

where z is defined by equation (4 *b*). On putting the values of $T_1 \Delta \left(\frac{\partial Y}{\partial x}\right)_{x=a}$ for different epochs we get the corresponding pressure. From equations (32 *b*, *c*), (51), and from the relation $T_1 = c^2\rho$, we get for the pressure exerted by the hammer during the first epoch

$$P_1 = P_0 + 2\rho v_1 c A\{e^{-qt_1} - e^{-pt_1}\}, \quad . \quad . \quad . \quad (58)$$

where P_0 is the pressure attained at the instant $t_1 = 0$.

Equation (57), with the help of (45 *b*, *c*), gives the pressure (P_2) exerted by the hammer during the second epoch,

$$P_2 = P_1 + 2\rho v_1 c A^2[e^{-qt_2}(A - qt_2) - e^{-pt_2}(A + pt_2)], \quad (59)$$

where (P_1) is given by equation (58).

In the same way, from equations (58), (56 *b*, *c*) we get for the pressure (P_3) during the third epoch

$$\begin{aligned} P_3 = P_2 + 2\rho v_1 c A^3 \Big[& e^{-qt_3} \left\{ A^2 \left(2 - \frac{p}{q+p}\right) - \frac{q}{q-p} \right. \\ & \left. - qt_3 \left(1 + A - \frac{q}{q-p}\right) + \frac{q^2 t_3^2}{2} \right\} \\ & - e^{-pt_3} \left\{ A^2 \left(2 - \frac{q}{q+p}\right) + \frac{p}{q-p} \right. \\ & \left. + pt_3 \left(A - 1 - \frac{p}{q-p}\right) + \frac{p^2 t_3^2}{2} \right\} \Big] . \quad . \quad . \quad . \quad . \quad (60) \end{aligned}$$

Proceeding as above, the expressions for the pressure at any epoch higher than the third can easily be obtained.

Reflexion from both Ends.

Hitherto the analysis that we have undertaken has been subjected to the restriction that one of the extremities of the string is so remote from the struck point that the impact terminates before any reflexion from this end

reaches the hammer. This limitation can easily be got rid of in some special cases, to be discussed below.

If the struck point be near the middle of the string, so that $(b-a)$ is small where $(a+b)=l$, the length of the string, then the wave from the end $x=l$ overtakes the hammer before it leaves the string at the instant $t=\frac{2b}{c}+\tau$. Hence during the interval $2b/c<t_1<4a/c$ the displacement at different points on the string are given by

$$\left.\begin{aligned}
(\mathrm{Y}_2)_{x_1=0} &= y_1(t_1)_{x_1=0} - y_1(t_2)_{x_1=0} + y_2(t_2)_{x_1=0} \\
&\quad - y_1(t_2')_{x_1=0} + y_2(t_2')_{x_1=0}, \\
(\mathrm{Y}_2)_{x_1<0} &= y_1(t_1)_{x_1<0} - y_1(t_2)_{x_1>0} + y_2(t_2)_{x_1<0} \\
&\quad - y_1(t_2')_{x_1<0} + y_2(t_2')_{x_1<0}, \\
(\mathrm{Y}_2)_{x_1>0} &= y_1(t_1)_{x_1>0} - y_1(t_2)_{x_1>0} + y_2(t_2)_{x_1>0} \\
&\quad - y_1(t_2')_{x_1<0} + y_2(t_2')_{x_1>0},
\end{aligned}\right\} \quad (61)$$

where $t_2=t_1-2a/c$ and $t_2'=t_1-2b/c$.

The wave $y_2(t_2)_{x_1<0}$ being reflected as $-y(t_3)_{x_1<0}$ from the end at $x=0$ reaches the hammer at $t_2=2a/c$ as the wave $-y_2(t_3)_{x_1=0}$, and while crossing generates two new waves, $y_3(t_3)_{x_1<0}$ and $y_3(t_3)_{x_1>0}$.

So at the instant $2a/c<t_2<2b/c$ we have

$$\begin{aligned}
(\mathrm{Y})_{x_1=0} &= y_1(t_1)_{x_1=0} - y_1(t_2)_{x_1=0} + y_2(t_2)_{x_1=0} \\
&\quad - y_1(t_2')_{x_1=0} + y_2(t_2')_{x_1=0} - y_2(t_3)_{x_1=0} + y_3(t_3)_{x_1=0}. \quad (62)
\end{aligned}$$

At the instant $t_1=2(a+b)/c$ the waves $-y_1(t_2')$ and $-y_1(t_2)$, after being reflected from the respective ends $x=0$ and $x=l$ as $y_1(t_2'-2a/c)$ and $y_1(t_2-2b/c)$, will generate two new waves, $-y_2(t_2'-2a/c)$ and $-y_2(t_2-2b/c)$. On the other hand, the waves $y_2(t_2')$ and $y_2(t_2)$, being reflected from the two ends $x=0$ and $x=l$ as $-y_2(t_2'-2a/c)$ and $-y_2(t_2-2b/c)$, will give rise to the waves $y_3(t_2'-2a/c)$ and $y_3(t_2-2b/c)$ respectively; so at the interval $2a/c<t_2'<2b/c$ we have for the struck point $x=a$, i. e., $x_1=0$,

$$\begin{aligned}
(\mathrm{Y})_{x_1=0} &= (\mathrm{Y})_{x_1=0} \text{ of equation (62)} + y_1(t_2-2b/c)_{x_1=0} \\
&\quad + y_1(t_2'-2a/c)_{x_1=0} - 2y_2(t_2-2b/c)_{x_1=0} \\
&\quad - 2y_2(t_2'-2a/c)_{x_1=0} + y_3(t_2'-2a/c)_{x_1=0} \\
&\quad + y_3(t_2-2b/c)_{x_1=0}. \quad \ldots\ldots\ldots \quad (63)
\end{aligned}$$

Again, at the instant $t_2' = 2b/c$ the wave $y_2(t_2')$, being reflected as $y_2(t_3')$ from the end $x=l$, reaches the struck point $x=a$, producing a fresh wave $y_3(t_3')$; so at the interval $4b/c < t_1 < (4b+2a)/c$ we have for the displacement of the struck point

$$(Y)_{x_1=0} = (Y)_{x_1=0} \text{ of equation (63)} + y_3(t_3')_{x_1=0} - y_2(t_3')_{x_1=0}. \quad . \quad . \quad . \quad (64)$$

Proceeding in a similar manner we can derive the expression for the displacement at any instant.

In the case when the hammer strikes exactly at the middle we get the expression for the displacement of the struck point at any instant during impact by putting $b=a$. Hence, from (61) we have for the value of $(Y)_{x_1=0}$ during $2a/c < t_1 < 4a/c$

$$(Y_2)_{x_1=0} = y_1(t_1)_{x_1=0} - 2y_1(t_2)_{x_1=0} + 2y_2(t_2)_{x_1=0}, \quad . \quad (65a)$$

which, with the help of (32a), (34), and (38a), can be written as

$$\begin{aligned}(Y_2)_{x_1=0} &= Av_1\left[\frac{1-e^{-qt_1}}{q} - \frac{1-e^{-pt_1}}{p}\right] - 2Av_1\left[\frac{1-e^{-qt_2}}{q} - \frac{1-e^{-pt_2}}{p}\right] \\ &\quad + 2A^3v_1\left[\frac{1-e^{-qt_2}}{q} - \frac{1-e^{-pt_2}}{p}\right] \\ &\quad + 2A^2v_1\left[\frac{e^{-qt_2}}{q}(1+qt_2) - \frac{1}{q} + \frac{e^{-pt_2}}{p}(1+pt_2) - \frac{1}{p}\right]. \quad (65b)\end{aligned}$$

In the same manner from (64) we get the displacement $(Y_3)_{x_1=0}$ of the mid-point during the interval $4a/c < t_1 < 6a/c$ as

$$(Y_3)_{x_1=0} = (Y_2)_{x_1=0} \text{ of equation (65}a\text{)} + 2y_1(t_3)_{x_1=0} - 6y_2(t_3)_{x_1=0} + 4y_3(t_3)_{x_1=0}. \quad . \quad . \quad . \quad . \quad (66a)$$

On putting the values of the different expressions as previously obtained we get, after simplification,

$$\begin{aligned}(Y_3)_{x_1=0} &= \text{sum of the terms in (65}b\text{)} \\ &\quad - 2Av_1\left[\frac{e^{-qt_3}}{q}(\alpha_1+\alpha_2qt_3+A^2q^2t_3^2) - \frac{\alpha_1}{q}\right. \\ &\quad \left. - \frac{e^{-pt_3}}{p}(\beta_1+\beta_2pt_3+A^2p^2t_3^2) + \frac{\beta_1}{p}\right], \quad . \quad . \quad (66b)\end{aligned}$$

where

$$\alpha_1 = 1+3A(1-A)-2A^3\{1+A(2-p/(q+p))\},$$

$$\alpha_2 = 2A^2\{q/(q-p)-A\}+3A,$$

$$\beta_1 = 1-3A(1+A)+2A^3\{1+A(2-q/(q+p))\},$$

$$\beta_2 = -[2A^2\{p/(q-p)-A\}+3A].$$

Special Cases.

(1) If the string is free from damping, i. e., $k=0$, and if the compression of the hammer takes place according to Hooke's law from the very beginning of the impact, *i e.*. if Hertz's law is absent, which gives $\tau=0$ and $v_1 \to v_0$, equations (32), (45), (56), (58), (59), and (60) reduce to those obtained by Das [8].

(2) When E is large enough compared to ρ/m, and Hertz's law is not called into play (*i. e.*, $\tau=0$), the values of q and p reduce to

$$q = \frac{2\rho c}{m} - \frac{k}{2} = q_0 \quad \text{say,} \quad . \; . \; . \; . \; (67a)$$

$$p = \frac{Ec}{2T_1} - \frac{k}{2} = Ec/2T_1 = p_0 \quad \text{say,} \quad . \; (67b)$$

when k is taken to be small, and the corresponding value of A as given in (33) becomes unity. The above values of q, p, and A reduce the expressions (32), (45), (56), (59), and (60) to those obtained by the author in a previous paper [10].

(3) If E, *i. e.*, p, is equal to infinity and $\tau=0$ we come to the case of a hard hammer. The expression for the pressure during different epochs as given by equations (58), (59) and (60) become

$$P_1 = 2\rho v_0 c e^{-q_0 t}, \quad . \; . \; . \; . \; . \; . \; . \; . \; . \; . \; . \; . \; . \; (68a)$$

$$P_2 = P_1 + 2\rho v_0 c e^{-q_0(t-2a/c)}\{1-q_0(t-2a/c)\}, \quad . \; . \; . \; . \; (68b)$$

and

$$P_3 = P_2 + 2\rho v_0 c e^{-q_0(t-4a/c)}\{1-2q_0(t-4a/c)+q_0^2(t-4a/c)^2/2\}.$$

$$. \; . \; . \; (68c)$$

(4) If in addition to the assumptions made in (3) above, we assume that the hammer is massive, *i. e.*,

$\rho/m \to 0$ and $k=0$, we shall get all the expressions obtained by Delemer. Thus equations (32 *a*, *b*, *c*) reduce to

$$(Y_1)_{x_1=0} = \frac{P_1}{2T_1} ct, \quad . \quad . \quad . \quad . \quad . \quad . \quad (69a)$$

$$(Y_1)_{x_1<0} = \frac{P_1}{2T_1} (ct+x-a), \quad . \quad . \quad . \quad . \quad (69b)$$

$$(Y_1)_{x_1>0} = \frac{P_1}{2T_1} (ct-x+a), \quad . \quad . \quad . \quad . \quad (69c)$$

and from (68 *a*) we have

$$P_1 = 2\rho v_0 c \quad \text{(a constant)}. \quad . \quad . \quad . \quad (69d)$$

These equations are the same as given by Delemer, who assumed in his theory that the pressure exerted by the hammer during impact is constant. The derivation of Delemer's formulæ as above clearly shows that his theory is applicable only to the case of a massive hammer.

(5) If we suppose the elastic constant E as given by Hooke's law of compression to be great, the hammer tends to become hard. Thus in the limiting case, when E is infinite, the hammer becomes perfectly rigid as soon as Hertz's period is over. This assumption, though it appears at the outset to be not quite justified, has certain experimental interest which we shall discuss below ; we have from (35), (65), and (68) for the mid-point (when $E=\infty$, *i. e.*, $p=\infty$)

$$(Y_1)_{x_1=0} = \frac{v_1}{q_0}(1-e^{-q_0 t_1}), \quad . \quad . \quad . \quad . \quad . \quad . \quad . \quad . \quad . \quad (70a)$$

$$(Y_2)_{x_1=0} = (Y_1)_{x_1=0} + \frac{2v_1}{q_0}\{e^{-q_0 t_2}(1+q_0 t_2)-1\}, \quad . \quad . \quad (70b)$$

$$(Y_3)_{x_1=0} = (Y_2)_{x_1=0} - \frac{2v_1}{q_0}[e^{-q_0 t_3}(1+q_0 t_3+q_0{}^2 t_3{}^2)-1], \quad (70c)$$

and the corresponding pressures are given by

$$P_1 = P_0 + 2\rho v_1 c e^{-q_0 t_1}, \quad . \quad . \quad . \quad . \quad . \quad . \quad . \quad (70d)$$

$$P_2 = P_1 + 4\rho v_1 c e^{-q_0 t_2}(1-q_0 t_2), \quad . \quad . \quad . \quad . \quad (70e)$$

$$P_3 = P_2 + 4\rho v_1 c e^{-q_0 t_3}(1-3q_0 t_3+q_0 t_3{}^2) \quad . \quad . \quad (70f)$$

where t_1, t_2, and t_3 are given by (27 *b*), (34 *a*), (47) respectively when $\tau=0$, which makes $P_0=0$, and when $k=0$ the above expressions are very easily reduced to those obtained by Kaufmann.

(6) In the case when the hammer is highly elastic, soft, and light we have the condition

$$4\left(\frac{2T_1}{mc}-\frac{k}{2}\right)>\frac{Ec}{2T_1} \quad . \quad . \quad . \quad . \quad . \quad (71)$$

from (25), and so q, p become partly real and partly imaginary; we have

$$[q, p]=\mu\mp i\nu, \quad . \quad . \quad . \quad . \quad . \quad (72)$$

where $i=\sqrt{-1}$ and

$$\left.\begin{aligned}\mu &= Ec/4T_1,\\ \nu &= \frac{1}{2}\sqrt{\frac{4Ec}{2T_1}\left(\frac{2T_1}{mc}-\frac{k}{2}\right)-\left(\frac{Ec}{2T_1}\right)^2}\end{aligned}\right\} \quad . \quad . \quad (73)$$

Thus with the values of q and p given in (72) we can easily rewrite all the expressions obtained previously; but here, in order to avoid the unnecessary lengthening of the paper, we shall discuss only a few of them which are more or less important.

From equations (32 *a*) and (45 *a*), giving the displacements of the struck point, we have

$$(Y_1)_{t_1=0}=B\{\sin\delta-e^{-\mu t_1}\sin(\nu t_1+\delta)\} \quad . \quad . \quad (74\,a)$$

and

$$(Y_2)_{t_1=0}=(Y_1)_{t_1=0} \text{ in equation (74 } a)$$

$$-B\left[(1-\mu^2/\nu^2)\{\sin\delta-e^{-\mu t_2}\sin(\nu t_2+\delta)\}\right.$$

$$\left.-\frac{\mu}{\nu}\{\cos\delta-e^{-\mu t_2}\cos(\nu t_2+\delta)+\sqrt{\mu^2+\nu^2}.t_2e^{-\mu t_2}\cos\nu t_2\}\right],$$

$$. \quad . \quad . \quad (74\,b)$$

where

$$B=2\mu r_1/\nu\sqrt{\mu^2+\nu^2} \quad \text{and} \quad \delta=\tan^{-1}\frac{\nu}{\mu}. \quad . \quad . \quad (75)$$

Similarly from the pressure equations (58) and (59) we have

$$P_1=P_0+\frac{Ev_1}{\nu}e^{-\mu t_1}\sin\nu t_1 \quad . \quad . \quad . \quad . \quad (76)$$

and

$$P_2=P_1+\frac{Ev_1\mu^2}{\nu^3}e^{-\mu t_2}\left\{\frac{\nu\sqrt{\mu^2+\nu^2}}{2\mu}t_2\cos(\nu t_2-\delta)-\sin\nu t_2\right\}, \quad . \quad . \quad . \quad (77)$$

where t_1, t_2, μ, ν, and δ are given by (27 *b*), (34 *a*), (73), and (75) respectively.

Bhargava and Ghosh have got an expression for the pressure exerted by the felt hammer similar to that given in (76). The minor difference in the value of the constant involved in the equation is due to the fact that they have assumed the shorter segment of the string to remain straight as a rigid rod during impact. They have further made some improper approximation in solving the differential equation. This was pointed out by Das [14], who, however, has made a similar assumption about the shorter segment. Now this assumption goes completely against the experimental fact, as is seen from the beautiful photographs obtained by R. N. Ghosh [15] in a recent paper, where he has attempted to explain it by arbitrarily taking an additional term to represent the free vibration of the shorter segment.

(7) In the case when $\tau=0$, the string is free from damping, i. e., $k=0$, and the hammer is soft and plastic, *i. e.*, $Ec/2T_1$ is very small. we have from (73) and (76)

$$P_1=\frac{Ev_0}{c}\sin\nu_0 t, \quad . \quad . \quad . \quad . \quad . \quad (78a)$$

where

$$\nu_0=\sqrt{\frac{E}{m}}. \quad . \quad . \quad . \quad . \quad . \quad . \quad (78b)$$

This is the form of the pressure which Helmholtz assumed in solving the problem of the pianoforte string. In this connexion he remarked that "the magnitude of ν_0 increases as the elastic power of the hammer increases and its weight decreases." This, however, is evident from (78 *b*).

Duration of Contact.

The duration of contact Φ, as generally defined, is the value of (t) for which the expression for the pressure (P_n) falls to zero; but such a definition is possible only in the

case of a rigid hammer. It is otherwise in the case of the felt hammer, where contact commences according to Hertz's law. In this case while leaving the string the hammer may be in contact with it even after the pressure according to Hooke's law falls to zero, *i. e.*, the pressure falls to the value P_0. This extension of the period is due to the relaxation of the felt which was compressed during the Hertz's period up to the pressure P_0. So this extension, which may be called the Hertz period at the end, has the same magnitude (τ) as given by (10).

Now we shall consider the case where during the first epoch Hooke's pressure falls to zero, and therefore the actual pressure becomes P_0. This happens in the case denoted by equation (76), where the actual pressure falls to the value P_0 when $t=\pi/\nu+\tau$; so the duration of contact Φ is the sum of t and τ the time required to destroy the pressure P_0, which is equal to

$$\Phi=\pi/\nu+2\tau. \quad . \quad . \quad . \quad . \quad . \quad . \quad . \quad (79)$$

Thus when the striking distance a from the fixed end is large and the hammer is light and soft Φ is constant for a constant value of (v_0), and the impact terminates before any reflexion reaches the hammer from the end.

Next we shall consider the case when the impact terminates during the second or any higher epoch. It may be remarked that it is extremely difficult to solve the pressure equation algebraically in the general case. However, in the case of the rigid hammer it is possible to solve the pressure equations algebraically up to the fifth epoch, since general algebraic solutions of the biquadratic and the cubic equations are known. In other cases graphic methods should be adopted.

The case when the hammer after Hertz's period at the beginning behaves as a hard one, owing to the large value of E, has already been treated for the mid-point. Here the hammer does not leave the string before the waves reflected from the two ends reach it. This is evident from the fact that $P_1=P_0$ given by equation (70*d*) has no finite root. The hammer may, however, leave the string before any second reflexion reaches it, in which case P_2 given in equation (70*e*) falls to the value P_0 at the time

$$t=\Phi_0+\tau, \quad . \quad . \quad . \quad . \quad . \quad (80\,a)$$

where

$$\Phi_0 = \frac{2l}{c}\left[\frac{1}{2} + \frac{1}{4}\frac{m}{m'(1-km/4\rho c)}\left\{1+\frac{1}{2}e^{-\frac{2m'}{m}(1-km/4\rho c)}\right\}\right], \quad \ldots (80\,b)$$

and $m'=l\rho$ and τ given by equation (10). So the duration of impact Φ, as before, is the sum of t and the time (τ) required to destroy the pressure P_0. This gives

$$\Phi = \Phi_0 + \frac{2u_0}{v_0}\left(1+\frac{n^2u_0^{5/2}}{7v_0^2}+\frac{n^2u_0^5}{16v_0^4}+\cdots\right) \quad \text{(from (10) and (80}a\text{), (80}b\text{))}.$$

$$\ldots (81)$$

In the above we have supposed $E=\infty$, although actually it is large and finite; this will not materially

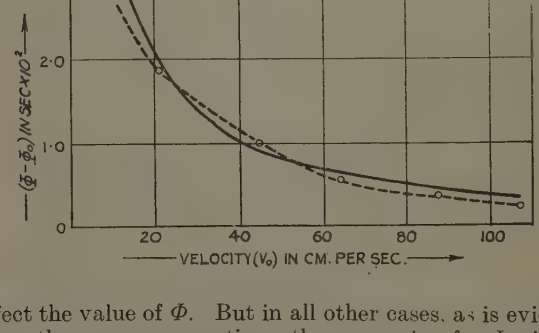

affect the value of Φ. But in all other cases, as is evident from the pressure equations, the expression for Φ will be of the same form as given by (81), only the value of Φ_0 differs in each case.

The continuous curve in the figure shows the theoretical variation of $(\Phi-\Phi_0)$ with (v_0).

In calculating the theoretical values the expression within the brackets in (81) is taken to a first approximation and $2u_0=0{\cdot}4$ cm. The dotted curve shows the corresponding variation of the experimental values obtained by the writer [16]. The theoretical value of Φ_0 from (80b) is $2{\cdot}997\times10^{-2}$ sec., whereas the observed value is $3{\cdot}086\times10^{-2}$ sec. From the figure it is evident that the

theory put forward agrees fairly well with the experiment, the slight discrepancy being perhaps due to the approximation made during the calculation of Φ_0 from the pressure equation (70*e*).

In conclusion, we may remark that the existence of the small pressure during the Hertzian periods at the beginning and at the end of the impact, which is the basis of the present analysis, naturally reminds one of Lamb's [6] assumption that "the pressure exerted by the hammer on the string becomes appreciable after a certain instant when it comes in contact and leaves the string long after the pressure falls to a very small value."

Summary.

1. A general theory of the impact of the elastic hammer of any elastic value with a damped stretched string is developed.

2. It is shown that the impact begins and ends with Hertz's law of compression, and that Hooke's law obtains in the interval between these two periods.

3. The general expressions for the displacement of any point of the string during contact and expression for the pressure for the hammer striking at the end and also at the middle, have been derived up to the third epoch. The method may be extended for higher epochs.

4. The special case in which the hammer strikes at a little distance away from the centre of the string is also discussed.

5. The theories of Helmholtz, Delemer, Kaufmann, and Das are shown to be the special cases of the present theory.

6. Lamb and Bhargava-Ghosh theories are also discussed from the standpoint o ' the author's theory.

7. The expressions for the duration of contact are also discussed. It is shown that in the case of the felt hammer, the duration depends on the velocity of impact.

8. The theoretical as well as the experimental values of the variation of the duration of contact with the velocity before impact have been compared and found to be in very good agreement.

Finally, the author wishes to thank Prof. K. C. Kar, D.Sc., for his valuable advice and lively interest in this work.

References.

(1) Raman and Banerjee, Proc. Roy. Soc. A, xcvii. pp. 99–110 (1920).
(2) K. C. Kar, Phil. Mag. vi. pp. 276–280 (1925); Ind. Phys. Math. Journ. iii. pp. 103–104 (1932).
(3) Helmholtz, 'Sensations of Tone,' translated by Ellis, 3rd edit. pp. 380–384.
(4) Kaufmann, *Ann. d. Phys.* Bd. liv. p. 675 (1895).
(5) J. Delemer, *Ann. Soc. Sci. de Bruxell.* xxx. parts 3–4, pp. 299–310 (1905–1906).
(6) H. Lamb, 'Dynamical Theory of Sound.'
(7) Bhargava and Ghosh, Phil. Mag. xlvii. pp. 1141–1148 (1924).
(8) Das, Proc. Ind. Ass. Cult. Sci. ix. p. 297 (1926).
(9) K. C. Kar and M. Ghosh, Phil. Mag. ix. pp. 306–324 (1930); xii. pp. 676–685 (1931); *Zeit. f. Phys.* Bd. lxi. h. 7 & 8, pp. 525–536 (1930); Bd. lxvi. h. 5 & 6, pp. 414–424 (1930); *Zeit. f. Andw. Math. u. Mec.* Bd. xi. h. 5, pp. 361–372 (1931).
(10) M. Ghosh, Ind. Phys. Math. Journ. iii. pp. 15–25 (1932).
(11) C. K. Weak, Amer. Journ. Sci. xxxii. pp. 366–368 (1884).
(12) J. P. Andrews, Phil. Mag. viii. p. 781 (1929); ix. p. 593 (1930); Proc. Phys. Soc. pp. 1–25 (1931); Approved Doctorate Thesis of the London University.
(13) Rayleigh, 'Theory of Sound,' i. 2nd edit. (1926), art. 133, p. 195.
(14) Das, Proc. Phys. Soc. xl. p. 29 (1927).
(15) R. N. Ghosh, Phil. Mag. ix. p. 1174 (1930); similar photographs were obtained previously by Kaufmann (*loc. cit.*) and Banerjee and Ganguli, Phil. Mag. vii. pp. 345–352 (1929).
(16) M. Ghosh, Ind. Journ. Phys. vii. part 5, pp. 365–382 (1932).

Physical Research Laboratory,
Presidency College, Calcutta.
October 1933.

XLV. *Some Measurements of the* K-*Absorption Edges of Carbon, Nitrogen, and Oxygen, and of the Components of Carbon* Kα. *By* F. C. Chalklin, *Ph.D., Lecturer in Physics, and* L. P. Chalklin, *Ph.D., University College, London* *.

[Plates XIX. & XX.]

A. *Absorption Measurements.*

THE K-edges of the light elements occur in the region of the very soft X-rays, and it is, therefore, only recently, with the development of the grazing incidence grating spectrograph, that it has become possible to observe and measure them. In the present investigation we have employed a plane grating vacuum spectrograph, which we have recently described †, to measure the K-edges of carbon, nitrogen, and oxygen.

* Communicated by Prof. E. N. da C. Andrade.
† Phil. Mag. xvi. p. 363 (1933).

The carbon, nitrogen, and oxygen which give rise to these absorption effects, occur naturally in the vacuum spectrograph as residual gases or components of these gases. Since the X-ray tube is connected to the spectrograph these gases also produce emission spectra consisting in each case, of the Kα line. This line is naturally close to the K-edge, and being, for the light elements, very wide and diffuse, extends right up to it. A photometer record from one of our plates shows this effect rather clearly (fig. 1, Pl. XIX.). It is also evident from this record that the determination of the absorption edges under such circumstances is a matter of considerable uncertainty. In the work to be described we have attempted to obviate these troublesome emission lines, and in this way to obtain more accurate values for the wave-lengths of the edges.

With the order of vacuum attainable in the X-ray tube of our spectrograph the emission lines of oxygen and carbon originate from the surface of the anti-cathode, and not directly from the residual gases. This is demonstrated by the fact that we rarely obtain the nitrogen emission line with appreciable intensity, and it is conclusively proved by our subsequent results. The carbon is deposited on the anti-cathode, probably as a result of the breakdown, during the running of the X-ray tube, of hydrocarbons, CO and CO_2, from the walls and joints of the spectrograph. An examination of our plates leads us to believe that the oxygen is mainly due to the deposition of tungsten oxide from the filament of the tube. To minimize these deposits, we have adopted the procedure of allowing the anti-cathodes to run hot. This was done by employing as anti-cathode a metal sheet folded over and in poor thermal contact with a water-cooled base. The temperature of the metal sheet could then be varied by altering the thermionic current. Many different anti-cathode metals have been employed, but, for the present purpose, those most successful were the ones possessing high melting-points such as tungsten and molybdenum. In fig. 2 (Pl. XIX.) is shown a spectrogram and its photometer record obtained by the method described. The almost complete absence of the carbon K_α-emission line and the strength of the carbon K_a-edge are the most noteworthy features of the curve. The nitrogen edge can also be seen. Although the oxygen K_α-line is weak,

it has not been completely eliminated on this, nor on any other plate. Another interesting feature is the sharpness of the edges. These cover a range of about ·8 Å. for carbon, ·6 Å. for nitrogen, and ·3 Å. for oxygen.

Measurements of the edges have been made and are listed in Table I. The values refer to the centres of the edges, where the measurements are most accurately made and where they are independent of corrections for the resolution of the apparatus.

TABLE I.

Element.	Determinations.	Mean.
Carbon ...	Order I. 43·1. Order II. 43·0, 42·9, 43·0, 43·0	43·0 Å. ± ·2
Nitrogen..	Order I. 30·9. Order II. 31·2, 30·9, 30·8,	31·0 Å. ± ·2
Oxygen...	Order II. 23·2.	23·2 Å. ± ·2

TABLE II.

Author.	Carbon.			Nitrogen.			Oxygen.		
	Å.	Volts.	ν/R.	Å.	Volts.	ν/R.	Å.	Volts.	ν/R.
Thibaud ..	43·5	283·8	20·95	31·1	397	29·30	23·5	524	38·77
Magnusson.	43·3	285·1	21·04						
Prins and Takens ..	43·4	284·5	21·00						
Chalklin ..	43·0	287·1	21·19	30·9	399·5	29·49	23·2	532·1	39·28
Neufeldt .. K-edge		283·8			396·7			532·0	
Subsidiary edges		308·1			434·0			583·0	
		318·9			454·0			613·0	
		363·0			480·5			640·0	

The results of other workers * are included in Table II. Each of these investigators appears to have used cold anti-cathodes. Some results recently obtained by Neufeldt are included. This author used an ion counter to detect the soft X-rays and measured the absorption coefficient of celluloid for different wave-lengths. For each of the elements carbon, oxygen, and nitrogen he observed the K-discontinuity and three subsidiary edges. His results are not affected by emission lines, but we do

* Thibaud, 'Nature,' cxxi. p. 321 (1928). Prins and Takens, *Zeits. für Phys.* lxxv. p. 741 (1932). Magnusson, *Zeits. für Phys.* lxxix. p. 161 (1932). Neufeldt, *Zeits. für Phys.* lxviii. p. 659 (1931).

not know what accuracy he claims for the wave-lengths of the edges. For nitrogen and oxygen there appears to be no great difference between our results and those of previous workers. This is to be expected for nitrogen, since the emission line is weak and allowed us to get satisfactory results with cold anti-cathodes. For carbon, however, the difference is rather large. It is for this element that the effect of the emission line would be expected to cause the greatest error.

Thibaud, in his original note, says that the absorption seems to be limited by a "white line." Local absorption of this type has been observed by us for each of the elements under discussion. It is not, however, invariably present. When very hot anti-cathodes are employed the absorption seems to be almost entirely local. In fig. 2 (Pl. XIX.) it consists of a white line 4·9 Å. wide for carbon, 1·6 Å. for nitrogen, and 1·4 Å. for oxygen *. For cold anti-cathodes it may or may not occur, but a continuous absorption on the short wave side of the edge is always present.

It is of interest to note that the occurrence of both local and continuous absorption is to be expected for these elements, for it is a feature of the K-absorption of the lighter elements in the hard X-ray region.

It has been known for some time that, in order to obtain the local absorption structure at hard X-ray absorption edges, the absorbing screen should be thin. Aoyama, Kimura, and Nishina † pointed out the reason for this. With a thin absorbing screen the local absorption may be strong enough to give a white line on the photographic plate, whilst the continuous absorption, stretching out on the short wave side of the line, may be imperceptible. With increasing thickness of the screen the continuous absorption becomes appreciable, and the contrast between the white line and the continuous absorption region on the plate diminishes, and in the limit practically disappears. This explanation appears to be applicable to the present case. Thus, for hot anti-cathodes, for which we obtain the local absorption, the emission spectra are weak and thus show that there is little carbon, nitrogen, or oxygen on the

* Our measurements of the widths of the white lines vary considerably. Since they probably possess a fine structure, an examination of them with an instrument of higher dispersion would probably yield results of interest.

† *Zeits. für Phys.* xliv. p. 810 (1927).

surface. For cold anti-cathodes, on the other hand, there is a layer of carbon, oxygen, and sometimes nitrogen, and the soft X-rays, generated in this layer or in the metal surface beneath it, are partially absorbed before entering the spectrograph. Thus the hot anti-cathodes give the effect of a thin screen and the cold ones correspond to a thick screen.

Although the present experiments have shown definitely that for cold anti-cathodes much of the carbon and oxygen absorption takes place at the anti-cathode, it is not so evident where the absorption occurs when hot anti-cathodes are employed. A calculation based on the results of Dershem and Schein * for the absorption coefficients of various elements for carbon Kα-radiation makes it appear unlikely that the absorption, due to vapours in the spectrograph, is sufficient to give rise to the observed effects unless there is an enormous increase in absorption at the K-discontinuities and unless the vapour molecules are very complex, so that many atoms are present even at low pressures. It is perhaps possible that, even for the hottest anti-cathodes that we have used—with about one-third of the surface incandescent—there is, in the cooler portions, sufficient emission followed by carbon, oxygen, and nitrogen absorption to account for the observed absorption. It seems quite possible for sufficient oxygen in the form of oxides to be present. It is also possible for carbon. For nitrogen, however, it is extremely unlikely. It is, therefore, necessary to look for another absorbing medium. This may well be provided by the photographic plate, where absorption might occur in occluded gases or in the gelatin. It might be suggested that the difference between our value for the K-edge of carbon and the values of the other workers is due to a difference between the K-edge for the carbon at the anti-cathode and the K-edge for the gelatin of the plate. We have evidence against this. We have a plate, taken with a moderately hot anti-cathode, showing a weak carbon K_α-emission line and continuous as well as local absorption. There is, therefore, anti-cathode absorption taking place. The emission line is not, however, strong enough to mask the edge. The edge is not appreciably less sharp than

* Phys. Rev. xxxvii. p. 1238 (1931).

the edge found for the very hot anti-cathodes, and it does not show appreciable displacement.

B. *Fine Structure of Carbon* K_α.

Owing to its natural occurrence, the K_α-line of carbon has been studied more than any other soft X-radiation. The measurements of the wave-length of the line agree reasonably well at about 44·5 Å., but there has not always been agreement as to its structure. Most authors have described the line as broad and diffuse, but there has been a lack of agreement in the measurements of its width. It is likely that the apparent width depends upon the intensity. Bazzoni, Faust, and Weatherby announced a complex structure of the line, Faust * giving the following measurements of components :— 42·66, 43·23, 44·05, 44·66, 45·33, 46·2, 46·6, 47·21, 47·7 Å. These were obtained by the analysis of photometer records. These results have been the subject of investigations in Siegbahn's laboratory at Upsala, but no evidence of fine structure had been observed until recently. Soderman †, for instance, finds that the blackening rises steeply to a maximum on the short-wave side and falls away slowly on the long-wave side. The photometer curve appears quite smooth. Prins ‡, at Groningen, originally obtained a similar result.

The present authors have obtained this type of line on a large number of plates. A photometer record of one of them is shown in fig. 3 (Pl. XX.). Renninger § has investigated the effect of the crystal structure of the carbon on the shape of the K_α-line. He experimented with graphite, with diamond, and with carborundum. In each case the general shape of the photometer curve conformed to that of fig. 3 (Pl. XX.), but for graphite there was evidence of humps on the short-wave side.

Recently Morand and Hautot ‖ announced that they had resolved carbon K_α into two components separated by ·6 Å. Hautot ¶ shortly afterwards claimed to have resolved it into three— a strong long-wave line, a weaker

* Phys. Rev. xxxvi. p. 161 (1930).
† Phil. Mag. x. p. 600 (1930).
‡ *Zeits. für Phys.* lxix. p. 618 (1931).
§ *Zeits. für Phys.* lxxviii. p. 510 (1932).
‖ *Comptes Rendus*, cxcv. p. 1070 (1933).
¶ *Comptes Rendus*, cxcv. p. 1383 (1932). Also *Journ. de Phys.* iv. p. 236 (1933).

line ·2 Å. shorter, and a yet weaker line still shorter by ·5 Å. A number of tests were made to ensure that the components were real. The components appeared for exciting voltages ranging from 2600 down to 340. No values are given for the actual wave-lengths. Hautot has since obtained similar results for boron.

Our earlier spectrograms of carbon K_α, of which fig. 3 (Pl. XX.) is an example, were obtained with a slit of width about ·1 mm. at a distance of 14·2 cm. from the grating. The slit width was subsequently reduced to about ·06 mm. It was then noticed that the carbon K_α-line had split into two components, of which that at the longer wave-length was considerably the stronger. Fig. 4 (Pl. XX.) shows the duplicity of carbon K_α in successive orders. This structure has been consistently observed

TABLE III.

Plate.	Short-wave component. Order.					Long-wave component. Order.				
	I.	II.	III.	IV.	Mean.	I.	II.	III.	IV.	Mean.
E. 18.	—	43·91	—	—	43·91	—	44·71	—	—	44·71
E. 23.	—	43·89	—	43·99	43·94	—	44·71	—	44·70	44·71
E. 31.	—	43·85	43·86	—	43·86	—	44·73	44·68	—	44·71
U. 29.	43·79	43·82	43·83	—	43·81	44·93	44·57	44·52	—	44·67
				Final Mean...	43·88				Final Mean...	44·70

in successive orders on our plates during our experiments of the past eighteen months. During these experiments we have used two different gratings, one having 300 lines per mm. and the other 600. We have had occasion to rotate the grating through 180°. The angle of incidence of the X-rays has been varied from a little over 1° to a little over 2°. Different materials have been used as anti-cathode : some have been used cold and some moderately hot. The exciting voltage has been sometimes 4000 and sometimes 2000. Finally, we have observed the duplicity of the line with a solid carbon block allowed to run hot. The fine structure is on some plates clearer than on others, but, if one allows for this, the satisfactory result is obtained that the separation of the components remains constant. Table III. gives the measurements of the components. Each of the four plates given was chosen for its clearness, but each

was taken in different circumstances from the others in the table.

The wave-length 43·88 Å. is equivalent to 281·3 volts, and 44·7 Å. corresponds to 276·2 volts. The separation of the two lines is seen to be ·82 Å. or 5·1 volts. Since the separation of the components in these experiments is in reasonable agreement with that given by Morand and Hautot and since the relative intensities correspond, we may identify our results with theirs. We have not, however, succeeded in resolving the long-wave line into two components as Hautot has done. Prins * also has recently observed a fine structure for carbon K_χ. He obtains a maximum at 44·6 Å. and subsidiary maxima at 43·8 Å. and 43·3 Å. The first two of these components seem to be identifiable with our lines. He also obtains, however, another type of structure with principal maximum at 44·31 Å. and subsidiaries at 43·67 Å. and 43·28 Å. Although our experimental conditions have, as we have shown, varied widely, we have not observed this second type of structure. Siegbahn †, too, has recently published a photometer record of carbon K_χ which indicates a structure very similar to that found by us.

The conditions of our own experiments make it almost impossible that the short-wave component should be other than a genuine line, and it may be taken as certain that the short-wave component is a genuine soft X-ray line and not a "ghost." Again, the apparent constancy of the relative intensity of the components throughout the extensive series of plates shows that they are both due to the same element. Since, on a plate taken with a hot solid carbon anti-cathode, these two lines are practically the only radiations observable, there can be no doubt that the source of the two lines is carbon.

It is unlikely that the fine structure is the result of a chemical compound of carbon. Such compounds would be hydro-carbons, CO or CO_2. These are hardly likely to exist on the moderately hot anti-cathodes, yet it is for these anti-cathodes that the fine structure is often most clear.

Hautot, taking the values for the K_χ satellites of Si,

* *Zeits. für Phys.* lxxxi. p. 507 (1933).
† Proc. Phys. Soc. xlv. p. 689 (1933).

Al, Mg, and Na obtained by Wetterblad *, and applying Moseley's law, has identified his three components as follows:—Long-wave-component $K_{\alpha_{1,\ 2}}$. Middle component $K_{\alpha'}$ and $K_{\alpha_{3,\ 4}}$. Short-wave component $K_{\alpha_{5,\ 6}}$ †.

There seems no reason to doubt the identification of $K_{\alpha_{1,\ 2}}$, to which we are now able to give the wave-length 44·70 Å. We propose to attempt the calculation of the satellites directly from the Wentzel theory. K_{α_3}, according to Wentzel ‡, is the result of a transition from an L-level to a K-level, one electron being absent from the L-level throughout the process. Thus, initially one K- and one L-electron are missing from the atom, and at the end of the transition two L-electrons are missing.

Thus, $$\alpha_3 = KL - L^2,$$

where L^2 represents two L-electrons missing.

But KL = (work to take one K-electron out of the atom) + (work to take one L-electron out subsequently).

Hence $$\alpha_3 = K + L^+_{z+1} - (L + L^+),$$

where L^+ represents the work done in removing an L-electron from an atom already ionized in the L-shell. L^+_{z+1} represents the same thing for an element of atomic number one higher.

Now $$\alpha_{1,\ 2} = K - L.$$

Therefore $$\alpha_3 - \alpha_{1,\ 2} = L^+_{z+1} - L^+.$$

We propose to make the assumption that the carbon atom in the solid state has levels which do not differ appreciably from those of the free carbon atom. For L^+ we insert the ionization potential of singly ionized carbon taken from the summary given by Joos §. The value is deduced from the optical series. The nitrogen spectra similarly provide L^+_{z+1}.

We have, therefore, $\alpha_3 - \alpha_{1,\ 2} = 29{\cdot}54 - 24{\cdot}28 = 5{\cdot}26$ volts.

The agreement of this with the experimental result 5·1 volts, for the distance of the short-wave line from

* *Zeits. für Phys.* xlii. p. 611 (1927).

† A further discussion by Hautot is given in *Comptes Rendus*, cxcvi. p. 1729 (1933).

‡ See Lindh's "Rontgenspektroskopie," *Handbuch der Experimentalphysik*, xxiv. 2 Teil, p. 236.

§ "Ergebnisse und Anwendungen der Spektroskopie," *Handbuch der Experimentalphysik*, xxii. p. 231.

$K_{\alpha_{1,2}}$ is within the experimental error, and certainly within the error expected for the calculation. We therefore identify the line at 43·88 Å. with carbon K_{α_3}.

A similar calculation for the line K_{α_5} yields for it the value 282·3 volts, or 43·73 Å. Since this differs from our K_{α_3}-line by only ·15 Å., and since it would be probably much weaker than the latter, it is not very surprising that we have not succeeded in resolving it.

Similarly, we have attempted the calculation of K_{α_4} and K_{α_6}. Our calculations make it appear that these lines should be considerably displaced from $K_{\alpha_{1,2}}$. Two very weak unidentified lines agree with the calculated values, but, at the moment, we have not sufficient evidence to allow us to identify them as carbon radiations.

The structure of the unresolved carbon K_α-line is obviously not completely explained by the strong long-wave component and the weaker short-wave line. It is clear that there must be other radiations on the long-wave side of $K_{\alpha_{1,2}}$ to produce the gradual slope of the long-wave side of the composite line. These may be produced by further satellites or possibly by partial absorption of the type suggested by us * in our interpretation of the diffuse line at 51 Å. The latter alternative is rendered likely by the fact that the gradual slope is most noticeable for cold anti-cathodes, for which the absorption will be most pronounced.

The wave-lengths given in this paper are based on the L_α-line of copper (13·306 Å.) derived from crystal determinations. For planning the calibration equations and for supervising their computation, we wish to express our thanks to Dr. L. J. Comrie, Director of H.M. Nautical Almanac Office. We are indebted to Col. F. J. M. Stratton, of Cambridge, and to Prof. F. G. Donnan and Mr. H. Terrey, of this College, for photometer records of our plates, and greatly appreciate their kindness. We also wish to thank the Government Grants Committee of the Royal Society for a grant, with the aid of which much of our apparatus was purchased.

Finally, we have great pleasure in thanking Prof. E. N. da C. Andrade for his kind interest and encouragement during the course of this research.

* *Comptes Rendus*, cxcv. p. 374 (1932).

XLVI. *An Analogy between the Slow Motions of a Viscous Fluid in Two Dimensions, and Systems of Plane Stress.* *By* J. N. Goodier, *M.A., Ph.D., Ontario Research Foundation, Toronto* *.

Introduction.

An analogy between the two-dimensional, slow, steady motion of an incompressible viscous fluid between rigid boundaries and the *transverse* flexure of an elastic plate clamped along the same boundaries was pointed out by Rayleigh[1], and turned to account in the general discussion of a few examples. The stream function for the fluid and the transverse deflexion of the plate are solutions of the same differential equation—the biharmonic equation—and the mathematical analogy is complete when the boundary conditions are made to correspond. Another group of problems which shares the same differential equation is presented by the elastic plate strained by forces in its own plane—that is, in a state of two-dimensional or plane stress; but it seems to have been considered that the boundary conditions, involving the second derivatives of the stress function, are essentially different from the fluid boundary conditions, which of course involve only the first derivatives of the stream function. It is the purpose of this note to show that such is not the case, and that all (two-dimensional, slow, steady) fluid motions within rigid boundaries at rest or in uniform motion have their counterparts in distributions of plane stress in a plate with the same boundaries either free from stress or subjected only to uniform normal stress.

On account of their bearing on the theory of structures the special problems of plane stress (as well as the cognate problems of generalized plane stress and plane strain) have received much attention. The experimental methods of photo-elasticity[2] have been developed for the investigation of cases not readily tractable by calculation; the present analogy renders them available for the study of fluid motions.

A number of the solutions obtained analytically have, in the light of this analogy, an immediate interpretation as types of viscous flow. Thus the plane stress system

* Communicated by the Author.

in a tapered plate stretched by a force at its apex gives the flow between inclined plane boundaries in relative motion, while the bending stresses due to a couple at the apex give the flow under pressure between fixed inclined walls, and, as a special case, flow in a half-plane from a source on the edge. Pure bending of an incomplete circular ring corresponds to flow under pressure round a cylindrical bend. Stokes' well-known problem of a cylinder falling in a viscous fluid, for which there is no solution of the equations of slow motion when a finite limiting velocity is anticipated, has its analogue in a type of strain known as dislocation in an infinite plate with a hole. These cases are dealt with in detail later, as also is the motion due to a rotating elliptical cylinder. The latter affords an example of the analogy established between the motion due to rotation of cylinders in the fluid and the stresses in a plate due to internal pressure in a cylindrical hole. Other instances of related problems are found in disturbances of laminar flow by cylindrical obstacles, analogous to disturbances of simple tension by cylindrical holes, and disturbances of flow under pressure by cylindrical obstacles, analogous to the bending of plates with holes, together with dislocations. Dislocations may also be involved in the two preceding cases when certain types of symmetry are lacking.

Stress Functions: Analogy with Stream Functions.

Two-dimensional distributions of stress or strain in an elastic medium free from body forces can be represented in terms of a stress function χ satisfying the biharmonic equation

$$\nabla^4\chi \equiv \left(\frac{\partial^2}{\partial x^2}+\frac{\partial^2}{\partial y^2}\right)^2\chi = 0 \quad . \quad . \quad . \quad . \quad (1)$$

by means of the stress formulæ

$$\widehat{xx}=-\frac{\partial^2\chi}{\partial y^2}, \quad \widehat{yy}=-\frac{\partial^2\chi}{\partial x^2}, \quad \widehat{xy}=+\frac{\partial^2\chi}{\partial x\,\partial y} \quad . \quad . \quad (2)$$

The notation is evident from fig. 1. At a boundary (s) we have tractions X, Y according to the equations

$$-\mathrm{X}=\widehat{xx}\,.\sin\theta-\widehat{xy}\,.\cos\theta,$$

$$\mathrm{Y}=\widehat{yy}\,\cos\theta-\widehat{xy}\,.\sin\theta\,;$$

whence

$$-\mathrm{X}=\frac{\partial^2\chi}{\partial y^2}\cdot\frac{dy}{ds}+\frac{\partial^2\chi}{\partial x\,\partial y}\cdot\frac{dx}{ds}=\frac{d}{ds}\left(\frac{\partial\chi}{\partial y}\right), \quad . \quad . \quad (3)$$

$$\mathrm{Y}=\frac{\partial^2\chi}{\partial x^2}\cdot\frac{dx}{ds}+\frac{\partial^2\chi}{\partial x\,\partial y}\cdot\frac{dy}{ds}=\frac{d}{ds}\left(\frac{\partial\chi}{\partial x}\right). \quad . \quad . \quad (4)$$

If instead of the components X, Y of the boundary traction we consider the components N and T, normal and tangential to the boundary itself, the former directed outwards and the latter in the direction s-increasing, we have

$$-\mathrm{X}=\mathrm{N}\sin\theta-\mathrm{T}\cos\theta=\mathrm{N}\frac{dy}{ds}-\mathrm{T}\frac{dx}{ds},$$

$$\mathrm{Y}=\mathrm{N}\cos\theta+\mathrm{T}\sin\theta=\mathrm{N}\frac{dx}{ds}+\mathrm{T}\frac{dy}{ds},$$

Fig. 1.

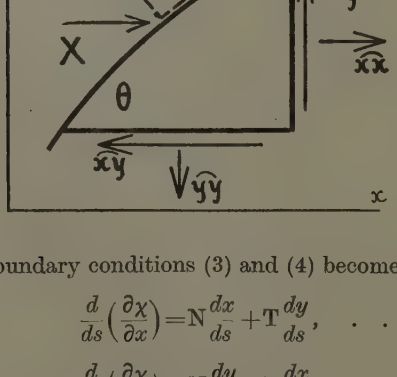

and the boundary conditions (3) and (4) become

$$\frac{d}{ds}\left(\frac{\partial\chi}{\partial x}\right)=\mathrm{N}\frac{dx}{ds}+\mathrm{T}\frac{dy}{ds}, \quad . \quad . \quad . \quad . \quad (5)$$

$$\frac{d}{ds}\left(\frac{\partial\chi}{\partial y}\right)=\mathrm{N}\frac{dy}{ds}-\mathrm{T}\frac{dx}{ds}. \quad . \quad . \quad . \quad . \quad (6)$$

If N and T are constant, these are integrable along the boundary, and if, further T vanishes, they become

$$\frac{\partial\chi}{\partial x}=\mathrm{N}x+\mathrm{A}, \qquad \frac{\partial\chi}{\partial y}=\mathrm{N}y+\mathrm{B}, \quad . \quad . \quad . \quad (7)$$

where A and B are constants for the boundary. We observe that if χ is interpreted as a two-dimensional stream function, N as an angular velocity, and A, B as velocities of translation, the conditions (7) are the kinematical conditions for a fluid at a moving rigid boundary. If the fluid is incompressible, the motion steady, and the effects of inertia negligible, the stream function is, like the stress function, a solution of the biharmonic equation (1). Consequently every problem of such fluid motion within rigid boundaries at rest or in motion with uniform velocities of translation and rotation may be regarded as mathematically identical with a problem of plane stress for the same boundaries free from stress or subjected only to uniform normal stress.

Fig. 2.

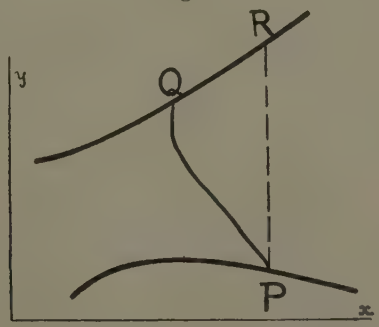

Continuing the discussion of the stress function, we shall have $N=0$ at any stress-free boundary, so that $\partial\chi/\partial x$, $\partial\chi/\partial y$ have constant values A, B along such a boundary. But boundaries between which any resultant force is being transmitted will not have the *same* constant values; for, considering an imaginary section PQ (fig. 2) between two boundaries, we shall have equations such as (3), (4) to give by integration along PQ

$$\int_P^Q X\,ds = \left[\frac{\partial\chi}{\partial y}\right]_P - \left[\frac{\partial\chi}{\partial y}\right]_Q, \quad \ldots \quad (8)$$

$$\int_P^Q Y\,ds = \left[\frac{\partial\chi}{\partial x}\right]_Q - \left[\frac{\partial\chi}{\partial x}\right]_P, \quad \ldots \quad (9)$$

and the left sides are the components of the resultant

force transmitted across PQ. Unit thickness, perpendicular to the representative plane, is understood throughout.

The values of $\partial\chi/\partial x$, $\partial\chi/\partial y$ may always be prescribed as zero on one of the stress-free boundary segments, since the subtraction of $Ax+By$ from χ leaves the stresses unaffected, introducing only rigid-body displacements. Consequently, if we are concerned only with the stresses, and no *resultant* force is transmitted between two boundaries, we may make $\partial\chi/\partial x$, $\partial\chi/\partial y$ vanish on both of them. This being the case, there is a very simple interpretation of the difference of χ for the two boundaries, for it is a measure of the moment of the couple transmitted between them. This moment is the same as that transmitted across a section PR parallel to the y-axis, the segment RQ being free from traction, and is therefore

$$\int_{\mathrm{P}}^{\mathrm{R}} \widehat{xx}\,.y\,.dy - \int_{\mathrm{P}}^{\mathrm{R}} \widehat{xy}\,.x\,.dy = \int_{\mathrm{P}}^{\mathrm{R}} \frac{\partial^2\chi}{\partial y^2}\,.\,y\,.dy + x\int_{\mathrm{P}}^{\mathrm{R}} \frac{\partial^2\chi}{\partial x\,\partial y}\,.\,dy$$
$$= \left[x\frac{\partial\chi}{\partial x} + y\frac{\partial\chi}{\partial y}\right]_{\mathrm{P}}^{\mathrm{R}} - \int_{\mathrm{P}}^{\mathrm{R}} \frac{\partial\chi}{\partial y}\,.dy \quad . \quad . \quad . \quad (10)$$

on integrating by parts. The first term vanishes at both limits under the conditions postulated, and the integral remaining is $\chi_{\mathrm{P}}-\chi_{\mathrm{R}}$ simply. This is the same as $\chi_{\mathrm{P}}-\chi_{\mathrm{Q}}$, since the gradient of χ vanishes at the boundary.

Laminar Motions and Stretched Plates.

In the fluid motion defined by a biharmonic stream function ψ the velocity components parallel to the x- and y-axes are respectively

$$u = -\frac{\partial\psi}{\partial y}, \qquad v = \frac{\partial\psi}{\partial x}.$$

When there are two rigid boundaries in relative motion we regard one as fixed and the other as having velocity components U, V. The boundary conditions are then

$$\frac{\partial\psi}{\partial x} = \frac{\partial\psi}{\partial y} = 0 \qquad \text{on the fixed boundary,} \quad . \quad (11)$$

$$\frac{\partial\psi}{\partial x} = \mathrm{V}, \qquad \frac{\partial\psi}{\partial y} = -\mathrm{U} \qquad \text{on the moving boundary.} \quad (12)$$

From (7) *et seq.* we may write down the conditions for the stress function corresponding to the same boundaries, free from stress, but transmitting between them a force $\bar{X}$, $\bar{Y}$, as

$$\frac{\partial \chi}{\partial x} = \frac{\partial \chi}{\partial y} = 0 \qquad \text{on one boundary,} \quad (13)$$

$$\frac{\partial \chi}{\partial x} = Y, \quad \frac{\partial \chi}{\partial y} = -X \quad \text{on the other.} \quad (14)$$

Since we are considering the equations of steady motion of the fluid the velocities and forms of the boundaries must be such as to permit steady motion. When this is so we conclude, comparing (11) and (12) with (13) and (14), that

(A) *the stream function for flow between two rigid boundaries due to their relative motion is the same as the stress function for a plate having the same boundaries, and transmitting between them a force in the same direction as the relative motion, except that the components of the force in the stress function take the places of the boundary velocity components in the stream function.*

The mode of application of the force to the loaded edges of the plate is related to the manner in which the fluid enters and leaves the region. The relationship is expressed by equations such as (8) and (9), since $\partial\chi/\partial y$, $\partial\chi/\partial x$ will have the same distribution as the velocity components in the fluid. When the fluid boundaries are long in comparison with their distances apart the "elastic analogue" is a long strip with forces applied at its ends. It is then well known, as an instance of Saint-Venant's principle, that the mode of application of the forces is immaterial except in the neighbourhoods of the ends. In the fluid motion therefore the motion in the central part will not depend on the manner in which the fluid enters and leaves the region. Such problems as the disturbance of laminar flow by local irregularities on one of the boundaries afford further examples of the same principle.

When the region is not simply connected there may be tensions transmitted between the boundaries although no external forces are applied to the plate, as, for instance,

if a thin sector is cut out of a ring and the ring closed again by cementing together the faces of the gap. This is an example of the type of internal strain known as dislocation. Three distinct types are possible in a plate, two in which the faces are given relative translations before joining, and a third in which the relative displacement is a rotation. In all three the values of $\partial\chi/\partial x$, $\partial\chi/\partial y$ are constant on the boundaries, because there are no applied forces, and the changes in their values on moving from one boundary to another still measure the resultant tensions transmitted.

It is shown below that the rotational type of dislocation corresponds to a fluid motion in which there is a pressure discontinuity, inducing a circulation round the inner boundary; consequently if the pressure is to be continuous in the region rotational dislocations are excluded from the elastic analogue. If we attempt to interpret a stress function for arbitrary translational dislocations as a stream function it will clearly lead to arbitrary translational velocities of the boundaries; but these will not in general be consistent with steady motion. Nevertheless they can sometimes be combined with others derived from another stress function in such a way as to give allowable motions.

Streaming Motion and Flexure.

When the fluid streams under pressure between two fixed boundaries, $\partial\psi/\partial x$ and $\partial\psi/\partial y$ vanish at both boundaries. In the elastic analogue therefore $\partial\chi/\partial x$, $\partial\chi/\partial y$ vanish at both boundaries, and it follows that no resultant force is transmitted between them. In the fluid motion there is a flow $\psi_1 - \psi_2$ between any two points 1, 2, and thus, according to (10), a couple $\chi_1 - \chi_2$ in the elastic analogue. Thus

(B) *the stream function for flow under pressure between two fixed boundaries is the same as the stress function for a plate having the same boundaries, and transmitting between them a pure couple, except that the couple (or bending moment) in the stress function takes the place of the total flow in the stream function.*

There is here clearly no restriction on the shape of the boundaries. The remarks made above on the application

of forces and the entrance and exit of the fluid apply again. The latter may now be regarded as governed by the terminal pressure conditions.

Rotational Motion and Pressure on a Boundary.

Consider now a region with closed boundaries, all but one of arbitrary shape and stationary, the other circular and rotating steadily about its centre. The motion of the fluid will then be steady. The conditions at the fixed boundaries are

$$\frac{\partial \psi}{\partial x} = \frac{\partial \psi}{\partial y} = 0,$$

and at the rotating boundary

$$\frac{\partial \psi}{\partial x} = \omega x, \quad \frac{\partial \psi}{\partial y} = \omega y,$$

the origin of the conventional x-y-axes being at the centre and ω being the counter-clockwise angular velocity. In an elastic plate having the same boundaries, if the circular one is loaded with uniform normal stress N and the others are free from stress, the boundary conditions are given by (7) for the loaded boundary whilst $\partial\chi/\partial x$, $\partial\chi/\partial y$ have (different) constant values on the others. By adding a linear function to χ we can make it satisfy the modified conditions

$$\begin{aligned}
&\frac{\partial \chi}{\partial x} = \mathrm{N}x, \quad \frac{\partial \chi}{\partial y} = \mathrm{N}y \quad \text{at the loaded boundary,} \\
&\frac{\partial \chi}{\partial x} = \mathrm{A}_1, \quad \frac{\partial \chi}{\partial y} = \mathrm{B}_1, \quad \text{on one free boundary,} \\
&\frac{\partial \chi}{\partial x} = \mathrm{A}_2, \quad \frac{\partial \chi}{\partial y} = \mathrm{B}_2 \quad \text{on another free boundary,}
\end{aligned} \tag{15}$$

and so on, according to the number of free boundaries. These differ essentially from the conditions for the stream function in that A_1, A_2, B_1, B_2 etc. appear in place of zero. The values of these constants depend, from (8) and (9), on the resultant forces transmitted between the respective boundaries. If the plate is free from dislocations it is clear that these forces depend on the applied forces, and they will be determinate when these are given. Analytically they will be determined by the condition that the

elastic displacements must be single-valued. It may not be assumed that in general they vanish when the plate is free from dislocation, but it is easily shown that they must for a doubly-connected region symmetrical about both coordinate axes; for then the shear stress $-\partial^2\chi/\partial x\,\partial y$ must vanish on the axes, and by integration it appears that $\partial\chi/\partial x$ is constant on the y-axis and $\partial\chi/\partial y$ is constant on the x-axis. On the circular boundary $\partial\chi/\partial x$ vanishes at the intersections with the y-axis and $\partial\chi/\partial y$ at the intersections with the x-axis by (15). It follows, also from (15), that $\partial\chi/\partial x$, $\partial\chi/\partial y$ vanish on the free boundary.

When the symmetry is lacking it is not to be expected that the shear stress will vanish or give zero resultant on any two axes between the boundaries, and A_1, B_1, etc. will not then vanish. But they will do so if the appropriate dislocation is superposed. We have then that

(C) *if a doubly-connected region has two-fold symmetry the stream function for the fluid motion due to rotation of a rigid circular boundary about its centre is the same as the stress function for a plate having the same boundaries, the circular boundary being subject to uniform normal stress, except that the applied stress in the stress function takes the place of the angular velocity in the stream function.*

The theorems (A), (B), and (C) cover most problems of interest, especially when extended to unsymmetrical cases by the introduction of dislocations.

General Correspondences

There are certain general correspondences between the fluid motions and their elastic analogues, valuable in the interpretation of photo-elastic observations.

Although a stress function is necessarily dimensionally different from a stream function, the numbers representing fluid velocities represent also force resultants to some scale in the elastic analogue; velocity gradient numbers represent stresses on the corresponding scale, and so on. In this sense we may speak of the stream function and the stress function as being the same function, and denote it by ϕ, imagining it as containing parameters which, when given the significance of boundary velocities, make

it a stream function, and when given the significance of forces make it a stress function.

In the fluid motion the mean pressure p is given by

$$\frac{\partial p}{\partial x} = -\mu \frac{\partial}{\partial y} \nabla^2\phi, \quad \frac{\partial p}{\partial y} = \mu \frac{\partial}{\partial x} \nabla^2\phi,$$

where μ is the coefficient of viscosity.

These define p as the function conjugate to the harmonic function $\mu\nabla^2\phi$. The Laplacian $\nabla^2\phi$ is the same as $\frac{\partial v}{\partial x} - \frac{\partial u}{\partial y}$, the vorticity in the fluid. In the elastic analogue the sum of the two normal stresses for any pair of perpendicular directions at a point is $\nabla^2\phi$, and the change of thickness of the plate (initially of unit thickness) at the point is proportional to this, being $-\frac{\sigma}{E}\nabla^2\phi$, where σ and E are Poisson's ratio and Young's modulus. Also the dilatation (for plane stress) is $\frac{1-2\sigma}{E} \cdot \nabla^2\phi$ and the (elastic) rotation is proportional to the conjugate function.

Thus, apart from factors, the change of thickness in the elastic analogue, which can be obtained from extensometer measurements, gives the vorticity in the fluid, and by construction of the conjugate function the rotation in the elastic analogue and the pressure in the fluid. The fact that the latter two are represented by the same function, conjugate to $\nabla^2\phi$, leads to the result, already quoted, that discontinuity in the one implies discontinuity in the other. We notice also that lines of constant thickness in the elastic analogue, of constant vorticity in the fluid, are the orthogonal trajectories of lines of constant elastic rotation and of constant fluid (mean) pressure.

In general of course the mean pressure p is not the actual normal stress on an element of surface within the fluid. If $\widehat{nn}$ is the normal stress on an element of area normal to a line element n, along which the extensional strain is e_{nn}, the general equations (Lamb, 'Hydrodynamics,' 5th ed. p. 544) give

$$\widehat{nn} = -p + 2\mu e_{nn},$$

the fluid being incompressible. However, the strain

along a rigid boundary vanishes because the fluid does not slip, so that the actual normal stress there is merely the mean pressure. The normal forces on the boundary are thus obtainable from thickness measurements on the elastic model. The effects of any statical pressure are, of course, ignored, being independent of the motion.

Correspondences between the rates of strain in the fluid and the stresses in the elastic analogue are easily perceived by writing the former in terms of the stream function and the latter in terms of the stress function. One of them is of particular interest. The rate of shearing strain in the fluid, the distortion for short, is expressed by

$$q(\theta)=2\,\frac{\partial^2\psi}{\partial x\,\partial y}\,.\sin 2\theta+\left(\frac{\partial^2\psi}{\partial x^2}-\frac{\partial^2\psi}{\partial y^2}\right).\cos 2\theta,$$

where θ is the angle between the x-axis and a side of the element considered. The shearing stress for the corresponding element in the elastic analogue is

$$s(\theta)=\frac{1}{2}\left(\frac{\partial^2\chi}{\partial x^2}-\frac{\partial^2\chi}{\partial y^2}\right).\sin 2\theta-\frac{\partial^2\chi}{\partial x\,\partial y}\,.\cos 2\theta,$$

so that

$$q(\theta)=2s\left(\theta+\frac{\pi}{4}\right)$$

numerically—that is, the distortion in the fluid for a given direction at a point is numerically equal (to some scale) to twice the shear stress at the corresponding point, for a direction inclined at 45°, in the elastic analogue. The directions for *maximum* shear stress in the latter are inclined at 45° to the principal stresses, which therefore indicate the directions of maximum distortion in the fluid. Thus lines of principal stress in the elastic analogue (which show the *directions* of the principal stresses at points on them) show the orientation of the elements having maximum distortion at points in the fluid.

The isochromatic lines of photo-elasticity are lines of constant principal stress difference or maximum shear stress, and therefore lines of constant maximum distortion in the fluid. For fluid boundaries in uniform motion the elastic analogue has boundaries either free from stress or loaded with uniform normal traction or pressure. In either case the tangent and normal at a boundary point are in the directions of principal stress, and thus for the

fluid, the directions of maximum distortion. It follows that the tangential drag on a fluid boundary is measured by the principal stress difference in the elastic analogue, and this is obtained immediately from photo-elastic observation. From this and the thickness measurements the reactions on a boundary are completely determined.

Applications.

As problems of plane stress and problems of fluid motion have hitherto been treated as though their respective boundary conditions were unconnected, it is to be expected that many solutions of the common problem have been duplicated, and that some of the more elaborate have been found for one subject and not for the other. It is interesting now, therefore, to review existing solutions in the light of the present analogy. As simple instances of pairs of problems for which the stream function is essentially the same as the stress function there are: laminar motion and simple tension in a strip; streaming between parallel planes and pure bending of a strip; rotation of a circular cylinder in the fluid and uniform pressure within a circular hole.

A type of problem which has some physical importance but is analytically very intractable is to find the disturbance of laminar flow by an irregularity in one of the bounding planes. The elastic analogue is by theorem (A) a stretched strip with a corresponding irregularity in one edge. There appears to be no accurate solution published of any such elastic problem, although it would be of practical significance in indicating the effects of notches etc. in a tension member, of course within the elastic limit. However, the fluid problem for a small plane projection at right angles to the boundary plane and also, of course, to the undisturbed flow has recently been investigated theoretically by Dean[3], and his results consequently provide (approximate) stress formulæ for a stretched strip with a small lateral cut extending normally inwards from one side.

The tension analogy can be extended to regions not simply connected, but, as in the case of theorem (C), complications arise unless there is two-fold symmetry. Consider, for instance, the disturbance of laminar flow by a fixed cylindrical obstacle. On the cylinder $\partial\psi/\partial x$

and $\partial\psi/\partial y$ vanish. At a distance, $\partial\psi/\partial y$ tends to the value αy and $\partial\psi/\partial x$ to zero. These conditions will define ψ, except for a constant, when the pressure is single-valued. In the corresponding plate with a hole, subjected at a distance to pure tension T parallel to the undisturbed laminar flow, the conditions are that $\partial\chi/\partial x$, $\partial\chi/\partial y$ vanish at the hole, and at a distance χ tends to the value $\frac{1}{2}\mathrm{T}y^2+\mathrm{A}x+\mathrm{B}y$ except for a constant—that is, $\partial\chi/\partial x$ at a distance is A, and $\partial\chi/\partial y$ is $\mathrm{T}y+\mathrm{B}$. However, if there is symmetry about both coordinate axes $\partial^2\chi/\partial x\partial y$ vanishes at the axes, and integration along the intercepts between the boundaries shows that A and B must be zero. There is then exact correspondence between stream function and stress function. When the symmetry is lacking the attempt to interpret the stream function as a stress function may be expected to show that the elastic analogue involves a dislocation as well as pure tension.

The stress problem has been solved for circular and elliptical holes [4] in infinite plates, and also for a circular hole in a strip of finite width[5]. The latter solution corresponds therefore to laminar flow between two planes a finite distance apart disturbed by a circular cylinder fixed between them, the planes having equal and opposite motions. In the two former the planes must be supposed separated by an infinite distance.

Theorem (B) shows that the steady motion in a channel when the (traces of the) walls are any two curves can be found from the stress distribution in a plate of the same form under flexure in its plane. The effects of notches in straight beams have been studied experimentally by Coker[6], and polariscope photographs of a beam with a series of notches have appeared in a paper by Frocht[7]. These photographs illustrate an effect which has also been noticed in fatigue tests of screwed rods. The stress concentrations due to a series of notches are *less* severe than that due to a single notch. The analogous fluid motion is flow between corrugated walls, or, if the corrugations are small, "laminar" motion past a corrugated boundary. This latter case was examined by Rayleigh[1] in connexion with the question of wave formation under the action of wind. As the fluid analogue of the stress effect referred to we may expect that a corrugated boundary disturbs fluid motion less than an isolated

projection of the same shape as the corrugations on an otherwise plane boundary.

Pure bending of a strip with a hole corresponds to translation of a cylinder in a stream. There is a resultant force transmitted in the elastic strip between the hole and either edge.

In order to bring the cylinder to rest, and so arrive at the case of a fixed cylindrical obstacle, it is necessary to superpose in the strip a discloation which will make the resultant stress system such that no resultant forces, but only couples, are transmitted between the hole and each edge. Both couples must be in the same sense, since the flow is in the same sense on each side of the obstacle. If the obstacle section, and therefore also the hole, is long and thin the elastic analogue may be modified by cutting off the part to one side of a section through the

Fig. 3.

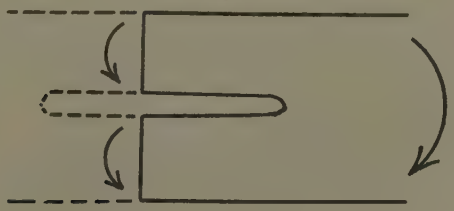

hole and applying couples directly to the two limbs of the remainder (fig. 3). The restriction to a single obstacle is clearly not essential. Bairstow[8] has obtained a solution for a circular cylinder fixed in a stream between parallel plane walls. A general procedure for biharmonic analysis of a perforated strip has recently been extensively developed by Howland, and applied to a group of stress problems including stretching, mentioned above in connexion with disturbed laminar flow, and bending[9]. The interpretation of the latter as a fluid motion has already been referred to. In order to apply similar analysis to the case of a fixed cylinder in a channel disturbing flow under pressure it would be necessary to introduce a dislocation which reduces the actions transmitted in the elastic analogue between the hole and each straight boundary to pure couples. The type of dislocation concerned is the same as that considered

below in the discussion of the falling cylinder. Another stress distribution for which Howland and Stevenson give a solution is that due to a point couple applied on the middle line of a strip[9], balanced by couples at infinity. This will have an interpretation in connexion with flow from a line source within parallel plane boundaries.

In the case of the rotating cylinder and the analogy expressed by theorem (C) the circular boundary may be regarded as stationary and the other as rotating if the coordinate axes are supposed to rotate with it. The elastic analogue has uniform pressure on the circular boundary, and if this is a relatively remote outer boundary the state of stress is uniform throughout ($\widehat{xx}=\widehat{yy}=$ constant, $\widehat{xy}=0$) except for a local disturbance round the inner boundary, in accordance with Saint-Venant's principle. We infer that the fluid motion is a uniform rotation disturbed only in the neighbourhood of the inner boundary, and hence that a rotor does not disturb the fluid remote from it. When the symmetry is lacking the case is different, for the dislocations then required to complete the analogy introduce effects which persist at infinite distances. An example occurs in the rotation of two parallel cylinders in opposite directions, considered by Jeffery[10]. The discussion of the falling cylinder given below throws some light on these difficulties.

The rotation of an isolated elliptical cylinder about its axis is considered in detail later.

Howland and Knight have obtained formulæ for the motion due to a rotating circular cylinder between parallel bounding planes[11]. According to theorem (C) they pertain also to the stress distribution in a slab or a strip, due to pressure in a cylindrical hole bored through it.

Solutions of Special Problems.

1. *Inclined Plane Boundaries with Sliding Motion.*—Let one plane be $y=0$, the other $y=x\tan\alpha$, so that α is the angle between them. The inclined plane may be supposed fixed and the horizontal one moving past it, parallel to itself, with velocity $-U$. The elastic analogue is, by theorem (A), a tapered strip transmitting a tension parallel to the x-axis. The appropriate form for stress function or stream function is [12]

$$By+(Cx+Dy)\tan^{-1}\frac{y}{x}.$$

It satisfies the boundary conditions

$$\frac{\partial\psi}{\partial x}=0, \quad \frac{\partial\psi}{\partial y}=U \quad \text{at} \quad y=0,$$

$$\frac{\partial\psi}{\partial x}=\frac{\partial\psi}{\partial y}=0, \qquad \text{at} \quad y=x\tan\alpha,$$

if

$$B=-\frac{U\alpha^2\operatorname{cosec}^2\alpha}{1-\alpha^2\operatorname{cosec}^2\alpha}, \qquad C=\frac{U}{1-\alpha^2\operatorname{cosec}^2\alpha},$$

$$D=\frac{U(\alpha^2\operatorname{cosec}^2\alpha-\cot\alpha)}{1-\alpha^2\operatorname{cosec}^2\alpha}.$$

The total flow across any section vanishes, for there is no aperture at the apex through which the fluid can escape.

Fig. 4.

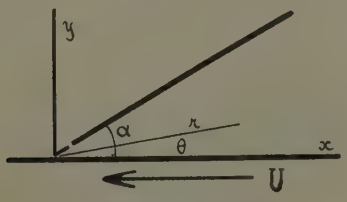

If we suppose the region limited by two sections to the right of the origin the pressure will be higher at the narrow end. The pressure formula is easily found as the function conjugate to $\mu\nabla^2\psi$:

$$p=2\mu(C\cos\theta+D\sin\theta)/r$$

in polar coordinates.

2. *Flow through a Channel with Inclined Walls.*—The elastic analogue is by theorem (B) a tapered strip transmitting a bending moment. There are many variations of this problem according to the manner in which the couples at the ends are applied, each mode corresponding to a mode of entry and exit for the fluid. When the tapering is slight the state of an intermediate region will be the same in all modes.

A simple stress function for a bent tapered strip has been given by Inglis[13], in the form

$$\mathrm{M} \cdot \frac{\sin\theta\cos\theta - \theta\cos\alpha}{\alpha\cos\alpha - \sin\alpha},$$

$\theta=0$ being the middle line and $\theta=\pm\alpha/2$ the boundaries. This, then, will be the stream function for a type of flow between fixed inclined walls, due to a pressure gradient, if M is interpreted as the total flow. The stream-lines are radii from the apex.

The pressure is

$$p=\frac{2\mu\mathrm{M}}{\alpha\cos\alpha-\sin\alpha}\cdot\frac{\cos 2\theta}{r^2}.$$

This motion may be alternatively regarded as due to a line source at the intersection of the bounding planes. It may be combined with the foregoing type to give another motion possible between moving inclined walls. M can be adjusted to make the pressure the same at two points, and if these are on one of the planes, one at each end of the region, the resulting formulæ, when the apical angle is small, become the same as the approximate formulæ applied in the theory of lubrication to the wide bearing block[14]. The condition of uniform pressure over complete cross-sections at each end calls for a more general solution of the differential equation.

3. *Line Source on the Boundary of a Semi-infinite Region.*—This is the special case of the preceding solution, in which $\alpha=\pi$. The elastic analogue is a semi-infinite plate with an isolated point-couple acting at a point on the edge. The stream-lines, radii from the source, have the same configuration as when the fluid is inviscid, but whereas in the latter the flow is uniform in all directions in the representative half-plane, the viscous flow is markedly concentrated about the direction normal to the boundary —that is, $\theta=0$. About half the flow takes place between the radii $\theta=\pm 23°$, as against $\theta=\pm 45°$ in inviscid flow.

4. *Flow round a Cylindrical Bend.*—The bending of an incomplete annulus, which is the elastic analogue of this type of motion, has been investigated by several authors[15]. With polar coordinates, the pole being the centre of the circular boundaries, the simplest stress function, corre-

sponding, of course, to a particular mode of application of the couples, is independent of θ, having the form

$$Br^2+C\log r+Dr^2\log r.$$

The stream-lines are concentric circular arcs, and the fluid is stationary on the two arcs $r=a$, $r=b$, if

$$B=-\left[\frac{1}{2}+\frac{b^2\log b-a^2\log a}{b^2-a^2}\right]D,$$

$$C=\frac{2a^2b^2}{b^2-a^2}\log\frac{b}{a}\cdot D.$$

The total flow Q is given by

$$\frac{2D}{b^2-a^2}\cdot\left[\left(ab\log\frac{b}{a}\right)^2-\left(\frac{b^2-a^2}{2}\right)^2\right].$$

It is easily seen that $\nabla^2\psi=4B+4D\log r$, so that, ignoring a constant, the conjugate function is $4D\theta$, and therefore

$$p=-2\mu Q\cdot\frac{b^2-a^2}{\left(ab\log\frac{b}{a}\right)^2-\left(\frac{b^2-a^2}{2}\right)^2}\cdot\theta$$

except for a constant. This reduces to the usual formula for a straight channel when $b-a$ is small compared with a.

It is interesting to compare the pressure gradient required for a given discharge through the curved channel, terminated by radii, with that required for the same discharge through a straight channel of the same width and length equal to that of the arc midway between the walls of the curved channel. The latter length is $\frac{1}{2}(a+b)\theta$, θ being the angle of the bend, and by a well-known formula

$$p=-\frac{12\mu Q}{(b-a)^3}\cdot\tfrac{1}{2}(a+b)\theta.$$

The ratio of the pressure gradients is consequently

$$R=-\frac{4}{3}\cdot\frac{(\rho-1)^4}{(2\rho\log\rho)^2-(\rho^2-1)^2},$$

where $\rho=b/a$. Values of this ratio are given in the table. It appears that the curvature of the channel introduces

only a very slight increase in resistance unless the inner radius is made extremely small.

ρ	1	2	4	6	8	10	∞
R	1	1·016	1·059	1·092	1·118	1·134	1·333

5. *The Falling Cylinder.*—Bairstow[8] has found a definite resistance to the motion of a cylinder between parallel walls for a finite velocity of translation parallel to them, although it is known that no solution can be found if the walls are removed to infinity. The parallel planes may

Fig. 5.

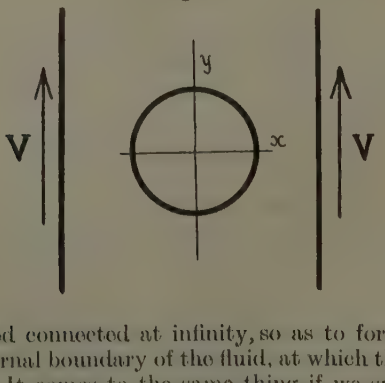

be imagined connected at infinity, so as to form a single closed external boundary of the fluid, at which the velocity vanishes. It comes to the same thing if we suppose the cylinder at rest and this boundary moving past it with velocity V (fig. 5). On the cylinder then $\partial\psi/\partial x$, $\partial\psi/\partial y$ vanish, and on the outer boundary $\frac{\partial\psi}{\partial x}=\mathrm{V}$, $\frac{\partial\psi}{\partial y}=0$. These conditions define a state of stress in the elastic analogue which is not due to boundary tractions, on account of the constancy of the first derivatives of ψ on the boundaries. But there is a y-component of force measured by V, transmitted between the inner and outer boundaries, since the respective values of $\partial\psi/\partial x$ differ by this amount. Such characteristics indicate a dislocation, which might be realized by cutting out a thin parallel slice along the

intercept on the positive x-axis, drawing the faces of the gap together, and rejoining. The stress function will be proportional to the width of the gap. Clearly if the distance between cylinder and walls is infinite the gap cannot be finite unless an infinite tension is used to close it. If the tension (*i.e.*, the velocity of the cylinder) is restricted to be finite, the gap, and with it the stress function, becomes evanescent.

With the outer boundary at infinity it makes no difference what shape we assign to it. Taking it as circular, we can adopt an existing solution for a dislocation in a circular ring[16]. In polar coordinates the stress function is

$$\frac{E\delta}{8\pi}\left\{-\frac{r^3\cos\theta}{a^2+b^2}+\frac{a^2b^2}{a^2+b^2}\cdot\frac{\cos\theta}{r}+2r\log r\cos\theta\right\}$$
$$+Ar\cos\theta+Br\sin\theta,$$

and no difficulties are introduced if b, the outer radius, is supposed infinite in comparison with a, the inner radius, or radius of the cylinder in the fluid problem, provided that δ, the width of the gap, remains small but finite.

If we interpret this function as a stream function it appears that it satisfies the velocity conditions at the boundaries, but requires the relative velocity to be logarithmically infinite (the outer radius being infinite, as it must be to permit steady motion). Otherwise the relative velocities within the fluid at finite distances from the cylinder become evanescent, implying no finite force on the cylinder. A falling cylinder consequently does not, on the basis of the equations of slow motion, attain a limiting velocity as a sphere does, and it does not present a proper problem within the scope of the assumptions involved in the differential equation.

6. *Elliptical Cylinder rotating in Infinite Fluid.*—The motion relative to the cylinder is the same if we suppose it fixed and the fluid at infinity given the opposite angular velocity, ω. The circular boundary of theorem (C) is then at infinity, and the stream function is obtainable from the stress function for an infinite plate with an elliptical hole, the stress at infinity being all-round tension

($\widehat{xx}=\widehat{yy}=\omega$, $\widehat{xy}=0$). This stress function is known to be[17]

$$\tfrac{1}{4}c^2\omega(\sinh 2\xi - 2\xi\cosh 2\alpha)$$

in the elliptic coordinates defined by $x+iy=c\cosh(\xi+i\eta)$. The elliptical hole is bounded by $\xi=\alpha$ and $2c$ is the distance between the foci. When ω is interpreted as the angular velocity at infinity the stream function is given by the same expression. It is independent of the coordinate η, so that the ellipses $\xi=$constant, confocal with the inner boundary, the section of the elliptical cylinder, are the stream-lines. By direct differentiation

$$\nabla^2\psi = 2\omega \cdot \frac{\sinh 2\xi}{\cosh 2\xi - \cos 2\eta},$$

Fig. 6.

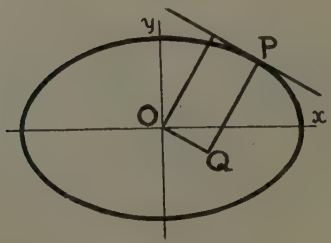

which is the real part of $2\omega\coth(\xi+i\eta)$. The pressure formula, derived from the imaginary part of this function, is

$$p = -2\mu\omega \cdot \frac{\sin 2\eta}{\cosh 2\xi - \cos 2\eta}.$$

The peripheral stress at the hole in the plate and the distortion in the fluid on the cylinder are represented by the same function. The distortion is

$$q = 2\omega \cdot \frac{\sinh 2\alpha}{\cosh 2\alpha - \cos 2\eta}.$$

From these two formulæ we can evaluate the torque on the cylinder. If PQ is the normal, and OQ the perpendicular from the origin (fig. 6), the formulæ of analytical

geometry give, on transformation to the present elliptic coordinates,

$$\mathrm{PQ}=c\sinh 2\xi[2(\cosh 2\xi-\cos 2\eta)]^{-\frac{1}{2}},$$

$$\mathrm{OQ}=c\sin 2\eta[2(\cosh 2\xi-\cos 2\eta)]^{-\frac{1}{2}}.$$

The element of arc ds along one of the ellipses is

$$\frac{c}{\sqrt{2}}\cdot\sqrt{\cosh 2\xi-\cos 2\eta}\cdot d\eta.$$

The pressure contributes to the (counter-clockwise) torque an amount

$$-4\mu\int_{\eta=0}^{\eta=\pi/2}p\cdot\mathrm{OQ}\cdot ds=4\mu\omega c^2\int_0^{\pi/2}\frac{\sin^2 2\eta}{\cosh 2\alpha-\cos 2\eta}\cdot d\eta.$$

The integral reduces to familiar forms, and the result for the pressure torque is

$$2\pi\mu\omega c^2(\cosh 2\alpha-\sinh 2\alpha).$$

Expressing this in terms of the semi-axes of the ellipse, $a=c\cosh\alpha$ $b=c\sinh\alpha$, it becomes

$$2\pi\mu\omega(a-b)^2.$$

The torque contributed by the viscous drag on the cylinder is

$$4\mu\int_{\eta=0}^{\eta=\pi/2}q\cdot\mathrm{PQ}\cdot ds=4\mu\omega c^2\sinh^2 2\alpha\int_0^{\pi/2}\frac{d\eta}{\cosh 2\alpha-\cos 2\eta}$$
$$=2\pi\mu\omega c^2\sinh 2\alpha=4\pi\mu\omega ab.$$

When the axes are equal this reduces to the well-known formula for a circular cylinder, and the pressure contribution vanishes. When they are nearly equal, and $(a-b)/a=\delta$, a small number, the torque is, neglecting δ^2, $4\pi\mu\omega a^2(1-\delta)$, so that δ will be the proportional error made if the cylinder is assumed perfectly circular.

Note added in proof.—An exact solution for the problem 2, of the last section, not neglecting the inertia terms in the equations of motion was given by Jeffery [18]. In the same paper he shows also that the stream function of 4, above, is still appropriate when the motion is not slow, although the pressure formula is then different. The function discussed in (5) was derived otherwise by Berry and Swain [19]. The solution for the rotating elliptical cylinder agrees with two previous solutions by Edwardes [20] and Wilton [21].

References.

(1) Rayleigh, Phil. Mag. (5) xxxvi. p. 354 (1893) [*Papers*, iv. p. 78].
(2) Coker and Filon, "Photo-elasticity," C. U. P. (1931).
(3) W. R. Dean (i.) Phil. Mag. (7) xiii. p. 585 (1932); (ii.) Phil. Mag. (7) xiv. p. 929 (1933).
(4) Ref. (2), chap. vi.
(5) R. C. J. Howland, Phil. Trans. ccxxix. p. 49 (1930).
(6) Ref. (2), art. 5.24.
(7) M. M. Frocht, Trans. Am. Soc. Mech. Eng. liv. p. 87 (1932).
(8) L. Bairstow and others, Proc. Roy. Soc. A, c. p. 394 (1922).
(9) R. C. J. Howland and A. C. Stevenson, Phil. Trans. A, ccxxxii. (1933).
(10) G. B. Jeffery, Proc. Roy. Soc. A, ci. p. 169 (1922).
(11) R. C. J. Howland and R. C. Knight, Camb. Phil. Soc. Proc. xxix. (2) p. 277 (1933).
(12) Ref. (2), art. 4.15.
(13) Ref. (2), art. 4.26.
(14) Lamb, 'Hydrodynamics,' art. 330 *a*.
(15) Ref. (2), art. 4.12.
(16) Ref. (2), art. 4.29.
(17) Ref. 2, art. 6.23. The original source, C. E. Inglis, Trans. Inst. of Naval Arch. 1913, is not correctly quoted by Coker and Filon.
(18) G. B. Jeffery, Phil. Mag. xxix. pp. 445 & 455 (1915).
(19) A. Berry and L. M. Swain, Proc. Roy. Soc. A, cii. p. 766 (1923).
(20) D. Edwardes, Quart. Journ. Math. xxvi. pp. 70 & 157 (1893).
(21) J. B. Wilton, Phil. Mag. ser. vi. vol. xxx. p. 761 (1915).

Ontario Research Foundation,
August 10th, 1933.

XLVII. *On the Radiation from the Inside of a Circular Cylinder.*—Part III. *By* H. Buckley, *M.Sc., F.Inst.P., of the National Physical Laboratory* *.

IN a paper entitled "Recherche d'un Radiateur Integral au moyen d'un Corps Cylindrique" Yamauti † discusses the defect from full radiation of the radiation from the inside of a uniformly heated cylinder closed at one end.

The method he uses is the same as that developed by the author ‡ for open cylinders in 1927, but the approximation to the kernel of the integral equations involved is given by means of a three-exponential-term approximation as compared with the author's single- and two-term exponential approximations.

* Communicated by the Author.

† Yamauti, Com. Int. des Poids et Mes., Proc. Verb., xvi. p. 243 (1933).

‡ Buckley, Phil. Mag. iv. p. 753 (1927); vi. p. 447 (1928); Rec. Trav. Com. Int. d'Eclair, 7e Sess., p. 888 (1928).

It so happens that in 1929 the author also worked out the solution for the uniformly heated cylinder closed at one end which approximates to the type of black body which is used in actual practice in optical pyrometry, and lately as a primary standard of light. The solution was obtained in precisely the same way as Yamauti's, but the results cover a wider range of cylinder lengths and also the case when the walls and closed end of the cylinder have different emissive properties. A single exponential term approximation to the kernel was used.

Consider a cylinder of length l closed at one end by a flat disk, where the distances x and x_1 from the open end and l are expressed in terms of the radius. It is further assumed that the radiation emitted by the end disk after inter-reflexions are taken into account is uniform over its surface. This is approximately correct, but is very closely true for all cylinders which are not very short. Then

$$\Phi(x_1) = \epsilon_1 + (1-\epsilon_1)\int_0^l \Phi(x) - \mathrm{K}(x-x_1)\,dx + (1-\epsilon_1)\Phi_0\mathrm{K}_0(l-x_1), \quad . \quad . \quad (1)$$

$$\Phi_0 = \epsilon_2 + (1-\epsilon_2)\int_0^l \Phi(x)\mathrm{K}_0'(l-x)\,dx. \quad . \quad . \quad . \quad . \quad (2)$$

These are identical with equations 4 *a* and 4 *b* in Yamauti's paper, where

$\Phi(x_1)$ = total radiation per unit area emitted at x_1 on the side of cylinder.

Φ_0 = total radiation per unit area emitted by end disk—assumed constant.

ϵ_1 = emissivity of side of cylinder.

ϵ_2 = emissivity of end disk.

$\mathrm{K}(x-x_1)$ = radiation received per unit area at x_1 from an annulus of the cylinder of unit width at x when the annulus at x is radiating unit radiation per unit area.

$\mathrm{K}_0(l-x_1)$ = radiation received per unit area at x_1 from the end disk at l when the end disk is radiating unit radiation per unit area.

$K_0'(l-x)$ = radiation received per unit area by the end disk at l from an annulus of the cylinder of unit width at x when the annulus at x is radiating unit radiation per unit area.

$$K(x)=\frac{1}{4}\frac{d^2}{dx^2}F(x)\doteq e^{-x}/2\,;$$

$$K_0(x)=-\frac{1}{4}\frac{d}{dx}F(x)\doteq e^{-x}/2\,;$$

$$K_0'(x)=2K_0(x)\,;$$

$$\pi/2.F(x)=\pi\{x^2+2-x\sqrt{x^2+4}\}/2$$

= radiation received by a circular disk of unit radius from an equal coaxial disk at a distance x, radiating unit radiation por unit area.

If equation (2) is substituted in equation (1) an equation for $\Phi(x_1)$ is obtained. For the single-term approximation it can be shown that

$$\Phi(x)=A_0+Ae^{\alpha x}+Be^{\beta(l-x)}.$$

If this value is substituted for $\Phi(x)$, and the equation for $\Phi(x_1)$ integrated, comparison of the various terms gives :

$$A_0=1,$$

$$\alpha=\beta=-\sqrt{\epsilon_1},$$

$$A=\frac{(1-\epsilon_1)\{(1+\sqrt{\epsilon_1})-(1-\epsilon_2)(1-\sqrt{\epsilon_1})\}}{\{(1-\epsilon_1)(1-\epsilon_2)-(1+\sqrt{\epsilon_1})^2\}-\{(1-\epsilon_1)(1-\epsilon_2)-(1-\sqrt{\epsilon_1})^2\}e^{-2\sqrt{\epsilon_1}l}},$$

$$B=\frac{(1-\epsilon_1)\{(1-\epsilon_2)(1+\sqrt{\epsilon_1})-(1-\sqrt{\epsilon_1})\}e^{-\sqrt{\epsilon_1}l}}{\{(1-\epsilon_1)(1-\epsilon_2)-(1+\sqrt{\epsilon_1})^2\}-\{(1-\epsilon_1)(1-\epsilon_2)-(1-\sqrt{\epsilon_1})^2\}e^{-2\sqrt{\epsilon_1}l}};$$

so that

$$\Phi(x)=1+\frac{(1-\epsilon_1)\{(1+\sqrt{\epsilon_1})-(1-\epsilon_2)(1-\sqrt{\epsilon_1})\}e^{-\sqrt{\epsilon_1}x}}{D}$$

$$+\frac{(1-\epsilon_1)\{(1-\epsilon_2)(1+\sqrt{\epsilon_1})-(1-\sqrt{\epsilon_1})\}e^{-\sqrt{\epsilon_1}(2l-x)}}{D},$$

where D is the denominator of the expressions for A and B. If $\epsilon_2=1$ this reduces to

$$\Phi(x)=1-\frac{(1-\epsilon_1)\{(1+\sqrt{\epsilon_1})e^{-\sqrt{\epsilon_1}x}+(1-\sqrt{\epsilon_1})e^{-\sqrt{\epsilon_1}(2l-x)}\}}{(1+\sqrt{\epsilon_1})^2-(1-\sqrt{\epsilon_1})^2e^{-2\sqrt{\epsilon_1}l}}$$

or $\Phi(x)$

$$=1+\frac{(1-\epsilon_1)\{(1-\sqrt{\epsilon_1})e^{-\sqrt{\epsilon_1}(l+x)}-(1+\sqrt{\epsilon_1})e^{-\sqrt{\epsilon_1}(l-x)}\}}{(1+\sqrt{\epsilon_1})^2-(1-\sqrt{\epsilon_1})^2e^{-2\sqrt{\epsilon_1}l}}$$

if x is measured from the end disk where $\epsilon_2=1$, *i. e.*, if $l-x$ is substituted for x. This result is given in a previous paper * for the case of a finite cylinder closed at one end by means of a non-reflecting fully radiating disk for which $\epsilon_2=1$.

If, also, $l\to\infty$,

$$\Phi(x)=1-(1-\sqrt{\epsilon_1})e^{-\sqrt{\epsilon_1}x},$$

a result which has also previously been obtained for the neighbourhood of the end of an open infinite cylinder †. If $\epsilon_1=\epsilon_2=\epsilon$,

$$\mathrm{A}=\frac{(1-\epsilon)\{(1+\sqrt{\epsilon})\quad(1-\epsilon)(1-\sqrt{\epsilon})\}}{\{(1-\epsilon)^2-(1+\sqrt{\epsilon})^2\}-\{(1-\epsilon)^2-(1-\sqrt{\epsilon})^2\}e^{-2\sqrt{\epsilon}l}},$$

$$\mathrm{B}=\frac{(1-\epsilon)\{(1-\epsilon)(1+\sqrt{\epsilon})-(1-\sqrt{\epsilon})\}e^{-\sqrt{\epsilon}l}}{\{(1-\epsilon)^2-(1+\sqrt{\epsilon})^2\}-\{(1-\epsilon)^2-(1-\sqrt{\epsilon})^2\}e^{-2\sqrt{\epsilon}l}}.$$

The following tables give the values of $-\mathrm{A}$ and $-\mathrm{B}$ for various values of ϵ_1, ϵ_2, and l :—

	$\epsilon=\epsilon_1=\epsilon_2$.	$l=0$.	$l=2$.	$l=4$.	$l=6$.	$l=8$.
$-\mathrm{A}$	0·75	0·1320	0·1339	0·1119	0·1339	0·1339
	0·50	0·2759	0·2918	0·2929	0·2929	0·2929
	0·25	0·4219	0·4900	0·4986	0·4986	0·5000
	0·10	0·4986	0·6189	0·6641	0·6781	0·6821
$-\mathrm{B}$	0·75	0·0240	0·0043	0·00076	0·00013	0·00002
	0·50	0·0991	0·0255	0·0062	0·00151	0·00037
	0·25	0·2344	0·1001	0·3747	0·0138	0·0051
	0·10	0·3564	0·2350	0·1349	0·0728	0·0389

* Buckley, Phil. Mag. vi. p. 447 (1928).
† Buckley, Phil. Mag. iv. p. 753 (1927).

$l=6$, $\epsilon_1=0{\cdot}50$.

	$\epsilon_2=1{\cdot}00$.	$\epsilon_2=0{\cdot}75$.	$\epsilon_2=0{\cdot}50$	$\epsilon_2=0{\cdot}25$.	$\epsilon_2=0{\cdot}10$.	$\epsilon_2=0$.
—A..	0·2929	0·2929	0·2929	0·2929	0·2929	0·292
—B..	0·00072	0·00034	0·0015	0·0028	0·0036	0·004

$l=4$, $\epsilon_1=0{\cdot}50$.

	$\epsilon_2=1{\cdot}00$.	$\epsilon_2=0{\cdot}075$.	$\epsilon_2=0{\cdot}50$.	$\epsilon_2=0{\cdot}25$.	$\epsilon_2=0{\cdot}10$.	$\epsilon_2=0$.
—A..	0·2929	0·2929	0·2929	0·2929	0·2928	0·2927
—B..	$0{\cdot}0032_2$	0·00142	0·0062	0·0115	0·0149	0·0173

The value of Φ_0 is obtained by substituting A and B in equation (2) and integrating. From this

$$\Phi_0=1+\frac{4\sqrt{\epsilon}(1-\epsilon)e^{-\sqrt{\epsilon}l}}{\{(1-\epsilon)^2-(1+\sqrt{\epsilon})^2\}-\{(1-\epsilon)^2-(1-\sqrt{\epsilon})^2\}e^{-2\sqrt{\epsilon}l}}.$$

The curves in the figure show the variation of Φ_0 for different values of ϵ and l. From these curves the values of the length required so that the radiation shall be within 1 per cent. of full radiation can be deduced. These are

$$l=3{\cdot}8 \quad \text{for} \quad \epsilon=0{\cdot}75,$$

$$l=5{\cdot}8 \quad \text{for} \quad \epsilon=0{\cdot}50,$$

$$l=9{\cdot}0 \quad \text{for} \quad \epsilon=0{\cdot}25.$$

These values fit on the curve in fig. 4 of Yamauti's paper *, in which he gives the length of cylinder required so that the radiation is within 1 per cent. of full radiation. The agreement, of course, only applies to Yamauti's one-term approximation.

The values obtained from the three-term approximation of Yamauti are 4·8, 7·0, and 10·7 respectively. The radiation is varying so slowly in these regions that any very small difference from the true value due to the

* In Yamauti's fig. 4 the dashed lines refer to the one-term approximation and the full lines to the three-term approximation to the kernel instead of the converse, as is stated on the figure.

necessity of using an approximation to the kernel makes a considerable difference in the length calculated to give within 1 per cent. of full radiation. These results may be compared with those quoted by Dorgelo *, who states that calculation by Zwikker and de Groot show that a cylindrical hole in tungsten with diffusely reflecting walls and bottom gives full radiation to within 1 per cent. when the length is twenty times the radius.

If it be assumed that the emissivity of tungsten is 0·30, the curves show that the length required to give

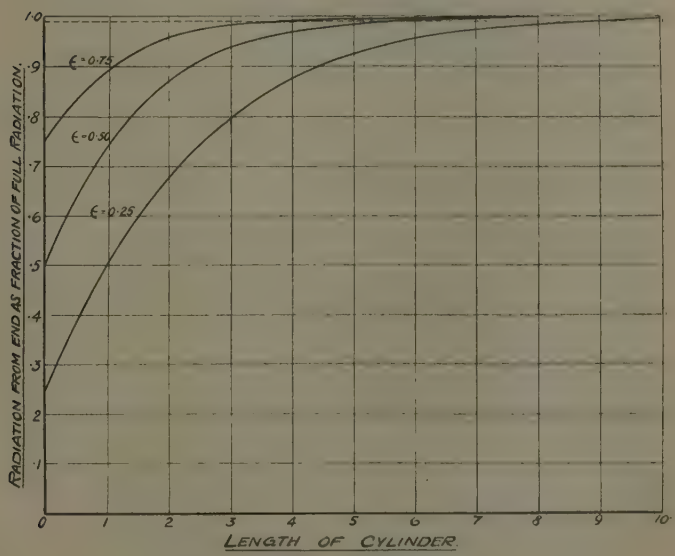

Variation of radiation from end of cylinder as a function of emissivity and length.

within 1 per cent. of full radiation is about eight times the radius. Yamauti's three-term approximation gives about nine and one half times. Both these values are very different from the twenty times given by Zwikker and de Groot. As, however, no details of their method of calculation is given, it is impossible to trace the cause of the discrepancy.

23rd August, 1933.

* Dorgelo, *Phys. Zeit.* xxvi. p. 756 (1923).

XLVIII. *Revised Figures for the Electrical Conductivity of Aqueous Solutions of Sodium and Potassium Hydroxides, and the Limiting Mobility of the Hydroxyl Ion at 25°.* By GEORGE HAROLD JEFFERY, *B.Sc.(Lond.)*, *A.I.C.*, *and* ARTHUR ISRAEL VOGEL, *D.Sc.(Lond.)*, *D.I.C.*, *F.I.C.**

IN a previous communication (Phil. Mag. (7) xv. p. 395 (1933)) we described accurate determinations of the conductivities of aqueous solutions of sodium and potassium hydroxides over the range 0·0001–0·01 N, and the solvent correction was applied on the assumption that carbonic acid was the only impurity in the equilibrium water used. The values for the primary and secondary dissociation constants of carbonic acid employed were $3{\cdot}50\times10^{-7}$ (Kendall, J. Amer. Chem. Soc. xxxviii. p. 1486, (1916)) and $4{\cdot}1\times10^{-11}$ (Seyler and Lloyd, J. Chem. Soc. cxi. p. 138 (1917); Walker, Bray, and Johnston, J. Amer. Chem. Soc. xlix. p. 1246 (1927)) respectively. Recent determinations of MacInnes and Belcher (*ibid.* lv. p. 2630 (1933)), however, give the valuec $4{\cdot}54\times10^{-7}$ and $5\,61\times10^{-11}$ for K_1 and K_2 respectively, and we havc therefore recalculated our results with the aid of the new constants.

The corrected figures are tabulated below, the symbols having the same significance as in our previous paper. The values of "x" calc. and Δ (J. Chem. Soc. p. 1720 (1931)) are for sodium hydroxide 116·6 and +15·2 per cent., and for potassium hydroxide 122·1 and +17·3 per cent. respectively.

Sodium Hydroxide at 25°. (M=40·01.)

$\Lambda_0^n=\Lambda_c+64{\cdot}4\ C^{0{\cdot}204}$. $\Lambda_0^n=260{\cdot}85$.
$\Lambda_0^s=\Lambda_c+132{\cdot}1\ C^{0{\cdot}5}$. $\Lambda_0^s=248{\cdot}60$.

Series.	κ.	$C\times10^4$.	$\Lambda_c$obs.	Λ_c corr.	$\Lambda_c$calc.	Diff.	Λ_0^n.
1 (V)....	0·793	0·945	236·9	247·0		—	—
First		4·462	243·0	247·6		—	—
specimen.		9·668	242·71	244·74	244·64	+0·10	260·92
		19·65	241·40	242·43	242·50	−0·07	260·82
		34·24	239·91	240·53	240·50	+0·03	260·82
		50·06	238·41	238·80	238·75	+0·05	260·74
		65·31	236·98	237·46	237·36	+0·10	(260·22)

* Communicated by the Authors.

Sodium Hydroxide at 25°. (M=40·01.) (*Cont.*)

$\Lambda_0^n = \Lambda_c + 64{\cdot}4\,C^{0{\cdot}204}$. $\Lambda_0^n = 260{\cdot}85$.

$\Lambda_0^s = \Lambda_\epsilon + 132{\cdot}1\,C^{0{\cdot}5}$. $\Lambda_0^s = 248{\cdot}60$.

Series.	κ.	$C\times10^4$.	$\Lambda_c$obs.	$\Lambda_c$corr.	$\Lambda_c$calc.	Diff.	Λ_0^n.
2 (S)....	0·715	2·756	241·0	247·25	—		—
Second		5·295	243·20	246·51	(245·56)	(+0·95)	261·04
specimen.		9·901	242·62	244·62	244·44	+0·18	260·94
		19·66	241·52	242·42	242·44	−0·02	260·78
		28·68	240·61	241·24	241·16	+0·08	260·79
		37·52	239·65	240·13	240·10	+0·03	260·65
		80·11	235·70	235·93	(235·24)	(+0·69)	(260·14)
		95·12	234·65	234·84	—		(259·42)
3 (V)....	1·13	1·462	216·1	244·2	—		—
Specimen		4·624	237·2	245·0	—		—
prepared as (2).		8·606	239·92	244·83	245·09	−0·26	260·92
		12·56	240·34	243·81	243·69	+0·12	260·82
		24·27	239·92	241·63	241·68	−0·05	260·82
		45·70	238·16	239·05	239·19	−0·14	260·74
		71·06	236·08	236·72	237·86	−0·14	(260·22)
4 (S)....	0·465	3·306	246·9	248·4	—		—
Specimen		5·462	245·7	246·3	246·42	−0·12	(261·45)
prepared as (2).		8·686	244·52	245·41	245·48	−0·07	260·99
		13·00	243·24	243·85	243·31	+0·54	260·75
		50·80	238·70	238·80	239·91	−0·11	260·73
		79·66	235·86	235·96	(236·34)	(+0·54)	(260·19)

Potassium Hydroxide at 25°. (M=56·11.)

$\Lambda_0^n = \Lambda_c + 59{\cdot}9^{\,0{\cdot}199}$. $\Lambda_0^n = 283{\cdot}92$.

$\Lambda_0^s = \Lambda_\epsilon + 151{\cdot}2\,C^{0{\cdot}5}$. $\Lambda_0^s = 273{\cdot}10$.

Series.	κ.	$C\times10^4$.	$\Lambda_c$obs.	$\Lambda_c$corr.	$\Lambda_c$calc.	Diff.	Λ_0^n.
1 (S)....	0·638	1·524	261·4	271·0	—		—
First		3·536	266·8	272·2	—		—
specimen.		7·297	266·80	269·16	269·26	−0·10	284·02
		10·06	266·42	268·31	268·23	+0·08	284·04
		21·15	265·10	265·96	266·04	−0·08	283·84
		48·47	262·51	262·81	262·40	+0·41	283·77
		63·44	261·30	261·53	(262·05)	(+0·52)	283·90
		99·95	258·60	258·76	—		(282·10)

Potassium Hydroxide at 25°. (M=56·11.) (*Cont.*)

$\Lambda_0^n = \Lambda_c + 59{\cdot}9^{0{\cdot}199}$. $\Lambda_0^n = 283{\cdot}92$.

$\Lambda_0^g = \Lambda_c + 151{\cdot}2\,C^{0{\cdot}5}$. $\Lambda_0^g = 273{\cdot}10$.

Series.	κ.	$C\times10^4$.	$\Lambda_c$obs.	$\Lambda_c$corr	$\Lambda_c$calc.	Diff.	Λ_0^n.
2 (V)....	0·717	1·816	263·9	271·5	—		—
Second		3·513	266·50	271·3	—		—
specimen.		8·648	266·61	268·69	269·85	−0·16	283·99
		16·10	265·90	267·00	266·94	+0·06	283·95
		27·52	264·51	265·14	265·02	+0·12	283·94
		65·59	261·02	261·29	(261·85)	(−0·56)	283·82
		87·95	259·42	259·62	—		(283·12)

Λ_c at Round Concentrations.

$C\times10^4$.	NaOH.	KOH.
5·0	246·51	270·05
10·0	244·68	268·22
20·0	242·52	266·23
30·0	241·12	264·85
40·0	239·81	263·69
50·0	238·75	262·05
60·0	237·78	261·75
70·0	236·85	260·93
80·0	236·02	260·18
90·0	235·23	259·30
100·0	234·49	258·88

The most probable values of Λ_0 for sodium and potassium hydroxides are 260·85 and 283·92, which lead to 211·05 and 210·52, or a mean value of 210·78 for the limiting mobility of the hydroxl ion at 25°.

The revised values of the conductivities are in good agreement with the determinations of Goworecka and Hlasko (*Rocz. Chem.* xii. p. 403 (1932)) and over the more dilute range ($5–20\times10^{-4}$ N) the agreement is better than that previously noted (Phil. Mag. (7) xvi. p. 64 (1933)).

University College, Southampton.
Woolwich Polytechnic, London, S.E. 18.

XLIX. *Studies in Paramagnetism.—*I. *On the Mechanism of Quenching of Orbital Magnetic Moment in Paramagnetic Ions of the Iron Group. By* S. Datta, *Ghosh Research Scholar in Physics, Calcutta University* *.

IN this paper the magnetic behaviour of ions belonging to the first transition group with special reference to the influence of interaction with neighbouring ions, atoms, or molecules will be discussed. It is well known that, assuming the carriers of magnetic moment to be "free ions" in the spectroscopic sense, (i.) the temperature-susceptibility relation is given by the Curie law, viz., χT=constant, and (ii.) the magnetic moment can be calculated from the formula $\mu=4{,}97\ g\sqrt{J(J+1)}$ according to Hund's[1] method. Some of the assumptions on which Hund's formula is derived are not valid in the case of the ions of the Iron group, where the magnetic electrons occupy the outermost shells and are exposed to the perturbing force of their immediate neighbours. This interaction limits the applicability of Hund's method to the case of these ions; but the difficulty is greatly removed if, following Bose[2], we suppose that in the case of these ions only the spin-vectors can orient in the magnetic field and contribute to the ionic magnetic moment. According to the latter view the magnetic moment is given by the formula

$$\mu=4{\cdot}97\sqrt{4s(s+1)}, \quad . \quad . \quad . \quad . \quad . \quad (1)$$

where μ is expressed in Weiss-units. Though there is substantial agreement with experimental values for the first half of this group, for some ions in the second half the agreement is less satisfactory.

Van Vleck[3], on the other hand, has developed a theory of paramagnetic susceptibility based on quantum mechanics and has shown that where the multiplet intervals are very small compared to kT, which is precisely the case for the Iron group of ions, the magnetic moment will be given by the formula

$$\mu=4{\cdot}97\sqrt{4s(s+1)+l(l+1)}. \quad . \quad . \quad . \quad . \quad (2)$$

* Communicated by Prof. D. M. Bose.

Stoner[4] first pointed out that since the magnetic electrons in this group of ions are in the outermost "$3d$" shell and exposed to the perturbing force of their neighbours, the interatomic forces would quench the magnetic effect of the orbital angular momentum but leave the spin free, so that the actual magnetic moments of these ions would agree best with formula (1), and in case of any deviations the values would lie between the limits given by (1) and (2). Also de Haas and Gorter[5], as well as Pauling[6], have pointed out that for the l-vectors to be immobile the decomposition of the energy-levels caused by the perturbing force would have to be large compared to the multiplet separation of the free ions. Since in the second half of the Iron group, the multiplet separations are larger than in the first half, they can be of the same order of magnitude as the Stark effect splitting of the ionic terms in the electric field due to the distribution of atoms and molecules round them, so that for these ions deviations from the "spin only" value are to be expected.

In the present investigation the magnetic moment of the Co^{++} and Ni^{++} ions have been experimentally studied by subjecting them to different types of interaction with a view to find out how the orbital magnetic moments are quenched and how for the results agree with formula (1). In the first part of the paper has been described the measurement of magnetic moment, over a considerable range of temperature, of some coordination compounds in the state of powdered crystals and the results have been given in Table I. In Table II. are compared the magnetic moments and Δ-values for different types of compounds of Co^{++} and Ni^{++}, viz., the anhydrous, the hydrated, and the complex salts all in the state of powders. The second part of the paper relates to the magnetic measurement of different solutions of $CoCl_2$ and $NiCl_2$ over as large a range of temperature as is possible, and the results have been given in Table III. An attempt has been made to interpret the experimental results in terms of the theories which have recently been put forward to account for the quenching of orbital moments, viz., the one proposed by Bose and the writer, and the other by Van Vleck and his collaborators.

A second effect of this interaction with neighbouring ions, atoms, or molecules is to cause a deviation from the relation given by Curie for the variation of the suscepti-

bility with temperature, viz., $\chi T = C$; the experimental results are much better represented by a modified relation first proposed by Weiss, viz., $\chi(T - \Delta) = C$.

In a subsequent paper, the origin of the term "Δ" will be discussed in the light of experimental evidence gathered here and with particular reference to some recent theories.

I. *Magnetic Moment of* Co^{++} *and* Ni^{++} *Ions in some Coordination Compounds.*

Ray and Bhar[7] measured the magnetic susceptibility of a large number of complex compounds of the Iron group of elements; but as their intention was only to determine the nearest Bohr magneton values, the measurements were made only at room-temperature with a simple Curie balance. On the basis of these results Bose[8] showed that for ions whose simple salts gave values of magnetic moment higher than that given by formula (1), the values obtained for the corresponding four-fold coordination compounds were in better agreement with the latter. To test if the approach towards this calculated value is real, it was considered worth while to carry on measurements with this class of compounds with a more sensitive arrangement and over a large range of temperature, so that a determination of the correct magnetic moment might be possible.

The compounds were all prepared from Merck's extra-pure nickel-free cobalt and cobalt-free nickel salts in the Inorganic Chemistry Laboratory of this College under the direction of Prof. P. Ray, to whom the author's best thanks are due. The magnetic measurements were carried out with a Weiss-Foëx magnetic balance, a description of which will be found in a paper by Foëx and Forrer[9]. With this arrangement the susceptibility of the substances used in these experiments could be measured within an accuracy of ·1 to ·2 per cent. As the complex compounds under investigation slightly decompose at high temperature, all measurements were made between $+80°$ C. and $-80°$ C., the latter being the temperature of solid CO_2. At all temperatures other than the room-temperature there was a certain lag between the constant temperature of the high or low temperature both surrounding the substance in the ampule and that actually

acquired by the substance. The lag at different temperatures was actually determined by measuring the constant temperature of the surrounding bath and that of the substance within the ampule, by inserting a fine thermocouple inside the substance. Another method used was that given by Welo[10], and is as follows:—The temperature variation of the susceptibility of Mohr's salt is known accurately from the measurements of Foëx. A known quantity of the salt is put in a glass ampule and the latter placed in different constant temperature baths. From the known value of the susceptibility the temperature

TABLE I.

Ion.	Compound.	Δ.	Observed magnetic moment in Weiss magnetons.	Calculated. Van Vleck.	Bose.
Co^{++}	$[Co(N_2H_4)_2]Cl_2$	+ 9	23·2	25·8	19·3
	$[Co(N_2H_4)_3]SO_4$	−15	23·3	,,	,,
	$[Co(N_2H_4)_2(H_2O)]SO_3$.	− 4	23·1	,,	,,
	$[Co(C_5H_5N)_4](SCN)_2$ ..	+ 7	23·6	,,	,,
	$[Co(N_2H_4)_2](SCN)_2$ ...	+12	23·8	,,	,,
	$[Co(N_2H_4)_2](CH_3COO)_2$	+ 2	23·8	,,	,,
Ni^{++}	$[Ni(N_2H_4)_2]Cl_2$	+21	14·4	22·2	14·1
	$[Ni(N_2H_4)_3]SO_4$	−40	14·0	,,	,,
	$[Ni(N_2H_4)_3(H_2O)]SO_3$.	−24	14·0	,,	,,
	$[Ni(N_2H_4)_2](NO_3)_2$	+12	14·8	,,	,,

of the salt in the ampule is determined, and a calibration curve is drawn between the latter and the temperautre of the bath. The curve was used to determine the temperature-correction in all later experiments.

The results are given in Tables I. and II.

II. *Variation of the Magnetic Moment of Cobalt and Nickel Salts in different Solutions.*

A large amount of experimental work has been done on the magnetic susceptibility of salts in solution belonging to the Iron group of elements. The results of various

workers [11] definitely indicate that the magnetic moment of the same ion in solution varies slightly with the concentration and to a somewhat greater extent on the nature of the solvent. Most of the work was done at a time before any satisfactory theory of paramagnetism of these ions was developed, so that no theoretical interpretation of the results could be attempted nor any systematic investigation could be carried on to test the validity of any theory. Moreover, in the earlier investigations the susceptibility was measured at only one temperature

TABLE II.

Compound.	Δ.	Observed magnetic moment.	Temp. range.	Calculated.	
				Van Vleck.	Bose.
$CoCl_2$	+47*	24·96	273° K.–598° K.	25·8	19·3
$[Co(H_2O)_6]Cl_2$.	+ 8	24·2	91° K.–306° K.	„	„
$[Co(N_2H_4)_2]Cl_2$	+ 9	23·2	193° K.–353° K.	„	„
$CoSO_4$	−45†	25·2	77° K.–289° K.	„	„
$[Co(H_2O_6)]SO_4.H_2O$	−14†	25·04	64° K.–294° K.	„	„
$[Co(N_2H_4)_3]SO_4$	−15	23·3	193° K.–350° K.	„	„
$NiCl_2$	+67‡	15·7	63° K.–292° K.	22·2	14·1
$[Ni(H_2O)_6]Cl_2$	+24	15·7	91° K.–302° K.	„	„
$[Ni(N_2H_4)_2]Cl_2$	+21	14·4	193° K.–350° K.	„	„
$NiSO_4$	−70†	16·9	77° K.–289° K.	„	„
$[Ni(H_2O)_6]SO_4.H_2O$.	−3 §	16·01	14° K.–290° K.	„	„
$[Ni(N_2H_4)_3]SO_4$	−40	14·4	193° K.–350° K.	„	„

* P. Theodorides. † L. C. Jackson. ‡ H. R. Woltjer. § C. J. Gorter.

and the magneton number was calculated on the assumption that the simple Curie law, viz., $\chi T = C$ holds, which is not certainly the case. Even in later investigations the temperature range within which the susceptibility has been measured is too small to justify an extrapolation up to absolute zero for the determination of Δ.

Some very interesting results have been recorded by Chatillon[12], who carried out exhaustive investigations on the magnetic moment of the Co^{++} ion. He observed a definite lowering of magnetic moment in certain cases when $CoCl_2$ was dissolved in an alcohol or water con-

taining excess of HCl. The observed lowering of magnetic moment was interpreted as due to the formation of some complex anions like $[CoCl_4]^{--}$, etc. This complex-forming tendency was supposed to be a characteristic property of cobalt. Recently Fahlenbrach[13] has carried out magnetic measurement of solutions of Co^{++}, Ni^{++} and Cr^{+++} salts etc. of largely varying concentrations, and recorded some anomalous values of the magnetic moment and of Δ at large dilutions which seem difficult of any interpretation. Some criticisms[16] of his work have also appeared.

The present writer has studied the absorption and Raman spectra at different temperatures of solutions in ethyl alcohol and in HCl of different concentrations of salts belonging mainly to the Iron group, and has also carried out magnetic measurements over as large a range of temperature as possible on fairly concentrated solutions of $CoCl_2$ and $NiCl_2$ in the above-mentioned solvents *. From the results of these investigations some interesting conclusions on the influence of temperature and the nature of the solvent on the kind of the valency-binding between the ions in solution have been deduced. The results of the magnetic measurements are discussed in this paper, and the results of spectroscopic measurements will appear elsewhere.

The experimental arrangement and procedure were similar to that described in the earlier part of the paper. In the case of solutions however the temperature-range within which the measurement could be made is bound to be limited, and errors are liable to creep in owing to evaporation taking place at high temperatures. In the present arrangement the measurement is carried out with the solution in sealed ampules; the temperature could therefore be raised even above the boiling-point of the solvents without any evaporation taking place. The lowest temperature at which measurements were made was that of liquid oxygen. In no case, even at the lowest

* With the experimental arrangement used, it was very difficult to carry out precision-measurement with solutions at extreme dilution when any slight error in the correction for diamagnetism of the solvent etc. may seriously affect the result, so that the problem of any small dependence of magnetic moment on concentration has been excluded from the present investigations. To avoid the effect of change of concentration, if any, on the magnetic moment all the solutions used had more or less the same concentration.

temperature, did any salt crystallize out, though in certain cases the whole solidified *en masse* because of the very sudden cooling. The susceptibility at each temperature was determined after making proper correction for the diamagnetism of the glass ampule as well as for the diamagnetic part of the solution. On plotting the $\frac{1}{\chi}$-T graph (see fig. 1) it is found that for most of the solutions

Fig. 1.

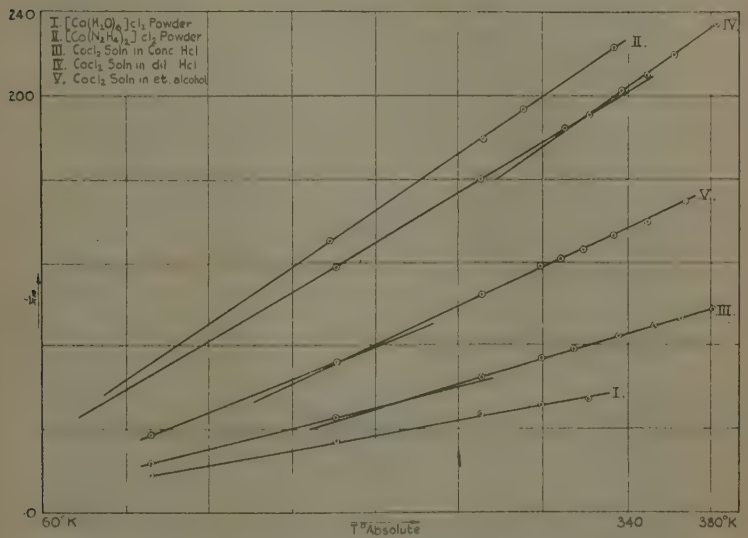

the points do not lie on one straight line, but on two with different slopes indicating a discontinuous change of the magnetic moment and of the Δ-value of the solution. The results are given in Table III.

Discussion of Results.

In Tables I. and II. we have collected together the magnetic moments of several compounds of Co^{++} and Ni^{++} in different states of aggregation, viz., (i.) simple anhydrous salts, (ii.) hydrated salts, (iii.) complex salts,

TABLE III.

Substance.	Condition in which measurement is made.	Temp. range.	Colour.	Observed magnetic moment.	Calculated. Van Vleck.	Calculated. Bose.
$CoCl_2$	Powdered crystals of $[Co(H_2O)_6]Cl_2$.	−182° C.–+ 33° C.*	Red	24·2	25·8	19·3
	17·5 p.c. solution in anhydrous ethyl alcohol.	− 65° C.–+100° C.	Blue	22·4	,,	,,
		−182° C.–− 65° C.	Red	24·2	,,	,,
	18·5 p.c. solution in concentrated HCl (26 p.c.).	− 48° C.–+113° C.	Blue	21·9	,,	,,
		−182° C.–− 48° C.	Red	24·0	,,	,,
	18·3 p.c. solution in dilute HCl (4·5 p.c.)	+ 59° C.–+114° C.	Blue	21·6	,,	,,
		− 80° C.–+ 59° C.	Red	23·5	,,	,,
$NiCl_2$	Powdered crystals of $[Ni(H_2O)_6]Cl_2$.	−182° C.–+ 29° C.*	Green	15·7	22·2	14·1
	22·5 p.c. solution in ethyl alcohol.	−182° C.–+ 95° C.	Green	15·3	,,	,,
	19·4 p.c. solution in concentrated HCl (30 p.c.).	+ 17° C.–+108° C.	Yellowish-green	14·4	,,	,,
		− 80° C.–− 17° C.	Green	15·1	,,	,,
	22·5 p.c. solution in dilute HCl (7 p.c.)	+ 54° C.–+113° C.	Yellowish-green	15·2	,,	,,
		− 80° C.–+ 54° C.	Green	16·2	,,	,,

The concentration in each case was estimated from analysis of the solution.

* At higher temperatures the salts begin to dissolve in their water of crystallization.

all of them being in the form of powders. While the magneton number of the same ion in the states (i.) and (ii.) agree with one another there is a definite lowering in its value in the case of the complex salts, which approach towards the limit given by the "spin only" value. The value of Δ is lower in the case of the hydrated salt in comparison to that in the anhydrous ones.

Again, from Table III. and fig. 1 it will be observed that in each of the solutions (except $NiCl_2$ solution in ethyl alcohol, which will be considered later) there is a break in the $\frac{1}{\chi}$—T line, and a consequent change in the magnetic moment of the ion. For the acid solutions it is found that the transition-temperature is higher the less the concentration of the acid. The magnetic moment at the higher temperature range is appreciably lower than the moment of the hydrated or anhydrous salt, while that at the lower temperature range is nearly equal to the latter.

It is, however, remarkable that even with simple salts the value of the magnetic moment deviates much more in the case of Co^{++} ions than Ni^{++} ions from the value calculated on Bose-Stoner "spin only" hypothesis, though the two ions are adjacent in the periodic table. Moreover, with Ni^{++} the "spin only" value of the magnetic moment is almost perfectly reached in co-ordination compounds and certain solutions, though under similar conditions there is still considerable deviation from the spin-only-value in the case of Co^{++}, showing that the orbital moments are not equally quenched in the two cases. We will now discuss the experimental results in the light of theories which have been recently put forward to account of the behaviour of the paramagnetic ions belonging to the first transition group.

Bose and Datta[15] have recently discussed the nature and behaviour of paramagnetic complexes in hydrated crystals and aqueous solutions, and have pointed out that the moment of the paramagnetic ion in such cases can be represented by the following modification of Van Vleck's formula for "free" ions of this group, viz.,

$$\mu = 4{\cdot}97\sqrt{4s(s+1) + l(l+1)}\, f(\mathrm{A/T}).$$

The additional term in VanVleck's formula is attributed

to the fact that there is a certain energy of coupling * between the central paramagnetic ion and the surrounding dipole molecules of water forming the complex. In this complex group the associated molecules are in a state of thermal oscillation with respect to the central ion. If the energy u of such oscillation is greater than A, the energy of coupling, then the latter breaks down, so that out of a total n_0 ions present only $n = n_0 f(A/T)$ are not subject to such coupling, and thus contribute to the orbital moment, where $f(A/T)$ diminishes from unity to zero as A/T increases from zero to infinity. A consequence of this is that as T is raised n diminishes and as T is lowered n increases †. With the help of these assumptions it has been possible to correlate (i.) the temperature shift in the absorption spectra of $[Ce(H_2O)_6]^{+++}$ with the lowering of its magnetic moment, and (ii.) the relation between the position of the absorption maxima of the different complexes of the same paramagnetic ion and their magnetic moments.

We will now point out certain results contained in the present paper which cannot be interpreted in terms of our theory :–

(i.) If we take as our standards of comparison the position of the absorption maxima and the magnetic moment of the hydrated complex of a given ion then, according to our theory, it is to be expected that if the replacing of the water molecules by other groups in the complex leads to a diminution of the latter's magnetic moment, then the position of the absorption maxima

* Expressed in terms of the theory of the splitting up of the degenerate energy states of the paramagnetic ion in the presence of the electric field due to its neighbours, our assumption implies that the ion can exist in either of two energy-levels, the lower one corresponding to zero orbital moment and the upper one to that of the free ion, the fraction in the upper level being proportional to $e^{-A/T}$, where A is the difference in the potential energy of the ion in the two levels. Intermediate levels which are considered in Van Vleck's theory are not taken into account (see p. 600 for an exposition of Van Vleck's theory).

† Recently the writer has observed some fairly sharp lines (as is characteristic of the rare-earth salts) in addition to the familiar broad bands in the absorption spectra of certain solutions of $CrCl_3$ and $CoCl_2$. These lines are to be attributed to free Cr^{+++} and Co^{++} ions, whereas the broad bands are due to the hydrated complexes $[Cr(H_2O)_6]^{+++}$ and $[CO(H_2O)_6]^{++}$ etc. It was observed that the intensity of these absorption lines depends on the temperature, gradually increasing with the latter. These experiments, the details of which will be published shortly, seem to afford qualitative confirmation of the above view.

should shift towards the violet side. It is found that solution of $CoCl_2$ and $NiCl_2$ is ethyl alcohol and HCl leads to a diminution of the magnetic moments of these ions and also a shift of the absorption maxima to the red side.

(ii.) A further consequence to be expected from our theory is that the magnetic moments of all the ionic complexes should tend to the limiting value of $4{\cdot}97\sqrt{4s(s+1)}$ by taking (A/T) sufficiently large, *i. e.*, by making either A large by a suitable choice of the associated groups or the temperature of observation sufficiently low. From the data given before it will be seen that it is possible to reach this limiting value in the case of the Ni^{++} complexes, but not for the Co^{++} complexes. In the latter case no Co-complex has been found with a magneton number less than 21, while the Bose Stoner limiting value is 19·2.

It will be shown that these deviations from the predictions of our theory can be accounted for by the assumption that in alcoholic and acidic solutions the paramagnetic ions exist in a new form of aggregation, other than as complexes of the type considered above; it is very probable that they exist in the form of homopolar chlorides; further, the difference in the behaviour of the Co^{++} and Ni^{++} ions can be interpreted in terms of the theory of quenching of orbital moments of paramagnetic ions, which has been worked out in quantitative details by Van Vleck, Penney, Schlapp, and others[16].

We will first give an account of the theory of asymmetric crystal field developed by Kramers[17], Bethe[18], Van Vleck and his collaborators. They have shown that exactly the type of quenching of orbital moment leading to Bose Stoner formula takes place if the electrons in each paramagnetic atom or ion are subjected to sufficiently large asymmetrical electrical forces arising from the effect of neighbouring atoms or molecules in a solid crystal or solution. The potential energy of any electron of a given atom in an external field may be developed as a series of powers of the coordinates of the electron, and in a crystal the terms of lowest order which do not vanish are of the form $Ax_i^2 + By_i^2 + Cz_i^2$ when two of the coefficients are equal, *e. g.*,

$$A=B, \quad \text{and} \quad |A-C|\,\Sigma x_i^2 > kT,$$

there will be in general a partial quenching of orbital moment ; full quenching being possible only when the state corresponding to the lowest potential energy corresponds to zero orbital moment. When, however, A, B, and C are sufficiently large and all unequal, the magnetic effect of the orbital angular momentum will be practically fully suppressed, giving very good agreement with Bose-Stoner formula.

In regular crystals, however, it is necessary to retain in the expression for potential energy higher order terms than the second in order to reveal the exact degree of symmetry ; as, for example, Van Vleck[19] has shown that to account for the magnetic behaviour of cobalt and nickel ions it must be assumed that the crystalline field

Fig. 2.

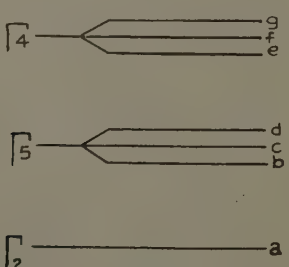

Stark-splitting in Ni^{++} and Co^{++} (inverted).

in the case of hydrated salts of the Iron group generally possesses only rhombic symmetry with relatively small departure from cubic symmetry. Neglecting the departures from cubic symmetry in the fourth-order terms the development of crystalline potential takes the form

$$V=\Sigma[f(r_i)+Ax_i^2+By_i^2-(A+B)z_i^2+D(x_i^4+y_i^4+z_i^4)].$$

If the fourth-order part of the above is the dominant non-central term, from Bethe's group theory of levels in crystalline fields the Stark-splitting for an ion in the F-state (Co^{++} and Ni^{++}) will be as shown in the adjacent figure (see fig. 2). Van Vleck [19] has shown that to obtain agreement with experiment it is necessary to assume that in Ni^{++} the singlet energy level lies lowest, and then the orbital magnetic moment will be largely suppressed and

the residual moment will be nearly isotropic, as is the case with this ion. Now the crystals of Co^{++} and Ni^{++} hydrated salts have so nearly the same structure and ionic arrangement that it is plausible to assume similar fields in both cases, so that A, B, D have the same sign and magnitude. If that be so the magnetic behaviour of Co^{++} can be explained only on the supposition that an inversion of the energy levels takes place (Van Vleck has shown that this is to be expected theoretically) so that the lowest energy level is a triplet and the highest level a singlet. The orbital magnetic moment in such a case will be much less completely quenched and there will be much greater anisotropy. In this way the magnetic anisotropy of crystals of Co^{++} salts and their residual orbital moment can be accounted for. Penney and Schlapp[20] have quantitatively tested Van Vleck's suggestions and found satisfactory agreement with experimental data for Ni^{++}; owing to computational difficulty and insufficiency of experimental data for the Co^{++} ion it has not been possible to test if the agreement is equally satisfactory in this case also.

Van Vleck[19] has also concluded that D must be positive for the hydrated salts of the Iron group, and Gorter [21] has pointed out that this is the case when the metal ion is surrounded by six oxygen ions or water dipoles definitely oriented in an octahedral arrangement. If, on the contrary, the ion is surrounded by 8 or 4 negative charges in a cubic or tetrahedral arrangement D will be negative. The contribution to D again due to different charges in the neighbourhood of the central ion is prop. to R^{-5} so that only the immediate neighbours appreciably contribute to it, and very small charges in interatomic distances affect the constants of the crystalline field.

Unfortunately the X-ray analyses of crystal structure of the above anhydrous, hydrated, and complex salts which have been investigated in the present work, as well as sufficient magnetic data for their single crystals (along different axis and over considerable range of temperature) are wanting, so that the present discussion of the above results is bound to be of a tentative and qualitative nature. An inspection, however, of the results given in Tables I. and II. indicates that the magnetic moments do not change appreciably as we pass from the anhydrous to the hydrated salts. The inference

would be that the nature and constants of the crystal field acting on the central paramagnetic ions are the same in both class of salts, it being likely that the ions and water-dipoles surrounding the paramagnetic ion have the same effect, being in the same relative positions in the two salts. As, however, we pass on to the case of co-ordination compounds, with the change in the coordination number the nature of the crystal field may assume a different type of symmetry or its constants changed owing to different atomic grouping round the paramagnetic ion. As the magnetic moment of the ions in this class of compounds shows a definitely lower value than those of corresponding anhydrous or hydrated simple salts, and is in better agreement with the Bose-Stoner value, it seems that in these cases the crystalline field assumes a still lower type of symmetry (than that of simple salt crystals), and so the magnetic effect of the orbital angular momentum has been suppressed to a greater degree. Also the shift of the absorption maxima towards the violet side observed in some of the aqueous solutions of these complexes[15] indicates that the lowering of the magnetic moment of the ion is due to the increase in the force of binding between the ion and the associated molecules (*i. e.*, increase in the magnitude of the electrical field due to neighbours).

We shall now try to interpret the results of measurements with solutions. Without entering into the details of some later experimental work carried on by the writer, an account of which will be published shortly, it may be mentioned here that when a substance such as $CrCl_3$ is dissolved in a solvent like ethyl alcohol, whose di-electric constant is lower than that of water, or in water containing excess of HCl, the absorption spectrum is shifted towards the longer wave-length side with respect to that due to the hydrated complex and approaches towards that due to the free ion. Also the continuous absorption edge in the ultra-violet region shifts to a much longer wave-length limit and is approximately in the same position as in $CrCl_3$ vapour given by Saha and Deb[25]. But at very low temperatures even in these solutions the absorption spectra again assume the form as due to hydrated complexes. The other paramagnetic ions of this group in solution behave similarly. Thus it seems in the alcohol or acid solutions there is a tendency of the

central paramagnetic ion to break its association with the dipole molecules and to get surrounded by the Cl ions, resulting in the formation of homoplar molecules *. This tendency for molecule formation increases with the lowering of the di-electric constant of the solvent and increasing the concentration of the Cl ions ; the tendency for the formation of hydrated complexes increases with the lowering of the temperature of the solution. From the above considerations it is reasonable to infer that at low temperatures the absorption centres, which are also the paramagnetic carriers are the hydrated complexes, and those at the higher temperatures are the homopolar molecules.

Further evidence of molecule formation in the above cases has been collected from the study of Raman spectra of these type of solutions, the details of which will be published shortly. It is now well known, from the work of Krishnamurti [22] and others, that inorganic halides with electrovalent bonds give no Raman lines, whereas those with homopolar bonds give Raman lines. The paramagnetic salts of this group have strong absorption in the visible region of the spectrum, and it is very difficult, and in some cases impossible, to obtain their Raman spectra. However, Raman lines of very small frequency-shift have been observed with alcoholic or acidic solutions of some of the paramagnetic chlorides (*e. g.*, $CoCl_2$ in ethyl alcohol, $MnCl_2$ in ethyl alcohol or in excess of HCl, etc.) whose aqueous solutions give no such lines, thereby proving definitely the homopolar character of the salts in such solutions.

Admitting, therefore, that in these solutions at higher temperature ranges the paramagnetic ions are associated with the Cl ions resulting in the formation of homopolar molecules we must seek an explanation for the observed lowering of magnetic moment. In his treatment of the quenching of orbital magnetic moment by asymmetric external fields Van Vleck [24] has shown that the interatomic forces within a homopolar molecule may be considered as equivalent to a constant external field

* From a study of the position and intensity of the absorption-maxima in the near ultra-violet region obtained with solutions of certain alkali and alkaline earth-halides, in water and alcohol, Scheibe[23] has come to similar conclusions. His results indicate that in alcoholic solutions there is a much greater tendency for the formation of covalent bonds between the cations and the halogen anions.

on each constituent atom, and though such representation is a poor quantitative approximation, it does not affect the symmetry considerations. In a diatomic molecule there is an axis of symmetry, and the orbital magnetic moment perpendicular to this axis is blotted out, while the parallel component is quenched only when the state corresponding to zero orbital moment falls considerably below the others in energy. In unsymmetrical polyatomic molecules in general the orbital magnetic moment is largely quenched, since all symmetry in the field is lost in such complicated molecules. It is seen from the table that all the values of the magnetic moment lie between the calculated values of Van Vleck and Bose-Stoner, and in those cases where we have reasons to assume the formation of homopolar molecules, the moments diminish considerably and approach the Bose-Stoner value. The lowering of magnetic moment is therefore to be anticipated from Van Vleck's theory, and is a beautiful confirmation of the same.

Again, it is seen from Table III. that in each case at the lower temperatures the colour of the acid and the alcoholic solutions change and approach that of the aqueous solution indicating that the absorbing carriers are now the associated complexes ; hydrated ones in the acid solutions and alcoholated ones in the alcoholic solutions. Simultaneously with the above change there is, as anticipated, a change in the magnetic moment, the latter rising very nearly to the value for hydrated or anhydrous salts. That the alcohol molecules can form complexes similar to hydrated ones must be concluded from the behaviour of the $CoCl_2$ solution in ethyl alcohol. The solution contained no trace of water, as the anhydrous salt was dissolved in perfectly dry ethyl alcohol. At and below the temperature of solid CO_2 the colour was clear red, exactly similar to that of the hydrated complexes, and the magnetic moment also approached the value obtained for the latter.

Anomalous Behaviour of Alcoholic Solution of $NiCl_2$.

It is not possible to dissolve anhydrous $NiCl_2$ to any appreciable extent in dry ethyl alcohol. Alcohol solution of the salt is possible only when the $NiCl_2$ is taken in the hydrated form, so that some water molecules are present

in the solution. Under such condition the Ni^{++} ion has a tendency to retain its hydrated complex character in the alcoholic solution, and therefore did not show similar change of magnetic moment with temperature, as has been found in the case of the alcoholic solution of $CoCl_2$.

Summary.

The paper describes the experimental measurement of the magnetic moments of Co^{++} and Ni^{++} ions in different states of aggregation, viz., as (i.) hydrated salts, (ii.) co-ordination compounds containing different groups like N_2H_4 etc., and (iii.) solutions of $CoCl_2$ and $NiCl_2$ in ethyl alcohol and HCl solutions of different concentration, over wide range of temperature (from 90° K. to 390° K.). It has been observed that while the magnetic moment of the ions remains practically the same in powdered crystals of hydrated and anhydrous salts, there is a definite lowering of magnetic moment in the case of the co-ordination compounds the value in each case approaching that calculated according to the Bose Stoner "spin only" formula. Moreover, in the alcoholic and acid solutions it is observed that there is a break in the $\frac{1}{\chi}$—T diagram indicating a change in the magnetic moment as well as in the value of Δ, with an accompanying change in colour. It has been found that the moment in the higher temperature range is definitely lower than that in the lower temperature range when it is of the same order as in hydrated or anhydrous salts. The spectroscopic behaviour of these solutions (their characteristic absorption spectra, and in certain cases Raman spectra as well) suggests that at the lower temperature ranges the ions exist in the form of hydrated complexes in the acid solutions and alcoholated complexes in alcoholic solutions, whereas at the higher temperature ranges they exist in the form of homopolar chlorides. It has also been observed that for Ni^{++} ion the "Bose Stoner" value is reached in many of the complex compounds as well as in the solutions under certain conditions of temperature and nature of the solvent. But in no state of aggregation for the Co^{++} ion is the Bose-Stoner value reached.

These magnetic behaviours have been interpreted in the light of recent theories proposed by Bose and the writer and Van Vleck and his collaborators to explain the quenching of the orbital magnetic moments for ions of the Iron group.

In conclusion, the writer desires to express his grateful thanks to Prof. D. M. Bose for his kind interest and helpful advice during the progress of the work.

References.

(1) F. Hund, *Zeits. f. Phys.* xxxiii. p. 855 (1925).
(2) D. M. Bose, *Zeits. f. Phys.* xliii. p. 864 (1927).
(3) J. H. Van Vleck, Phys. Rev. xxxi. p. 587 (1928).
(4) E. C. Stoner, Phil. Mag. viii. p. 250 (1929).
(5) W. J. de Haas and C. J. Gorter, Proc. Amst. Acad. xxxiii. p. 1101 (1932).
(6) L. Pauling, Journ. Am. Chem. Soc. liii. p. 1367 (1931).
(7) P. Ray and H. Bhar, Journ. Ind. Chem. Soc. v. p. 497 (1928).
(8) D. M. Bose, *loc. cit.*
(9) G. Foëx and R. Forrer, *Journ. de Phys.* vii. p. 180 (1926).
(10) L. A. Welo, Phil. Mag. vi. p. 481 (1928).
(11) E. C. Stoner, 'Magnetism and Atomic Structure' (1926).
J. H. Van Vleck, 'Theory of Electric and Magnetic Susceptibilities' (1932).
(12) A. Chatillon, *Ann. de Phys.* ix. p. 187 (1928).
(13) H. Fahlenbrach, *Ann. d. Phys.* xiii. p. 265 (1932); xiv. p. 521 (1932).
(14) G. Foëx, *Journ. de Phys.* iii. p. 337 (1932); H. Auer, *Phys. Zeits.* xxxiii. p. 869 (1932); A. Lallemand, *Journ. de Phys.* iv. p. 21 (1933); C. J. Gorter, *Phys. Zeits,* xxxiii. p. 546 (1932).
(15) D. M. Bose and S. Datta, *Zeits. f. Phys.* lxxx. p. 376 (1933).
(16) Van Vleck, 'Theory of Electric and Magnetic Susceptibilities' (1932); Phys. Rev. xli. p. 208 (1932); W. G. Penney and R. Schlapp, Phys. Rev. xli. p. 194 (1932); xlii. p. 666 (1932); xliii. p. 485 (1933); W.G. Penney, R. Schlapp, and O. M. Jordahl, Phys. Rev. xl. p. 637 (1932).
(17) H. A. Kramers, Proc. Amst. Acad. xxxii. p. 1176 (1929).
(18) H. Bethe, *Ann. d. Phys.* iii. p. 133 (1929); *Zeits. f. Phys.* lx. p. 218 (1930).
(19) J. H. Van Vleck, *loc. cit.*
(20) W. G. Penney and R. Schlapp, Phys. Rev. xlii. p. 666 (1932).
(21) C. J. Gorter, Phys. Rev. xlii. p. 437 (1932).
(22) P. Krishnamurti, Ind. Journ. Phys. v. p. 113 (1930).
(23) G. Scheibe, *Zeits f. Electrochemie,* xxxiv. p. 497 (1928).
(24) J. H. Van Vleck, 'Theory of Electric and Magnetic Susceptibilities' (1932), p. 293.
(25) M. N. Saha and S. C. Deb, Bul. Acad. Sciences, U.P. i. p. 1 (1931–32).

Ghosh Physical Laboratory,
University College of Science,
Calcutta.

L. *The Heavy Elastica.* *By* W. G. Bickley, *D.Sc.*, *Imperial College of Science and Technology* *.

1. *Introduction.*

THE primary object of this paper is to provide numerical data of an accuracy greater than that of experimental results for use in reducing the observations made in certain tests of the physical properties of cotton fabrics, tests developed and employed in the laboratories of the British Cotton Industry Research Association at the Shirley Institute, Didsbury[1].

The differential equations of the problems do not seem to admit of formal solution, but can, of course, be solved numerically in particular cases. Numerical methods have therefore been used throughout. The particular process used has been described by the present writer[2] and has largely been developed in the course of the present investigation. The majority of the solutions for the "cantilever" (see *infra*) were originally worked out by Adams's method, but have since been recalculated to an extra place of decimals by the new method. The accuracy of the new and much less laborious method was found by comparison to be adequate, as well as being tested by a device recently discovered[3].

The cases considered fall into two classes, the "cantilever" (§§ 3–5) and the "heart loop" (§§ 6–8), which are in use for ordinary and very flimsy materials respectively, and the kernel of the paper is the set of tables and graphs of the results obtained.

2. *General Equations.*

The central problem of the paper is to determine the shape of a uniform strip of elastic material, due to its weight and certain definite methods of support. The latter lead to boundary conditions which must be satisfied by the solutions of the general differential equation for the shape. We therefore consider first this general differential equation.

The notation that will be used is collected here :—

B=flexural rigidity of strip,

w=weight of strip, per unit length,

* Communicated by Dr. R. H. Pickard, F.R.S.

$c=\sqrt[3]{B/w}$="bending length"[1],

s=arc, measured from a convenient origin,

ψ=angle between the tangent and the horizontal,

x, y=Cartesian co-ordinates in the plane of the loop, horizontal and vertical respectively,

S=shearing force,
T=tension,
M=bending moment,
} at any point,

together with non-dimensional quantities denoted by the corresponding Greek letters, *i. e.*,

$$\sigma=s/c, \quad \xi=x/c, \quad \eta=y/c,$$
$$\tau=T/wc, \quad \mu=M/wc^2.$$

A suffix $_0$ will be used to indicate the value of any quantity at the origin, and a suffix $_1$ to indicate the value at the other end of the strip.

The fundamental assumption throughout, an assumption which is borne out by Peirce's experiments[1], is that curvature is proportional to bending moment, or, in symbols,

$$\frac{d\psi}{ds}=\frac{M}{B}. \quad . \quad . \quad . \quad . \quad . \quad . \quad . \quad (2.1)$$

The forces acting on an element δs of the bent strip are shown in fig. 1. The equations of equilibrium are. resolving horizontally,

$$\delta(T\cos\psi)-\delta(S\sin\psi)=0,$$

or
$$T\cos\psi-S\sin\psi=\text{const.}=T_0; \quad . \quad . \quad (2.21)$$

resolving vertically,

$$\delta(T\sin\psi)+\delta(S\cos\psi)=w\,\delta s,$$

or
$$T\sin\psi+S\cos\psi=S_0+ws; \quad . \quad . \quad . \quad (2.22)$$

taking moments about P,

$$M+\delta M=M-S\,\delta s,$$

or
$$S=-dM/ds. \quad . \quad . \quad . \quad . \quad . \quad . \quad (2.23)$$

From these we derive

$$dM/ds=-S=T_0\sin\psi-(S_0+ws)\cos\psi, \quad . \quad (2.31)$$

i. e.,

$$Bd^2\psi/ds^2=T_0\sin\psi-(S_0+ws)\cos\psi, \quad . \quad . \quad (2.32)$$

which is the general differential equation for the shape of the bent strip.

Integrating (2.31) between 0 and s, we have

$$M = M_0 + T_0 \int_0^s \sin\psi\, ds' - S_0 \int_0^s \cos\psi\, ds' - w \int_0^s s' \cos\psi\, ds'$$

$$= M_0 + T_0 y - S_0 x - w \int_0^s s' \cos\psi\, ds', \quad . \quad . \quad . \quad . \quad (2.41)$$

dashes being used to distinguish between a variable of

Fig. 1.

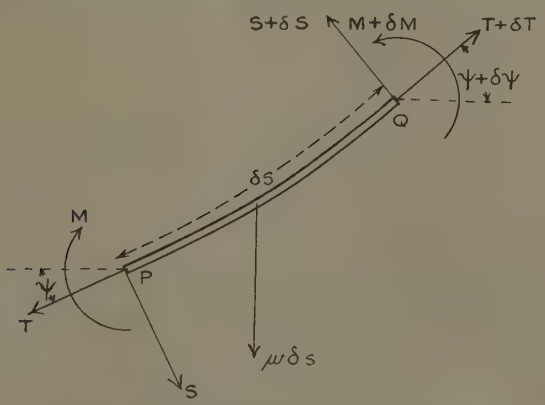

Forces and moments acting on element of elastica.

integration and its value at the limit. Now the last integral is equal to

$$\int_{s'=0}^{s'=s} s'dx' = \Big[s'x'\Big]_{s'=0}^{s'=s} - \int_0^s x'ds'$$

$$= \int_0^s (x - x')ds', \quad . \quad . \quad . \quad . \quad (2.42)$$

from which it is seen that the last term of (2.41) represents the moment of the weight of the segment OP (O being the origin) about P, so that the physical interpretation of (2.41) is complete.

In the two cases that we shall consider in detail S_0 vanishes, so that our differential equation is

$$Bd^2\psi/ds^2 = T_0 \sin\psi - ws\cos\psi, \quad . \quad . \quad . \quad (2.51)$$

or, in terms of non-dimensional variables,

$$d^2\psi/d\sigma^2 = \tau_0 \sin\psi - \sigma\cos\psi. \quad . \quad . \quad . \quad (2.52)$$

3. *The Cantilever.*

The method most commonly employed in measuring the " bending length " of a material is the " cantilever " method, described by Peirce[1]. In this one end of a

Fig. 2.

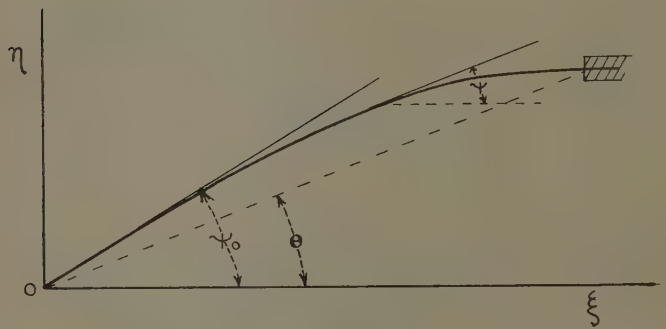

" Cantilever."

strip of the material is clamped horizontally, and the strip allowed to sag under its own weight. The angle θ between the chord and the horizontal (fig. 2) is measured. The bending length is deduced from θ and the length of the strip by means of a not very satisfactory empirical formula based on experiment. We propose to give accurate numerical results to replace the use of this formula in reducing observations.

To do this we integrate (2.52) numerically, with appropriate boundary conditions. Taking the origin at the free end of the strip (fig. 2), and denoting the inclination there by ψ_0, it is possible to integrate the special form of (2.52) step by step along the strip until ψ passes

zero. It will be noticed that both T_0 and S_0 vanish, so that the differential equation for this case is

$$d^2\psi/d\sigma^2 = -\sigma \cos \psi. \quad . \quad . \quad . \quad . \quad (3.1)$$

M_0 is also zero, so that the boundary condition at the free end is equivalent to the vanishing of $d\psi/d\sigma$ there.

The numerical integration has been performed for the values 10°, 20°, 30°, 40°, 50°, 60°, and 70° of ψ_0, with an interval 0·05, and using Simpson's Rule as an integration formula[2]. The value of σ corresponding to $\psi=0$ is denoted by σ_1, and is found by interpolation from the results. If l is the length of the overhanging portion of the strip, $\sigma_1 = l/c$. From the values of ψ as a function of σ we then calculate

$$\left.\begin{aligned} \xi = x/c &= \int \cos \psi \, d\sigma, \\ \text{and} \quad \eta = y/c &= \int \sin \psi \, d\sigma, \end{aligned}\right\} \quad . \quad . \quad . \quad . \quad (3.2)$$

again using Simpson's Rule, so that the form of the cantilever is determined. Finally, θ is found from the fact that

$$\tan \theta = \eta_1/\xi_1. \quad . \quad . \quad . \quad . \quad . \quad (3.3)$$

When ψ_0 and θ are small we approximate to the case of the uniformly loaded cantilever of engineering, the formulæ for which are well known, and reduce in our notation to

$$\sigma_1^3 = (l/c)^3 = 8 \tan \theta = 6 \tan \psi_0. \quad . \quad . \quad . \quad (3.5)$$

The numerical results are given in Table I., and the gradual divergence from (3.5) is there exhibited.

4. *Results for Cantilever.*

The results given in the Table are made visible by graphs showing relations between selected pairs of the tabulated quantities (figs. 3–7). In these relations depending upon the approximations given by (3.5) are shown by dotted lines. The shapes of the overhanging portion are exhibited in figs. 8 and 9. The first of these is drawn with c as unit, so that it shows the successive forms of the overhanging strip as material is gradually pushed out from the support. In the other the length of the overhanging strip is the unit, so that it shows the

TABLE I.

Results for Cantilever.

ψ_0.	σ_1.	$\tan\theta$.	θ.	σ_1^3.	$6\tan\psi_0$.	$8\tan\theta$.	$\frac{\sigma_1^3}{\tan\theta}$.	$\frac{1/\sigma_1}{c/l}$.
0°	..	..	..	..	..	..	8·000	..
10°	$1{\cdot}0190_5$	0·13176	7° 30′·4	1·0582	1·0580	1·0541	8·031	0·9813
20°	$1{\cdot}2976_4$	0·26885	15° 2′·9	2·1850	2·1838	2·1508	8·127	0·7706
30°	$1{\cdot}5129_6$	0·41761	22° 39′·9	3·4632	3·4641	3·3408	8·293	0·6610
40°	$1{\cdot}7112_6$	0·58691	30° 24′·5	5·0113	5·0346	4·6952	8·538	0·5844
50°	$1{\cdot}9152_7$	0·79119	38° 21′·0	7·0257	7·1505	6·3295	8·880	0·5221
60°	$2{\cdot}1464_8$	1·05699	46° 35′·2	9·8896	10·3923	8·4559	9·356	0·4659
70°	$2{\cdot}4398_8$	1·44648	55° 20′·6	14·5246	16·4849	11·5718	10·041	0·4099

effect of increasing the weight per unit length without altering the flexibility.

Fig. 3.

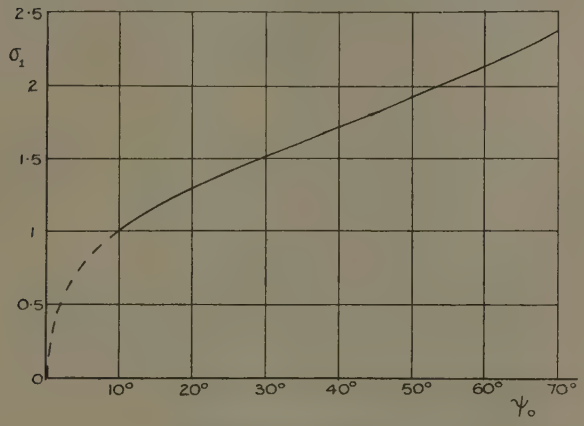

Results for cantilevers.

Fig. 4.

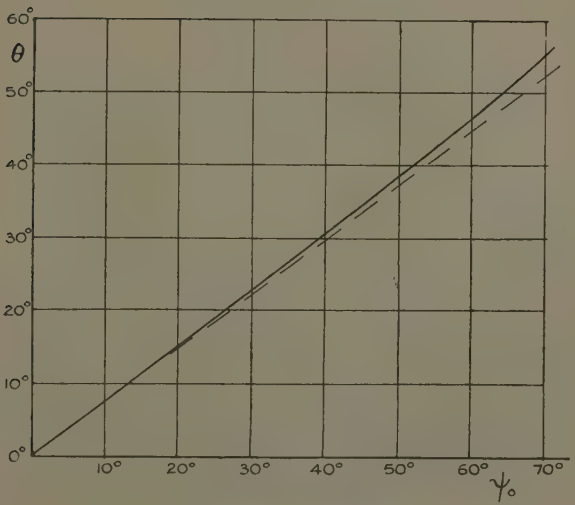

Results for cantilevers.

Fig. 5.

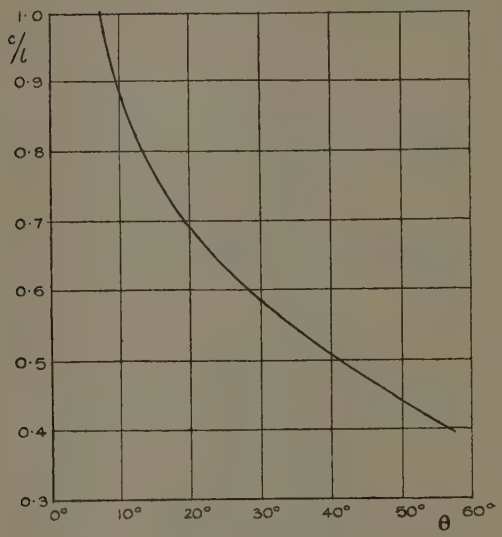

Results for cantilevers.

Fig. 6.

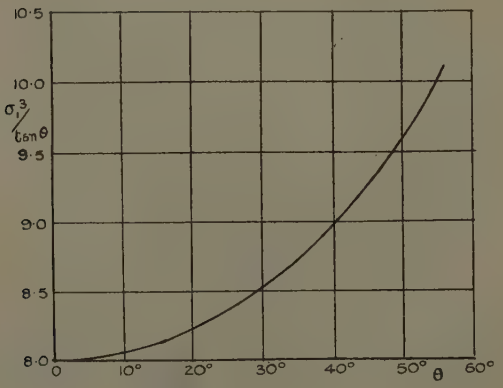

Results for cantilevers.

Similar results have been given by Hummel and Morton[4] as far as $\psi_0=45°$ from a solution of the differential equation in series, but they were unable to go further on account of the increasing slowness of convergence of the series. Over the common range the results of the two methods agree.

Fig. 7.

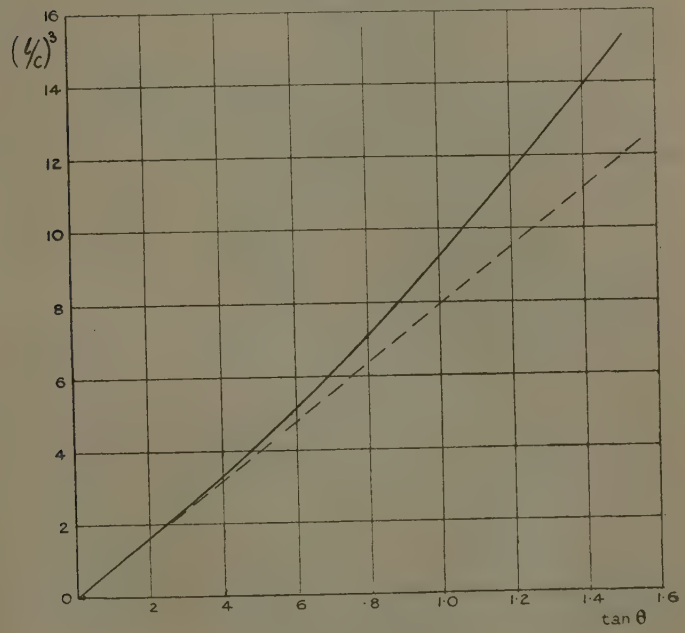

Results for cantilevers.

5. *Discussion of Cantilever Results.*

The interest of fig. 3, which shows the relation between $\sigma_1(=l/c)$ and ψ_0, is mainly mathematical, since it is impossible to measure ψ_0 experimentally with any accuracy.

Fig. 4 shows how closely the approximate form of (3.5),

$$\theta=\tfrac{3}{4}\psi_0, \quad . \quad . \quad . \quad . \quad . \quad . \quad (5.1)$$

holds over the range considered.

Figs. 5, 6, and 7 are three ways of exhibiting the results in a form suitable for the determination of c from observed

Fig. 8.

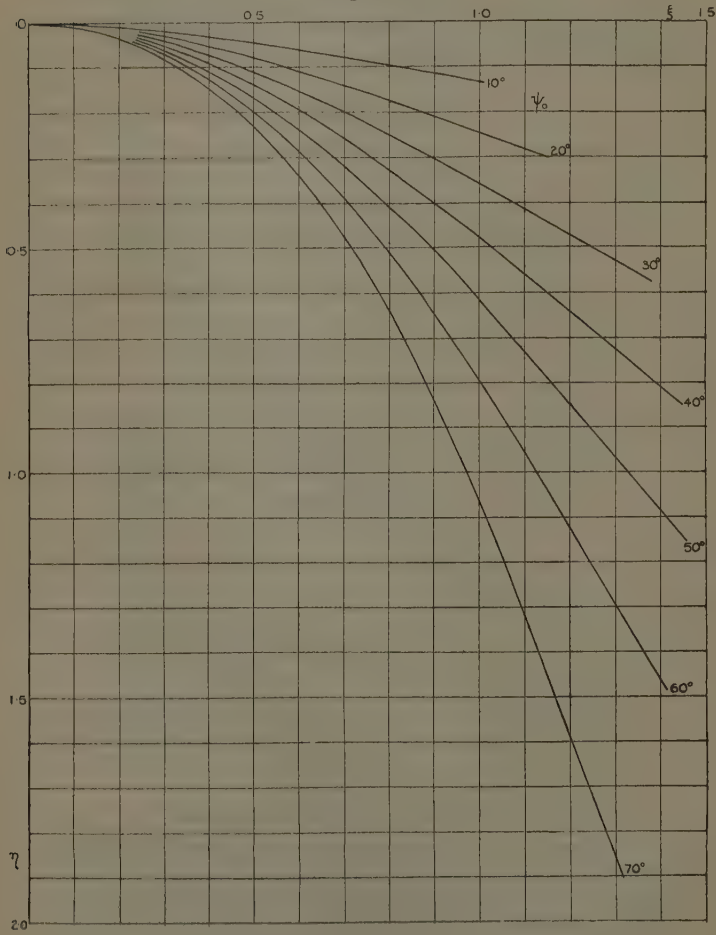

Cantilevers, with c as unit.

values of l and θ. In fig. 5 the value of c/l is plotted as a function of θ, and the accuracy obtained by direct

reading of this graph (drawn, of course, on a larger scale and on paper with intermediate squares) may often be sufficient, and the value of c is obtained by multiplying the length of the strip by the appropriate ordinate. If greater accuracy is desired the use of figs. 6 or 7 is recommended. The ratio $\sigma_1{}^3/\tan\theta$ varies comparatively little, and fig. 6 shows this as a function of θ. In use the ordinate corresponding to the measured θ is multiplied by $\tan\theta$, and the cube root of the product divided

Fig. 9.

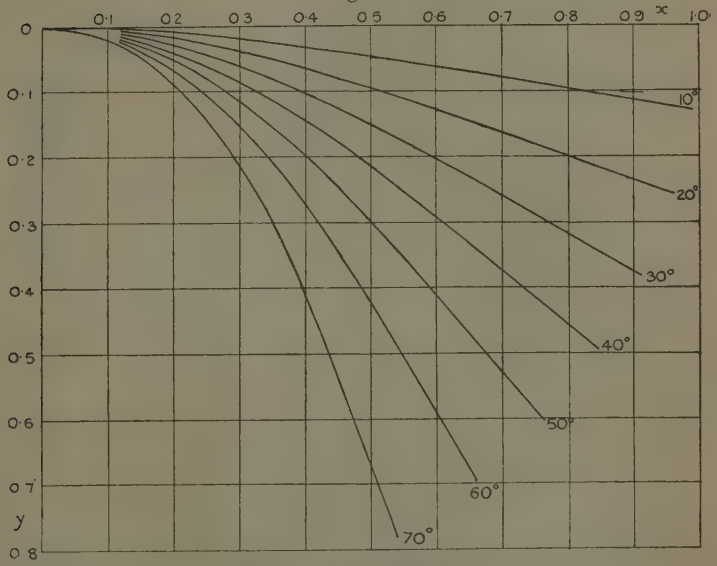

Cantilevers of equal length.

into l to give c as the quotient. Finally, in fig. 7 we plot $\sigma_1{}^3$ against $\tan\theta$ and see that the graph has only small curvature throughout. This implies that interpolation from the numerical results by simple proportional parts will give results of considerable accuracy. It also suggests the advisability of modifying the design of the flexometer * so as to enable $\tan\theta$ to be read directly—a very simple matter. To facilitate this a table has been

* See photographs facing p. 86 of Peirce's paper (1).

prepared by interpolation, giving σ_1^3 as a function of $\tan\theta$ at interval 0·1, along with second differences, so that it can be interpolated further with ease.

As illustrations of the employment of these methods we give the details for $\theta=36°$:

From fig. 5,

$$c/l = 0{\cdot}537 \pm {\cdot}002\,;$$

from fig. 6,

$$\sigma_1^3 = (8{\cdot}77 \pm {\cdot}01)\tan 36°,$$

whence $$0{\cdot}5392 < c/l < 0{\cdot}5396.$$

Interpolating in Table II.,

$$\sigma_1^3 = 6{\cdot}3694,$$

$$c/l = 0{\cdot}5395.$$

TABLE II.

For Reducing Cantilever Observations.

$\tan\theta$.	σ_1^3.	Δ^2.
0·0	0·0000	0
0·1	0·8019	107
0·2	1·6145	199
0·3	2·4470	287
0·4	3·3082	339
0·5	4·2033	371
0·6	5·1355	386
0·7	6·1063	389
0·8	7·1160	389
0·9	8·1646	390
1·0	9·2522	..

6. *Heart Loops.*

The "heart loop" (fig. 10) is used for testing more flimsy materials, for which the "cantilever" is unsuitable, since such materials fall nearly vertically. From the ratio of the sag ($AB=y_1$) to the length l of the arc APB it is required to find the "bending length," c.

The differential equation to be solved is (2·52),

$$d^2\psi/d\sigma^2 = \tau_0 \sin\psi - \sigma\cos\psi.$$

Each value of τ_0 defines the shape of a loop, whose size is determined by the value of c, so that there is again a singly-infinite series of shapes. The integration, however, is not so straightforward as with the cantilevers, since there is now no free end at which all the conditions are known *à priori*. If we are to integrate step by step from A we need the value of $d\psi/d\sigma$ at A, which we shall denote by μ_0, and there is apparently no means of determining this otherwise than by trial and error. A trial value of μ_0 is therefore assumed for each value of τ_0, and the integration carried through until ψ passes $3\pi/2$.

Fig. 10.

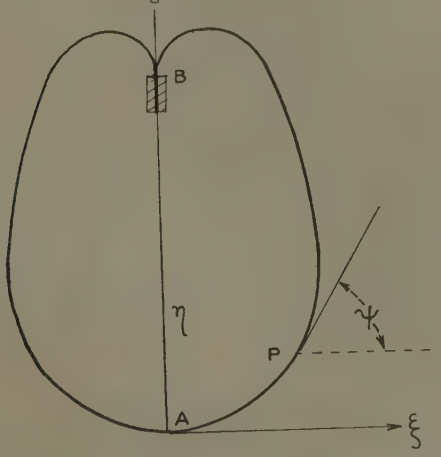

Heart loop.

The correctness of the assumed value of μ_0 is then tested by finding

$$\xi_1 = \int_0^{\sigma_1} \cos\psi \, d\sigma, \quad . \quad . \quad . \quad . \quad . \quad (6.1)$$

which, with the correct value of μ_0, will be zero, and where σ_1 is the value of σ corresponding to $\psi = 3\pi/2$. This is found by interpolating, using Taylor's series, which is here convenient, since $d^2\psi/d\sigma^2$ and $d\psi/d\sigma$ are known, and three terms prove to be sufficient. In actual practice rough trials were made until μ_0 was approximately located. Two integrations, with two near values of μ_0,

preferably such as to give values of ξ_1 of opposite sign, were then carefully carried through. By interpolation a better value of μ_0 was found, and this checked by a third integration. At best, then, three integrations were needed for each loop, so that the process is laborious ; and since the interpolation is not linear, with sufficient accuracy, unless the values of μ_0 differ but little, it was not rare for four or more integrations to be carried through before a result that could be regarded as satisfactory was obtained, *i. e.*, until ξ_1 was between $\pm$ 0·00005. It will be realized, however, that the third and successive integrations are considerably assisted by the first two, and also that the examination of the gradual and regular divergence of the trial solutions is a very sensitive check against casual numerical error. All other possible checks of accuracy, including the author's correction of the integration formula[3] have been applied. For the shorter loops, the table of sines and cosines in Milne-Thomson and Comrie's 'Standard Four-Figure Tables,' with a radian argument, have been invaluable. For the longer loops, where the '$4\frac{1}{2}$' figure accuracy of these tables was not quite sufficient, the similar tables from the British Association's Mathematical Tables, vol. i., were employed, using five figures. As the interval of σ employed was never less than 0·1, it is believed that at least four figures in the results are correct, and that the fifth is probably correct.

7. *Results for Heart Loops.*

The numerical results for the five loops calculated are given in Table III., and graphs exhibiting the relations between selected pairs are given in figs. 11–15.

Fig. 11 shows the relation between τ_0 and μ_0. This would be of considerable assistance if it were desired to compute further loops *within* the range shown. *Extrapolation* is not recommended. The minimum between 0·5 and 0 explains the unpleasantly large number of trials that had to be made for $\tau_0 = 0$ when the work for 2, 1, and 0·5 had been completed, and before this sudden change of behaviour of the curve had been detected !

Fig. 12 shows the relation between τ_0 and σ_1, σ_1 being, of course, the length of the arc APB (fig. 10) in terms of c as a unit, *i. e.*,

$$\sigma_1 = l/c, \quad . \quad . \quad . \quad . \quad . \quad . \quad . \quad (7.1)$$

Table III.

Results for Heart Loops.

τ_0.	μ_0.	σ_1.	η_1.	$\sigma_2/\eta_1=l/y_1$.	$1/\eta_1=c/y_1$.	$1/\sigma_2=c/l$.	$\eta_1/\sigma_1=y_1/l$.
∞	..	..	..	3·7358	..	..	0·2675
2·0	1·4895	1·8702	0·6054	3·0892	1·6518	0·5347	0·3237
1·0	1·2880	2·3487	0·8561	2·7434	1·1680	0·4258	0·3645
0·5	1·2015	2·7876	1·1889	2·3446	0·8411	0·3587	0·4265
0·0	$1·1724_5$	3·7472	2·0969	1·7870	0·4769	0·2669	0·5596
−0·1	$1·1874_0$	4·1929	2·5798	1·6250	0·3876	0·2386	0·6154
−0·2	$1·2292_5$	5·0839	3·5780	1·4207	0·2795	0·1967	0·7039
−0·3	1·2782*	..	..	..	..	..	..

* μ_0 located approximately, but the loop is so sensitive to a small change in μ_1 that six places seem necessary to obtain satisfactory results.

Fig. 11.

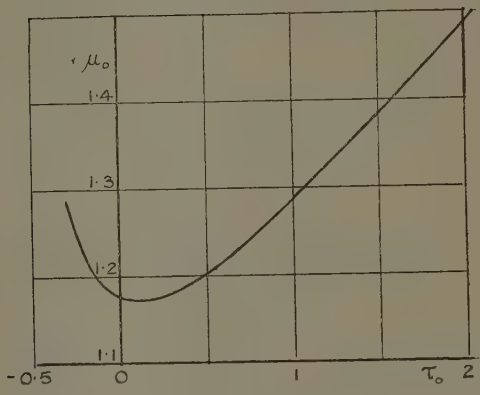

Results for heart loops.

Fig. 12.

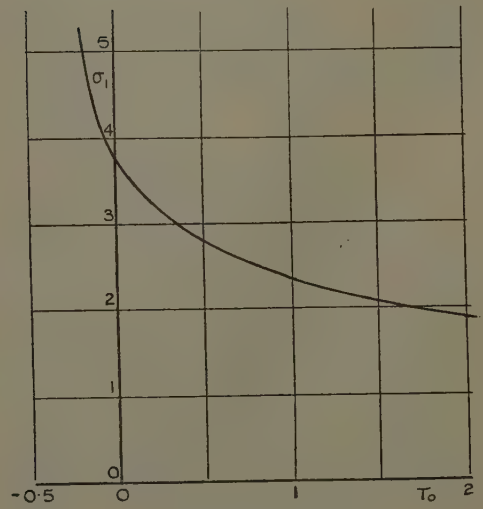

Results for heart loops.

and shows the increase in the lengths of the loops as τ_0 decreases.

Fig. 13 shows $\eta_1 (= y_1/c)$ as a function of τ_0. Figs. 11–

Fig. 13.

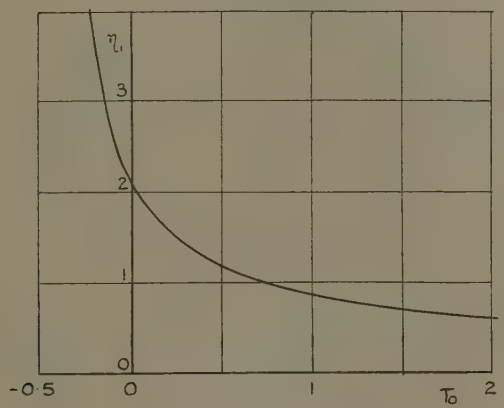

Results for heart loops.

13 thus exhibit the fundamental numerical results.

In use the measurable quantities are l and y_1, and c is required. Evidently a loop is determined, except as to scale, by the ratio of y_1 to l. Fig. 14 shows l/y_1 as a

Fig. 14.

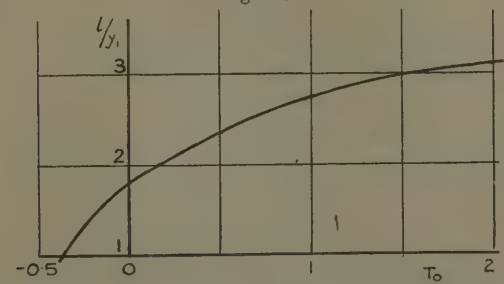

Results for heart loops.

function of τ_0. For long loops this ratio must evidently approach unity as a limit, and the graph indicated that the limit is reached for a value of τ_0 between $-0{\cdot}35$ and

$-0{\cdot}4$. For values of τ_0 below this, then, *no loops exist*, a fact which explains the inability to obtain results for $\tau_0 = -0{\cdot}5$ after prolonged effort and before any other negative values of τ_0 had been dealt with.

Fig. 15.

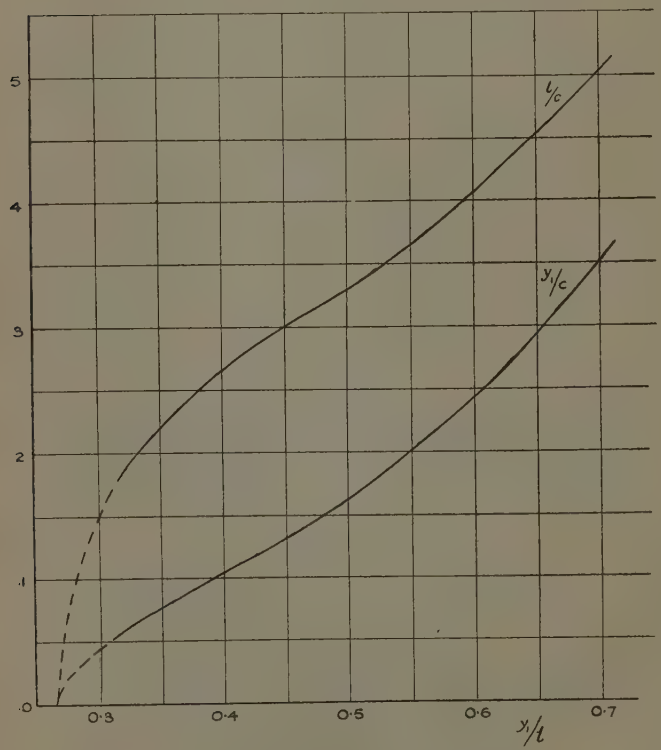

Reduction graph for heart loops.

Fig. 15 is drawn to enable the experimental results (*i. e.*, the values of l and y_1) to be used to determine c. This last can be obtained from its ratio to either l or y_1. The figure shows l/c and y_1/c as functions of y_1/l. The choice of these ratios, and not their slightly more convenient reciprocals, have been dictated by the greater

accuracy to be expected by correlating larger numbers with longer loops.

Fig. 16.

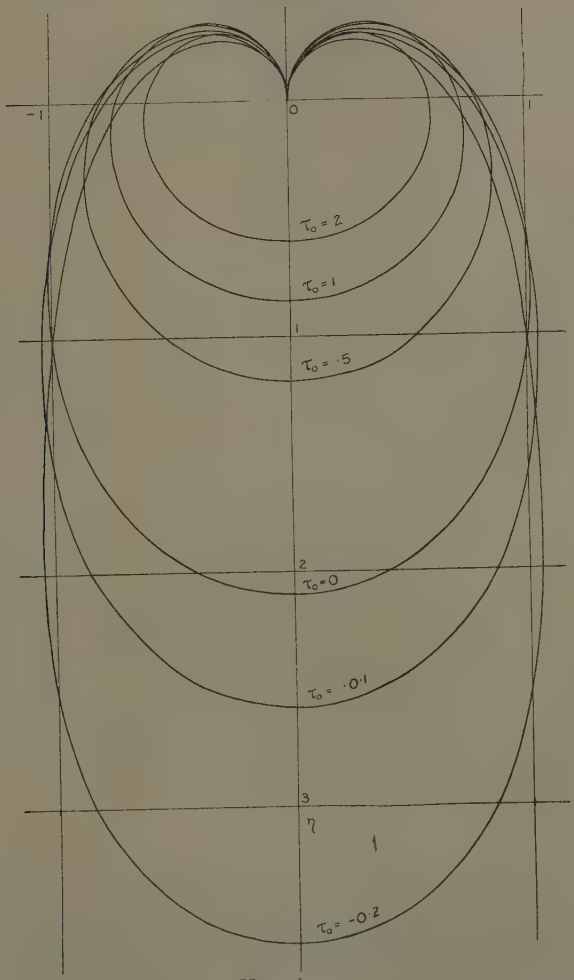

Heart loops.

In fig. 16 are shown, on the same scale, the shapes of all the loops computed. Finally, in fig. 17 the shape of

the weightless heart elastica, computed from the formulæ given by Peirce[1], and which corresponds to the limit as $\tau_0 \to \infty$, is given for comparison.

Fig. 17.

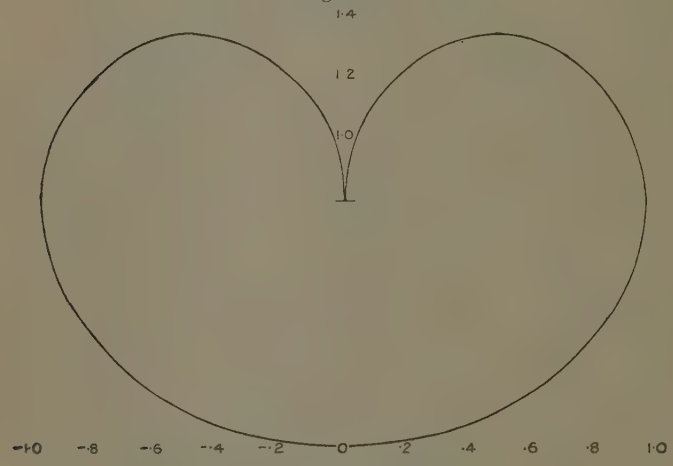

Heart elastica (weightless).

9. *Acknowledgments.*

9. In conclusion, my grateful thanks are due to Mr. Rupert S. Scott, of 70 Harley Street, by whose treatment my failing eyesight has been so far restored that this work, begun long since, carried on with increasing difficulty, and then put aside for some months, has finally been completed. I also wish to thank Dr. R. H. Pickard for his continued interest in this work.

References.

(1) F. T. Peirce, "The 'Handle' of Cloth as a Measurable Quantity," Shirley Institute Memoirs (9) viii. p. 83 (1930).
(2) W. G. Bickley, "A Simple Method for the Numerical Solution of Differential Equations," Phil. Mag. (7) xiii. p. 1006 (1932).
(3) W. G. Bickley, "A Simple Method for the Numerical Solution of Differential Equations: Note on Error and its Avoidance," *ibid.* xv. p. 1174 (1933).
(4) Hummel and Morton, Phil. Mag. (7) iv. p. 348 (1927).

Imperial College of Science and Technology,
July 1933.

LI. *Note on the Computation of the Disturbed Motion of a Synchronous Motor. By* W. H. INGRAM, *School of Engineering, Columbia University*.*

THE equations of motion of synchronous machines, as given by the Lagrangean formula, contain coefficients which are sinusoidal functions of the rotor position angle and (in steady running) of the time of a period of the order of 1/60 second, so that the equations are not in a form suitable for application of any of the classical methods for numerical solution of differential equations because of the fact that the period of the coefficients occurring in the equations are short in comparison to the time-interval for which integration usually has to be carried out. A reduced system of differential equations is here derived in which the period (in a loose sense of the term) of the coefficients is of the order of 100 times that of the coefficients in the original system, so that numerical integration of the Runge type becomes practically applicable. The discussion is confined for simplicity to the simplest case that takes account of all essential features of a synchronous motor.

Consider a synchronous motor without amortisseur or salient poles operating on an infinite bus. For disturbances in the external forces Δe_k, $\Delta \mathrm{E}$, and $-\Delta f$, suddenly arising at time $t=0$, the equations of motion are

$$\left.\begin{aligned} e_k+\Delta e_k \mathrm{H}(t) &= r\dot{q}_k+\frac{d}{dt}\left[l^*\dot{q}_k+\mathrm{M}_k(\theta)\mathrm{I}\right] \\ \mathrm{E}_0+\Delta \mathrm{E}\mathrm{H}(t) &= \mathrm{R}\mathrm{I}+\frac{d}{dt}\left[\mathrm{L}\mathrm{I}+\Sigma \mathrm{M}_k\dot{q}_k\right] \\ -f-\Delta f\,\mathrm{H}(t) &= \Theta\ddot{\theta}+s\dot{\theta}-\mathrm{I}\Sigma \mathrm{M}_k'\dot{q}_k \end{aligned}\right\} \quad . \quad . \quad (1)$$

where

$$\left.\begin{aligned} e_k &= \sqrt{2}e_0\cos(\omega t-2k\pi/3) \\ \mathrm{M}_k &= \mathrm{M}_0\sin(\theta-2k\pi/3) \\ \Delta e_k &= \mathrm{A}\cos(\omega t-\alpha+\varsigma-2k\pi/3) \end{aligned}\right\} \quad . \quad . \quad . \quad . \quad (2)$$

The disturbance in the bus-bar voltage is thus assumed to be positive phase-sequent of maximum value A and phase-angle $\alpha-\varsigma$ with respect to the e_k's; the angle ς is

* Communicated by the Author.

introduced for convenience and later definition. The Heaviside unit function is used merely to denote the sudden appearance of the disturbing forces.

The new method suggested itself from the observation that the armature currents can be eliminated when r is zero to obtain reduced equations of much simpler form, and the first step in obtaining reduced equations which take account of the armature resistance proceeds from the observation that the solutions of the equations

$$\left.\begin{aligned} e_k+\Delta e_k\mathrm{H}(t)&=r\dot{x}+l^*\ddot{x}\\ -\frac{d}{dt}[\mathrm{M}_k(\theta)\mathrm{I}]&=l^*\ddot{\xi}\end{aligned}\right\} \quad . \quad . \quad . \quad . \quad (3)$$

may be added together to give a much better solution, in terms of the remaining variables, of the equation for $\dot{q}_k$,

$$e_k+\Delta e_k\mathrm{H}(t)-\frac{d}{dt}[\mathrm{M}_k(\theta)\mathrm{I}]=r\dot{q}_k+l^*\ddot{q}_k \quad . \quad . \quad (4)$$

than the solution obtained by putting r equal to zero in (4).

The solutions of (3) are

$$\begin{aligned}\dot{x}=&\sqrt{2}e_0z^{-1}\cos(\omega t-\varsigma-2k\pi/3)\\ &+\mathrm{A}z^{-1}[\cos(\omega t-\alpha-2k\pi/3)-\epsilon^{-\sigma t}\cos(\alpha+2k\pi/3)], \quad (5)\end{aligned}$$

$$\dot{\xi}=-\mathrm{M}_k(\theta)\mathrm{I}/l^*, \quad . \quad . \quad . \quad . \quad . \quad . \quad . \quad . \quad . \quad . \quad (6)$$

so that

$$\left.\begin{aligned}\Sigma\mathrm{M}_k\dot{x}_k=&a\sin(\theta-\omega t+\varsigma)\\ &+\mathrm{A}_1[\sin(\theta-\omega t+\alpha)-\epsilon^{-\frac{\sigma t}{4}}\sin(\theta+\alpha)]\\ \Sigma\mathrm{M}_k\dot{x}_k=&a\cos(\theta-\omega t+\varsigma)\\ &+\mathrm{A}_1[\cos(\theta-\omega t+\alpha)-\epsilon^{-\sigma t}\cos(\theta+\alpha)]\end{aligned}\right\}, \quad (7)$$

$$\left.\begin{aligned}\Sigma\mathrm{M}_k\dot{\xi}_k&=-\tfrac{3}{2}\mathrm{M}_0^2\mathrm{I}/l^*\\ \Sigma\mathrm{M}_k\dot{\xi}_l&=0\end{aligned}\right\}, \quad . \quad . \quad . \quad . \quad . \quad . \quad . \quad . \quad . \quad . \quad (8)$$

where

$$\begin{aligned}a&=\tfrac{3}{2}\sqrt{2}e_0\mathrm{M}_0z^{-1},\\ \mathrm{A}_1&=\tfrac{3}{2}\mathrm{M}_0\mathrm{A}z^{-1},\\ z&=[r^2+(\omega l^*)^2]^{\frac{1}{2}},\\ \varsigma&=\arctan(\omega l^*/r),\\ \sigma&=r/l^*.\end{aligned}$$

On making the substitution of variable

$$\left.\begin{aligned}\theta&=\omega t-\varsigma+\pi/2-\psi_0-\psi(t)\\ \mathrm{I}&=\mathrm{I}_0+y\end{aligned}\right\}, \quad . \quad . \quad . \quad (9)$$

the last two equations in (1) become

$$\left.\begin{aligned}\{\Delta\mathrm{E}+\mathrm{A}_1[\dot\theta\cos(\theta+\alpha)-\sigma\sin(\theta+\alpha)]\epsilon^{-\sigma t}\}\mathrm{H}(t)&\\ =\mathrm{R}y+\mathrm{L}^*\dot y+\mathbf{M}\dot\psi&\\ \{\Delta f+\mathrm{A}_1\mathrm{I}\epsilon^{-\sigma t}\cos(\theta+\alpha)\}\mathrm{H}(t)&\\ =\Theta\ddot\psi+s\dot\psi-y\mathbf{M}-\mathrm{I}_0\mathbf{N}&\end{aligned}\right\}, \quad (10)$$

when the steady-state relations

$$\left.\begin{aligned}\mathrm{E}_0&=\mathrm{RI}_0\\ -f&=s\omega-\mathrm{I}_0 a\sin\psi_0\end{aligned}\right\} \quad . \quad . \quad . \quad . \quad (11)$$

are made use of, and where

$$\mathbf{M}=-a\sin(\psi_0+\psi)-\mathrm{A}_1\sin(\psi_0+\varsigma-\alpha+\psi),$$

$$\mathbf{N}=\mathbf{M}+a\sin\psi_0,$$

$$\mathrm{L}^*=\mathrm{L}-\tfrac{3}{2}\mathrm{M}_0^2/l^*.$$

In obtaining (10) terms which oscillate comparatively rapidly in an almost periodic manner are placed on the left with the forces $\Delta\mathrm{E}$ and Δf. These terms come into existence at the time $t=0$, and their amplitudes die out exponentially. The terms on the right either contain the unknown variables as factors, are in existence before the time $t=0$, or do not vary rapidly with the time. The moment of inertia Θ of the rotor is always so great that the effect of active and reactive forces on the rotor of periodic or almost periodic oscillatory form is small in magnitude and unimportant in character if the period is of the order of magnitude of π/ω, or thereabouts; accordingly such oscillatory components in $y\mathbf{M}$, when they can be isolated, may be neglected on the right-hand side of (10) and the constant component of I may be neglected on the left.

Regarding the field winding as a system in itself, it is clear that the oscillatory component in y, having the character mentioned, can be obtained if the equations

$$\left.\begin{aligned}\dot\theta\epsilon^{-\sigma t}\cos(\theta+\alpha)&=\kappa u+\dot u\\ \sigma\epsilon^{-\sigma t}\sin(\theta+\alpha)&=\kappa u+\dot u\end{aligned}\right\} \quad . \quad . \quad . \quad (12)$$

can be solved. Both of these equations can be put in the form

$$\mu(t)\cos(\omega t-\beta)=\kappa u+\dot{u}, \quad . \quad . \quad . \quad . \quad (13)$$

which has a series solution of the form

$$u=a_0(t)\mu+a_1(t)\dot{\mu}+a_2(t)\ddot{\mu}+\ldots, \quad . \quad . \quad (14)$$

where

$$a_n=(-1)^n(\omega^2+\kappa^2)^{-\frac{1}{2}(n+1)}\cos(\omega t-\beta-(n+1)\varepsilon.$$

This series converges for any probable function $\psi(t)$, and, moreover, the first term would appear to be a good enough approximation in most cases*. Knowing the solution of the equation (13) it is not difficult to build up solutions of (12) when θ has the form (9) and when $\dot{\theta}$ is large in comparison to higher derivatives. Thus, a solution of

$$A_1[\dot{\theta}\cos(\theta+\alpha)-\sigma\sin(\theta+\alpha)]\epsilon^{-\sigma t}H(t)=Ru+L^*\dot{u}, \quad (15)$$

is, omitting terms which are comparatively small in ordinary practical cases,

$$u=A_1Z^{-1}[\dot{\theta}\cos(\theta+\alpha-\varsigma_1)-\sigma\sin(\theta+\alpha-\varsigma_1)]\epsilon^{-\sigma t}+U(\psi), \quad (16)$$

where

$$U(\psi)=-A_1Z^{-1}[\omega\sin(\psi_0-\alpha+\varsigma+\varsigma_1) \\ -\sigma\cos(\psi_0-\alpha+\varsigma+\varsigma_1)]\epsilon^{-\sigma t},$$

$$Z=[R^2+(\omega L^*)^2]^{\frac{1}{2}},$$

$$\varsigma_1=\arctan(\omega L^*/R).$$

On substituting this value of u into the second equation of (10), and neglecting tremors, one obtains

$$\left.\begin{aligned} \Delta EH(t)&=R\eta+L^*\dot{\eta}+\mathbf{M}\dot{\psi} \\ (\Delta f+\mathbf{F})H(t)&=\Theta\ddot{\psi}+s\dot{\psi}-(U+\eta)\mathbf{M}-I_0\mathbf{N} \end{aligned}\right\}, \quad (17)$$

where

$$\mathbf{F}=\tfrac{1}{2}A_1^2\omega L^*Z^{-2}(\sigma+R/L)\epsilon^{-2\sigma t}.$$

This system is of a form suitable for numerical study of the rotor transient In obtaining it the field current was resolved into three components—a constant component I_0, an oscillatory component having the period $2\pi/\dot{\theta}$ given by (16), and a term given by (17), which pre-

* *Cf.* Ingram, Camb. Phil. Soc. xxix. p. 530 (1933).

sumably is oscillatory and of a much greater but not well definable period.

A more exact set of equations is now obtainable by the Picard method of successive approximations. The force **F** rapidly attenuates when r is not small, but the expression for it is exact when r is zero, so there is little point in obtaining a more exact value for it than that already given, and its presence may be ignored in carrying out the Picard process. The first approximate solution in this process may be taken as that which satisfies the equations

$$\left.\begin{aligned} \Delta \mathrm{EH}(t) &= \mathrm{R}y_1 + \mathrm{L}\dot{y}_1 + \mathbf{M}_1\dot{\psi}_1 \\ \Delta f\mathrm{H}(t) &= \Theta\ddot{\psi}_1 + s\dot{\psi}_1 - y_1\mathbf{M}_1 - \mathrm{I}_0\mathbf{N}_1 \end{aligned}\right\}, \quad . \quad . \quad (18)$$

and, as a next approximation, a solution is sought of the system

$$\left.\begin{aligned} \Delta \mathrm{EH}(t) &= \mathrm{R}y + \mathrm{L}\dot{y} + \mathbf{M}\dot{\psi} + \frac{d}{dt}\Sigma \mathrm{M}_k\dot{\xi}_k \\ \Delta f\mathrm{H}(t) &= \Theta\ddot{\psi} + s\dot{\psi} - \mathbf{M}y + \mathbf{N}\mathrm{I}_0 + \mathbf{T} + \mathrm{I}_1\Sigma \mathrm{M}_k\dot{\xi}_k \end{aligned}\right\}, \quad (19)$$

where **T** is a term in the steady-state equation

$$-f = s\omega - \mathrm{I}_0 a \sin\psi + \mathbf{T},$$

which gives the drag on the rotor due to the Foucault effect in the armature circuits, and where $\dot{\xi}_k$ is the particular integral of the equation

$$-(\mathrm{I}_0 + y_1)\mathrm{M}_k(\theta_1) = r\xi_k + l^*\dot{\xi}_k. \quad . \quad . \quad . \quad (20)$$

The last equation may be solved when $\dot{\psi}$ is small in comparison to ω to give, very accurately,

$$\dot{\xi}_k = -\mathrm{M}_0\omega z^{-1}\mathrm{I}_1\cos(\theta_k - \varsigma) - \mathrm{M}_0 r z^{-2}\dot{\psi}\sin(\theta_k - 2\varsigma), \quad (21)$$

where $\theta_k = \theta - 2k\pi/3$. On substitution into (19), this yields

$$\left.\begin{aligned} \Delta \mathrm{EH}(t) &= \mathrm{R}y + \mathrm{L}^*\dot{y} - \rho\ddot{y} + \mathbf{M}\dot{\psi} \\ (\Delta f + \mathbf{F})\mathrm{H}(t) &= \Theta\ddot{\psi} + s\dot{\psi} - \mathbf{N}\mathrm{I}_0 - (\mathrm{U} + y)\mathbf{M} \\ &\quad - (\mathrm{I}_1^2 - \mathrm{I}_0^2)\omega\rho + 2r\rho\dot{y} \end{aligned}\right\}, \quad (22)$$

where, it is now found,

$$\mathbf{T} = \mathrm{I}_1^2\omega\rho,$$
$$\rho = \tfrac{3}{2}\mathrm{M}_1^2 r z^{-2}.$$

This system degenerates to (17) when $r=0$ and the terms in (22) not found in (17) are small; further iteration of the Picard process merely introduces small corrections in these terms. It is to be noted that the Foucault drag is given correctly in this second application of the Picard process. The system (22) may be taken as final in the type of problem contemplated.

LII. *The Calculation of Modulation Products.*—II. *By* A. C. Bartlett, *M.A.** (Communication from the Research Staff of the M.O. Valve Co., Ltd., at Wembley.)

Summary.

The method described before (Phil. Mag. xvi. p. 845 (1933)) of calculating the modulation products when any number of sine waves of voltage are applied to the electrodes of a thermionic valve is extended so as to deal with amplitude- and frequency-modulated waves.

Section I.

Amplitude-modulated Waves.

In a previous paper† a method was given of deriving the multiple Fourier series of a function of cosines directly from the Taylor series. This was applied to calculating the modulation products when any number of sinusoidal voltages are applied to any number of electrodes of a thermionic valve.

In practice it is often necessary to deal with amplitude-modulated waves of the form $v_1 \cos\theta(1+m\cos\phi)$. Consider the case of a valve with one control electrode in which the anode current i is related to the control voltage v by a series

$$i = \mathrm{F}(v) = a_0 + a_1 v + a_2 v^2 + \ldots$$

If to the grid of the valve a voltage

$$b + v_1 \cos\theta(1+m\cos\phi)$$

* Communicated by C. C. Paterson, M.I.E.E.

† Phil. Mag. ser. 7, xvi. p. 845 (Oct. 1933).

is applied, then

$$i = \mathrm{F}(b + v_1 \cos\theta(1 + m\cos\phi))$$

$$= e^{v_1 \cos\theta(1+m\cos\phi)\frac{d}{db}} \mathrm{F}(b),$$

and it is required to express this as a double Fourier series in θ and ϕ.

Proceeding as before, it is necessary to express $e^{z\cos\theta(1+m\cos\phi)}$ as a double Fourier series of the form

$$\sum_{s=0}^{\infty} \sum_{r=0}^{\infty} \mathrm{A}_{sr}(m, z) \cos s\theta \cos r\phi,$$

where each coefficient $\mathrm{A}_{sr}(m, z)$ is a function of m and z: a method of calculating A_{sr} is given in the Appendix.

To deal with the operator

$$e^{v_1 \cos\theta(1+m\cos\phi)\frac{d}{db}}$$

it is only necessary to replace z by $v_1 \frac{d}{db}$. Thus

$$e^{v_1 \cos\theta(1+m\cos\phi)\frac{d}{db}} = \sum_{s=0}^{\infty} \sum_{r=0}^{\infty} \mathrm{A}_{sr}\left(m, v_1 \frac{d}{db}\right) \cos s\theta \cos r\phi.$$

As an example consider the case where two modulated signals are applied simultaneously to the grid, so that

$$v_1 = b + v_1 \cos\theta_1(1 + m_1\cos\phi_1) + v_2 \cos\theta_2(1 + m_2\cos\phi_2).$$

The anode current will be

$$i = e^{v_1 \cos\theta_1(1+m_1\cos\phi_1)\frac{d}{db}} e^{v_2 \cos\theta_2(1+m_2\cos\phi_2)\frac{d}{db}} \mathrm{F}(b)$$

$$= \left\{ \sum_{s=0}^{\infty} \sum_{r=0}^{\infty} \mathrm{A}_{sr}\left(m_1, v_1 \frac{d}{db}\right) \cos s\theta_1 \cos r\phi_1 \right\}$$

$$\times \left\{ \sum_{p=0}^{\infty} \sum_{q=0}^{\infty} \mathrm{A}_{pq}\left(m_2, v_2 \frac{d}{db}\right) \cos p\theta_2 \cos q\phi_2 \right\} \mathrm{F}(b).$$

From this expansion any modulation product may be picked out; the following table gives a few of the simpler and more important terms:—

Constant term is $\mathrm{A}_{00}\left(m_1, v_1 \frac{d}{db}\right) \mathrm{A}_{00}\left(m_2, v_2 \frac{d}{db}\right) \mathrm{F}(b).$

Coefficient of $\cos\theta_1$ is

$$A_{10}\left(m_1, v_1\frac{d}{db}\right)A_{00}\left(m_2, v_2\frac{d}{d\bar{b}}\right)F(b).$$

,, ,, $\cos\theta_1\cos\phi_1$ is

$$A_{11}\left(m_1, v_1\frac{d}{db}\right)A_{00}\left(m_2, v_2\frac{d}{d\bar{b}}\right)F(b).$$

,, ,, $\cos\theta_1\cos\phi_2$ is

$$A_{10}\left(m_1, v_1\frac{d}{db}\right)A_{01}\left(m_2, v_2\frac{d}{d\bar{b}}\right)F(b).$$

Thus the output current of frequency θ_1 is modulated by the frequency ϕ_1 to the extent of

$$\frac{A_{11}\left(m_1, v_1\frac{d}{db}\right)A_{00}\left(m_2, v_2\frac{d}{db}\right)F(b)}{A_{10}\left(m_1, v_1\frac{d}{db}\right)A_{00}\left(m_2, v_2\frac{d}{d\bar{b}}\right)F(b)} \times 100 \text{ per cent.},$$

while it is also modulated by the frequency ϕ_2 to the extent of

$$\frac{A_{10}\left(m_1, v_1\frac{d}{db}\right)A_{01}\left(m_2, v_2\frac{d}{db}\right)F(b)}{A_{10}\left(m_1, v_1\frac{d}{db}\right)A_{00}\left(m_2, v_2\frac{d}{d\bar{b}}\right)F(b)} \times 100 \text{ per cent.}$$

The coefficients A_{00}, A_{01}, A_{10}, and A_{11} are given at the end of the Appendix, worked out as far as the tenth power of z, which is sufficient to deal with the intermodulation between modulated signals in the case of a valve whose characteristic can be expressed as a polynomial of degree not higher than ten.

Section 2.

Frequency-modulated Waves.

It is necessary to deal with voltages of the form

$$v_1\cos(\theta+m\cos\phi),$$

and therefore with operators of the form

$$e^{v_1\cos(\theta+m\cos\phi)\frac{d}{db}}.$$

Thus a double Fourier series for $e^{z\cos(\theta+m\cos\phi)}$ is required. This is seen to be given by

$$\mathrm{I}_0(z)+2\sum_{n=1}^{\infty}\mathrm{I}_n(z)\cos n(\theta+m\cos\phi),$$

together with the formula

$$\begin{aligned}&\cos n(\theta+m\cos\phi)\\&=\cos n\theta\{\mathrm{J}_0(mn)-2\mathrm{J}_2(mn)\cos 2\phi+2\mathrm{J}_4(mn)\cos 4\phi-\ldots\}\\&\quad+\sin n\theta\{2\mathrm{J}_1(mn)\sin\phi+2\mathrm{J}_3(mn)\sin 3\phi+\ldots\}.\end{aligned}$$

Hence the term of order $r\theta, s\phi$ in the required expansion of $e^{z\cos(\theta+m\cos\phi)}$ is

$$\epsilon_r\epsilon_s\mathrm{J}_s(mr)\mathrm{I}_r(z)\sin r\theta\sin s\phi$$

if s is odd, and

$$(-1)^{s/2}\epsilon_r\epsilon_s\mathrm{J}_s(mr)\mathrm{I}_r(z)\cos r\theta\cos s\phi$$

if s is even, where ϵ_n is Neumann's factor

$$\left.\begin{aligned}\epsilon_n&=2\ \text{when}\ n\neq 0,\\&=1\ \text{when}\ n=0.\end{aligned}\right\}$$

Replacing z by $v_1\dfrac{d}{db}$ gives the required operator, and the calculation proceeds as in Section 1.

Appendix.

It is required to express $e^{z\cos\theta(1+m\cos\phi)}$ as a double Fourier series.

By the expansion for $e^{z\cos\theta}$ already used

$$e^{z\cos\theta(1+m\cos\phi)}=\sum_{s=0}^{\infty}\epsilon_s\mathrm{I}_s\{z(1+m\cos\phi)\}\cos s\theta.$$

To complete the expansion it is now necessary to express

$$\mathrm{I}_s\{z(1+m\cos\phi)\}$$

as a Fourier series in ϕ. If

$$f(x)=\mathrm{I}_s\{z(1+mx)\}$$

then, by the method used in the previous paper but using Maclaurin's Theorem,

$$\begin{aligned}\mathrm{I}_s\{z(1+m\cos\phi)\}&=f(\cos\phi)\\&=\sum_{n=0}^{\infty}\epsilon_n\cos n\phi\,\mathrm{I}_n\left(\frac{d}{dx}\right)_{x=0}\mathrm{I}_s\{z(1+mx)\}.\end{aligned}$$

Hence A_{sr}, the coefficient of $\cos s\theta \cos r\phi$ in the Fourier series for $e^{z\cos\theta(1+m\cos\phi)}$, is

$$\epsilon_s\epsilon_r \mathrm{I}_r\left(\frac{d}{dx}\right)_{x=0} \mathrm{I}_s\{z(1+mx)\}.$$

A_{sr} may now be expanded in powers of z; the coefficient of z^{s+2k} is

$$\epsilon_s\epsilon_r \frac{1}{\lfloor k \rfloor \overline{s+k}} \cdot \frac{1}{2^{s+2k}} \mathrm{I}_r\left(\frac{d}{dx}\right)_{x=0} (1+mx)^{s+2k}.$$

To simplify further, if

$$\left(\frac{d}{dx}\right)^p_{x=0} (1+mx)^q$$

is written as ${}_p\mathrm{D}_q$, then it is easily seen that

$$\begin{aligned} {}_p\mathrm{D}_q &= m^p \frac{\lfloor q}{\lfloor q-p} \quad \text{if } p \not> q, \\ &= 0 \qquad\qquad \text{if } p > q. \end{aligned}$$

Hence

$$\mathrm{I}_r\left(\frac{d}{dx}\right)_{x=0} (1+mx)^{s+2k} = \sum_{w=0}^{\infty} \frac{1}{w \lfloor r+w} \cdot \frac{1}{2^{r+2w}} \cdot {}_{r+2w}\mathrm{D}_{s+2k},$$

but all the terms in which $r+2w > s+2k$ are zero, so that it is only necessary to sum over the range of w and k for which $r+2w \not> s+2k$.

A_{00}, A_{01}, A_{10}, and A_{11} have been calculated as far as the tenth power of z, and are given here:

$$\begin{aligned} A_{00} = 1 &+ \frac{z^2}{4}\left(1+\frac{m^2}{2}\right) + \frac{z^4}{64}\left(1+3m^2+\frac{3}{8}m^4\right) \\ &+ \frac{z^6}{9\times 2^8}\left(1+\frac{15}{2}m^2+\frac{45}{8}m^4+\frac{5}{16}m^6\right) \\ &+ \frac{z^8}{9\times 2^{14}}\left(1+14m^2+\frac{105}{4}m^4+\frac{35}{4}m^6+\frac{35}{128}m^8\right) \\ &+ \frac{z^{10}}{225\times 2^{16}}\left(1+\frac{45}{2}m^2+\frac{315}{4}m^4+\frac{525}{8}m^6 \right. \\ &\qquad\qquad \left. + \frac{1575}{128}m^8+\frac{63}{256}m^{10}\right). \end{aligned}$$

$$A_{01}=z^2\frac{m}{2}+\frac{z^4}{32}\left(2m+\frac{3}{2}m^3\right)$$
$$+\frac{z^6}{9\times 2^7}\left(3m+\frac{15}{2}m^3+\frac{15}{8}m^5\right)$$
$$+\frac{z^8}{9\times 2^{13}}\left(4m+21m^3+\frac{35}{2}m^5+\frac{35}{16}m^7\right)$$
$$+\frac{z^{10}}{225\times 2^{15}}\left(5m+45m^3+\frac{315}{4}m^5+\frac{525}{16}m^7+\frac{315}{128}m^9\right),$$

$$A_{10}=z+\frac{z^3}{8}\left(1+\frac{3}{2}m^2\right)$$
$$+\frac{z^5}{192}\left(1+5m^2+\frac{15}{8}m^4\right)$$
$$+\frac{z^7}{9\times 2^{10}}\left(1+\frac{21}{2}m^2+\frac{105}{8}m^4+\frac{35}{16}m^6\right)$$
$$+\frac{z^9}{45\times 2^{14}}\left(1+18m^2+\frac{189}{4}m^4+\frac{105}{4}m^6+\frac{315}{128}m^8\right),$$

$$A_{11}=mz+\frac{z^3}{8}\left(3m+\frac{3}{4}m^3\right)$$
$$+\frac{z^5}{96}\left(\frac{5}{2}m+\frac{15}{4}m^3+\frac{5}{16}m^5\right)$$
$$+\frac{z^7}{9\times 2^9}\left(\frac{7}{2}m+\frac{105}{8}m^3+\frac{105}{16}m^5+\frac{35}{128}m^7\right)$$
$$+\frac{z^9}{5\times 2^{13}}\left(\frac{m}{2}+\frac{7}{2}m^3+\frac{35}{8}m^5+\frac{35}{32}m^7+\frac{7}{256}m^9\right).$$

The author desires to tender his acknowledgment to the General Electric Company and the Marconiphone Company, on whose behalf the work was done which led to this publication.

LIII. *On the Elastic Extension of Metal Wires under Longitudinal Stress.*—Part III. *Theoretical* *. *By* L. C. Tyte, *Ph.D., F.Inst.P., Research Department, Woolwich*†.

Introduction.

THE linear relation between stress and the resulting strain produced in a material, first determined by Robert Hooke (1678), although questioned by Bulfinger (1729), who suggested a power law, was generally accepted till the middle of the last century.

The variation in the extension of cast iron was first observed by Hodgekinson (1822), and confirmed by Bauschinger, the results being represented by an algebraic formula,

$$x = ap + bp^2 + cp^3, \quad . \quad . \quad . \quad . \quad . \quad (1)$$

where x is the extension, p the load, and a, b, and c constants. The resulting expressions for Young's Modulus are

$$E = p/x = 1/(a + bp + cp^2),$$

or

$$E' = dp/dx = 1/(a + 2bp + 3cp^2).$$

Bach [1] extended the investigation to many materials, in all cases finding deviations from the simple law, his results being satisfied by the expression

$$x = a'p^m, \quad . \quad . \quad . \quad . \quad . \quad . \quad . \quad (2)$$

where a' and m are constants whose values varied from specimen to specimen, the following being typical values :—

Material.	m.	$1/a'$ (kgm./sq. cm.).
Cast iron (tension)	1·083	1 338 000
Cast iron (compression)	1·035	1 043 000
Copper	1·093	2 084 000
Brass	1·085	947 000

* Portion of Thesis approved for the degree of Doctor of Philosophy in the University of London.

† Communicated by Prof. C. H. Lees, D.Sc., F.R.S.

This yields, as expressions for Young's Modulus,

$$E = p/x = 1/ap^{m-1},$$

or

$$E' = dp/dx = 1/amp^{m-1}.$$

The disadvantage of the power law is that for small loads it does not approximate to Hooke's law.

Stradling [2] and Thompson [3] expressed their results by the algebraic formula (1), the latter giving the following values for his coefficients (x being the extension in mm. of the specimen and p the load in kgm.):—

Material.	Length (metres).	Sectional area (sq. mm.).	a.	b.	c.
Brass	22·700	0·0627	34·924	0·2386	0·1487
Copper	22·69	0·0641	27·461	0·2883	0·0538
Steel	22·70	0·03263	34·672	0·6498	−0·0525
Silver	22·69	0·0687	38·907	0·4462	−0·0313

Expressing x as the extension per unit length, and p, the load, in kgm./sq. mm., a, b, and c assume the values:—

Material.	$1/a$(kgm./sq. mm.).	a.	b.	c.
Brass	10 370	$9·647 \times 10^{-5}$	$6·592 \times 10^{-7}$	$4·11 \times 10^{-7}$
Copper	12 890	7·759	8·147	1·52
Steel	20 050	4·984	9·340	−0·755
Silver	8 490	11·79	13·51	−0·948

Similarly G. S. Meyer [4] expressed the extension of an aluminium wire, 18·315 metres long, whose deviation he found to be very great, as

$$x = 62·863p + 14·312p^2,$$

where x is the actual extension in mm. and p the load in kgm. weight, no cross-sectional area being given.

More recently Grüneisen [5] has made observations on cast iron, using small tensile forces and correspondingly small extensions (measured by an optical interference system), and linked them up with Bach's observations for larger tensile forces by acoustical measurements. This series showed that the power law was valueless and the algebraic expression was not very suitable.

He adopted Hartig's suggestion, and expressed the elastic modulus E′ (kgm./sq. mm.) for any load p (kgm./sq. mm.) as

$$E' = dp/dx = E_0 - cp,$$

E_0 being the elastic modulus for zero load and c a constant; and hence the extension x

$$x = \log_e (E_0/(E_0 - cp))/c.$$

Grüneisen's values of the elastic modulus are :—

Material.	Young's Modulus (kgm./sq. mm.).
Cast iron, GK	$10\,603 - 923\,p$
Cast iron, A	$14\,019 - 505\,p$
Copper (Bach)	$11\,732 - 185\,p$
Copper (Thompson) ...	$12\,920 - 24\,p$
Brass	$10\,576 - 30\,p$
Silver	$8\,462 - 10\,p$
Steel	$19\,975 - 18\,p$

Similar results were obtained by Schulze [6] from experiments on the longitudinal vibrations of loaded wires, giving the "adiabatic" modulus, which was found to decrease linearly with the load for steel, brass, silver, and German silver.

Lastly Kyrillov [7], experimenting on steel wire, found that Young's Modulus was nearly constant for all loads, the deviation from Hooke's law being less than a quarter of that found by Thompson.

It will be remarked that there are considerable differences in the values obtained by different experimenters for the same material, but from considerations of the methods of experiment and of the different heat- and cold-work treatments to which the specimens had been subjected this is hardly surprising.

Relation between the Length and the Stretching Force.

It was suggested by Professor Lees that the results obtained in the present investigation (see Part II. [8]) could be represented by the expression

$$L = L_0 e^{\alpha p}, \quad . \quad . \quad . \quad . \quad . \quad . \quad . \quad (3)$$

where L is the length under a tensile force p per unit area of a wire of initial length L_0 and α a constant.

Now consider two wires of similar cross-sectional area A and of length L and KL, loaded by means of the ratio-bar by a weight M, so that a load kM was on the shorter L, and $(1-k)$ M on the longer KL.

Thus the wire of length L becomes $L e^{k\alpha M/A}$ and the wire of length KL becomes $KL e^{(1-k)\alpha M/A}$. This will cause an extension of the shorter wire in excess of that of the longer wire, given by

$$\epsilon = Le^{k\alpha M/A} + (K-1)L - KLe^{(1-k)\alpha M/A}.$$

If d is the distance between the knife-edges attached to the wires this excess extension will cause a tilt θ of the ratio-bar, given by

$$\theta = \frac{L}{d}\{e^{k\alpha M/A} - 1 - K(e^{(1-k)\alpha M/A} - 1)\}. \quad . \quad . \quad . \quad (4)$$

Now in the experiments K differs only very slightly from 2, let it be $2+\Delta K$, and k is nearly 2/3, say $2/3+\Delta k$; hence

$$\frac{\theta d}{L} = e^{(2/3+\Delta k)\alpha M/A} - 1 - (2-K)\{e^{(1/3-\Delta k)\alpha M/A} - 1\}.$$

Expanding

$$\frac{\theta d}{L} = 1 + \overline{2/3+\Delta k}.\alpha M/A + \frac{1}{2}\{2/3+\Delta k.\alpha M/A\}^2 + \frac{1}{3}\{\overline{2/3+\Delta k}.\alpha M/A\}^3 + \ldots . - 1 - (2+\Delta K)\Big[1 + \overline{1/3-\Delta k}.\alpha M/A - \frac{1}{2}\{1/3-\Delta k.\alpha M/A\}^2 + \frac{1}{3}\{\overline{1/3-\Delta k}.\alpha M/A\}^3 + \ldots . - 1\Big].$$

Collecting terms and neglecting errors of the second order

$$\frac{\theta d}{L} = \frac{\alpha M}{A}\{3\Delta k - \Delta K/3\} + \frac{\alpha^2 M^2}{2A^2} - \{2/9 + 8\Delta k/3 - \Delta K/9\} + \frac{\alpha^3 M^3}{3A^3}\{2/9 + 2\Delta k - \Delta K/27\} + \quad . \quad . \quad . \quad (4')$$

The error ΔK in the ratio of the lengths of the wires is caused by an error in their lengths—taking them as $100+\Delta l_1$ and $200+\Delta l_2$ cm., the following values of ΔK are obtained for the corresponding values of Δl_1 and Δl_2:—

Δl_1 ...	0·1 cm.	0·1 cm.	0·0 cm.	0·1 cm.	0·01 cm.
Δl_2 ...	−0·1	0·1	0·1	0·0	0·00
ΔK ...	−0·0030	0·0010	0·0010	−0·0020	−0·0002

By assuming an error of 0·1 cm. in the lengths of the wires, as in the table, the error in K is made the greatest that could possibly arise, the general accuracy attained being more closely represented by taking the error in the lengths as 0·01 cm., which reduces the error in K to one-tenth, as shown. The error from this cause in the mean value of a series of experiments would be further reduced by the random distribution of sign of the small increments Δl_1 and Δl_2.

The error Δk in the distribution of the load (see Part I. [9]) consists of :

(*a*) Error in the ratio of the ratio-bar from the strict value.

Material.	Load (kgm.).	Error in ratio-bar.	Error due to knife-edges in different planes.	Error due to initial load.	Δk.
Steel, heat treatment A ..	1	$-5{\cdot}57\times10^{-4}$	..	$44{\cdot}24\times10^{-4}$	$38{\cdot}67\times10^{-4}$
	6	$-5{\cdot}57\times10^{-4}$	$-0{\cdot}29\times10^{-4}$	$8{\cdot}03\times10^{-4}$	$2{\cdot}18\times10^{-4}$
	11	$-5{\cdot}57\times10^{-4}$	$-0{\cdot}53\times10^{-4}$	$4{\cdot}16\times10^{-4}$	$-1{\cdot}93\times10^{-4}$
Copper, specimen II., heat treatment A ..	0·5	$0{\cdot}77\times10^{-4}$	..	..	$0{\cdot}77\times10^{-4}$
	1·25	$0{\cdot}77\times10^{-4}$	$-0{\cdot}41\times10^{-4}$	..	$0{\cdot}36\times10^{-4}$
	1·75	$0{\cdot}77\times10^{-4}$	$-1{\cdot}29\times10^{-4}$	..	$-0{\cdot}52\times10^{-4}$
Tin	0·00	$0{\cdot}77\times10^{-4}$	..	..	$0{\cdot}77\times10^{-4}$
	0·05	$0{\cdot}77\times10^{-4}$	$-0{\cdot}48\times10^{-4}$	..	$0{\cdot}29\times10^{-4}$
	0·10	$0{\cdot}77\times10^{-4}$	$-1{\cdot}79\times10^{-4}$	..	$-1{\cdot}02\times10^{-4}$

(*b*) Error due to the knife-edges not being in the same plane, making the ratios $2(1-0{\cdot}1\tan\theta):1$ for the steel bar and $2(1-0{\cdot}6\tan\theta):1$ for the aluminium bar.

(*c*) Error due to small initial loads m_1 and m_2 on the wires L and KL respectively, causing the ratio to be $2\mathrm{M}-3m_1 : \mathrm{M}-3m_2$.

The total error Δk in the ratio has been taken as the sum of the three, and has been calculated at different loads for three typical materials (steel, heat treatment A; copper, specimen II., heat treatment A; tin).

The effect of these errors on the coefficients in equation (4′) can now be calculated, and is shown in the following table; $\Delta\mathrm{K}$ has been given the value of $\pm 0{\cdot}0010$.

Material.	Load (kgm.).	Error in coefficient $(3\Delta k-\Delta\mathrm{K}/3)$ having value 0·00000 for no error.	Error in coefficient $(2/9+8\Delta k/3-\Delta\mathrm{K}/9)$ having value 0·22222 for no error.	Error in coefficient $(2/9+2\Delta k-\Delta\mathrm{K}/27)$ having value 0·22222 for no error.
Steel, heat treatment A.	1	$0{\cdot}01160\pm0{\cdot}00033$	$0{\cdot}01031\pm0{\cdot}00011$	$0{\cdot}00773\pm0{\cdot}00004$
	6	$0{\cdot}00065\pm0{\cdot}00033$	$0{\cdot}00058\pm0{\cdot}00011$	$0{\cdot}00044\pm0{\cdot}00004$
	11	$-0{\cdot}00059\pm0{\cdot}00033$	$-0{\cdot}00051\pm0{\cdot}00011$	$-0{\cdot}00039\pm0{\cdot}00004$
Copper, specimen II., heat treatment A.	0·5	$0{\cdot}00023\pm0{\cdot}00033$	$0{\cdot}00021\pm0{\cdot}00011$	$0{\cdot}00015\pm0{\cdot}00004$
	1·25	$0{\cdot}00012\pm0{\cdot}00033$	$0{\cdot}00010\pm0{\cdot}00011$	$0{\cdot}00007\pm0{\cdot}00004$
	1·75	$-0{\cdot}00016\pm0{\cdot}00033$	$-0{\cdot}00014\pm0{\cdot}00011$	$-0{\cdot}00010\pm0{\cdot}00004$
Tin	0·00	$0{\cdot}00023\pm0{\cdot}00033$	$0{\cdot}00021\pm0{\cdot}00011$	$0{\cdot}00015\pm0{\cdot}00004$
	0·05	$0{\cdot}00009\pm0{\cdot}00033$	$0{\cdot}00007\pm0{\cdot}00011$	$0{\cdot}00006\pm0{\cdot}00004$
	0·10	$-0{\cdot}00031\pm0{\cdot}00033$	$-0{\cdot}00027\pm0{\cdot}00011$	$-0{\cdot}00020\pm0{\cdot}00004$

Consideration of these representative values of the effect of the instrumental errors leads to the conclusion that they can be safely neglected.

Equation (4) thus becomes

$$\frac{\theta d}{\mathrm{L}} = e^{2\alpha\mathrm{M}/3\mathrm{A}} - 2e^{\alpha\mathrm{M}/3\mathrm{A}} + 1.$$

Hence $$\alpha\mathrm{M}/3\mathrm{A} = \log_e(1+\sqrt{d\theta/\mathrm{L}}).$$

Now θ, the angle of tilt of the mirror on the ratio-bar, will cause a deflexion δ on a scale placed a distance λ from the mirror, and as it is always small

$$\theta = \delta/2\lambda,$$

and the " excess extension per unit length of the shorter wire "

$$\eta = d\delta/2\lambda L.$$

Thus $$\alpha M/3A = \log_e(1+\sqrt{\eta}), \quad . \quad . \quad . \quad . \quad . \quad (5)$$

and a straight-line plot can be obtained between the load and excess extension.

Fig. 1.

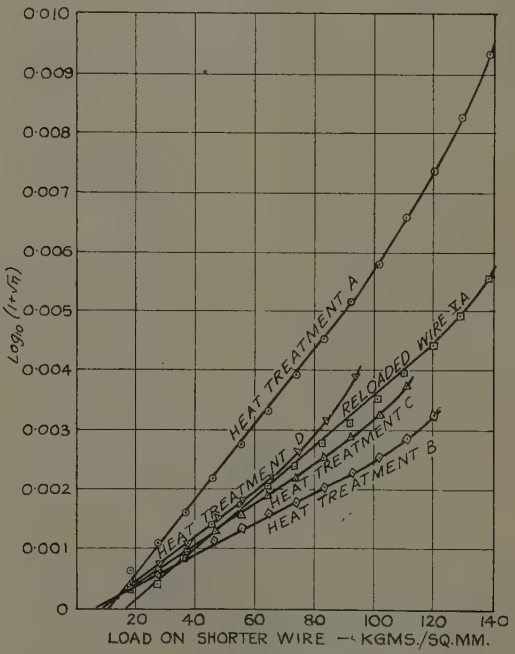

$\mathrm{Log}_{10}(1+\sqrt{\eta})$—load curves for steel.

For convenience values of $P=2M/3A$, the force per unit area on the shorter wire, have been plotted against $\log_{10}(1+\sqrt{\eta})$, the equation of the line thus becoming

$$\alpha P/2 = 2{\cdot}3026 \log_{10}(1+\sqrt{\eta}).$$

The curves are given in figs. 1–4, and in all cases are straight lines up to a critical load. The curves do not

pass through the origin as they should for the ideal case, but have an intercept on the load axis, the value of which

Fig. 2.

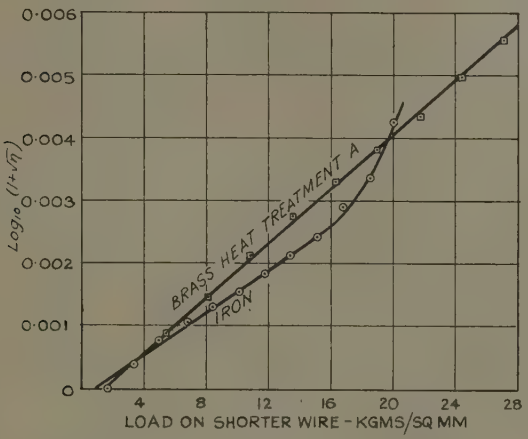

$\mathrm{Log}_{10}(1+\sqrt{\eta})$—load curves for iron and brass.

Fig. 3.

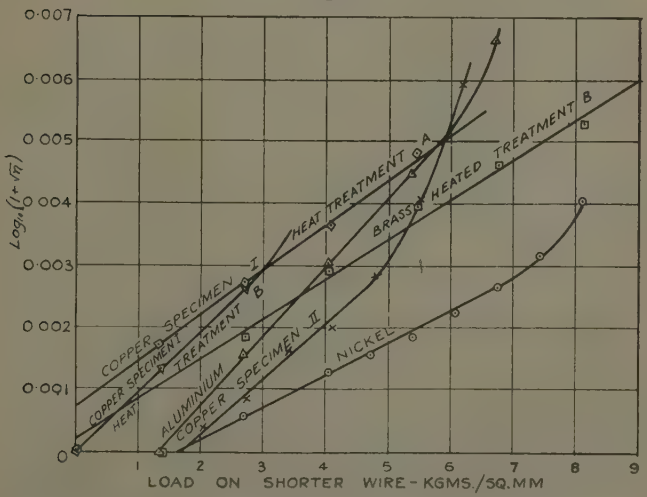

$\mathrm{Log}_{10}(1+\sqrt{\eta})$—load curves for nickel, copper, aluminium, and brass.

depends on the material, being largest for steel, decreasing in value for materials of smaller tensile strength, and becoming negative for the very soft metals, viz., zinc, tin, lead.

Fig. 4.

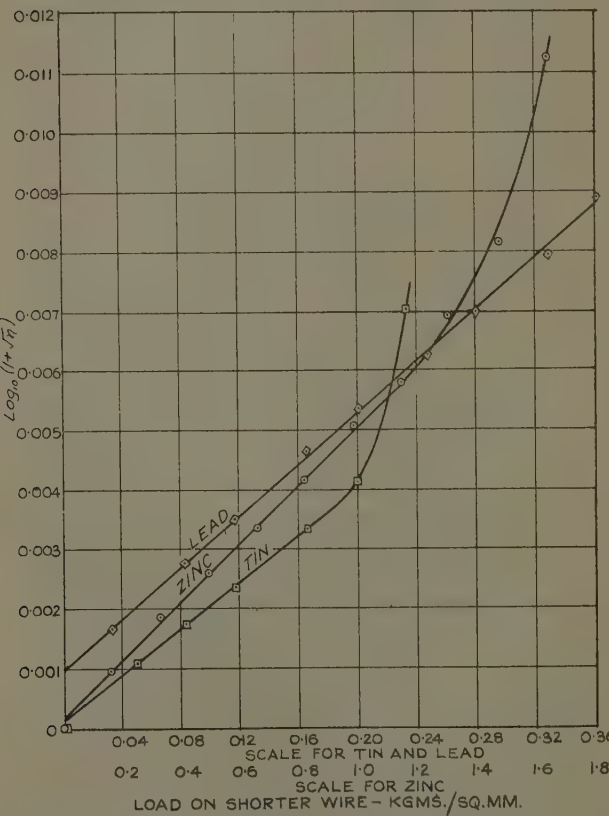

$\mathrm{Log}_{10}(1+\sqrt{\eta})$—load curves for lead, tin, and zinc.

An explanation of this may be offered by the fact that the harder wires require a definite load to keep them taut, this load being applied before excess extension measurements could be made, while the soft wires

experience an excess extension for the zero value of the applied load.

The values of α, based on the original length and cross-sectional area of the wires, have been calculated from the slopes of the curves, and are given below, together with the values of $1/\alpha$ and Young's Modulus for the metals according to Landolt and Börnstein.

Material.	$\alpha \times 10^4$.	$\frac{1}{\alpha}\left(\frac{\text{kgm.}}{\text{sq. mm.}}\right)$.	Young's Modulus $\left(\frac{\text{kgm.}}{\text{sq. mm.}}\right)$.
Steel, heat treatment A	2·94	3401	
,, ,, ,, reloaded VA ..	2·00	5000	
,, ,, ,, B	1·21	8264	20 000
,, ,, ,, C	1·61	6211	
,, ,, ,, D	1·84	5435	
Iron	8·03	1245	20 000
Nickel	23·4	427	22 000
Brass, heat treatment A	10·1	990	10 000
,, ,, ,, B	29·9	334	
Copper, specimen I., heat treatment A.	34·8	287	
,, ,, I., ,, ,, B.	44·2	226	12 000
,, ,, II., ,, ,, A.	39·8	251	
Aluminium	51·2	195	7 200
Zinc	227	44	10 000
Tin	901	11·1	5 000
Lead	1005	9·96	1 600

Attempts to fit the algebraic and power laws to the experimental results showed that they failed to express the observations, and hence it may be concluded that the simple expression

$$L = L_0 e^{\alpha p}$$

best represents the extension of a metal wire under longitudinal stress.

The Value of the Elastic Constant.

It will be seen that the exponential expression readily reduces on expansion to the algebraic form for the extension. Further, since

$$L = L_0 e^{\alpha p},$$

the extension per unit length

$$x=(L-L_0)/L_0=e^{\alpha p}-1,$$

and hence, if the elastic modulus is defined as

$$E=p/x=p/(e^{\alpha p}-1)=1/(\alpha+\alpha^2 p/2\ \ldots.),$$

which agrees with (1) while, if it is defined as

$$E'=dp/dx=1/\alpha e^{\alpha p}=\frac{1}{\alpha}(1-\alpha p+\frac{\alpha^2 p}{2}\ \ldots.),$$

which approximates to the Grüneisen expression

$$E'=E_0-cp,$$

E_0 having the value $1/\alpha$.

It will be observed that the values of $1/\alpha$ are very much smaller than the corresponding values of Young's Modulus. Within the last few years considerable attention has been devoted in engineering circles to the development of "short" and "long" time tensile and other tests of the strength of materials (*vide* Tapsell, 'Creep of Metals,' Oxford, 1931). These investigations have shown that if the duration of an experiment be considerably extended continuous "creep" is observed, which gives a resulting total extension far in excess of the initial "elastic" deformation on which Young's Modulus is calculated. The magnitude of the creep varies with the load and temperature, and will either increase and finally cause fracture or decrease and ultimately cease. For the small loads and low temperatures (relative to the melting-point) employed in the present experiments the creep observed is of the latter class, and it was after the cessation of the creep, as exhibited by the sensitive extensometer employed, that the extension measurements were made (see Part II.). Thus the values of $1/\alpha$ are determined by the total extension of the specimen after creep, and comparison with the values of Young's Modulus, which have been obtained from special experiments of short duration, is not justified. It is worthy of note that the "softer" the metal, *i. e.*, the greater the capacity for flow, the greater the difference between the values.

Experimental determinations in support of this hypothesis are offered by a recent paper on the Pomp-Enders short-time creep test [10] for a 0·1 per cent. carbon steel at 500° C. The results are given in the following table for the initial creep and total percentage extensions

of six specimens under a load of 5 kgm./sq. mm., and the corresponding values of "Young's Modulus" calculated for initial and total extension.

	Initial load extension per cent.	Creep time extension per cent.	Total extension per cent.	"Young's Modulus." Initial extension $\left(\frac{\text{kgm.}}{\text{sq. mm.}}\right)$.	"Young's Modulus." Total extension $\left(\frac{\text{kgm.}}{\text{sq. mm}}\right)$.
I.	0·051	0·181	0·232	19 610	4 310
II.	0·040	0·096	0·136	25 000	7 350
III.	0·038	0·138	0·176	26 300	5 680
IV.	0·042	0·098	0·140	23 800	7 140
V.	0·040	0·088	0·128	25 000	7 810
VI.	0·058	0·184	0·242	17 230	4 130

It will be noted that these values of "Young's Modulus" for initial and total extensions are in excellent agreement with the values as usually accepted and those given by the present "complete extension" readings.

Limit of the Law.

In the literature of elasticity there is much confusion in the definition of the elastic constants. Thus, the "elastic limit" may be defined as the least load producing permanent "set," or as the "limit of proportionality"—which it is recognized depends on the sensitiveness of the testing machine or as the load necessary to cause a given small deviation from Hooke's law, and for practical purposes it is sometimes considered to be coincident with the "yield point," defined as the load for which the extension increases without increase of the load. Further, Tammann [11] used the method of observing the first signs of slip to determine the elastic limit, and obtained very low values.

The position is not simplified by the marked difference in behaviour of the ferrous and non-ferrous metals. Thus the stress-strain curve for a non-ferrous metal has a curved path almost from the start, and no elastic limit or yield-point can be accurately defined. On the other hand, the ferrous metals give almost linear curves up to a very well defined yield-point, which is only slightly greater than the elastic limit. If, however, the ferrous metal

has been severely cold-worked it will behave similarly to the non-ferrous metals. Excellent curves illustrating these points have been obtained by Dalby [12] with his optical recorder.

A. 'Strength and Structure of Steel and other Metals' (Dalby). Arnold, 1923.

B. 'The Properties of Engineering Materials' (Popplewell and Carrington). Methuen, 1923.

C. 'Mechanical Engineer's Handbook.' McGraw-Hill Book Co.

D. 'Comprehensive Treatise on Inorganic and Theoretical Chemistry' (Mellor, vols. v. & vii.). Longmans and Co.

E. Tammann, *Zeits. für Phys. Chem.* vol. lxxv. pp. 108–126.

Material.	Limit of law $\left(\frac{\text{kgm.}}{\text{sq. mm.}}\right)$.	Elastic limit $\left(\frac{\text{kgm.}}{\text{sq. mm.}}\right)$.	Yield point $\left(\frac{\text{kgm.}}{\text{sq. mm.}}\right)$.
Steel, heat treatment A ..	101	Crucible Steel Wire 100 (C)	—
Steel, heat treatment reloaded VA	109		—
Steel, heat treatment B ..	102		—
Steel, heat treatment C ..	102		—
Steel, heat treatment D ..	74·5		—
Iron	15·1	14·8–18·3 (C)	14·8–17·4 (B) 19·7–23·9 (C)
Nickel	6·7	7·8 (E)	—
Brass, heat treatment A ..	27*	—	8·45–20·4 (B)
Brass, heat treatment B ..	10·8*	—	
Copper, specimen I., heat treatment A.....	5·4*	2·03 (E)	3·94 (B)
Copper, specimen I., heat treatment B.....	2·7		4·1 (A)
Copper, specimen II., heat treatment A.....	4·8		5·67 (A)
Aluminium	5·3	2·8–4·57 (C)	5·5–6·3 (D)
Zinc	1·14	1st slip bands Limit of proportionality	1·75 1·20 (D)
Tin	0·165	0·1575 (D)	—
Lead	0·360*	0·08 (D)	1·5 (B)

* For this stress, the largest measured, the law was still obeyed.

The maximum values of the load for which the exponential law holds are compared in the preceding table with the values of the elastic limit and of the yield-point as given by the following authorities, reduced for convenience to metric measurements.

The variations of the values of the limit for steel subjected to various heat treatments is in agreement with the experiments of Aitchinson (see Adam[13], p. 130), showing the mechanical properties in tension of steels as drawn, and after blueing at different temperatures.

Specimen I.			Specimen II.		
Blueing temperature.	Elastic limit $\left(\frac{\text{tns.}}{\text{sq. in.}}\right)$.	Yield point $\left(\frac{\text{tns.}}{\text{sq. in.}}\right)$.	Blueing temperature.	Elastic limit $\left(\frac{\text{tns.}}{\text{sq. ins.}}\right)$	Yield point $\left(\frac{\text{tns.}}{\text{sq. in.}}\right)$.
—	18·2	36·8	—	18·2	26·1
250° C.	20·5	36·6	250° C.	20·5	31·2
400	28·1	28·4	400	25·0	30·5
550	25·0	26·4	550	20·5	27·2

From this table it seems reasonable to identify the limit of the exponential law and the yield point for all metals, and this view receives support from the behaviour of the metals above this critical load. Thus the new law simplifies the position, requiring only one critical stress the yield point.

Theory.

Many suggestions have been put forward to explain the deviation from Hooke's law. For example, the decrease of cross-sectional area and increase of length caused by loading would make the extension exceed that expected by Hooke's law; but, as Schulze [6] pointed out, this effect is only 1/1000th of that observed by Thompson[3].

It is generally accepted that the forces between the atoms or molecules of a body consist of a force of attraction and a force of repulsion, the total force being represented as

$$f = mA/r^{m-1} - nB/r^{n-1},$$

r being the distance apart of the molecules and A, B, m and n constants.

Joffé [14] has shown that, expanding by Maclaurin's series,

$$f=f_0-f'(\Delta r)-\frac{1}{\underline{2}}f''(\Delta r)-\frac{1}{\underline{3}}f'''(\Delta r)\ldots,$$

and assuming $f_0=0$, and neglecting all terms containing r in a power higher than the first, we obtain Hooke's law,

$$f=f'(\Delta r).$$

Thus no proportional limit can really be expected to exist.

However, it seems very probable that this hypothesis is also inadequate to account for the large deviation found experimentally, and consideration of the crystalline structure of the metal offers a far more fruitful field, particularly in view of the recent production of metal single crystals and the investigation of their mechanical properties. To quote Prof. Carpenter [15] :—

"The softness of single crystal bars indicates that they can only possess a very low limit of proportionality under stress, and, indeed, raises a doubt whether they can properly be described as possessing any limit of proportionality at all. This point has been carefully tested by Gough, Hanson, and Wright [16] in the case of the metal aluminium. The limit of proportionality in tension of a polycrystalline bar is just about one ton per square inch. These investigators found that the single crystal bars possess no primitive limit of elasticity, but plastic straining occurred under the least stress applied. Furthermore, they conclude from the slope of the stress-strain diagram, even at the 10–40 lb. range, that no primitive state of elasticity existed. It is clear, therefore, that the well-defined elastic limit found in the polycrystalline bar is not a property of the metal crystal but of the crystal aggregate in the case of aluminium." It seems permissible to extend this last statement to all metals.

Jenkin [17] has offered an explanation of the slip in certain crystal units at very low stresses. Arguing from a study of simple models, he suggests that it is purely an accidental condition due to certain of the crystal units being under initial stress, so that slip occurs in these when a slight additional load is put on, thus causing minute yielding of the test piece and a slight departure from the

proportionality of stress and strain. This condition he showed by his model could be removed by submitting it to alternating stresses of sufficient magnitude to bring all the units into a "stress free" condition. Acting on this hypothesis, Gough found that copper could be restored to the elastic condition by previously applying alternating stresses. This idea of certain crystal units being in a state of stress seems particularly applicable to metals in the cold-worked condition, since some of the crystals must be left just on the point of slipping after the last application of cold work, and only a very slight additional load would be sufficient to cause slip; hence the low elastic limit. This hypothesis also affords an explanation of the recovery of elasticity by ageing and mild blueing, which must be expected to release the internal stresses, thus agreeing with the present experiments. Further, limited loading can be considered to cause flow in almost all the initially strained crystals without sufficiently straining others to the critical conditions, thus accounting for the much smaller deviation on reloading.

It is difficult, however, to reconcile these conditions of crystals under initial stress with the usual ideas of metals which have been annealed above the recrystallization temperature, when they should be completely stress free.

It is known that when a metal is stressed yield does not occur in all crystals simultaneously, but occurs first in a few specially situated, so that shear takes place on the 45° plane. Thus, as the crystals themselves slip under very small forces it can be assumed that certain crystals, orientated so that their slip planes are coincident with the plane of maximum stress, will undergo plastic deformation. As slip occurs the crystals harden, and slipping will finally be stopped by internal resistance. Further, the crystals being differently orientated, the motion of those in the plastic state will also be restricted by their neighbours, thus further limiting the amount of the extension. As Hopkinson first demonstrated, it takes time for the crystal to slip, and he further showed that for a very short duration of the stress, say one-thousandth of a second, metals were elastic far beyond their ordinary limit. This is in line with the experimental observation (see Part II.) that the deviation from Hooke's law

increased with time to a maximum value. Further, the greater the size of the crystal units the greater the amount of flow in the crystals; experimental evidence in support of this statement is supplied by the increase of ductility with increase of crystal size found by Carpenter and Elam [18] for aluminium. Hence an explanation is offered for the observations (see Part II.) that the deviation from Hooke's law was greater for non-ferrous metals the higher the annealing temperature, *i. e.*, resulting crystal size.

To recapitulate: the behaviour may be regarded as follows:—On immediate loading the material extends elastically, a property which is solely that of the crystal aggregate; slip then begins to occur in certain suitable crystals, giving the elastic after-effect and causing the deviation from proportionality of stress and strain.

This view would also enable us to appreciate the significance of Schulze's statement that the "adiabatic" elastic modulus depends only on the load, and is independent of the amount and duration of the after-effect; for it is quite conceivable that slip could occur in many individual crystals (causing the after-effect) without affecting the elastic modulus (which is solely a property of the aggregate).

Summary.

1. The stress and total extension have been shown to be connected by an exponential relation even at small loads.

2. The upper limit of the range for which this relation holds has been identified with the yield point.

3. The deviations from proportionality of stress and strain have been attributed to plastic distortion in certain suitably disposed crystals.

Acknowledgment.

In conclusion, I have to thank Professor Lees for granting facilities in the Physical Laboratories of the East London College for performing this work, and for the interest he has taken in it. I desire also to express thanks for a grant from H.M. Department of Scientific and Industrial Research, and to Dr. Crow and the Ordnance Committee for permission to publish this paper.

References.

(1) C. Bach, *Zeitschr. Ver. d. Ing.* 1888, pp. 193, 221, 1089; 1895, p. 489; 1896, p. 1381; 1897, p. 1. See also 'Elastizitat und Festigkeit.'
(2) G. Stradling, Wied. *Ann.* xli. p. 332 (1890).
(3) Thompson, *Ann. d. Phys.* xliv. p. 555 (1891).
(4) G. S. Meyer, Wied. *Ann.* lix. p. 668 (1896).
(5) Grüneisen, *Verh. phys. Ges.* p. 469 (1906); *Phys. Zeitschr.* vii. p. 901 (1906); *Ann. d. Phys.* xxii. p. 81 (1907); xxv. p. 825 (1908).
(6) Schulze, *Ann. d. Phys.* xxxi. p. 1 (1910).
(7) Kyrillov, *Jurn. Russk. Kisik-chimičesk. Obščestva*, xxxix. no. 3, p. 64 (1907).
(8) Tyte, Phil. Mag. xiii. p. 49 (1932).
(9) Tyte, Phil. Mag. x. p. 1043 (1930).
(10) 'Engineering,' cxxxiv. p. 232 (Aug. 26, 1932).
(11) Tammann, *Zeits. f. Phys. Chem.* lxxv. pp. 108–126.
(12) Dalby, 'Strength and Structure of Steel and other Metals' (Arnold, 1923); and numerous papers.
(13) Adam, 'Wire Drawing and the Cold Working of Steel' (Witherby, 1925).
(14) Joffé, 'The Physics of Crystals.'
(15) Carpenter, 'Nature,' cxxvi. p. 17 (July 5, 1930).
(16) Gough, Hanson, and Wright, Phil. Trans. Roy. Soc. A, ccxxvi. p. 1 (1925).
(17) Jenkin, 'Engineering' cxxxiv. p. 612 (Dec. 8, 1922).
(18) Carpenter and Elam, Proc. Roy. Soc. A, c. p. 329 (1921).

LIV. *Oscillations in High-Speed Jets of Compressible Fluid.*

By S. G. Hooker, *B.Sc., A.R.C.S., Brasenose College, Oxford* *.

1. A CHARACTERISTIC property of a jet of elastic liquid, issuing from a nozzle with a velocity exceeding that of sound, is that it exhibits a regular periodic structure due to oscillatory fluctuations of velocity and density.

This phenomenon has been recognized for many years, for in his book on 'Steam Turbines' † Stodola mentions that the presence of oscillations at the exit of steam from nozzles was observed previous to 1903 by Kienast, Gutermuth, and Emden ‡, and has given an account of much experimental evidence on the point.

2. More recently, in a paper "On the Production of Acoustic Waves by Means of an Air Jet of a Velocity

* Communicated by Prof. R. V. Southwell, M.A., F.R.S.
† 2nd Edition (English), 1906, p. 85.
‡ R. Emden, Wiedemanns *Annalen*, lxix. p. 264 (1899).

exceeding that of Sound." Dr. J. Hartmann * has described some of the properties of a high-speed jet as determined experimentally.

Fig. 1, which has been taken from his paper, shows an air jet J, moving with a super-sound velocity, being discharged from a nozzle N. The condition necessary to produce the jet (if emitted into the free atmosphere) is that the excess pressure in the container shall be greater than 0·9 atmosphere. If the excess pressure is not too high (say 2 to 4 atmospheres), the periodic features of the air jet obtained are easily demonstrated: a Pitot tube S is directed along the axis against the outcoming jet, and the pressures recorded by a manometer M are plotted against X the distance from the nozzle. The

Fig. 1.

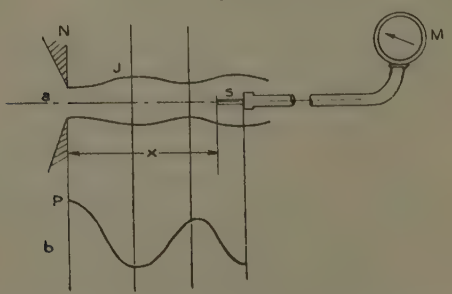

resulting curve is always periodic by nature as shown in (*b*) fig. 1.

Hartmann says: "It should be noted that a Pitot curve of periodic character is a characteristic of the jet if the velocity is greater than that of sound: with a jet whose velocity is less than sound the Pitot pressure is nearly constant."

The periodic structure of the jet is also shown in photographs taken by the method of striæ, and the theoretical explanation of the structure is due to Prandtl †.

3. Prandtl considered the case of a uniform jet of fluid of circular section escaping from a pipe of radius ϖ_0. Assuming that the free surface of the jet is oscillating,

* Phil. Mag. xi. p. 926 (1931).

† L. Prandtl, *Phys. Zeit.* 1904 and 1907.

while the axis remains an axis of symmetry throughout the disturbed motion which ensues, he found the appropriate expression for the velocity potential ϕ to be

$$\phi = -Ux + AJ_0(m\alpha\varpi)\cos mx, \quad . \quad . \quad . \quad (1)$$

where m is the frequency of the oscillation, and

$$\alpha^2 = \frac{(\gamma+1)(U^2-1)}{\gamma+1-\gamma-1U^2}. \quad . \quad . \quad . \quad . \quad . \quad . \quad (2)$$

U is the velocity of the undisturbed jet measured as a fraction of the speed of sound; and γ is the ratio of the specific heats for the gas under consideration.

From (1) it follows that the resultant velocity q at any point is given by

$$q^2 = U^2 - 2AmJ_0(m\alpha\varpi)\sin mx,$$

provided that the square of the small arbitrary constant A may be neglected. Now the pressure p is a function of q and γ only, and hence the constancy of p, for all values of x, at the free surfaces $\varpi = \varpi_0$ demands that

$$J_0(m\alpha\varpi_0) = 0.$$

The smallest root of this equation is

$$m\alpha\varpi_0 = 2{\cdot}405.$$

For any given speed U, using (2) to determine the value of α, we find that the fundamental frequency of the possible stationary oscillations is given by

$$m = \frac{2{\cdot}405}{\alpha\varpi_0}, \quad . \quad . \quad . \quad . \quad . \quad . \quad . \quad (3)$$

and the jet will appear to "bulge" and "contract" at regular intervals of x given by $2\pi/m$.

4. Hartmann includes in his paper some very beautiful photographs of jets, taken by the method of striæ, which illustrate in a striking manner the regular periodic formation of an undisturbed jet. In fig. 3 (pl. vii.) of his work he gives eight pictures showing the change in the structure of the jet as the excess pressure is raised by steps from 3·0 to 6·5 atmospheres. Numerical values are not given in his paper, but it is possible to measure

up these jets, and I have done so to obtain the following values :—

Excess pressure ..	3·0	3·5	4·0	4·5	5·0	5·5	6·0	6·5
λ/ϖ_0	2·8	3·0	3·4	3·8	4·0	4·20	4·60	4·60

In this table ϖ_0 denotes the radius of the jet (which was circular) and λ the wave-length of the oscillations as determined from the photographs. The values of the wave-length given in the last two columns—corresponding to excess pressures of 6 and 6·5 atmospheres—were difficult to determine, as the jet was beginning to break up.

In the absence of more accurate information, these rough measurements will be used to check Prandtl's theory. In the first place it is necessary to calculate the velocity of the stream corresponding with a given excess pressure: once this has been done, α can be determined, and hence the theoretical wave-length of oscillation, which can then be compared with the experimental measurements given above.

5. If p_0 and ρ_0 are the pressures and density of the air in the container, where we will assume the velocity to be zero, Bernouilli's equation gives

$$\frac{a^2}{\gamma-1}\left(\frac{p}{p_0}\right)^{\gamma-1/\gamma}+\tfrac{1}{2}q^2=\text{const.}, \quad . \quad . \quad . \quad (4)$$

where

$$a^2=\frac{\gamma p_0}{\rho_0},$$

and p is the pressure at a point where the fluid velocity is q.

Putting in the appropriate constant to make $p=p_0$ when $q=0$, we have from this equation

$$\frac{q^2}{a^2}=\frac{2}{\gamma-1}\left\{1-\left(\frac{p}{p_0}\right)^{\gamma-1/\gamma}\right\}. \quad . \quad . \quad . \quad . \quad (5)$$

If the jet is emitted into the free atmosphere, the static pressure p in the jet must be equal to the atmospheric pressure p_1. If we assume that the air in the container was compressed *isothermally* from atmospheric pressure and density to the pressure and density p_0, ρ_0, then

$$\frac{p_0}{\rho_0}=\frac{p_1}{\rho_1},$$

so that $$a^2=\frac{\gamma p_0}{\rho_0}=\frac{\gamma p_1}{\rho_1},$$

and a is the velocity of sound in stationary air at atmospheric condition.

In the theoretical work we used as the unit of velocity the local speed of sound; that is, the speed of sound at a point where the velocity of the fluid and sound are equal. If a_0 is the velocity of sound corresponding with a density ρ, then

$$\frac{a^2}{a_0^2}=\frac{\gamma p_0}{\rho_0}\cdot\frac{\rho}{\gamma p}=\frac{p_0}{p}\cdot\frac{\rho}{\rho_0}=\frac{1}{\left(\frac{p}{\rho_0}\right)^{\gamma}}\cdot\frac{\rho}{\rho_0}$$

$$=\frac{1}{\left(\frac{\rho}{\rho_0}\right)^{\gamma-1}}=\frac{1}{\left(\frac{p}{p_0}\right)^{\gamma-1/\gamma}},$$

or

$$\frac{a^2}{a_0^2}\left(\frac{p}{p_0}\right)^{\gamma-1/\gamma}=1. \quad . \quad . \quad . \quad . \quad . \quad (6)$$

But, from (5),

$$\left(\frac{p}{p_0}\right)^{\gamma-1/\gamma}=1-\frac{\gamma-1}{2}\cdot\frac{q^2}{a^2},$$

and we wish to determine the velocity of sound a_0 at a point where $q=a_0$. Therefore

$$\left(\frac{p}{p_0}\right)^{\gamma-1/\gamma}=1-\frac{\gamma-1}{2}\cdot\frac{a_0^2}{a^2},$$

and on substituting in (6) we have

$$\frac{a^2}{a_0^2}\left\{1-\frac{\gamma-1}{2}\cdot\frac{a_0^2}{a^2}\right\}=1,$$

or

$$\frac{a^2}{a_0^2}=\frac{\gamma+1}{2} \quad . \quad . \quad . \quad . \quad . \quad . \quad . \quad (7)$$

Giving γ the value it has for air, viz. :—

$$\gamma=1{\cdot}408,$$

we can write (5) in the form

$$\frac{q^2}{a^2}=4{\cdot}9\left\{1-\left(\frac{p}{p_0}\right)^{0{\cdot}29}\right\}, \quad . \quad . \quad . \quad (8)$$

Excess pressure (atmospheres).	$\frac{p_1}{p_0}$.	$\log\frac{p_1}{p_0}$.	$\cdot 29\log\frac{p_1}{p_0}$.	antilog.	$1-\left(\frac{p_1}{p_0}\right)^{0\cdot29}$.	$4\cdot9\left\{1-\left(\frac{p_1}{p_0}\right)^{0\cdot29}\right\}$.	$\frac{q}{a}$.	$\frac{q}{a_0}=\mathrm{U}$.	α.
3·0	$\frac{1}{4}$	−·602	−·1745	·668	·332	1·625	1·275	1·400	1·20
3·5	$\frac{1}{4\cdot5}$	−·653	−·1895	·646	·354	1·735	1·317	1·446	1·30
4·0	$\frac{1}{5}$	−·699	−·203	·627	·373	1·826	1·35	1·460	1·40
4·5	$\frac{1}{5\cdot5}$	−·741	−·2146	·610	·390	1·91	1·38	1·515	1·47
5·0	$\frac{1}{6}$	−·778	−·226	·594	·406	1·990	1·41	1·545	1·54
5·5	$\frac{1}{6\cdot5}$	−·813	−·236	·580	·420	2·06	1·435	1·575	1·60
6·0	$\frac{1}{7}$	−·846	−·245	·568	·432	2·12	1·455	1·599	1·66
6·5	$\frac{1}{7\cdot5}$	−·875	−·254	·557	·443	2·17	1·473	1·618	1·71

and then (7) becomes

$$\frac{a}{a_0} = \sqrt{\frac{\gamma+1}{2}} = 1{\cdot}097. \quad . \quad . \quad . \quad . \quad (9)$$

In (8), p is atmospheric pressure and p_0 the pressure in the container, which is given by Hartmann in terms of atmospheric pressures. The value of q/a can be determined immediately; and on multiplying its value by 1·097 we obtain q/a_0, which has been denoted by U in § 3.

6. In the preceding table values of q/a_0 are given corresponding with an excess pressure in the container which increases by steps from 3·0 to 6·5 atmospheres. In the last column are given values of α corresponding with the values of U, and calculated from formula (2).

More photographs showing the nature of jets have been given by Bailey and Wood *. Their pictures (figs. 5 *a* and 5 *b* of their paper) demonstrate the difference in structure of the jet when the velocity is below and above that of sound. In the former case no oscillations are evident, while in the latter—with an excess pressure in the container of approximately 2·74 atmospheres—the wave-length of the oscillations is such that

$$\lambda/\varpi_0 = 2{\cdot}70.$$

These figures furnish the last column of the following table :—

	Hartmann.								Bailey and Wood.
Excess pressure	3·0	3·5	4·0	4·5	5·0	5·5	6·0	6·5	2·74
λ/ϖ_0 ...	2·8	3·0	3·4	3·8	4·0	4·20	4·60	4·60	2·70
α	1·20	1·30	1·40	1·47	1·54	1·60	1·66	1·71	1·15

7. It has been shown earlier that the frequency m of the possible stationary oscillations in a jet of circular section (radius ω_0) is given by

$$m\alpha\varpi_0 = 2{\cdot}405.$$

* A.R.C. Reports T. 3362 (477), 'An Investigation of the Principles of the Air Injectors,' Feb. 1933.

Hence
$$\alpha = \frac{2{\cdot}405}{m\varpi_0} = \frac{2{\cdot}405}{2\pi} \cdot \frac{2\pi}{m\varpi_0}$$
$$= \frac{2{\cdot}405}{2\pi} \cdot \frac{\lambda}{\varpi_0},$$

or
$$\alpha = 0{\cdot}382\lambda/\varpi_0, \quad . \quad . \quad . \quad . \quad . \quad . \quad . \quad (10)$$

where λ is the wave-length of the oscillations. Thus α and λ are linearly related, and a graph showing this

Fig. 2.

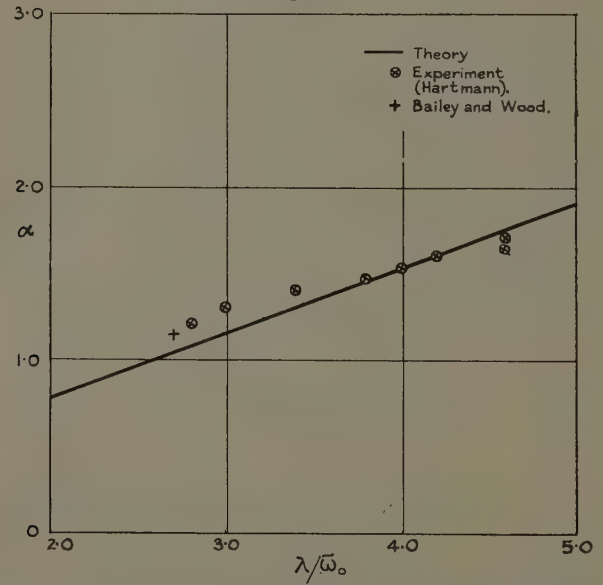

relation is drawn in fig. 2, where the experimental values determined in the preceding table are compared with the theoretical. Taking into consideration the roughness of the measurements the agreement appears to be good.

8. I have remarked earlier that when the excess pressure was 6 and 6·5 atmospheres it was difficult to determine λ/ϖ_0 from the photographs. In this case a white line appeared perpendicular to the axis of the jet, which was the more pronounced the higher the excess pressure, and occurred at the minimum section. Quoting Hartmann,

" . . . this line represents a compression wave, the like of which is always formed in front of any object stopping a flow with a velocity exceeding that of sound (or moving like a bullet through the air with super sound velocity)." The line therefore marks a region of low velocity and, as a result, high static pressure ; the tendency is for the air to flow radially outwards from the axis of the jet to the atmospheric pressure ; and in this process the structure of the jet is destroyed. This is an example of what happens when the critical amplitude of oscillation is exceeded.

9. A further point of interest arises in considering the stability of these jets. The outer bounding stream surfaces obviously constitute surfaces of discontinuity, and it is easy to see that the argument commonly used to demonstrate the instability of such a sheet does not hold if the fluid velocity exceeds that of sound.

Consider a two-dimensional jet. We suppose the outer surface to be displaced into a sine curve, as indicated in the following diagram :—

Fig. 3.

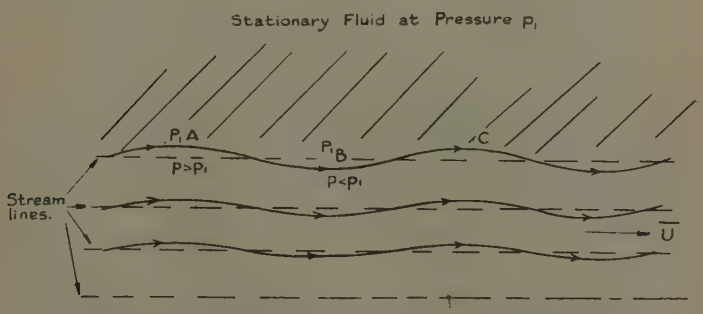

Consider first the normal argument applicable at low speeds when the fluid is sensibly incompressible. The stream lines are concave at A and convex at B, so that the speed of flow at A is less than the speed at B. Consequently, since the static pressure in the undisturbed jet is equal to the pressure p_1 of the surrounding fluid, in the disturbed state the pressure just inside the bounding stream line is greater than p_1 at A and less than p_1 at B. The pressures developed by the disturbance are therefore

of a nature which tends to increase the displacement of the stream lines, and the surface is consequently unstable.

This argument does not apply if the speed of the stream exceeds that of sound. For then the speed in the disturbed state is greater at A than at B, because the stream tube sections are larger at A. Consequently the pressure is less at A and greater at B than that of the surrounding air. The pressures developed by the disturbance therefore tend to restore the stream lines to their original linear course, and we must deem the surface *stable*.

10. Regarding the origin of oscillations in a jet of compressible fluid which is escaping from a nozzle of finite length, we observe that if the pressure p into which the fluid is discharged is lower than the value p_1 which corresponds with the adiabatic expansion required to fill entirely the exit cross-section of the diverging nozzles, then at the moment of leaving the nozzles the jet enters a region of pressure lower than that of the static pressure in the jet, and accordingly experiences a sudden increase of expansion down to the surrounding back pressure In actual fact, the jet overshoots the expansion to p; and too much potential energy is converted into kinetic energy, with the result that oscillations are developed.

This paper has been written during the course of an investigation which the author is conducting under the supervision of Prof. R. V. Southwell at the Engineering Laboratory, Oxford, with the aid of a Senior Research Award from the Department of Scientific and Industrial Research.

LV. *Yellow-Blue Ratio and Personal Errors in Heterochromatic Photometry.* *By* W. S. Stiles, *The National Physical Laboratory**.

Summary.

In this note an approximate formula is derived which gives the personal error when matching brightnesses of different colour temperature, in terms of the yellow-blue

* Communicated by Sir J. E. Petavel, K.B.E., D.Sc., F.R.S.

ratio of the observer. The formula gives results in satisfactory agreement with the errors computed using the complete visibility curves, and also with the errors observed directly.

WHEN making a photometric match between brightnesses of different colour, different observers obtain different results owing to variations in the shapes of their visibility curves. When the brightnesses to be compared are produced by incandescent light sources, a close approximation to the correct result (*i. e.*, the result which would be given by an observer with the standard visibility curve) is obtained by plotting the values given by a group of observers against the yellow-blue (Y/B) ratios of these observers, and taking the value on the best straight line through the results which corresponds to Y/B=1*. This presupposes that the group contains sufficient observers with their Y/B ratios suitably distributed on either side of unity to enable a representative straight line to be drawn. Alternatively, if only one or two observers are available and their Y/B ratios are known, a correction to their values may be applied provided it is known for the colour difference in question how the error of the reading varies with Y/B ratio. Crittenden and Richtmyer † have obtained empirically the relation between personal error and Y/B ratio for photometric matches between the light from a 4 w.p.c. carbon lamp and the light of several other colour temperatures. The object of this note is to derive a general formula giving the personal error in matching any two colour temperatures in terms of the Y/B ratio of the observer.

Suppose we have a brightness whose relative energy distribution is represented by E_λ; E_λ is adjusted to have the value unity at $\lambda=0{\cdot}555\,\mu$. Let the absolute energy in a wave-length interval λ to $\lambda+d\lambda$ be given by $xE_\lambda d\lambda$. Then x is a measure of the brightness in energy units. For an observer whose visibility curve is given

* The yellow-blue ratio is the ratio of the transmissions of two special colour filters, as measured by an observer by a photometric method in which total brightnesses are compared. For a concise statement of the properties of the Y/B filters and the principles underlying their use see Guild, Optical Convention Proc. 1926, p. 100.

† 'Bulletin, Bureau of Standards,' xiv. p. 87 (1918).

by U_λ and whose mechanical equivalent of light is N, the value of the brightness in photometric units will be

$$P = \frac{x}{N}\int_{\cdot 40}^{\cdot 76} U_\lambda E_\lambda d\lambda.$$

Splitting this integral into two parts at the wave-length $\lambda = 0{\cdot}555\ \mu$ (the wave-length at which the standard visibility curve for the light adapted eye has its maximum value), we obtain

$$P = \frac{x}{N}\left\{\int_{\cdot 40}^{\cdot 555} U_\lambda E_\lambda d\lambda + \int_{\cdot 555}^{\cdot 76} U_\lambda E_\lambda d\lambda\right\}$$
$$= \frac{x}{N}(R+S),$$

where

$$R = \int_{\cdot 40}^{\cdot 555} U_\lambda E_\lambda d\lambda,$$
$$S = \int_{\cdot 555}^{\cdot 76} U_\lambda E_\lambda d\lambda.$$

We now make the simplifying assumption that for the various visibility curves met with in practice and for the different energy distributions with which we shall be concerned, R and S can be represented as simple products, $R = U_r e_r$, $S = U_r e_s$, in which U_r and U_s vary from observer to observer, but are independent of the energy distribution, whilst e_r and e_s are the same for all observers but vary with the energy distribution. This assumption would be strictly true whatever the energy distribution, if all visibility curves had the same *shape* in the two halves of the spectrum and differed only in the relative values of the visibility on either side of the central wave-length ($0{\cdot}555\ \mu$). It would also be strictly true whatever forms the visibility curve might assume, provided the energy distribution remained the same in each half of the spectrum, different energy distributions corresponding merely to different values of the energy on either side of the central wave-length. With the mild variations of the visibility curve from the standard visibility curve which occur in practice, and with continuous energy distributions of regular character such as are given by incandescent light sources, we may accept the assumption as an approximation.

We have, then, if E_λ (1) and E_λ (2) are two energy distributions

$$\frac{R_1}{R_2}=\frac{U_r e_{r1}}{U_r e_{r2}}=\frac{e_{r1}}{e_{r2}}=\frac{\bar{U}_r e_{r1}}{\bar{U}_r e_{r2}}=\frac{\bar{R}_1}{\bar{R}_2}, \quad . \quad . \quad . \quad (1)$$

$$\frac{S_1}{S_2}=\frac{U_s e_{s1}}{U_s e_{s2}}=\frac{e_{s1}}{e_{s2}}=\frac{\bar{U}_s e_{s1}}{\bar{U}_s e_{s2}}=\frac{\bar{S}_1}{\bar{S}_2}, \quad . \quad . \quad . \quad (2)$$

$$\frac{S_1}{R_1}=\frac{U_s e_{s1}}{U_r e_{r1}} \qquad \frac{\bar{S}_1}{R_1}=\frac{\bar{U}_s e_{s1}}{\bar{U}_r e_{r1}} \quad . \quad . \quad . \quad (3)$$

Here the suffix 1 or 2 denotes the value of a quantity which corresponds to the energy distribution E_λ (1) or E_λ (2), and symbols with a bar over the top refer to an observer having the standard visibility curve. The ratio of the photometric brightnesses having energy distributions E_λ (1) and E_λ (2) is clearly

$$\frac{P_2}{P_1}=\frac{x_2 R_2+S_2}{x_1 R_1+S_1}=\frac{x_2 R_2}{x_1 R_1}\frac{1+S_2/R_2}{1+S_1/R_1} \text{ for any observer,}$$

$$\frac{P_2}{\bar{P}}=\frac{x_2 \bar{R}_2+S_2}{x_1 \bar{R}_1+S_1}=\frac{x_2 R_2}{x_1 \bar{R}_1}\frac{1+\bar{S}_2/R_2}{1+\bar{S}_1/R_1} \text{ for the standard observer.}$$

Thus $$z=P_2/P_1\Big/\bar{P}_2/\bar{P}_1=\frac{1+S_2/R_2}{1+S_1/R_1}\Big/\frac{1+\bar{S}_2/R_2}{1+\bar{S}_1/R_1}.$$

Putting $\sigma=\dfrac{U_s}{U_r}\Big/\dfrac{\bar{U}_s}{\bar{U}_r}$ and using equations (3), we have

$$z=\frac{1+\sigma\bar{S}_2/\bar{R}_2}{1+\sigma S_1/R_1}\Big/\frac{1+\bar{S}_2/R_2}{1+\bar{S}_1/R_1}. \quad . \quad . \quad . \quad . \quad (4)$$

Knowing the energy distributions E_λ (1) and E_λ (2), $S_1R_1\bar{S}_2R_2$ can be calculated using the standard visibility curve, and z is determinable provided we can find the value of σ.

The measured Y/B ratio determines σ. If E_λ (y) and E_λ (b) represent the energy distributions of the radiation passed by the Gibson Y, B filters with a source at a colour temperature of 2080° K., then the ratio of the (Y/B) ratio for any observer to the Y/B ratio of the standard observer will be given by our formula (4) as

$$A=z=\frac{1+\sigma\bar{S}_y/\bar{R}_y}{1+\sigma\bar{S}_b/\bar{R}_b}\Big/\frac{1+S_y/R_y}{1+S_b/R}.$$

Thus $$\sigma=\frac{\bar{R}_y-R_b A\rho}{\bar{S}_b A\rho-\bar{S}_y},$$

where $$\rho=\frac{\bar{R}_y+\bar{S}_y}{\bar{R}_b+\bar{S}_b}.$$

Putting $A=1+n$, it follows that

$$\sigma=\frac{1-n\rho R_b/(\bar{R}_y-\rho R_b)}{1+n\rho\bar{S}_b/(\bar{R}_y-\rho R_b)} \quad . \quad . \quad . \quad . \quad . \quad (5)$$

Reverting to equation (4) we have, putting $\sigma=1+m$ and after some reduction,

$$z=1+\frac{(G_2-G_1)m}{1+G_1 m},$$

where

$$G_1=\bar{S}_1/(R_1+\bar{S}_1),\ G_2=\bar{S}_2/(R_2+\bar{S}_2).$$

Eliminating m with the aid of (5), we have, finally,

$$z=1-\frac{n\rho(G_2-G_1)(\bar{R}_b+S_b)/(R_y-\rho\bar{R}_b)}{1+\frac{n\rho}{\bar{R}_y-\rho\bar{R}_b}\{\bar{S}_b-G_1(\bar{R}_b+\bar{S}_b)\}} \quad . \quad . \quad . \quad (6)$$

S_y, $\bar{R}_y$, S_b, and R_b have been computed using Gibson's * values for the transmission of the Y/B filters, the energy distribution of a source at 2080° K., and the standard visibility curve (I.C.I. revised values, Geneva, 1924). We have

$$S_y=6{\cdot}345 \quad R_y=0{\cdot}191,$$

$$S_b=4{\cdot}313 \quad R_b=2{\cdot}307,$$

$$\rho=0{\cdot}987.$$

Inserting these numerical values in (6), we obtain

$$z=1+\frac{3{\cdot}13n(G_2-G_1)}{1-2{\cdot}04n\{1-G_1 1{\cdot}53\}} \quad . \quad . \quad . \quad . \quad (7)$$

Table I. gives the values of $G=\bar{S}/\bar{R}+\bar{S}$ when the energy distribution corresponds to a black body of temperature T. Thus to find the error made by an observer for whom A equals $1+n$, in determining a brightness of colour temperature T_2 in terms of a brightness of colour temperature T_1 taken as standard, we insert

* Journ. Op. Soc. America, ix. p. 113 (1924).

the corresponding values of G_2 and G_1 in equation (7) above.

For values of G_1 corresponding to any temperature in the range given in Table I., the denominator of the second term in (7) reduces to unity with sufficient accuracy for our purpose. The percentage error of an observer with an A value of $1+n$ then becomes

$$(100)(z-1)=+313\,n(G_2-G_1).$$

We have defined A as the ratio of the transmissions of the yellow and blue filters for the given observer divided by the same ratio for an observer possessing the standard visibility curve. In practice, the ratio of the

TABLE I.

T.	$G=S/S+R.$	T.	$G=\overline{S}/\overline{S}+R.$
2000° K.	·747	2640° K.	·673
2080	·737	2720	·665
2160	·726	2800	·658
2240	·716	2880	·651
2320	·706	2960	·645
2400	·697	3040	·639
2480	·688	1203	·633
2560	·681		

transmissions of the yellow and blue filters is taken as the Y/B ratio. This ratio for the standard observer equals

$$\frac{R_y+S_y}{R_b+S_b}=\rho=0{\cdot}987.$$

Thus $A=(Y/B)/0{\cdot}987$, and putting $Y/B=1+r$ we have

$$A-1=n=\frac{r+0{\cdot}013}{0{\cdot}987}.$$

Hence

$$\text{percentage error}=(z-1)100=+317(r+0{\cdot}013)(G_2-G_1) \quad . \quad . \quad . \quad (8)$$

Taking values of G_2 and G_1 corresponding respectively to temperatures $T_2=2760°$ K. and $T=2040°$ K., the variation with $(Y/B)=1+r$ of the error given by the

above formula is shown as the straight line in fig. 1. In the same figure the plotted points were obtained by taking a number of the more abnormal visibility curves measured by Gibson and Tyndall* and calculating directly the Y/B ratio and the error in matching distributions of colour temperatures T_2 and T_1 †. It is clear that the formula (8) above gives a satisfactory approximation to the errors involved.

A further test of the formula is provided from data obtained at the National Physical Laboratory for the

Fig. 1.

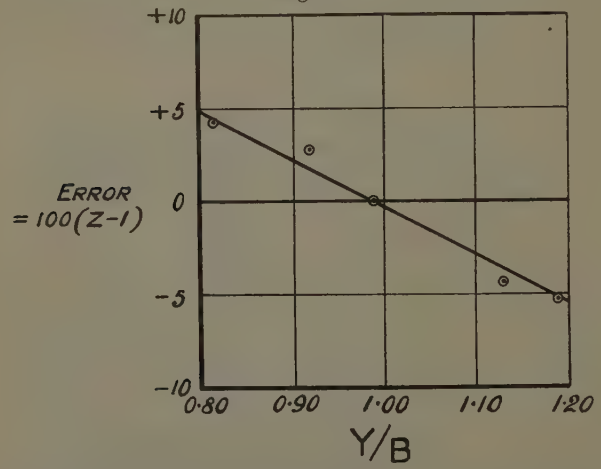

Percentage error in matching brightnesses of colour temperatures 2760° K. and 2040° K. respectively, plotted against observer's Y/B ratio.

transmission of certain blue glasses for light of colour temperature 2080° K. or 2360° K., as measured by different observers whose Y/B ratios were also determined. We shall consider two sets of observations in which the flicker method of photometry was employed. If L_2 and L_1 represent respectively the measured luminosities with and without the blue glass filter in the beam, then the measured transmission of the filter is given by $\tau = L_2/L_1$.

* 'Bureau of Standards, Sci. Papers' No. 475 (1923).

† The calculations of these points were made by Mr. B. H. Crawford in connexion with a photometer employing a variable colour difference. See Journ. of Sci. Inst., Jan. 1934.

The points in fig. 2 represent the observed transmissions of the glass R. 1.28 for light of colour temperature 2080° K. plotted against measured Y/B ratio. To apply formula (8) we take for G_1 the value in Table I. corresponding to T=2080° K. As the transmission of the blue glass throughout the spectrum was also measured, G_2 can be calculated using the spectral transmission of the glass, the energy distribution for T=2080° K. and the standard visibility curve. We find $G_1=0{\cdot}737$, $G_2=0{\cdot}699$. Thus the percentage error in the transmission obtained by an observer with Y/B ratio $1+r$ should equal $317(r+0{\cdot}01)(0{\cdot}699-0{\cdot}737)=-12{\cdot}0(r+0{\cdot}01)$.

Fig. 2.

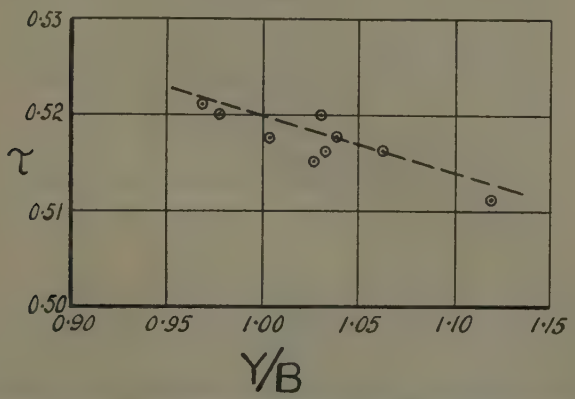

Transmission τ of blue glass R. 1.28 for light of colour temperature 2080° K. plotted against Y/B ratio of the observer.

The total transmission of the glass for a standard observer is found by computation to equal 0·5207, and using this value and the above result for the error we obtain the dotted straight line in fig. 2. As far as the test of the formula for the variation of error with Y/B ratio is concerned, it is legitimate to displace the theoretical line downwards slightly, keeping its gradient constant, until the best fit with the experimental points is obtained. It is clear that the agreement between the experimental points and the theoretical line is satisfactory. The results of a similar comparison using data for the transmission of blue glass R. 1.28 for light of colour temperature

2360° K. are shown in fig. 3. Again the agreement is satisfactory.

Fig. 3.

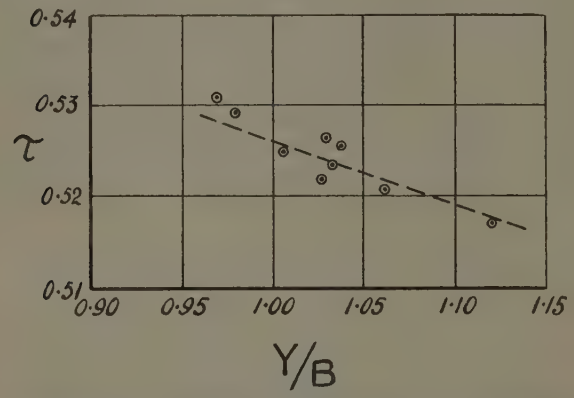

Transmission τ of blue glass R. 1.28 for light of colour temperature 2360° K. plotted against Y/B ratio of the observer.

August 1933.

LVI. *The Fourier Discontinuities: a Chapter in Historical Integral Calculus.* *By* Sir Joseph Larmor *.

THE representation of functions, so far as the functional idea had been introduced, by series of sines and cosines, had been not unfamiliar in use in tentative manner in the hands of the school of Euler. It was left for Fourier, apparently, to develop it into a method of general analysis †. The difficulties and prejudices that lay in the way are indicated by the remonstrances of the great analysts of the time, his colleagues, against the notion that any zigzag or discontinuous graph whatever could be capable of expression by an algebraic formula: and Fourier's memoirs appear to have been put into cold storage, to emerge ten years later when

* Communicated by the Author.

† For a more detailed exposition *cf.* an Address (1916) to the Lond. Math. Soc. "On the Fourier Harmonic Analysis and its scope in Physical Science," in the writer's 'Mathematical and Physical Papers,' vol. ii. pp. 528–567, with later (1928) additions.

their author himself came into office, about the same time as his classic book on the Theory of Heat appeared. His procedure then was in course of time to introduce wider notions of abstract functionality just when the science was in danger of being regarded as completed. It is of interest to note that in the national collection of Fourier's work the editor, Gaston Darboux, no mean authority on analysis, recognized features of rigorous demonstration comparable with the later niceties of Dirichlet and his successors. But what one remembers of early days of instruction in the British School of Natural Philosophy, then headed by W. Thomson (Lord Kelvin), was not any great zeal for the abstract strengthening of foundations of which they knew little but supreme content that they had a calculus by which the numerical tables of experimental results could be prepared in elegant manner for analytic reasoning. Yet the question may be put, how far all this belongs to Fourier: for did not Laplace, one of his more severe critics, essay to reduce the arithmetical complexities of the tides into regular formulæ involving their essential components, one of his greatest and most enduring achievements.

In the early days it was the custom of W. Thomson, and of the successors who gained their attitude of mind in his environment to illustrate the marvellous potency of the Fourier mode of expansion by constructing graphs exhibiting its application to zigzag functions, even to functions with abrupt changes in value, to show how rapidly the series closed down on the function as the number of terms is increased. Such illustrations are familiar nowadays in the textbooks, especially of engineering applications (*cf.* many examples in Prof. Byerly's recent text).

There are two qualities that an expansion in series must possess, if it is to be of utility for purposes of physical science. In the first place there is the property of locality: if a Fourier series is to represent adequately a turbulent curve, the type of fine structure of the series at each place should be governed by the form of the local irregularity in the function and depend not at all on distant features. Thus in analyzing a tidal motion into its harmonic elements, we would not expect an internal complication at any restricted place to affect the relative

amplitudes of the tidal components at a distance from it. This principle is now isolated into a theorem, and established with the rigour and limitation of the abstract analysis as applied to unrestricted functionality.

Again, if an undulating motion, such as radiation, is resolved into its harmonic components, one would expect the sum of their energies, each energy as if existing separately, to make up the energy of the light thus resolved. There should be none of that energy remaining unclaimed, over and beyond the energy-spectrum of the radiation. This physically essential result requires mathematical proof, which indeed gave considerable trouble to Stokes in the ancient pre-analytic days, using a mode of approach afterwards simplified by Rayleigh. The proposition is now accepted as a fundamental theorem in the pure abstract theory, relieved from all physical implication or intuitions, and passes currently by the name of an investigator which readily slips from memory.

More than formalism is involved here. One can remember the astonishment which the early performance of the telephone created: how the sound put in at one end was resolved into its pure tones, each separately transmitted, and how these should all be combined again at the receiver to reproduce the same sound without any confusion introduced. The tale runs that Helmholtz, then in the midst of his work on acoustics and the nature of audition, when in conversation on the subject, explained why he could not participate in the surprise, for did he not awake every morning with Fourier's theorem ringing in his ears. He had spent much effort to verify that the character of a note depends on the energies of the component tones combined in it, but not at all on their phases.

An early general investigation of the anomaly of discontinuous change (later than Dirichlet's comprehensive analysis however) is in a memoir, which long remained classical, by Stokes. He finds the explanation in the fact that the series loses its convergence,—hardly indicating how,—in passing to the critical value, as he calls the place of discontinuity where the function abruptly changes, recovering it after this place has been passed. A graphical representation of mode of change of a Fourier continuous function S_n, restricted to a series of n terms, on its way to the limit when n becomes infinite,

can illuminate more clearly. It was familiar in W. Thomson's environment of practical physical analysis that in approaching the critical place where there is a break in the limiting value of the function, the graph of S_n begins to oscillate, more and more widely as it comes up nearer, the numerical density of the fluctuations increasing with increase of the value of n. A final stroke of the fluctuation jumps continuously across the gap at the limiting Fourier discontinuity, and the process starts off again on the other side of it with a complementary set of fluctuations about the new level, gradually dying away into the new smooth curve. This mode of transition is for our finite series S_n here an affair of sheer ultimate fact, not to be explained further: except that in the general case of such expansions, as *infra*, the terms of the series (the dynamical "normal functions" of Rayleigh) are themselves functions of increasing fluctuation, a feature which adapts them to this *rôle*. The questions to be asked are with regard to the frequency of continuous fluctuations of this limited series in relation to n, and the law of their amplitude. Both as it happens will be sufficiently illustrated *infra* by an example, to enable the mode of transition to a limit to be grasped.

But a more general path of discussion is readily at hand. The function expressed by the series S_n is purely continuous so long as n is not pressed to the infinite limit: the upper and the lower sets of fluctuations, about the two mean base curves, on the two sides of the discontinuous break, which need not be straight when the range covered by the fluctuations becomes short, must thus join together smoothly at some point on the critical ordinate, and the final lines of fluctuation therefore oscillate beyond the two mean levels to a total range, namely doubled amplitudes up and down, which is equal to twice the break in continuity. By symmetry this prolongation of the limiting ordinate must be equally divided into parts passing on beyond the upper and the lower mean levels. Thus when n becomes very great the fluctuations, now congested, have condensed into a sort of thickened line or band which suddenly rises from the upper mean level to a height equal to half the discontinuity, then falls as an ordinary thin connecting line to an equal distance below the lower level, into which it subsides nearly abruptly by another return thick line of transition. This somewhat remarkable

course of transition across the break in continuity was, as appears, left to be pointed out by Willard Gibbs as an accidental *aperçu* or rather correction to a previous hasty remark : if indeed this be the " Gibbs phenomenon " about which much has been written. One may notice as a corollary that as the break of continuity increases, so does the amplitude of the fluctuation, thus increasing even without limit, an apparent exception to the principle of local structure resolved in modern terms by due analytic reason assignable. But if the two sides of the gap in the function thus interact, it becomes a question how precise in general are the fluctuations on either side. We can to this end consider the difference of a longer series $S_{n'}$ from S_n (*infra*) as made up of a set of terms each fluctuating rapidly when n is great, superposing completely in angular phase at the gap, but in passing away from it very soon getting out of step, into opposed phases, and so cancelling out. The local fluctuations of the sum would remain but would not be regular, though closer for larger values of n which is the main point; while the jump across to the new base of fluctuations would appear for this continuous function S_n as an ultimate fact. The fine structure of S_n appears as determined locally. It thus emerges as the essential characteristic at a place of discontinuity for Fourier's and cognate expansions in series, that the terms of the series have angular phases that are there coincident; this arises from their Fourier mode of formation as integrals reaching up to the gap from both sides : the effect is that the terms are there cumulative, but on leaving the gap their values soon work into opposing phases, producing fluctuations which soon cancel in the aggregate, so that the sum goes on smoothly at the two levels. The vast range of theory of discontinuous functionality has developed historically around the Fourier series which, passing from early rejection, has become the dominating influence in modern theory of functions as expanded in order to include its vagaries.

The particular illustration employed, rather obscurely, by Gibbs (' Nature,' April 1899, or ' Works,' vol. ii. p. 259) in elucidation of a query by Michelson as *infra*, is the series of n terms

$$S_n = 2(\sin x - \frac{1}{2}\sin 2x + \ldots \pm \frac{1}{n}\sin nx).$$

This expression S_n as it passes towards the limit for increasing n, is, as is readily verified from determination of the coefficients as integrals, the Fourier representation of a discontinuous graph made up of oblique lines whose ordinate is equal to x from $x=-\frac{1}{2}\pi$ to $\frac{1}{2}\pi$, equal to $x-\pi$ from $x=\frac{1}{2}\pi$ to $\frac{3}{2}\pi$, and so onward, thus repeating its previous range of values after every increment π along x, and representing a set of zigzags made up of oblique segments connected at the breaks by vertical joins. If the series S_n of this illustration could be summed for any value of n, or if the envelope bounding the set of purely continuous fluctuations near the position of each abrupt Fourier discontinuity, be determined as the locus $\partial S_n/\partial x$ null, the decay of the fluctuations could be explored over a range of values of n. The apices of the fluctuations are the positions at which the gradient of S_n vanishes, and if one mistakes not they form in this example an equidistant set determined by vanishing of the readily summable gradient of S_n, though that is a series which does not tend to a limit with n increasing. Thus in this example the fluctuations disappear by their amplitudes gradually fading away, without shrinkage of their distance apart. When n is increased, on the way to the Fourier limit, they become closer, their interval being inversely as n. All this, if worked out on suitable examples, would rather elegantly illustrate the general position as regards the Fourier discontinuities, stopping short however of abstractions leading into generalized ideas on the definition of an integral. Near the break in the function the limited sum S_n, elsewhere definite, may be said in the congestion of fluctuations to cease to have a recognizable succession of values, and in that sense cease to have a gradient * ; a remark which is on the way toward the constructs, also called functions, provided by Weierstrass and other analysts, to which may be ascribed continuity but not rate of change, or in the Leibnitzian terminology not a differential coefficient anywhere along their range whose value is as a warning against trusting (as here) to geometrical intuition.

A diagrammatic graph (like the different one given *infra*) would represent the trend of S_n, which is purely

* *Practically*, for applications in bulk, it is the local aggregate of the function that counts, the fluctuations that express superfine local structure cancelling themselves out at a distance.

continuous so long as the number of its terms is finite, close to the position of the limiting Fourier discontinuity at $x=\frac{1}{2}\pi$. Beginning as the straight line of ordinate rising to $\frac{1}{2}\pi$, it breaks out into undulations of increasing amplitude as the critical position is approached, then one of the undulations flashes across through the central critical point on the axis, and initiates a new set of undulations based on the line whose ordinate starts from $-\frac{1}{2}\pi$, and along this oblique line they gradually fade away. As n is increased the two sets of zigzags shut themselves up bellows-like towards the critical ordinate, and in the limit the graph simplifies to a form of the type of the second diagram. (The graph actually drawn *infra* represents coarsely a different series S'_n, very close to the critical place, when n is large.)

As Gibbs phrases it abstractly, the transition towards a limit as x increases is a different process from the transition towards a limit as n increases. It is hardly likely that these simpler matter-of-fact representations are entirely novel. They may be utilized to illustrate more closely the general Dirichlet analysis. But the writer, now away from library collections, is not aware even of the names of the texts (other than the French general courses) from which the preliminary elementary ideas of the Integral Calculus are now usually acquired for practical use. The arrival of new journals indicates a reversion towards technique suitable for applied mathematics, as important now as when Helmholtz promoted the translation of Thomson and Tait, and Klein that of Routh. As in all beginnings in knowledge, no care is of course superfluous to get relations into forms which if incomplete are not abstruse, which may not include traces of indefiniteness or errors that are readily avoidable and so conduce to dispiriting associations of scrapping involving reconstructions afterwards. In this general way the feature of the sets of "normal functions" which make them a suitable foundation for the expression of an arbitrary graph by a series is that they belong to the class of what may be called *undulating* functions, their own individual graphs being from their definition everywhere concave to the base line and of undulations increasing along each set. The general features of this fitness for unrestricted representation were brought out with zest by Rayleigh in his early time, in a condensed

and paraphrased account of the Sturm-Liouville theory, itself based doubtless on the ideas of the Fourier analysis, in the 'Theory of Sound,' vol. i. § 142. The run of this explanation is in keeping with a remark attributed to Sylvester, that Sturm had told him that his classical theorem on the separation of the roots of numerical equations had presented itself in the course of investigations on compound pendulums. There were even dynamical vibrating systems improvised, said to be suitable for the demonstration of Fourier's and cognate expansions: though the term demonstration in place of illustration grates on the ideas of the pure analysts. There is also an early memoir, once famous, by W. R. Hamilton with significant title 'On Fluctuating Functions.'

The historians of the last age appear to have judged rightly in the main (*cf.* Kelvin's appreciations) in ascribing to Fourier, after d'Alembert, the initiative in reduction of the discussion of physical fields, in Faraday's later sense, into smooth continuous partial differential analysis. It is the essence of the procedure that it had not to pass to limits: what was concerned physically was the amount of the quantity represented that was within a differential element of volume: thus fluctuations, such as are here traced, would cancel out, for atomic theory at best could provide only a coarse-grained foundation or frame of reference. The exploration of the transition of the Fourier sum S_n towards a limit, as n becomes infinite, could not lead to invalidation of this Fourier physical procedure, for there is no other. It is the introduction of extended ideas of abstract quantity, continuous itself but without gradient or rate of change, either locally or over a range, thus quite outside the bounds of ordinary intuition, which has promoted enlarged abstract conceptions of discontinuous integration, of increasing intricacy, following out a procedure (Riemann Lebesgue, Borel, Denjoy) said to be now complete. Human intellect however remains limited: and unwittingly to confuse these two disciplines, the practical and the purely abstract, is to do much less than justice to either.

The critical remarks *supra* on the too brief explanations of Gibbs arose from a highly valued presentation copy of his writings, which alone is at present accessible. Their origin appears (Cajori's 'History of Mathematics,'

p. 465) to have been a summation of the particular Fourier series S_n above, a specially sensitive one, which was extended by A. A. Michelson and S. W. Stratton as far as 160 terms as a test of an integrating machine invented by them. They found out that it "recorded certain unexpected small towers in the curve for the sum, as n increased." Their natural inclination was to suspect the reliability of the machine, until Gibbs explained that they "were true mathematical phenomena." They are called the Gibbs' phenomenon, but perhaps they might be named equally well after Michelson or Kelvin, and "have received further attention from Maxime Bôcher, T. H. Gronwall, H. Weyl, and H. S. Carslaw." The circumstances permitting such discontinuity had been worked out logically and rather expansively by Stokes long before, in a memoir now forgotten as a source: but it is surely very interesting to find two purely practical men knocking their heads hard against this barrier that destroys convergence, thus asserting a new and very welcome entry into the most abstract domain of modern analysis. We here introduce new features, for the "small towers in the curve for the sum" would be expected to range on both sides of the mean curve, beyond it and within it, if this is right, and to be describable rather as *erratic* distribution of the ordinates of summation within the region of rapid sensible fluctuation, which the machine cannot be sensitive enough to arrange on a curve at all. It would have been interesting to find how far the actual impressions of the operators of the machine would coincide with this point of view.

The diagrams will help to elucidate the passage towards a limit that is here expressed. They happen to have been sketched for a different zigzag, represented by S_n' with cosines in place of sines and n odd; thus

$$S_n' = 2(\cos x - \tfrac{1}{3}\cos 3x + \ldots \pm \frac{1}{n}\cos nx)$$

with its segments parallel to the axis instead of oblique, each of length π. In fig. 1 the two sets of fluctuations that arise are roughly indicated: as the number of terms n increases, they condense towards the ordinate of the discontinuity: but as the curve is continuous so long as n remains finite, they must unite across the graph by one definite stroke which passes across through the central

point of the gap. As each fluctuation is symmetrical above and below the mean curve, an outer bound of the wanderings from the mean curve, which also are both above and below, would be half the range of the discontinuity. But Gibbs' argument that this outer bound is an actual value at the place of discontinuity, by quoting a result in definite integrals, belongs to a field of more

Fig. 1.

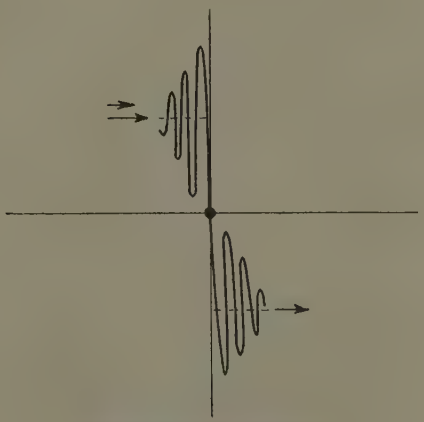

Course of fluctuations for S_n'.

Fig. 2.

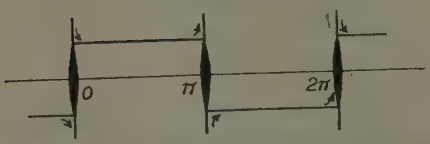

The rectangular zigzag that is represented in the limit.

unlimited abstract precision that need not here be pursued. In any case, the main contribution brought out by the geometric map is that the amplitude of the fluctuation remains bounded to unchanged amount as n increases; whereas a not unnatural tendency might have been to assume it to become larger as the range of the fluctuations diminishes with increasing n. It does become larger when the width of the gap is increased.

In fig. 2, which is a graph of part of the broken curve with its centre at $x=\pi$, to which the series S_n' converges, this width of fluctuation is represented by thick vertical strokes, but of changing thickness, for the erratic summation points determined by ordinates of the graph would be most dense near the mean line of the curve, there being in fact only one point at the extreme value expressed by the Gibbs' integral.

Holywood, Co. Down.
Dec. 31, 1933.

LVII. *Ionization by Collision in Helium.* *By* J. S. Townsend, *Wykeham Professor of Physics, Oxford, and* S. P. MacCallum, *Fellow of New College, Oxford* *.

1. In the paper † on the "Electrical Properties of Neon" which was published some time ago we gave an account of the experiments which were made to determine the coefficients of ionization of electrons and positive ions in pure neon.

The results differed from previous experiments on the ionization of monatomic gases, as sufficient precautions had not been taken in the earlier experiments to eliminate impurities. It was found that small traces of impurities which have large effects on the conductivity of helium and neon cannot be detected by the ordinary method of observing the spectrum of a discharge in a narrow spectroscopic tube. Since then we have made similar experiments with pure helium with the apparatus which was used with neon.

The electrodes in this apparatus were two parallel plates of nickel 3·5 cm. in diameter. The distance between the plates was adjustable by means of a micrometer screw within a range from 1 mm. to 10 mm. The apparatus was set up in a quartz cylinder, as shown in the previous publication (*loc. cit.* pp. 858, 859), where the method of purifying the gas is also fully described.

2. In these experiments a number of electrons are set free by the action of ultra-violet light from the negative electrode and move under the action of a force X to the

* Communicated by the Authors.
† Phil. Mag. vi. p. 857 (Suppl. Nov. 1928).

positive electrode. The currents were very small, so that the field of force was not disturbed by the charge in the gas. The currents between the plates were measured with a constant force X and different distances x between the plates. The results of experiments with pure helium at different pressures and with a constant force of 100 volts per centimetre are given in Table I. The pressure of the gas, p, is given in millimetres in the first column of the table, and the ration X/p in the second column. The currents i_2, i_4, i_6, and i_8 obtained with the distances of 2, 4, 6, and 8 mm. between the plates are given in arbitrary units, the current i_2 obtained with the potential of 20 volts being taken to be 100 at each pressure.

TABLE I.

X = 100 volts per centimetre.

p.	X/p.	i_2.	i_4.	i_6.	i_8.
8·2	12·2	100	116	135	162
4·1	24·4	100	118	149	192
2·05	49	100	119	159	203
1·03	97	100	105	127	159
·55	182	100	103	116	136

In these experiments the currents were measured with the same intensity of light falling on the negative electrode. When the intensity of the light was changed it was found that the currents obtained with different distances between the plates were all changed in the same proportion.

3. Similar results were obtained with other forces. For each force there is a certain pressure at which the current between the plates attains a maximum value. In helium the maximum current is obtained when the ration X/p is about 40 or 50, as shown by the currents recorded in Table I., for the force of 100 volts per centimetre.

In general the current obtained with a given potential $x \times X$ depends only on the ratio X/p, so that experiments with different forces where the ratio X/p is constant, may be represented by a curve giving the currents in terms of the potentials $x \times X$.

Several such curves are given in fig. 1, where each curve corresponds to a particular value of the ratio X/p. The ordinates are proportional to the currents and the abscissæ are the potentials $x \times X$ in volts. The curves represent the results of some of the experiments recorded in Table I. and other experiments which were made with different electric forces.

4. There is a close resemblance between these experiments and the experiments with neon which were made under similar conditions.

Fig. 1.

Curve	1	2	3	4	5	6	7
X/p	6	12	30	50	64	97	182

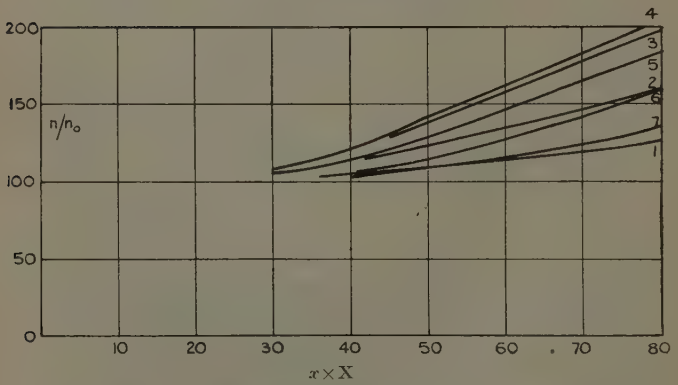

In both of these investigations and in many others on the conductivity of monatomic gases which have been made in this Laboratory the results have been found to be in good agreement with the original theory of ionization by collisions * which is given in books on modern physics.

The more recent theories of the conductivity of gases depending on the formation of metastable atoms are open to several objections.

These theories are advocated in papers published in the 'Proceedings of the Royal Society,' where it is said that they are generally accepted by most physicists excepting those

* 'Electricity in Gases,' Clarendon Press, Oxford (1915).

who have worked at the Electrical Laboratory, Oxford. It will, however, be noticed that the authorities who are responsible for these publications make no attempt to answer the objections to the theories which we have pointed out. It is unnecessary therefore to make any further reference to the more recent theories of ionization, except to state that it is impossible to reconcile any of them with many of the electrical properties of monatomic gases.

According to the original theory the ionization of the gas is attributed to single collisions of electrons with molecules of the gas where the energies of the electrons are above a certain critical value which may be expressed as a potential, and this potential is called the ionizing potential. The electrons lose a large proportion of their energy in the collisions in which the molecules are ionized, and also in the collisions where other molecular changes are produced when the energy of the electrons is of the order of the ionizing potential. These effects of collisions would include the changes which cause molecules to radiate or to be dissociated. As far as the conductivity of monatomic gases is concerned it is only necessary to take into account the large losses of energy in collisions which cause the atoms to radiate without considering the relative intensities of the radiations of different wave-lengths. The experiments on the currents between parallel plates show that in helium and neon electrons with energies much greater than the ionizing potential collide with large numbers of atoms without losing a large part of their energy, the number of collisions in which the atoms are ionized being comparatively small.

5. In most of the collisions of electrons with atoms of helium the transfer of energy is practically the same as in the collisions between elastic spheres, even when the energy of the electrons is as great as that corresponding to 25 or 30 volts. In some of these elastic collisions the electrons gain energy and in others they lose energy, but the mean result of a large number of collisions is the same as if there were a small loss of energy $\lambda . E$ in each collision, E being the energy of the electron *. A large number of these collisions makes an appreciable reduction

* J. S. Townsend, Phil. Mag. ix. p. 1145 (June 1930); xvi. p. 729 (October 1933).

in the energy of an electron, as shown by the curves (fig. 1), for the larger values of the ratio X/p.

The conductivity obtained with a constant force of 100 volts per centimetre increases as the pressure is increased from a small fraction of a millimetre to 2 mm., but with larger pressures the conductivity diminishes as the pressure is increased. This reduction in the conductivity, with increase of pressure, is due to losses of energy in small amounts λ . E, and the following calculations show that the effect becomes appreciable when the ratio X/p is 50.

6. In order to estimate these losses of energy it is necessary to find the number of collisons of an electron with atoms of the gas, as it moves under an electric force in the space between two planes A and B parallel to the electrodes. Let x_1 and x_2 be the distances of the planes from the negative electrode, the distance (x_2-x_1) between the planes being small. Let E be the energy of electrons expressed in volts, so that E . $e/300$ is the kinetic energy $mU^2/2$ in ergs, m being the mass of the electron, U the velocity of agitation, and e the atomic charge.

Let W be the mean velocity of the electron in the direction of the electric force, p the pressure of the gas in millimetres of mercury, and L the mean free path of the electron in the gas at 1 mm. pressure. In helium * it has been found that the coefficient λ is $2{\cdot}6\times10^{-4}$ in collisions where the energy E is greater than 2 volts. The mean free path depends on the definition of a collision.

In these calculations the collisions are defined as in the theory of the motion of electrons which gives the well-known relation between L and the velocities $\overline{U}$ and W.

The value of L depends on the energy E, but for an approximate investigation L may be taken to be ·05 cm., which is approximately the mean free path of electrons with the energy of 5 volts.

7. The average number of elastic collisions C of an electron with atoms of the gas in the space between the

* J. S. Townsend and V. A. Bailey, Phil. Mag. xlvi. p. 657 (Oct. 1923).

planes A and B is $U \cdot p \cdot (x_2-x_1)/WL$, and the formula for the mean velocity W in terms of U is

$$W=2 \cdot Z \cdot e \cdot L/3 \cdot m \cdot U \cdot p, \quad . \quad . \quad . \quad (1)$$

Z being the force in electrostatic units.

(In this case U is the actual velocity of an electron, so that the numerical factor, 2/3, in the above formula is not the same as in the ordinary formula for the mean velocity W of a number of electrons in terms of the mean velocity of agitation U in the steady state of motion.)

The number of collisions C may therefore be expressed in the form

$$C=3Ep^2(x_2-x_1)/XL^2, \quad . \quad . \quad . \quad . \quad . \quad (2)$$

E being the energy of the electron in volts and X the force in volts per centimetre.

The mean loss of energy in these collisions is $\lambda . E$, and the gain of energy of the electron is traversing the distance (x_2-x_1) between the plates under the force X is $(x_2-x_1)X$, so that the ratio R of the loss to the gain is

$$R=3E^2p^2/10X^2 \quad . \quad . \quad . \quad . \quad . \quad . \quad (3)$$

8. It is of interest to consider the changes in the number C and the energy $\lambda . E . C$ as the pressure is increased from 1 mm. to 20 mm., when the energy E, the force X, and the distance (x_2-x_1) are constant, E being 25 volts, X 100 volts per centimetre, and (x_2-x_1) half a millimetre.

With the pressure of 1 mm. $X/p=100$, the number of collisions C is 15, and the loss of energy $\lambda . E . C$ is one-tenth of a volt, which may be neglected in comparison with the gain of energy $(x_2-x_1)X$, which is 5 volts. Thus with the smaller pressures the losses of energy in the amounts λE may be neglected in comparison with the gain of energy due to the motion of the electrons in the direction of the force.

With a pressure of 2 mm. $X/p=50$, the number C is 60, and the loss of energy $\lambda . E . C$ is ·4 volts, which makes a considerable reduction in the gain of energy of 5 volts.

The number of collisions C increases in proportion to the square of the pressure, and at 10 mm. pressure $X/p=10$, the number C is 1500, and the loss $\lambda . E . C$ is 9·3 volts, which is greater than the gain of energy of 5 volts, so that the energy of the electron diminishes.

9. It follows from equation (3) that if all the electrons made the same number of collisions C with atoms of the gas, and lost the amount of energy $\lambda . E . C$ in each collision, none of them would attain energies greater than $1{\cdot}8_2 X/p$, which is the value of E when the loss of energy $\lambda . E . C$ is equal to the gain $(x_2 - x_1)X$.

Under these conditions when X/p is 10 the maximum energy acquired by the electrons is 18 volts, which is less than the ionizing potential of helium.

The curves (fig. 1) show that ionization by collision is obtained for values of X/p less than 6, so that some of the electrons do not lose the amount of energy $\lambda . E . C$ in collisions with atoms of the gas while moving the distance $(x_2 - x_1)$ in the direction of the electric force.

The coefficient λ, the velocity W given by equation (1), and the number C given by equation (2) are only average numbers, and the actual losses of energy of the different electrons are widely distributed about the mean value $\lambda . E . C$. The inequalities in the amounts of energy lost by electrons in collisions with atoms in the space between the planes A and B are principally due to large inequalities in the velocities of the electrons in the direction of the electric force, and to a lesser extent to the inequalities in the amounts of energy lost or gained in elastic collisions *.

Some of the electrons therefore acquire sufficient energy to ionize atoms of the gas even when the mean energy of the electrons is much less than the ionizing potential.

10. The current between parallel plate electrodes is constant and consists only of the electrons set free by the light from the negative electrode when the potential $x \times X$ between the plates is less than 20 volts. The current increases with the distance between the plates, but with potentials of 50 or 60 volts the increase is not more than half the current obtained with 20 volts.

These increases are to be attributed to the ionization of the gas by the electrons set free from the negative electrode, since the effect of positive ions may be neglected when the increase in the current is small.

The experiments therefore provide a simple means

* J. S. Townsend, Phil. Mag. ix. p. 1145 (June 1930); xvi. p. 729 (October 1933).

of determining many of the actions of the electrons in the collisions with atoms of the gas.

The number of electrons generated in the gas is comparatively small when the potential $x \cdot X$ is 30 volts, the maximum being about 6 per cent. of the total number when X/p is about 40.

The current increases continuously with the potential, and in the range of potentials from 20 to 30 volts the rate of increase of the currents is so small that it is imposible to determine the ionizing potential accurately.

11. The values of this potential, as found experimentally by different investigators, are between 20 and 25 volts. The value deduced from Bohr's theory of the spectral lines is 24·5 volts, and this may be taken as the minimum potential at which a small increase of current is obtained. Also, in accordance with Hanle's * experiments on the intensity of the line spectrum, it may be assumed that this type of radiation is excited in a small proportion of the total number of collisions where the energies of the electrons are about 24 volts. It† has been found that the intensities of the continuous spectrum and the band spectrum are small compared with the intensity of the line spectrum in currents where the ratio X/p is within the range of values taken in these experiments.

The losses of energy of the electrons which are required to maintain the band spectrum and the continuous spectrum may therefore be neglected in these calculations, as the object of the investigation is not to consider in detail all possible losses of energy of the electrons, but to determine the general principles on which a reasonable theory of the conductivity of monatomic gases may be based.

What is required is a general theory of collisions which is consistent with different well known properties of currents in gases.

12. It will therefore be assumed that, in addition to the collisions where the average loss of energy of an electron is λE, there are also collisions in which the electrons lose different large amounts of energy. In order to

* W. Hanle, *Zeits f. Physik*, lvi. p. 94 (1929).

† J. S. Townsend and M. Pakkala, Phil. Mag. xiv. p. 418 (September 1932); J. E. Keyston, Phil. Mag. xv. p. 1162 (June 1933).

simplify the calculations it will be assumed that these losses are all the same and equal to 24 volts.

In some of these collisions the atoms are ionized, but for the purpose of this investigation it is unnecessary to specify the different atomic changes which may result from the other collisions in which there are large losses of energy. It will also be assumed, for simplicity, that the electrons have small energies when set free from the atoms that are ionized, so that if an atom is ionized at a distance x_1 from the negative electrode the electron which is set free does not acquire sufficient energy to ionize another atom until it moves a distance x_2 from the negative electrode where the potential $(x_2-x_1)X$ is greater than 24 volts.

13. It is of interest to consider the conclusions which may be deduced in accordance with this simplified theory from the experiments on the currents between parallel plates when the potentials of the plates are less than 50 volts. The electric force may be taken as 100 volts per centimetre and the distances between the plates less than 5 mm.

With potentials less than 50 volts between the electrodes if an electron loses the amount of energy of 24 volts in a collision it does not again acquire an energy of 26 volts ; but the experiments show that there is very little ionization when the energies of the electrons are 26 volts, so that when the electrodes are 5 mm. apart an electron does not ionize an atom after it has lost 24 volts. Each electron set free from the negative electrode can therefore ionize only one atom. For a similar reason the electrons set free from the atoms of the gas do not ionize other atoms when the distance between the electrodes is less than 5 mm.

Under these conditions all the ionization in the space between the plates is due to the electrons set free from the negative electrode which have not lost the amount of energy of 24 volts in any collision before that in which the atom is ionized. Thus, if an atom is ionized at a distance x from the negative electrode the energy of the electron is $x \,.\, X - \Sigma\lambda \,.\, E$, where $\Sigma\lambda \,.\, E$ denotes the loss of energy in elastic collisions.

When the pressure is small the losses of energy in the small amounts λE may be neglected, but at large pressures

greater than 2 mm. the mean energies of the electrons are considerably diminished by these losses.

14. The following are the conclusions deduced by this theory from the results of the experiments where the force is 100 volts per centimetre and the pressure of the gas 2 mm. given by curve 4 (fig. 1). The experiments show that 12 per cent. of the electrons set free from the negative electrode ionize atoms of the gas when the plates are 3·5 mm. apart, and 40 per cent. when the plates are 5 mm. apart; thus at least 28 per cent. of the electrons set free from the negative electrode traverse the space between the distances of 2·5 and 3·5 mm. from the negative electrode without losing a large amount of energy, although the mean energies of these electrons in that space is about 29 volts and the average number of collisions of each electron with atoms of the gas is 140.

15. The number of electrons that lose energy in collisions that excite radiation may be estimated as follows :—

Let n_0 be the number of electrons set free from the negative electrode by the ultra-violet light. The number of collisions in which atoms that are ionized at distances less than 5 mm. from the negative electrode is $\cdot 4 \times n_0$.

Let $y \times n_0$ be the number of electrons that excite radiation in collisions at distances less than 5 mm. from the negative electrode. Thus the number of electrons that arrive at the distance of 5 mm. from the negative electrode with energies of about 26 volts is $(y - \cdot 4) \cdot n_0$, each having lost the amount of 24 volts in a collision. If there were no losses of energy in small amounts the energies of these electrons would all be 26 volts, but owing to the small losses the mean energy at 5 mm. from the negative electrode is 24·5 volts. When the electrodes are 6 mm. apart these electrons have the same energies in collisions at distances between 5 and 6 mm. from the negative electrode as the electrons at distances from 2·5 to 3·5 mm. from the electrode. The number of atoms ionized between the latter distances (2·5 and 3·5 mm.) is $\cdot 12 \times n_0$, so that the number of atoms ionized at distances between 5 and 6 mm. by the electrons which arrive there with the energies of approximately 24·5 volts is $\cdot 12 \times (y - \cdot 4) n_0$.

In addition there is a comparatively small number $n_0(\cdot 6 - y)$ of electrons that arrive at the distance of

5 mm. with energies of about 50 volts. Since these energies are large the electrons make a large number of collisions with atoms, and it may be assumed that most of them lose energy in amounts of 24 volts in collisions at distances between 5 and 6 mm. from the electrode and that the number of collisions in which the atoms are ionized is in the proportion of $\cdot 4/y$ to the number that excite radiation. The number of atoms ionized by the electrons with large energies is therefore $\cdot 4(\cdot 6-y)n_0/(y+\cdot 4)$, and the total number ionized at distances between 5 and 6 mm. from the negative electrode is

$$\cdot 12(y+\cdot 4)n_0 + \cdot 4(\cdot 6-y)n_0/(y+\cdot 4).$$

Equating this number to the increase in the current $\cdot 2 \times n_0$ obtained by increasing the distance between the electrodes from 5 to 6 mm. the value of y is found to be $\cdot 39$.

It may therefore be concluded that in the space from 2·5 to 5 mm. from the negative electrode the number of collisions which excite radiation is approximately the same as the number in which atoms are ionized when the ratio X/p is 50.

The mean energy of the electrons in these collisions is 37 volts.

16. The probability of collisions in which atoms are ionized or of collisions which excite radiation may also be deduced from the curves (fig. 1). The experiments with the larger pressures (X/p less than 30) show that the collisions which excite radiation become more numerous in comparison with those in which atoms are ionized when the energy of the electrons is diminished, but for an approximate estimate of the probabilities of these collisions it may be assumed that the proportion in which the two types of collision occur when the energy of the electrons is 29 volts is the same as in collisions where the energy of the electrons is 37 volts. Under these conditions the probability of ionizing an atom or of exciting radiation in a collision may be deduced from the curve 4 (fig. 1).

The number of electrons that ionize atoms at distances between 2·5 and 3·5 mm. from the negative electrode is $\cdot 12 \times n_0$, and a similar number excite radiation, so that

within this distance the total number of electrons that lose energy in large amounts is approximately $\cdot 24 \times n_0$.

The mean energy of the electrons in this space is 29 volts and the average number of elastic collisions made by each electron is 140, excluding those that lose energy in the large amounts of 24 volts. Let h be the probability of an electron, with energy of 29 volts, losing a large amount of energy in a collision. The value of h is obtained from the above numbers by the formula $\epsilon^{-140 \times h} = \cdot 76$, which gives $h = 1/500$.

Thus, if an electron with the energy of 29 volts collides with atoms of helium the probability of a collision in which atoms are ionized is 1/1000, and the probability of a collision that excites radiation is approximately the same.

17. The probability of collisions in which the electrons lose large amounts of energy increases with the energy of the electrons, as may be seen by considering the ionization in the space between the distances of 3·5 and 4·5 mm. from the electrode. As shown by the curve the number of atoms ionized in this space is $\cdot 17 \times n_0$, so that the total number of electrons that lose energy in large amounts is $\cdot 34 \times n_0$. The number that enter the spaces with sufficient energy to produce these changes in the atoms is $\cdot 76 \times n_0$, and the number that pass through without losing energy in large amounts is $\cdot 42 \times n_0$. The mean energy of these electrons in the space from 3·5 to 4·5 mm. from the negative electrode is 37 volts, and the number of collisions of each electron with atoms of the gas is 180. The probability of an electron losing a large amount of energy in a collision is in this case found by the equation $\epsilon^{-180 \times h} = 42/76$, which gives $h = 1/300$.

Thus if an electron with the energy of 37 volts collides with atoms of helium the probability of a collision in which an atom is ionized is 1/600, and the probability of a collision that excites radiation is approximately the same.

18. The other curves in fig. 1 may be analyzed in a similar manner, but with the larger pressures (X/p less than 25) the calculations become more complicated as the energies of the electrons are greatly reduced by the losses of energy in elastic collisions which are widely distributed about the average loss.

In some respects it is more convenient to determine the effects of collisions by the method depending on the coefficient of ionisation α deduced from experiments with larger electric forces *.

With the smaller forces and distances between the electrodes where the current is less than $1{\cdot}5 \times n_0$ the distribution of the energies about the mean changes with the distances of the electrons from the negative electrode. With large forces and distances between the electrodes a steady state is reached where the mean energy of the electrons and the distribution of the energy become constant after the electrons have moved a short distance from the negative electrode.

In helium, as in neon, the ionization by positive ions is not very small compared with the ionization by electrons, and there is no large range of distances between the electrodes where the current is given by a simple formula of the form $n = n_1 \epsilon^{\alpha(x-x_1)}$, the electric force X being constant.

19. In these gases the current n increases with the larger distance x between the electrodes, as in the formula

$$n = n_0 \frac{(\alpha - \beta)\epsilon^{(\alpha-\beta)(x-\delta)}}{\alpha - \beta\epsilon^{(\alpha-\beta)(x-\delta)}} \quad . \quad . \quad . \quad . \quad . \quad (4)$$

where the coefficients α and β are constant.

This formula represents the currents that would be obtained if both the electrons and positive ions ionized atoms of the gas, α being the coefficient of ionization of the electrons and β the corresponding coefficient for positive ions.

In general the positive ions also set free electrons from the negative electrode. When this action is taken into consideration the expression for n is of the same form as in equation (4), and is obtained from that equation by substituting $(\alpha + \gamma\alpha)$ for α and $(\beta + \gamma\alpha)$ for β, the coefficient of emission γ being the ratio of the number of electrons set free from the negative electrode to the number of positive ions impinging on the electode.

It is convenient to eliminate δ from the above formula and express n by a formula involving the distance S between the electrodes where a spark discharge is obtained with potential $S \times X$, since the distance S is easily found experimentally.

* J. S. Townsend, Phil. Mag. xlv. p. 1071 (1923).

When S is substituted for x the denominator of the formula for n becomes zero and the following relation is obtained between δ and S which may be used to eliminate δ :

$$(\alpha+\gamma\alpha)\epsilon^{(\alpha-\beta)\delta}=(\beta+\gamma\alpha)\epsilon^{(\alpha-\beta)S}.$$

The equation for n/n_0 thus becomes

$$n=\frac{n_0}{\beta+\gamma\alpha}\times\frac{\alpha-\beta}{\epsilon^{(\alpha-\beta)(S-x)}-1}. \quad . \quad . \quad . \quad . \quad . \quad (5)$$

The quantities $(\alpha-\beta)$ and $(\beta+\gamma\alpha)$ may therefore be found by substituting the values of n/n_0 found experimentally in this equation.

Other experiments are being made to find each of the coefficients β and γ for positive ions in helium, but they are not yet completed. The method of investigation is the same as that used to determine the coefficients β and γ for positive ions in hydrogen *.

20. As a first step towards a complete determination of the three coefficients α, β, and γ the coefficients $(\alpha-\beta)$ and $(\beta+\gamma\alpha)$ may be deduced from the experiments on the currents n between parallel plates. The value of $(\alpha-\beta)$ is easily found from measurements of the currents at three different distances between the plates. If n_a, n_b, and n_c be the currents obtained with a constant force X and the distances a, b, and c between the electrodes, where $(b-a)=(c-b)$, y_1 the ratio n_b/n_a, y_2 the ratio n_c/n_b, $(\alpha-\beta)$ is given by the formula

$$\epsilon^{(\alpha-\beta)(b-a)}=y_2(y_1-1)/(y_2-1). \quad . \quad . \quad . \quad . \quad (6)$$

The coefficient $(\alpha-\beta)$ may also be found from the ratio y_2 of the currents obtained with the plates at the distances apart c and b if $(c-b)=(S-c)$, S being the distance between the plates when a spark discharge is obtained with the potential $S\times X$. In this case

$$\epsilon^{(\alpha-\beta)(c-b)}=y_2-1. \quad . \quad . \quad . \quad . \quad . \quad (7)$$

The sparking potentials V in pure helium are given in volts in terms of the product $p\times S$ by the curve 1 (fig. 2), p being the pressure of the gas in millimetres, and S the distance between electrodes in centimetres. (The electrodes in this case were nickel plates 3·5 cm. in diameter.) These potentials were given in the previous paper on the

* J. S. Townsend and F. Ll. Jones, Phil. Mag. xv. p. 282 (Feb. 1933).

"Electrical properties of Neon," and were frequently verified when the apparatus was used to determine the photo-electric currents.

Several sets of experiments were made to determine the currents n with the force X chosen, so that $x \times X$ is the sparking potential, with the distance x between the plates an exact number of millimetres.

21. The results of the experiments in which the currents n_1, n_4, and n_6 obtained with the electrodes at the distances apart of 2, 4, and 6 mm. are given in Table II.

Fig. 2.

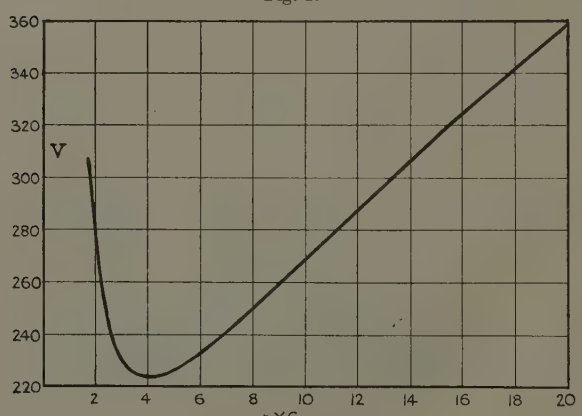

Helium. Sparking potentials, V, in volts; S, distance between plates, in centimetres; p, pressure of gas, in millimetres.

In these experiments the force X was chosen, so that the potential $\cdot 8 \times X$ with the plates 8 mm. apart was the sparking potential (given by the curve (fig. 2) at the point where the ordinate $p \times S$ is $\cdot 8p$).

The pressure p of the helium is given in the first column of the table, the force X in the second column and the ratios of the currents n_4/n_2 and n_6/n_4 in the third and fourth columns respectively.

In this case $y_1 = n_4/n_2$, $y_2 = n_6/n_4$, and $n_8 = \infty$, so that the quantity $\epsilon^{(\alpha-\beta)\times 2}$ is given by equation (6) as $y_2(y_1-1)/(y_2-1)$, and by equation (7) as (y_2-1). The following relation therefore should be obtained between

the values of y_1 and y_2 in order that the currents may be represented by equation (5):

$$y_1 = 1 + (y_2 - 1)^2/y_2. \quad . \quad . \quad . \quad . \quad . \quad . \quad (8)$$

The values Y_1 of the quantity on the right of this equation are given in the fifth column of the table, and they are seen to be in good agreement with the values of y_1 found experimentally, which are given in the third column.

TABLE II.

p.	X.	$\frac{n_4}{n_2}$.	$\frac{n_6}{n_4}$.	Y_1.	X/p.	$\frac{(\alpha-\beta)}{a}$.	$\frac{\beta+\gamma\alpha}{p}$.
4·7	278	2·30	2·97	2·31	59·3	·72	·074
9·4	305	2·33	2·97	2·31	32·5	·365	·031
14·0	250	2·44	3·15	2·47	25·0	·27	·0185
17·0	377	2·46	3·18	2·49	22·2	·225	·0145

Fig. 3.

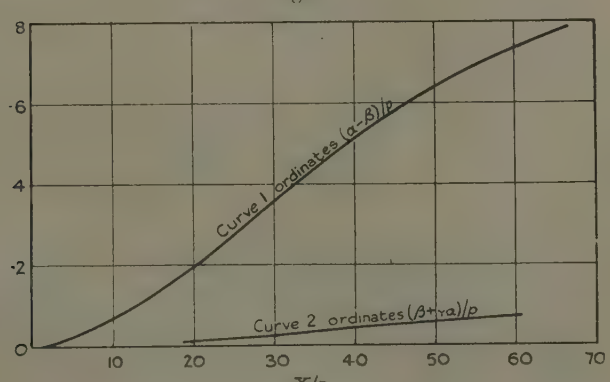

The values of $(\alpha-\beta)/p$ are given in the seventh column of the table.

These values of $(\alpha-\beta)/p$ and others obtained in a similar manner are given by the curve 1 (fig. 3) in terms of X/p.

22. Having found the values of $(\alpha-\beta)/p$ in terms of X/p the values of $(\beta+\gamma\alpha)$ may be obtained by equation (5). The quantity $(\alpha-\beta)(S-x)$ in the exponential term may

be written $(\alpha-\beta)(V-v)/X$, V being the sparking potential when the distance between the plates is S and v the potential between the plates at the distance apart x where the current is n. The ratio n/n_0 which occurs in equation (5) is given by the curves (fig. 1) for the different values of X/p.

Thus, taking X/p to be 50 the sparking potential V is 223 volts, the ratio $(\alpha-\beta)/X$ as given by curve 1 (fig. 2) is ·0128, and n/n_0 is 1·59 when the potential v is 60 volts as given by curve 4 (fig. 1). The ratio $(\alpha-\beta)/(\beta+\gamma\alpha)$ deduced by equation (5) from these numbers is 11, so that $(\beta+\gamma\alpha)/p$ is ·057.

23. The values of $(\beta+\gamma\alpha)/p$ thus obtained are given by the ordinates of curve 2 (fig. 3) and also in the last column of Table II. The sum of the numbers in the last two columns of the table is the value of $\alpha(1+\gamma)/p$, which is somewhat greater than α/p, and the numbers in the column $(\alpha-\beta)/p$ are somewhat smaller. An upper and a lower limit to the value of α/p are thus obtained.

The mean of the two limits is given in the second column of Table III., which is referred to as the value deduced from the curves (fig. 3).

In the initial stages of the process of ionization the rate of increase of the current n with the distance x between the plates is given approximately by the equation $n=n_1\epsilon^{\alpha(x-x_1)}$ for a small range of distances x, when n is less than $2n_0$ and the value of α may be found from the curves (fig. 1).

The values of α/p obtained from these curves are given in the third column of Table III., and the agreement between the numbers in the two columns shows that the action of the electrons in small photoelectric currents is the same as in the larger currents or in the continuous discharges which are maintained when the potential $x\times X$ is equal to the sparking potential.

23. It may also be inferred from these results that the mean energy of the electrons in the experiments where the currents n are within the range from $1\cdot1\times n_0$ to $2\times n_0$ is approximately the same as the mean energy E in the steady state attained with larger potentials.

The mean energy of the electrons at distances x from the negative electrode may easily be calculated when the current n is about $1\cdot2\times n_0$.

There are three groups of electrons to be considered: those that traverse the distance x without losing energy in large amounts, those that ionize atoms or excite radiation and lose energy in amounts of 24 volts, and those that are generated by the collisions of electrons with atoms of the gas. In each case there are losses in small amounts which increase in importance as X/p diminishes.

Thus in helium at 2 mm. pressure and a force of 100 volts per centimetre the current with the plates 3·5 mm. apart, as shown by curve 4 (fig. 1) is $1{\cdot}12 \times n_0$, so that the first group, consisting of 76 per cent. of the electrons, from the negative electrode, lose on an average 1·5 volts in small amounts, and the mean energy of this group at the distance 3·5 mm. from the negative electrode is 33·5 volts.

Table III.

$\frac{X}{p}$	α/p curves (fig. 3).	α/p curves (fig. 1).	E.
97	—	1·11	38
60	·76	·76	—
50	·67	·675	26
32·5	·418	·413	—
25	·28	·29	22
12	—	·095	16

The second group, consisting of 24 per cent. of the electrons from the negative electrode, which lose 24 volts in ionization or in exciting radiation, arrive at the distance of 3·5 mm. from the negative electrode with energies of 10 volts, having lost about 1 volt in small amounts.

The third group consists of the electrons ($\cdot 12 \times n_0$) which are generated in the gas. The mean distance they traverse is ·5 mm., so that mean energy of this group on arriving at the distance 3·5 mm. from the negative electrode is 5 volts. The mean energy of the total number $1{\cdot}12 \times n_0$ is 25·4 volts. The energies E thus obtained for different values of X/p are given in the last column of Table III.

The proportions in which collisions of different types occur in a gas, when the electrons are in steady motion

under the action of a uniform force, may be investigated by the method which has been described in a previous paper. In this case the mean energy of agitation E and the coefficient of ionization α of the electrons is the same for different distances from the negative electrode. The process of ionization by the collisions of electrons with atoms of the gas may be considered apart from actions of positive ions. Let n_1 be the number of electrons that pass through a plane at a distance x_1 from the negative electrode, and n_2 the number that pass through a plane at a distance x_2 from the electrode. The number n that pass through any plane at a distance x from the electrode is $n_1\epsilon^{\alpha(x-x_1)}$, and the total energy gained by the stream of electrons under the action of the force X in the space between the planes A and B at the distances x_1 and x_2 from the electrodes is

$$\int_{x_1}^{x_2} nX dx = X(n_2-n_1)/\alpha. \quad . \quad . \quad . \quad . \quad (8)$$

The energy of the electrons entering the space is n_1E and that of the electrons passing out is n_2E, so that the actual gain of energy is $(n_2-n_1)E$ and the amount lost in collisions with atoms of the gas is $(X/\alpha-E)(n_2-n_1)$.

If c_1 be the energy lost in a collision with an atom that is ionized, the total loss in these collisions is $(n_2-n_1)c_1$, and if F be the total loss in collisions with atoms that are not ionized the following relation between the energies F and $(n_2-n_1)c_1$ is obtained * :

$$(X/\alpha-E-c_1)(n_2-n_1)=F. \quad . \quad . \quad . \quad . \quad . \quad (9)$$

The quantity F includes the loss of energy in the collisions that excite radiation and the loss of energy in elastic collisions in the space between the planes A and B. The latter quantity is proportional to E^2, but it is impossible to find an accurate formula for this loss, as it depends on the distribution of the energies. The mean loss of energy in elastic collisions is $\lambda \,.\, E \,.\, C$, where C is the number given by equation (2). This quantity is proportional to the distance (x_2-x_1) between the planes, so that it is necessary to express the number of collisions (n_2-n_1) in which atoms are ionized and the number that excite radiation also in terms of (x_2-x_1). For this purpose (x_2-x_1) may be written as dx, and the number

* J. S. Townsend, Phil. Mag. xlv. p. 1071 (1923).

$(n_2 - n_1)$ as $n_1\alpha\,dx$. Let $n_1\alpha'dx$ be the number of collisions that excite radiation in the space between the planes at a distance apart dx, and c_2 the mean loss of energy in these collisions.

If $C\,dx$ be the number of elastic collisions in this space the coefficient C is $3Ep^2/XL^2$ (equation (2)), and the loss of energy in these collisions is $\lambda\,.\,E\,.\,C\,.\,n_1\,dx$. Equation (9) thus becomes

$$(X/\alpha - E - c_1)\alpha = c_2\alpha' + \lambda\,.\,E\,.\,C, \quad . \quad . \quad . \quad (10)$$

or

$$X/p = (E + c_1)\alpha/p + c_2\alpha'/p + \lambda\,.\,E\,.\,C/p. \quad . \quad . \quad (11)$$

From the values of E and α/p given in Table III. the values of $c_2\alpha'/p$ may be found by equation (11), taking c_1 to be 24 volts. The ratio $c_2\alpha'/c_1\alpha$ is given in the third column of Table IV.

The last term on the right of equation (11) increases in importance as X/p diminishes.

TABLE IV.

X/p.	$\frac{\lambda.E.C}{p}$.	$\frac{\alpha'.c_2}{\alpha.c_1}$.	$\frac{\alpha}{p}$.	$\frac{C}{p}$.
97	4·5	·8	1·11	470
50	4·0	·8	·67	600
25	6·0	1·8	·285	1000
12	6·6	3·6	·095	1600

This is shown by the values of $\lambda\,.\,E\,.\,C/p$ given in the second column of Table IV. The values of C/p are given in the last column of the table for comparison with the values of α/p, the ratio α/C being the ratio of the number of atoms that are ionized to the number of elastic collisions. The figures show that this ratio diminishes rapidly as X/p diminishes.

It will be observed from the numbers in the third column that the number of collisions α' in which radiation is excited increases in comparison with α the number in which the atoms are ionized as X/p diminishes.

If the loss of energy c_2 in the collisions that excite radiation be taken to be the same as c_1 (24 volts), the ratio α'/α for the larger values of X/p is approximately ·8. This is the ratio $y/\cdot4$ which was found to be approximately 39/40 by the method described in Section 15.

When c_2 is taken to be less than c_1 in equation (11) a closer agreement between the two methods of investigation is obtained.

It has been shown that similar conclusions are obtained from the corresponding experiments on photoelectric currents in pure neon. In neon the ratio α'/α of the number of collisions in which radiation is excited to the number in which atoms are ionized is approximately ·8 for values of from 160 to 60. The ratio increases as X/p diminishes, 1·5, 2·4, and 8 being the values of α'/α, which correspond to the values 30, 20, and 10 of X/p *.

Small traces of impurities have much the same effects on the conductivities of helium and neon.

When the gas contains a small amount of impurity the increase in the photoelectric current with the potential $X \cdot x$ between the plates is much greater than the increase when the gas is pure.

It has been found that the increase in the photoelectric currents in helium containing ·025 per cent. of argon, with a potential of 16 volts between the plates, is as great as the increase $\cdot 4 \times n_0$ in the currents in pure helium with a potential of 50 volts between the plates †.

This effect may be attributed to the ionization by single collisions of electrons with atoms of argon, which are more easily ionized than the atoms of helium. The conclusions to be drawn from these experiments with regard to the free paths of electrons in argon will be discussed in another paper.

LVIII. *A Theory of the Viscosity of Liquids.*—Part II. *By* E. N. da C. Andrade, *Quain Professor of Physics in the University of London* ‡.

1. *The Mechanism of the Temperature Variation of Viscosity: General Discussion.*

As pointed out in Part I. §, the sense of the temperature variation of the viscosity of liquids is sufficient to

* J. S. Townsend and S. P. MacCallum, Phil. Mag. xlv. p. 1071 (1928); Proc. Roy. Soc. A, cxxiv. p. 533 (1929).

† S. P. MacCallum and L. Klatzow, 'Nature,' cxxxi. p. 841 (June 10, 1933).

‡ Communicated by the Author.

§ Phil. Mag. xvii. p. 497 (1934).

show that the mechanism must be essentially different from that of gases. It is there suggested that in a liquid a communication of momentum from layer to layer takes place at the extreme libration of molecules oscillating about a very slowly displaced equilibrium position, and it is shown that if the frequency of oscillation be taken from the solid state a coefficient of viscosity agreeing closely with experiment can be calculated on this assumption. The view now put forward is that liquid viscosity decreases with temperature because the temperature agitation interferes with the interchange of momentum at the extreme librations. For greatest generality all that need be assumed, to account for the temperature variation, is that a certain mutual potential energy of the juxtaposed molecules is necessary if communication of momentum is to take place in the direction normal to the line of centres—that is, if the molecules are to behave momentarily as one. This energy is negative, since it is natural to suppose that for transfer the molecules must approach one another under conditions such that the forces of attraction are large. Then, in accordance with the general conceptions underlying Boltzmann's exponential distribution law, the number of cases favourable for transfer will decrease as the temperature rises, and the rate of decrease at a given temperature will depend upon the magnitude of the potential energy involved.

While all that need be postulated is that there is a certain potential energy of a molecule at the instant of close approach to another molecule, the magnitude of which can vary according to the nature of the approach, it seems well to suggest a mechanism by which this can be brought about. The temporary union which is postulated for transfer of momentum, while of far shorter duration, resembles that involved in association in the ordinary sense. It is well known in this connexion that, in the case of gases, of the impacts calculated on the kinetic theory only a percentage, which depends on the temperature, is favourable to combination of the molecules *. Boltzmann †, in his theory of association, put forward the assumption that there are certain "sensitive

* See, *e. g.*, Eucken, 'Lehrbuch der Chemischen Physik' (Leipzig, 1930); K. F. Herzfeld, "Kinetische Theorie der Wärme" (Müller-Pouillet's 'Lehrbuch der Physik,' iii. part 2 (Braunschweig, 1925).

† 'Kinetische Theorie der Gase,' ii. p. 177 *et seq.* (Leipzig, 1898.)

regions" or patches ("empfindliche Bezirke") at the surface of the molecules which must overlap if the molecules are to combine, thus making the occurrence of the temporary combination of ordinary association conditional on the relative orientation of the molecules. Eucken * enumerates three possibilities, of which the third includes the hypothesis of Boltzmann, namely, that combination depends upon whether the molecules at the instant of closest approach are favourably disposed "in respect of the relative position or inner state." We may, then, assume for our purpose that whether "instantaneous combination" (using the phrase to denote sufficient interaction for the molecules to transfer momentum normal to the line of centres) takes place or not depends upon relative orientation, this orientation being favourable in a large percentage, if not all, the cases of close approach in a fluid near freezing-point, but being progressively disturbed as the temperature agitation increases. The hypothesis is in accord with the modern view, particularly stressed by, for instance, Kossel †, that the field of force of a molecule, even a highly symmetrical molecule, shows marked variations from point to point of the surface. The evidence offered by the scattering of light ‡ is particularly significant, for it shows that for all molecules, even the highly symmetrical ones of the inert gases, the direction of the induced moment does not lie along the direction of the inducing force except for three principal axes. It is experimentally established therefore that the potential energy of a molecule, even a monatomic one, in the field of intermolecular force must depend upon its orientation. Theoretical considerations have been confined to the case of a uniform field of force, but the general conclusions are not affected by the non-homogeneity of the intermolecular field.

We suppose, then, that there is a local electrostatic field which tends to place the molecules in a condition favourable for communication of momentum—or, to particularize, to orient them—at extreme libration, this condition being disturbed by the heat agitation. The

* *Loc. cit.* p. 612.

† E. g., *Ann. der Physik*, xlix. p. 229 (1916); *Naturwissenschaften*, vii. pp. 339 & 360 (1919). See also Van Arkel and de Boer, 'Chemische Bindung als elektrostatische Erscheinung' (Leipzig, 1931).

‡ See, *e. g.*, Cabannes, 'La diffusion moléculaire de la lumière' (Paris, 1929).

direction of the local field may be supposed to be tolerably constant for a small group of molecules, but to vary from group to group in a random manner, the general picture being something like that offered by the Weiss theory of ferromagnetism for a solid. However, in the liquid case the boundaries of the groups are, of course, quite indefinite and continually fluctuating, the direction of the local field changing both in space and time. In the present theory the direction of the field is not involved, the tendency to induce transfer of momentum between adjacent molecules being alone in question. The same result would be obtained if the direction of the local field were everywhere the same, which is clearly impossible.

The local tendency to orientation of molecules in small groups, of fluctuating outline, lends the liquid a quasi-crystalline character. There is good independent experimental support for the quasi-crystalline structure in liquids under the effect of local intermolecular forces. G. W. Stewart * in particular has come to the conclusion, from his results on the X-ray diffraction in liquids, that crystalline, or as he prefers to call them cybotactic, groupings must be present in liquids, and that the space distribution consequent on the relatively large volume of the molecules compared to the fluid volume † (the so-called "volume effect") does not suffice to explain the effects. The intermolecular forces must, he finds, be involved in much the same way as is here demanded. Stewart ‡ says of the cybotactic groups that "these regions are very numerous, occupying a large fraction of the total volume of the liquid. A group does not retain its identity as determined by its constituent molecules. It is not a fragment of material, but it is a condition of position and potential energy which varies throughout the liquid." In the Faraday discussion (*loc. cit.*) he deduces, *e. g.*, that for ethyl ether at room-temperature only 7 to 10 per cent. of molecules are not in cybotactic groups. His general view, approaching liquids from a totally different direction, thus agrees well

* G. W. Stewart and R. L. Edwards, Physical Review, xxxviii. p. 1575 (1931); G. W. Stewart, 'Nature,' Oct. 24, 1931 (discussing the present writer's letter in 'Nature,' April 12, 1930, where the present theory was sketched); Faraday Society, Discussion on Liquid Crystals, 1933.

† J. A. Prins, *Naturwissenschaften*, xix. p. 435 (1931), where further references are given.

‡ Physical Review, *loc. cit.* p. 1576.

with that of the present writer, with the small modification that I prefer to think of the whole, or nearly the whole, of the liquid as being in "crystalline" groupings near the melting-point, the degree of orientation of the molecules in the groups being reduced by heat agitation as the temperature is raised, rather than the groups becoming smaller or less numerous. Attention may further be directed to the fact that W. Noll * and R. D. Spangler † have shown, by study of the X-ray diffraction, that as the temperature of ethyl ether is raised the evidence of cybotactic grouping becomes less and less, as demanded by the present theory.

My view is, then, that in certain respects the structure of a liquid approaches more closely that of a polycrystalline solid, such as an ordinary metal, than that of a gas. The crystallization is, of course, always imperfect, the tendency to local orientation being opposed by the heat agitation.

2. *The Temperature Variation of Viscosity: Quantitative.*

In accordance with what has been said we assume that for transfer of momentum to take place the molecules considered must possess a mutual potential energy $-E$. If ν, the frequency of vibration of the liquid molecule, is taken as constant, the variation of viscosity with temperature will be governed by the fraction of molecules possessing this energy at extreme libration. According to the Boltzmann distribution formula the ratio of number of molecules possessing energy $-E$ at temperature T to the number possessing this energy at temperature T′ is

$$e^{\frac{E}{k}\left(\frac{1}{T}-\frac{1}{T'}\right)},$$

which incidentally is the relation invoked in the theory of ordinary dissociation. This will be the main factor in the temperature variation of viscosity, for which an approximate formula will be

$$\frac{\eta_T}{\eta_{T'}}=e^{-\frac{E}{kT'}}e^{\frac{E}{kT}},$$

or

$$\eta_T=\eta_{T'}e^{-\frac{E}{kT'}}e^{\frac{E}{kT}}=Ae^{\frac{c}{T}}, \quad . \quad . \quad . \quad . \quad (1)$$

* Physical Review, xlii. p. 336 (1932).

† Quoted by Stewart, Faraday Discussions, *loc. cit.*

This formula does, in fact, give a very fair representation of the variation of the viscosity of liquids with the temperature *.

The approximate formula $\eta = Ae^{c/T}$ is often useful, and at once explains certain generalities about the viscosity of liquids, such as A. W. Porter's purely empirical relation †. This relation is that if the viscosity of a liquid I at any temperature T_1 be η, then, if the experimental range is sufficient, a temperature T_2 can be found for a second liquid II at which the viscosity is also η. If various values of T_1 are chosen and the corresponding T_2 be found for each, then T_1/T_2 plotted against T_1 gives a straight line. This follows at once from the formula $\eta = Ae^{c/T}$; for if A_1, c_1, and A_2, c_2 are the constants for liquids I and II, then

$$A_1 e^{c_1/T_1} = A_2 e^{c_2/T_2}$$

and $$\log A_1/A_2 = \text{constant for two liquids concerned}$$
$$= c_2/T_2 - c_1/T_1,$$

or $$T_1/T_2 = \alpha + \beta T_1,$$

where α and β are constants, which is the experimental relation.

In the deduction of formula (1) no account has been taken of the variation of volume with temperature. Owing to the expansion the average distance between molecules will increase with the temperature as $v^{1/3}$, where v is the specific volume, while the number of

* This formula was put forward by me in 'Nature,' March 1, 1930, and independently by S. E. Sheppard in 'Nature,' March 29, 1930. It subsequently proved that, unknown to either of us, the formula had been previously suggested by J. de Guzman (*Anales de la Sociedad Española de Fisica y Quiminca*, 1913), Kendall (footnote to paper in Journal Amer. Chem. Soc. xxxix. p. 1799 (1917)), and J. S. Dunn (Transactions of the Faraday Society, xxii. p. 401(1926)), all, apparently unknown to one another. The formula was further discussed by myself and others in 'Nature,' April 12, 1930. Since then I have found that Sir C. V. Raman suggested a logarithmic formula of this type in a letter to 'Nature,' iii. p. 532 (1923). He derives the constant from consideration of Sutherland's formula as applied to the vapour state, and quotes one liquid only, benzene, which bears out his conclusions very well. He does not appear to have made any subsequent publication on the subject.

† Phil. Mag. xxiii. p. 458 (1912). It may be noted that Porter's relation is satisfied by any formula of type $\eta = \phi(b + c/T)$, where ϕ is a universal function and b and c are special to each substance. Our form of function is the simple exponential, giving

$$\eta = e^{b + c/T}.$$

molecules per unit area will diminish as $v^{-2/3}$. On account of this effect alone the viscosity will diminish as $v^{-1/3}$. Further, the potential energy involved in the condition of communication will probably be a function of the volume, $f(v)$. These two effects of the temperature can be expressed by modifying the formula (1) to

$$\eta v^{1/3} = \mathrm{A} e^{\frac{cf(v)}{\mathrm{T}}}.$$

It remains to choose some simple form for $f(v)$. The average potential energy of a molecule is to the first approximation given by a in the a/v term of van der Waals' equation, and a simple course is to suppose that the part of the potential energy with which we are concerned varies in like manner. In this case the formula becomes

$$\eta v^{1/3} = \mathrm{A} e^{\frac{c}{v\mathrm{T}}}, \quad . \quad . \quad . \quad . \quad . \quad . \quad . \quad (2)$$

which is the formula which is generally employed in the remainder of this paper. Trial has also been made of a different function of v, namely $1/v^2$, and the formula

$$\eta v^{1/3} = \mathrm{A} e^{\frac{c}{\mathrm{T}v^2}} \quad . \quad . \quad . \quad . \quad . \quad . \quad . \quad (3)$$

was tentatively employed and fitted for a large number of liquids. On the whole the fit is not quite so good, but, owing to the slow variation of v with temperature, it does not differ much from the fit of (2) when the constants are suitably chosen. As it offers no advantage and is definitely behind (2) when comparison of energies with those derived from the equation of state is in question, it is not further discussed in this paper.

3. *The Characteristic Frequency.*

It has been assumed in the previous discussion that the value of the frequency ν for a given substance is independent of the temperature. In this connexion reference may be made to the theory of the specific heats of solids. To calculate the characteristic temperature θ from the mechanical properties, according to Debye's theory of the quasi-isotropic solid body, the elastic constants at ordinary temperature are always used, although the characteristic temperature in question is an exceedingly low one. The point is usually glossed over, although

Grüneisen * has drawn attention to this weakness of the theory. This is a particular aspect of the fact that the limiting value ν_m of ν is taken as independent of the temperature in the deduction of Debye's formula. The value of ν would be expected to be proportional to the square root of the elastic modulus, which varies markedly with temperature; but Eucken has shown that the attempt to allow for variation of ν_m in this manner leads to values which are in much worse accord with experiment than those derived on the assumption of constant ν_m †.

The ordinary theory gives

$$\nu = s\left(\frac{3N}{4\pi v_a}\right)^{1/3},$$

where s is the velocity of sound in the body, supposed in the present case homogeneous, and N, v_a are Avogadro's number and molar volume respectively ‡,

or

$$\nu = C v_a^{1/6} \frac{1}{\sqrt{\kappa}},$$

for a given body, where C is a constant and κ is the adiabatic compressibility. The A of the viscosity formula (2) is proportional to ν, so that if we utilize the value of ν just given, we have

$$\eta v^{1/6} = \frac{A'}{\sqrt{\kappa}} e^{\frac{c'}{vT}}. \quad . \quad . \quad . \quad . \quad (4)$$

The term $v^{1/6}$ varies very slowly with the temperature, but κ increases fairly rapidly with temperature for most liquids, the rise becoming more rapid as the temperature increases. With many liquids the adiabatic κ increases by about 60 per cent. for a rise of temperature from 0° to 60°, or $1/\sqrt{\kappa}$ decreases by 21 per cent.

Formula (4) and formula (2) have both been applied to liquids for which the adiabatic compressibility at different temperatures is recorded. It has been found that the fit given by (4), which allows for a variation of ν with temperature, is markedly worse than that given by (2). Typical results are given in the following tables. Table I. exhibits in detail the application of

* 'La Structure de la Matière,' Institut internationale de physique Solvay, 1921. See also Grüneisen and Goens, *Zeitschr. für Physik*, xxvi. p. 235 (1924).

† See Schrödinger, 'Handbuch der Physik,' Geiger-Scheel. x. p. 316 (1926).

‡ Born and Karman, *Phys. Zeitschr.* xiv. p. 15 (1913).

the two formulæ to the case of carbon tetrachloride. The constants A′ and c' and A and c respectively have been found by the method of least squares, as described in the next section. The percentage error is given in

TABLE I.

Carbon Tetrachloride.

t.	$\eta_{obs.}$	$\eta_{calc.}$		Percentage error.	
		Formula (4).	Formula (2).	Formula (4).	Formula (2).
0·60	1132	1295	1317	+2·9	+1·1
7·15	1188	1174	1184	+1·2	+ ·3
14·89	1047	1059	1050	−1·1	− ·3
21·21	951	962	957	−1·1	− ·6
27·56	870	882	875	−1·4	− ·6
35·21	785	795	789	−1·3	− ·5
42·08	719	728	722	−1·2	− ·4
49·17	656	664	659	−1·2	− ·4
56·29	607	609	607	− ·3	0
62·87	565	561	563	+ ·7	+ ·3
69·89	524	516	521	+1·6	+ ·5
74·16	501	491	497	+2·0	+ ·6

Formula (4) : $A' = 915 \times 10^{-8}$, $c' = 391$.
Formula (2) : $A = 397 \times 10^{-6}$, $c = 560$.

TABLE II.

Substance.	Formula (4).				Formula (2).			
	$A' \times 10^8$.	c'.	Greatest percentage error.		$A \times 10^6$.	c.	Greatest percentage error.	
			+	−			+	−
Carbon tetrachloride ..	980	380	3·2	1·4	397	560	1·1	·6
Chloroform	1253	245	·9	·7	607	412	·2	·2
Ethylene chloride.....	842	459	2·7	2·7	444	668	1·0	·6
Ethyl acetate	1099	433	2·0	1·2	440	767	·4	·3
Benzene	745	657	1·9	1·8	331	1007	·8	·7
Benzene chloride * ...	910	496	2·2	1·7	548	703	1·2	·9

* Owing to lack of data for κ the range of values to which formula (4) is fitted is from $\eta = \cdot01050$ to $\eta = \cdot00410$, while for formula (2) it is greater, viz., from $\eta = \cdot01050$ to $\eta = \cdot00320$.

the form $(\eta_{obs.} - \eta_{calc.})/100 \,.\, \eta_{obs.}$. It is clear that formula (2) gives a much better fit, the maximum percentage error over a range in which the viscosity varies from ·0133 to ·0050 being 1·1, whereas with formula (4) it is 2·9. Table II. gives the values of the constants

and the greatest positive and negative percentage error for other liquids for which the necessary values of κ are available. In all cases the error is much less for formula (2).

It would seem, then, that just as in the case of the specific heat of solids, so here there is some compensating effect which makes a value of ν invariant with temperature represent closely the experimental results on the variation of the quantity in question (viscosity or specific heat) with temperature. Little help on this point can be derived from the consideration of the specific heat of liquids, for small success has so far attended attempts to devise a theory to fit the experimental results on the variation of specific heat with temperature, even with such simple liquids as argon and mercury. With general liquids the energy of rotation and the intermolecular energy provide sources of complication which we can neglect in the first instance in the viscosity problem.

Supported by the considerations of the specific heat of solids and by the markedly better fit we shall adopt formula (2) for the discussion of the variation of viscosity with temperature. It is, however, emphasized that formula (4), which assumes that ν varies as $1/\sqrt{\kappa}$, gives a tolerable approach to a fit.

4. *Comparison with Experiment of Formula for Temperature Variation.*

The formula $\eta v^{1/3} = \mathrm{A}e^{\frac{c}{\mathrm{T}}}$ has been fitted to the chief liquids for which reliable data are available. In the case of most liquids Thorpe and Rodger's figures * are the best determinations available. There has been much dispute as to the application of the kinetic-energy (sometimes called the Hagenbach-Couette) correction to these figures, which were obtained with an apparatus in which the ends of the capillaries were submerged in the liquid. This correction may be written in the form $\frac{m\rho \mathrm{V}}{8\pi l}$, to be subtracted from Poiseuille's expression $\frac{\pi \mathrm{P} r^4}{8l\mathrm{V}}$ for η, where V is the volume delivered per unit time, ρ the density, r and l respectively the radius and the length of the tube, and m a constant. Thorpe and Rodger applied the correction with 1 as the value of m, as advocated by Couette, Finkener, Wilberforce, and

* T. E. Thorpe and J. W. Rodger, Phil. Trans. Roy. Soc. A, clxxxv. p. 397 (1894); clxxxix. p. 71 (1897).

others *. Stöckl, however, following L. Graetz † holds that the correction is inapplicable when the ends of the capillary are submerged, and accordingly, in Landolt and Börnstein's 'Tables,' 5th edition, 1923, in which he is responsible for the viscosity section, the values appear as derived without application of any correction, *i. e.*, m is taken as 0. Erk ‡ has recently published the results of a very careful study, in which he comes to the conclusion that, with submerged capillaries, as used by Thorpe and Rodger, the Hagenbach-Couette correction should be applied, with $m=1{\cdot}1$. Thorpe and Rodger's values, used for computing the constants, have accordingly been slightly modified from those given in their paper by taking $m=1{\cdot}1$ instead of 1. The change is very slight, never exceeding about 0·5 per cent.

The values of Meyer and Mylius § have been taken for the halogen derivatives of benzene, and of S. Mitsukuri and T. Tonomura ‖ for the low temperature determinations for methyl, ethyl, propyl, and isobutyl alcohol. For liquid chlorine and iodine the values of Steacie and Johnson ¶ have been used.

To fit the formula to the experimental data the logarithmic form of equation (2) was used, viz. :—

$$\log \eta+\frac{1}{3}\log v=\log \mathrm{A}+\frac{\mathrm{M}c}{\mathrm{T}v},$$

where M is the modulus of common logarithms, all logs being to base 10. Putting

$$\mathrm{C}=\log \mathrm{A},\quad x=\frac{\mathrm{M}}{\mathrm{T}v},\quad y=\log \eta+\frac{1}{3}\log v,$$

we have

$$y=\mathrm{C}+cx$$

as the equation to be fitted. The fitting was done by the method of least squares, the work of computation being done in the Nautical Almanac Office under the direction and supervision of Dr. L. J. Comrie, who very

* See Thorpe and Rodger, Phil. Trans. Roy. Soc. A, clxxxv. p. 397 (1894), or S. Erk, 'Forschungsarbeiten a. d. Geb. des Ingenieurwesens,' p. 288 (1927).

† Winkelmann, *Handbuch der Physik*, i. p. 1382 (1908).

‡ *Loc. cit.*

§ *Zeitschr. f. Phys. Chem.* xcv. p. 349 (1920).

‖ Proceedings of Imperial Academy of Japan, iii. p. 155 (1927); v. p. 23 (1929).

¶ Journ. Amer. Chem. Soc. lvii. p. 754 (1925).

kindly planned the routine, with proper controls *. Any desire of the writer to make a favourable estimate of the fit is therefore eliminated.

The residuals $y_{obs.}-y_{calc.}$ were found, and the percentage error determined as $\frac{100\ (y_o-y_c)}{M}$, a positive error thus denoting that the calculated is less than the observed value.

The fit is, broadly speaking, very good, the maximum percentage error depending in general as would be expected, on the range of viscosity, defined as the ratio of the viscosity at the lowest temperature of the experimental range to that at the highest temperature. Where the range is less than 2 the maximum percentage error rarely exceeds ·5, and in the worst case is ·7 ; for ranges between 2 and 3 it is generally about ·7 and never exceeds 1·1 ; for ranges between 3 and 4 it goes up to 2·3 in the case of ethylene bromide, but is generally much less, *e. g.*, for metaxylene, range 3·57, it is ·8. For ranges between 4 and 12 it does not generally exceed 2, although for benzene bromide (experiments of Meyer and Mylius) it is 3·3. The alcohols are particularly good, butyl alcohol, with a range of 11·9, showing a maximum percentage error of 1·4. There are, however, a few substances which stand right apart from the others, namely, trimethylcarbinol and dimethylethylcarbinol, with errors of over 20 per cent., while amyl alcohol (optically active) is also a very bad fit. These fall in the same class as water and must be considered anomalous substances. I understand from my colleague, Professor C. K. Ingold, that the tertiary alcohols are anomalous in other respects as compared with primary and secondary alcohols. The peculiarities of water need no special comment. The errors for water, when the whole range from $t=-10°$ to $t=160°$ C., $\eta=2600$ to $\eta=104\times10^{-5}$ is considered, are as high as 27 per cent.

The fit is exhibited in Table III. for some typical substances, chosen so as to exemplify different ranges and different chemical types. The experimental data are given as recorded by Thorpe and Rodger, who for some substances set down four or even five significant figures, and for others only three. To save printing the calculated

* The expenses of the computation were borne by a grant made to the author by the Imperial Chemical Industries Company.

TABLE III.

Methyl Acetate.
Range of $\eta = 1{\cdot}75$.

t.	$\eta \times 10^5$.	Percentage error.
0·34	475·6	−0·1
6·31	443·0	0
11·41	418·0	0
16·70	394·1	0
22·74	369·9	+0·1
28·37	348·4	0
33·85	329·6	−0·1
40·45	309·2	−0·1
46·06	293·4	0
50·34	282·0	0
54·33	271·8	0

Methyl Ethyl Ketone.
Range of $\eta = 2{\cdot}16$.

t.	$\eta \times 10^5$.	Percentage error.
0·32	535·6	+0·1
7·04	491·8	0
14·10	451·7	−0·1
21·31	416·4	−0·1
28·36	385·5	0
35·42	357·9	0
42·49	333·5	0
48·72	314·2	+0·1
55·92	293·6	0
63·74	274·2	+0·2
70·26	258·7	0
76·25	245·7	−0·1

Propyl Acetate.
Range of $\eta = 2{\cdot}95$.

t.	$\eta \times 10^5$.	Percentage error.
0·38	765·8	+0·6
9·78	665·5	0
20·59	575·8	−0·1
30·13	510·4	−0·3
39·75	455·8	−0·3
50·04	407·4	−0·1
61·36	361·8	−0·1

Propyl Acetate (*cont.*).
Range of $\eta = 2{\cdot}95$.

t.	$\eta \times 10^5$.	Percentage error.
69·89	332·4	0
79·99	302·1	+0·1
89·50	276·7	+0·1
96·90	259·4	+0·3

orthoXylene.
Range of $\eta = 4{\cdot}35$.

t.	$\eta \times 10^5$.	Percentage error.
0·49	1094	+1·7
13·88	885	+0·8
26·54	740	−0·7
39·33	629	−1·1
51·94	544	−1·0
65·41	472	−0·8
78·78	413	−0·8
90·82	371	−0·3
101·78	338	0
116·61	300	+0·3
128·15	275	+0·7
141·14	251	+1·2

Octane.
Range of $\eta = 3{\cdot}45$.

t.	$\eta \times 10^5$.	Percentage error.
0·25	700	−0·3
12·18	594	−0·4
22·92	520	0
32·96	463	+0·2
43·89	411	+0·4
54·73	367	+0·4
66·46	327	+0·3
77·82	295	+0·4
88·33	268	0
98·52	246	0
109·07	226	0
122·07	203	−0·8

TABLE III. (*cont.*).

Ethyl alcohol.
Range of $\eta = 3{\cdot}22$.

t.	$\eta \times 10^5$.	Percentage error.
7·16	1532·6	− ·9
13·23	1357·1	− ·4
19·22	1209·2	+ ·1
25·24	1078·9	+ ·3
31·89	955·7	+ ·6
37·51	864·1	+ ·6
42·84	787·2	+ ·5
49·37	704·3	+ ·4
55·57	635·0	+ ·1
61·07	581·0	− ·1
67·55	524·8	− ·3
73·57	475·9	−1·0

Ethyl alcohol:
low temperature values included.
Range of $\eta = 92{\cdot}5$.

t.	$\eta \times 10^5$.	Percentage error.
−98·11	43960	+1·4
−96·54	39010	−2·6
−89·80	28350	−1·4
−83·03	20350	−4·3
−74·22	14827	+0·7
−71·50	13230	+ ·1
−63·98	10007	−4·0
−59·42	8412	−1·3
−56·85	7875	+ ·9
−52·58	6874	−1·2
−37·65	4441	+2·6
−32·01	3835	+3·4
−26·56	3331	+3·7
−17·59	2684	+4·5
− 0·30	1798	+3·1
+ 7·16	1532	+2·1
13·23	1357	+1·9
19·22	1209	+1·6
25·24	1079	+1·7
31·89	956	+ ·7
37·51	864	+ ·1
42·84	787	− ·5
49·37	704	−1·3
55·57	635	−1·9
61·07	581	−2·9
67·55	525	−3·6
73·57	476	−4·9

Propyl alcohol.
Range of $\eta = 6{\cdot}61$.

t.	$\eta \times 10^5$.	Percentage error.
7·31	3145	+2·6
15·06	2555	+1·2
22·86	2101	+ ·1
30·83	1732	− ·7
31·02	1724	− ·7
38·79	1440	−1·3
46·47	1218	−1·3
54·33	1030	−1·4
61·74	880	−2·0
69·04	771	− ·6
76·75	666	− ·1
84·82	576	+ ·8
93·10	498	+1·7
95·59	476	+1·7

Propyl alcohol:
low temperature values included.
Range of $\eta = 67{\cdot}0$.

t.	$\eta \times 10^5$.	Percentage error.
−60·23	31890	0
−54·51	24570	− ·4
−49·46	19840	− ·5
−38·47	12810	− ·8
−34·27	11030	− ·3
−31·71	10210	+1·1
−29·54	9370	+ ·2
−20·26	7004	+1·9
− 9·69	5078	+2·0
− ·30	3825	+ ·2
+ 7·31	3145	+1·5
15·06	2555	+ ·2
22·86	2101	− ·7
30·83	1732	−1·4
31·02	1724	−1·4
38·79	1440	−1·8
46·47	1218	−1·7
54·33	1030	−1·6
61·74	880	−2·1
69·04	771	− ·5
76·75	666	+ ·1
84·82	576	+1·2
93·10	498	+2·2
95·59	476	+2·2

values are not given, but only the percentage error. The fit for octane is particularly good, the greatest percentage error over a range of viscosity from 700 to 203×10^{-5} c.g.s. units being ·8. For the two alcohols selected, viz., ethyl and propyl, two sets of figures are given: (*a*) the values of Thorpe and Rodger, and (*b*) the values of Thorpe and Rodger together with those of Mitsukuri and Tonomura, which gives a much greater range. The two sets (*a*) and (*b*) have been fitted separately. The results for all substances are summarized in Table IV., where in the first two columns the values of the constants A and *c* for each substance are set down. In the third column the range is given, while in the last column the *greatest* positive and negative percentage error is set down.

TABLE IV.

Constants and Percentage Error for Formula $\eta v^{1/3} = Ae^{c/vT}$.

Substance.	$A \times 10^6$.	*c*.	Range.	Greatest percentage error.	
				+	−
Pentane	434	855	1·36	·4	·2
Hexane	455	929	1·93	·3	·4
Heptane	453	990	2·29	·5	·8
Octane	437	1098	3·45	·4	·8
isoPentane	436	856	1·28	·1	·1
isoHexane	454	900	1·72	·3	·3
isoHeptane	449	974	2·37	·5	·9
Diethyl ether	444	728	1·28	·1	0
Methyl propyl ether	446	746	1·40	·2	·1
Ethyl propyl ether	425	843	1·84	·2	·3
Dipropyl ether	414	951	2·50	·5	·9
Methyl isobutyl ether	434	825	1·74	·3	·3
Ethyl isobutyl ether	412	925	2·25	·2	·1
Methyl formate	524	571	1·34	·2	·1
Ethyl formate	492	675	1·71	·3	·2
Propyl formate	451	799	2·33	·2	·2
Methyl acetate	463	668	1·75	·1	·1
Ethyl acetate	440	767	2·23	·4	·3
Propyl acetate	406	891	2·96	·6	·3
Methyl propionate	498	719	2·19	·5	·6
Ethyl propionate	433	838	2·62	·1	·2
Methyl butyrate	425	862	2·93	·6	·4
Methyl isobutyrate	437	827	2·59	·2	·2
Chlorine	1153	197	1·49	·6	·4
Propyl chloride	502	655	1·55	·7	·4
isoPropyl chloride	459	683	1·42	·1	·1
isoButyl chloride	443	797	2·02	·3	·3
Allyl chloride	478	611	1·51	·2	·2
Methylene chloride	577	422	1·44	·2	·1
Ethylene chloride	444	668	2·66	1·0	·6

TABLE IV. (*cont.*).

Substance.	$A \times 10^6$.	c.	Range.	Greatest percentage error. +	Greatest percentage error. −
Ethylidene chloride	498	557	1·63	·1	·2
Chloroform	607	412	1·74	·2	·2
Carbon tetrachloride	397	560	2·66	1·1	·6
Tetrachlorethylene	680	436	2·91	·5	·7
Bromine	708	213	1·76	·4	·3
Ethyl bromide	546	378	1·41	·1	·1
Propyl bromide	529	473	1·93	·5	·3
isoPropyl bromide	491	492	1·79	·1	·2
isoButyl bromide	480	605	2·55	·4	1·0
Allyl bromide	508	444	1·94	·3	·2
Acetylene bromide	652	315	2·68	·8	·5
Propylene bromide	473	505	4·91	2·8	1·5
isoButylene bromide	376	656	6·52	4·6	2·3
Ethylene bromide	479	446	3·87	2·3	1·4
Iodine	1535	220	1·54	·9	1·4
Methyl iodide	540	247	1·45	0	·1
Ethyl iodide	568	319	1·89	·2	·3
Propyl iodide	543	406	2·59	·4	·3
isoPropyl iodide	530	410	2·42	·7	·3
isoButyl iodide	490	499	3·21	1·9	·9
Allyl iodide	523	389	2·52	·4	·3
Thiophen	440	739	2·52	·9	·5
Methyl sulphide	530	610	1·38	·1	·1
Ethyl sulphide	508	779	2·32	·3	·6
Carbon disulphide	729	356	1·40	·5	·2
Isoprene	449	731	1·31	·1	·1
Diallyl	416	854	1·73	·2	·4
Trimethyl ethylene	470	721	1·33	·1	·1
Acetaldehyde	480	610	1·20	·1	·1
Dimethyl ketone	491	720	1·53	·5	·2
Methyl ethyl ketone	453	834	2·16	·1	·1
Diethyl ketone	476	848	2·60	·8	·7
Methy propyl ketone	472	884	2·68	·3	·5
Acetic anhydride	457	809	4·30	2·1	1·0
Propionic anhydride	418	952	6·30	3·1	1·7
Formic acid	225	1036	4·30	4·3	3·2
Acetic acid	428	927	2·54	·3	·2
Propionic acid	513	904	4·28	1·3	·8
Butyric acid	419	1107	6·53	2·7	1·4
isoButyric acid	455	1048	5·48	2·0	·8
Methyl alcohol *	269	1172	2·27	·6	·6
Ethyl alcohol *	176	1586	3·22	·6	1·0
Propyl alcohol *	109	1967	6·61	2·6	2·0
Butyl alcohol	78·3	2174	11·9	1·4	1·1
Allyl alcohol	133	1609	4·8	·9	·6
isoPropyl alcohol	35·2	2466	8·3	2·0	1·3
isoButyl alcohol *	34·9	2609	16·6	4·0	2·3

* The following values are obtained for the four alcohols named when the low temperature values of Mitsukuri and Tononura are included:—

Methyl alcohol	269	1171	22·7	4·3	3·2
Ethyl alcohol	228	1491	92·5	4·5	4·9
Propyl alcohol	104·5	1986	67·0	2·2	2·1
isoButyl alcohol	31·3	2658	56·2	5·8	3·2

TABLE IV. (*cont.*).

Substance.	$A \times 10^8$.	c.	Range.	Greatest percentage error.	
				+	−
Dimethyl ethyl carbinol ...	9·74	3111	29·8	22·0	12·8
Trimethyl carbinol	3·95	3574	9·1	20·5	7·9
Amyl alcohol (active)	29·8	2688	27·0	9·9	6·2
Amyl alcohol (inactive) ...	51·5	2640	21·0	6·0	3·6
Water	58·8	1534	14·9	27·1	14·9
Benzene (T. and R.)	331	1007	2·37	·8	·7
Benzene (M. and M.)	346	996	2·60	2·3	1·7
Phenyl fluoride	514	695	2·31	·7	·9
Phenyl chloride	548	703	3·28	1·2	·9
Phenyl bromide	571	563	4·05	3·3	2·4
Phenyl iodide	547	516	4·47	2·4	2·2
Ethyl benzene	458	922	3·61	·8	·3
o-Xylene	417	1007	4·35	1·7	1·1
m-Xylene.....	465	893	3·57	·8	·5
p-Xylene	436	931	3·37	·5	·4
Toluene	439	912	3·00	·7	·3
Mercury	2467	21·0	2·05	(See fig. 2)	

In considering the departure of the formula from experiment it must be remembered that the precision of viscosity measurements is not very high. The liquid on which the most extensive and most careful work has been done is water, and even here over the temperature range 0° to 100° C. Bingham and White contemplate an error of 1 per cent. as possible at the higher temperatures *. The range of viscosity for water between the temperatures in question is 6·3 ; the error for the other liquids over the same range is probably considerably greater. A systematic relative error in the measurements is by no means to be excluded as a possibility, since at high temperatures the flow is more rapid and the question of the Hagenbach-Couette correction becomes more important. The magnitude of this correction for water at 100 amounts to about 4·1 per cent. if m is taken as 1, so that even the difference between taking $m=1$ (Thorpe and Rodger) and $m=1{\cdot}12$ (Bingham and White) leads to a difference of ·5 per cent. For some substances the full correction amounts to 6 per cent. of the value. There is, further, the possibility of temperature effects not allowed for, such as non-isotropic expansion of the glass tube. The experiments on mercury,

* *Zeitschr. f. Physikalische Chemie,* lxxx. p. 670 (1912): "Wir glauben bewiesen zu haben, dass die innere Reibung von Wasser bei allen Temperaturen zwischen 0 und 100 mit einem Fehler von weniger als 1% bestimmt werden kann."

discussed in section 7 and illustrated in fig. 2, provide further evidence as to the experimental discrepancies which occur in viscosity measurements. On the whole it is probably not an exaggeration to say that in general differences between calculated and experimental value do not *demonstrably* exceed experimental error. In any case there is not sufficient evidence to enable a definite statement to be made as to departures from the formula in any particular direction.

As has been said the alcohols in general fit the formula particularly well. The low temperature determinations of Mitsukuri and Tonomura, taken together with the values of Thorpe and Rodger, give us an enormous range of viscosity, *e. g.*, for ethyl alcohol the range is 92·5, from $\eta = \cdot 4396$, which approaches the viscosity of olive-oil (given as ·99 by Faust and Tammann) to $\eta = \cdot 00476$, which is about that of carbon disulphide at room-temperature. One way of observing the accuracy of the formula is to note that if, with methyl alcohol, we obtain values of A and c from Thorpe and Rodger's figures ($t = 3 \cdot 77°$ to $t = 63 \cdot 26°$ C.), and then extrapolate to $-87 \cdot 5°$, where the viscosity lies outside Thorpe and Rodger's range by 4·4 times their whole range, the error is only 3·8 per cent. With propyl alcohol extrapolation from Thorpe and Rodger's figures ($\eta = \cdot 00476$ to $\eta = \cdot 03145$) to $-60 \cdot 23°$ C. gives a viscosity ·308, as against Mitsukuri and Tonomura's value ·319, an error of 3·5 per cent. From another point of view the worst departure from the formula for ethyl alcohol, range 92·5, is just under 5 per cent., while for propyl alcohol, range 67·0, it is 2·2 per cent. Even supposing that the experimental results are correct and that this departure is real, there can be few physical measurements where a single formula, with only two constants, holds so well over so wide a range. The agreement is, strangely enough, better than that generally obtained in attempting to fit the viscosity of gases and vapours, even when three constants are used.

5. *The Constant of Temperature Variation.*

The average potential energy of the molecule in a liquid can be estimated from van der Waals' equation, written in the form

$$\left(p + \frac{a_m}{v^2}\right)(v - b_m) = \mathrm{R}_m \mathrm{T},$$

where the constants a_m, b_m, R_m apply to the gram molecule, with the standard atmosphere as unit of pressure and the volume occupied by a gram-molecule of a perfect gas as unit of volume *. Applying the familiar formula

$$\frac{\partial U}{\partial v} = T^2 \frac{\partial}{\partial T}\left(\frac{p}{T}\right)$$

we have $$\frac{\partial U}{\partial v} = \frac{a_m}{v^2} \quad \text{and} \quad U = \psi(T) - \frac{a_m}{v},$$

so that the potential energy of the gram molecule which is a function of the volume is $-\frac{a_m}{v}$.

To obtain the constant for c.g.s. units of pressure and volume we must multiply the values of a_m tabulated in Landolt-Börnstein by $1{\cdot}013 \times 10^6 \times 2{\cdot}241^2 \times 10^8 = 5{\cdot}09 \times 10^{14}$. Debye † has worked out the van der Waals cohesion forces on the basis of polarization effects produced by one molecule on another; it is then easy to show that $E_{mol.}$, the energy per molecule due to the intermolecular field, is $\frac{2}{NW}\frac{a}{v}$, where a is the van der Waals constant per gram molecule in c.g.s. units of pressure and volume, W the molecular weight, and N Avogadro's number, or

$$E_{mol.} = \frac{2a_m}{NWv} \times 5{\cdot}09 \times 10^{14}.$$

The exponential term in the viscosity formula is $\frac{E}{kT} = \frac{c}{vT}$, where E is that part of the potential energy involved in the viscosity. We may therefore take $\frac{2a}{NWk} = \frac{a}{W} \times 2{\cdot}41 \times 10^{-8}$ to compare to c, the quantities being $1/k$th of, respectively, the total potential energy and of the energy involved in the viscosity variation with the temperature.

Table V. shows the results of the comparison, all substances for which the necessary data are available being embodied in the table. The first column is

* It is for these units—pressure in atmospheres, and 22·41 litres as unit of volume—that the value of van der Waals' a is given in Landolt-Börnstein's Tables.

† P. Debye, *Phys. Zeitschr.* xxi. p. 178 (1920).

TABLE V.

Comparison of van der Waals' a and the Viscosity Constant c.

Substance.	a per. gm. mol.	$a_0 = \frac{2a}{NWk}$	c.	$\frac{c}{a_0}$
1. Pentane	$19{\cdot}23\times10^{11}$	6430	855	·133
2. Hexane	25·08	7020	929	·132
3. Heptane	31·96	7690	990	·129
4. Octane	37·87	8000	1098	·137
5. isoPentane	18·58	6210	856	·138
6. Diethyl ether	17·63	5735	728	·127
7. Methyl formate	11·53	4630	571	·123
8. Ethyl formate	15·92	5183	675	·130
9. Propyl formate	20·80	5689	799	·140
10. Methyl acetate	15·97	5200	668	·128
11. Ethyl acetate	20·75	5675	767	·135
12. Propyl acetate	26·18	6179	891	·144
13. Methyl propionate	20·50	5607	719	·128
14. Ethyl propionate	25·88	6108	838	·137
15. Methyl butyrate	25·82	6093	862	·142
16. Chlorine	6·59	2209	197	·089
17. Chloroform	15·39	3106	412	·132
18. Carbon tetrachloride	19·81	3105	560	·180
19. Ethyl bromide	11·89	2629	378	·144
20. Carbon bisulphide	11·78	3730	356	·096
21. Thiophen	21·02	6028	739	·123
22. Acetic acid	17·80	7150	927	·130
23. Methyl alcohol	9·66	7274	1172	·162
24. Ethyl alcohol	12·19	6386	1586	·250
25. Propyl alcohol	16·54	6634	1967	·296
26. isoButyl alcohol	17·27	5618	2609	·464
27. [Water] *	5·54	7420	1534	·206
28. Benzene	18·97	5857	1007	·172
29. Phenyl fluoride	20·22	5060	695	·137
30. Phenyl chloride	25·80	5520	703	·127
31. Phenyl bromide	28·97	4430	563	·127
32. Phenyl iodide	33·55	3970	516	·130
33. Ethyl benzene	30·41	6580	922	·140
34. Toluene	24·41	6390	912	·143
35. o-Xylene	29·00	6900	1007	·146
36. Mercury	8·21	985	21·0	·021

* The fit for water is so bad that the order of c has no meaning.

$a=a_m\times5{\cdot}09\times10^{14}$, where a is taken from Landolt-Börnstein. The second column shows

$$a_0=\frac{2a}{NWk}=\frac{a}{W\times4{\cdot}17}\times10^{-7},$$

the third column shows c, and the fourth c/a_0.

It may be noted that the values in ergs per gm. mol. being $\frac{c}{v}kN$ and $\frac{2a}{Wv}$ respectively for the viscosity-energy * and the total potential energy of the molecules, and Nk having the value of $4{\cdot}15 \times 10^7$, while there are $4{\cdot}18 \times 10^7$ ergs to the calorie, the quantities tabulated, viz., $\frac{2a}{WNk}$ and c, give, when multiplied by the densities, the energies *in calories* within 1 per cent. If greater accuracy is required a multiplying factor ·993 must be used, but the experimental data do not justify its use. The order of magnitude of the energy term in the exponential viscosity formula is then a thousand calories per gram molecule.

It will be seen at once that, with certain exceptions, the ratio c/a_0 is tolerably constant, the average value being 0·134. The exceptions in question are chlorine, carbon tetrachloride, carbon bisulphide, benzene, mercury, and the alcohols. The results are graphically exhibited in fig. 1, where c is plotted as ordinate against a_0 as abscissa. The alcohols are shown separately in the left-hand top corner, where the line represents the line in the main part of the diagram. Their exceptional position is obvious.

Twenty-seven substances give points lying as close to a straight line as can, perhaps, reasonably be expected considering the nature of the experimental determinations. The greatest departure of the points from the line represents an error of 8 per cent. in the determination of a_0, and the discrepancies between the values found for a by different experimenters cited in Landolt and Börnstein's 'Tables' often approach this. For example, for benzene the following values are given :—3505 (Sajotschewsky), 2981 (Ramsay), 3588 (Altschul), 3727 (Young); while for ether the following are available : 3288 (Sajotschewsky), 3106 (Ramsay), 3496 (Battelli), 3396 (Galitzene and Wilip), 3332 (Schamhardt), 3464 (Young), 3489 (Schör). In general the values of Young have been adopted where available.

The slope of the line, as found by applying the method of least squares, is 0·1344.

Of the exceptional substances the alcohols are discussed

* By viscosity-energy is merely meant the energy coefficient in the exponential term which gives the variations of viscosity with temperature.

in section 6 and mercury in section 7. Of the remaining four it may be pointed out that the two which lie above the line have compact highly symmetrical molecules,

Fig. 1.

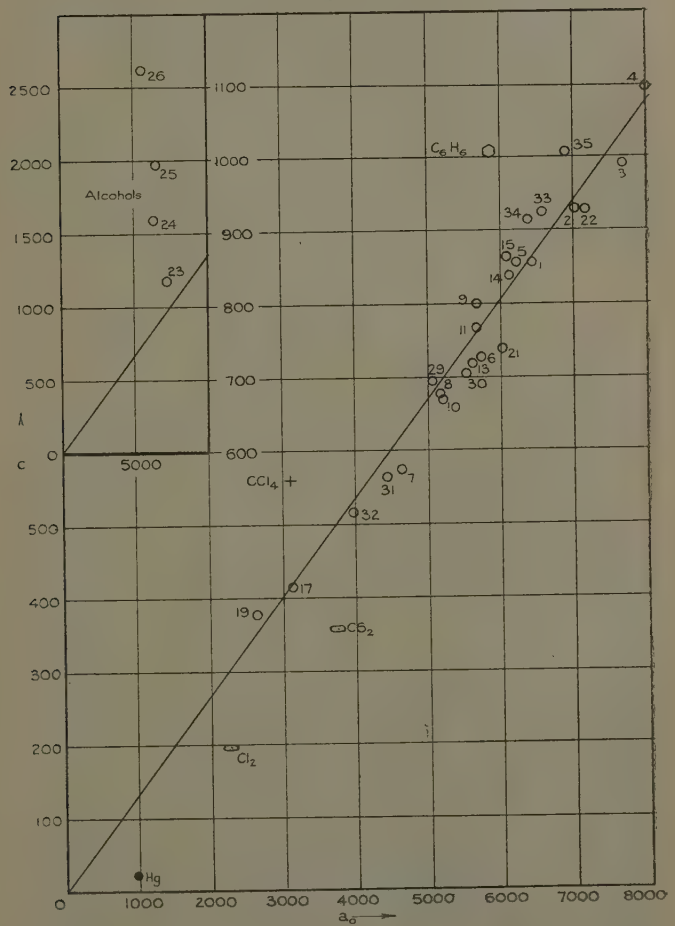

while the two which lie below, Cl_2 and CS_2, have short linear molecules. No explanation of their peculiar position is offered beyond their general structural differences from the substances which lie close to the line.

Anything which destroys the high symmetry of the molecule, *e. g.*, the substitution of a halogen in benzene or the substitution of a hydrogen for one chlorine in CCl_4 makes the behaviour of the substance normal.

It will be noted that there is apparently no distinction between polar and non-polar molecules from the point of view of viscosity. No success has been obtained in an attempt to involve the optical anisotropy of the molecule, for while the optical depolarization is exceptionally high for carbon disulphide it is also high for benzene and much the same for benzene, toluene, and ethyl benzene. The explanation of this is probably that the field with which we are concerned, namely, that which exists between a molecule and the closely neighbouring molecules, is very inhomogeneous, so that the effects are local to particular parts of the molecule, and its behaviour as a whole to a homogeneous field, such as an external electrostatic field or that of a plane electromagnetic wave, do not come into question.

A method of obtaining the potential energy of the liquid molecule is to calculate the inner latent heat, L_i, by subtracting the external work done, estimated from the vapour pressure and vapour density, from the latent heat as ordinarily measured. While there is nothing particularly novel about this *, I have been unable to find any extensive quantitative comparison of L_i with a/v from van der Waals' equation, and have consequently calculated L_i for liquids for which data are available, and obtained the ratio $L_i/\frac{a}{v}$. The value at different temperatures for one and the same liquid is tolerably constant, as may be seen, *e. g.*, from the case of benzene (Table VI.). All energies are given in ergs per gram molecule.

The fact that a/v follows L_i fairly closely (*e. g.*, from 0° to 100° L_i varies by 18 per cent., while $\frac{L_i v}{a}$ varies by only 4 per cent.) justifies the use that has been made of the function a/v to represent the internal energy as a first approximation.

The value of the internal energy as derived from the latent heat is always larger than that expressed as a/v.

* See, *e. g.*, Eucken, 'Lehrbuch der Chemischen Physik,' p. 224 (Leipsig, 1930).

The factor L_i/av differs little from 1·5, *e. g.*, for pentane, hexane, heptane, octane it is 1·48, 1·45, 1·47, 1·52 respectively, the average value for a number of liquids being 1·47.

It appears from Table V. and from fig. 1 that for most liquids the viscosity energy has the value of about 0·13 of the inner energy as calculated from van der Waals' formula, and about 0·087 of the inner energy as calculated from the latent heat—say about one-tenth of the total potential energy of the liquid. For the alcohols, however, the value is markedly greater, namely, 0·162 for methyl alcohol, ·250 for ethyl alcohol, 0·296 for propyl alcohol, and ·464 for isobutyl alcohol (all for the van der Waals' inner energy), while for water, as far as the constant

TABLE VI.

Benzene.

Temperature.	L_i.	a/v.	$L_i/\frac{a}{v}$.
0	$3{\cdot}17\times10^{11}$	$2{\cdot}19\times10^{11}$	1·45
80	$2{\cdot}83\times10^{11}$	$1{\cdot}98\times10^{11}$	1·43
100	$2{\cdot}68\times10^{11}$	$1{\cdot}93\times10^{11}$	1·39
		Average	1·42

has any meaning for a substance so badly fitted by the formula, it is 0·206.

In this connexion it is interesting to recall some results of F. A. Schultze *, who calculated from experimental data the values of $c_p - c_v$ per gram molecule for various liquids. He found that for all non-associated liquids of the types which we have been considering the value was about 10 calories per gram molecule. For the alcohols, however, Schultze found values which are much below 10 at normal temperature, but which vary with the temperature, increasing rapidly as it increases, *e. g.*, for propyl alcohol $c_p - c_v$ has the values 3·37, 7·40, 10·7 at 0°, 50°, 100° respectively †. This suggests that

* F. A. Schultze, *Physikalische Zeitzshr.* xxvi. p. 153 (1925).

† It is perhaps worth noting that propyl alcohol, for which Schultze gives the most rapid variation of association with temperature, shows, of the normal alcohols, the biggest departure from the relation of fig. 1.

the association of the alcohols diminishes strongly with the temperature, there being very little association at high temperatures, a result which is also obtained by other methods *. The point is discussed in the next section.

6. *Associated Liquids.*

It has often been pointed out † that a great difficulty in the way of devising a theory of viscosity of liquids is that many liquids are associated and the degree of association must change with the temperature. Since, however, on the theory put forward the viscosity effect is, in essence, due to a kind of association, governed by the same temperature law as ordinary association, the simple formula (2) should express the temperature variation of viscosity for even heavily associated liquids, and it is noteworthy that for primary and secondary alcohols the temperature variation is well represented by the formula. The effect on the viscosity of an association diminishing with the temperature will find expression in a value of c larger than that which would be correct if there were no change of association with temperature.

The theory of this paper does not give the quantitative effect of association on viscosity, but it is generally agreed by all workers that, from a study of the experimental evidence, association increases the viscosity ‡. Assuming this, it is clear that the effect of association in the alcohols will be to increase the temperature coefficient of viscosity above the value to be expected for a non-associated substance. The abnormally high value for the c/a_0 ratio can thus be naturally attributed to an association varying with the temperature. At the same time, as has been pointed out, there is no reason to expect association of ordinary type to affect the general fit of the formula.

It seems at first sight surprising that the liquid which with the alcohols is best known as an example of association, namely, acetic acid, should give a point falling well in line with the non-associated liquids. This point, however, instead of constituting a difficulty for the theory,

* See Errera, 'Polarisation Diélectrique' (Paris, 1928); and 'Leipziger Vorträge,' pp. 25, 105 (Leipzig, 1929).

† *E. g.*, Erk, Zähigkeitsmessungen an Flüssigkeiten Mitteilungen a. d. Phys-tech. Reichsanstalt, Heft, 288 (1927).

‡ See, *e. g.*, E. Hatschek, 'The Viscosity of Liquids,' chapter vii. (London, 1928),

proves a support. Recent work has shown that the degree of association of acetic acid is independent of the temperature. Briefleb *, for instance, concludes that the molecules are always double. From our point of view then there is no reason to expect an abnormal value of c. The constancy of the acetic acid molecule as against the varying complexity, with the temperature, of the alcohol molecule, gives the reason of the different behaviour of the two types of substance. Incidentally it may be remarked that in other respects acetic acid does not show the same departures from normality as do the alcohols. Acetic acid, for instance, shows no departure from the law of rectilinear diameters of Cailletet and Mathias, whereas alcohols and water show a marked curvature, which is explicable if with acetic acid both liquid and vapour are equally associated.

7. *Mercury.*

The case of mercury is of particular interest, as not only is it the elementary substance for which the most extensive and most concordant measurements are available, but it is the only monatomic liquid. Measurements have, it is true, also been made on bromine by both Thorpe and Rodger and by Steacie and Johnson, but only over a short range, and bromine is not mono-molecular, at any rate in the gaseous state, while for the liquid metals the measurements of the variation of viscosity with temperature are far from being satisfactory †.

The data for mercury have been critically considered by Erk ‡, who has also fitted an empirical formula, of the form $\log \eta = c\frac{t-a}{t-b}$, to give what he considers the best values. The formula $\eta v^{1/3} = Ae^{\frac{c}{vT}}$ can be made to follow Erk's three-constant formula with a greatest error of 1·2 per cent., but the experimental values are so scattered at the higher temperature that I have preferred to fit it direct (i.) to Koch's values, which cover the whole temperature range, (ii.) to the whole assembly of values. The results are shown in fig. 2, where the lower curve

* *Zeits. f. Phys. Chem.* x. B, p. 205 (1930).
† See footnote to Part I. (p. 508).
‡ *Zeits. f. Phys.* xlvii. p. 886 (1928).

with the scale of ordinates shown to the left of the η-axis refers to (i.), while the upper curve with the scale of ordinates to the right of the η-axis refers to (ii.). It will be seen that the regularity of the experimental results is not sufficient to establish definitely any insufficiency of the formula (2).

The striking thing is the very low value of c, which has respectively for (i.) and (ii.) the values 21·7 and 21·0,

Fig. 2.

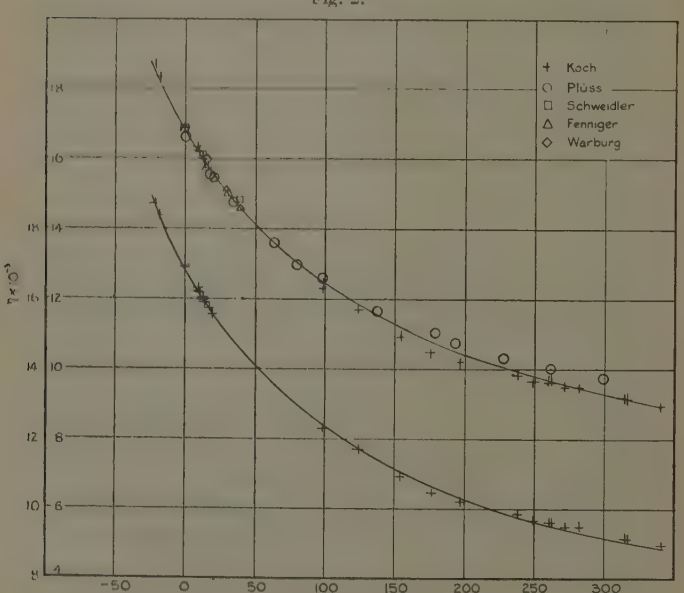

as compared with the other lowest values, 197 for liquid chlorine, 207 for bromine, 220 for iodine. An exceedingly low value for c, expressing the very slow variation of viscosity with temperature *, agrees excellently with the views put forward in this paper. The field of force of a monatomic molecule must be highly symmetrical compared

* Over a range of 360° C. the viscosity only drops to one-half its value, while for a typical substance like octane it drops to half its value over some 60° C., and for alcohol it suffers such a reduction over 40° C. or so.

to that of the general type of organic molecule for which data are considered in this paper, or even compared to a diatomic molecule such as that of chlorine. The energy cannot in this case vary much with orientation, and in consequence the constant c must be small. It is to be expected that in the case of the liquid form of the inert gases the constant c will be smaller still and the variation of viscosity with temperature very slow. Helium, neon, and argon offer too restricted a range of low temperatures to make experiment easy, but experiments with liquid krypton and xenon seem feasible, and I hope to find opportunity to investigate this point.

8. *Viscosity and Chemical Constitution.*

The expression of the viscosity with the aid of the two constants of the formula $\eta v^{1/3}=Ae^{\frac{c}{vT}}$, as against the usual expression with the three constants of Slotte's empirical formula

$$\eta=C/(a+t)^n,$$

is clearly favourable to the discovery of regularities between viscosity and chemical constitution, quite apart from the theoretical meaning here attributed to the formula. It is unfortunate that no accurate data are available for long series of homologues, four being the greatest number of members (*e. g.*, the paraffins). Certain regularities can, however, be observed.

The constant A expresses the viscosity at very high (infinite) temperature, supposing, of course, the substance to remain liquid, that is, the viscosity when the orientation of the molecules is purely random, unaffected by local fields. It involves, according to the theory put forward, many factors which cannot be disentangled: the frequency ν, the molecular dimensions, and distribution of the molecular field. In general it varies very little with a series, *e. g.*, by less than 5 per cent. with the paraffins, for which the extreme variations of c are 28 per cent.; by 8 per cent. for the ethers, where the variations of c are 30 per cent. A is the same for methyl and for propyl iodide, for which c is 247 and 406 respectively. Just as in the exponential formula for thermionic emission, A is less accurately determinable than c, but it seems clear that there is a small systematic decrease of A as we go from less to more

complex members in series of esters or ethers, and a slight increase as we go from chloride to iodide in the series of halogen salts.

The values of c for the few series available are shown in fig. 3, and the general regularity of the results appears

Fig. 3.

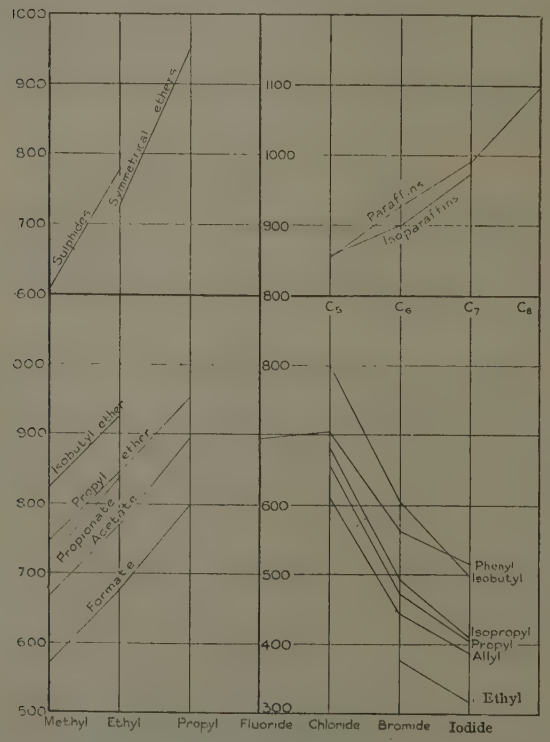

at once. Four groups of substances are shown. In the upper left-hand corner are the values of c for compounds with two methyl, ethyl, or propyl groups, plotted against the number of carbons in the alkyl radical; in the lower left-hand corner esters and double ethers, likewise plotted against the number of carbons in the alkyl radical (one alkyl radical in the case of the ethers); in the upper

right-hand corner the paraffins, plotted against the number of carbons, and below the halides of phenyl and of certain alkyl radicals, plotted against the four halogens as 1, 2, 3, 4. The following points are of interest :—

The paraffins show, as far as four substances can, a zigzag line. If this is real, and not due to inexactness of the experiments *, it is of great interest as confirming the alternating character of the paraffin series of homologues established by other investigations. I hope to be able soon to reach greater certainty on this point by measurements on the earlier numbers of the series.

The change from methyl to ethyl in the radical of an ester or an ether makes roughly the same change in c for the different substances, the average value being 104 ; from ethyl to propyl the average value is 119. Half the changes in the symmetrical ethers, *i. e.*, the change for one CH_2 group, is 112 for ethyl to propyl.

In the halides of phenyl the fluoride shows an anomaly which is paralleled in other physical-chemical properties, *e. g.*, the boiling-point. For the alkyl radicals the run from chloride to bromide to iodide is much the same, although the magnitude of the change in c is not very constant, *i. e.*, for allyl, propyl, isopropyl, isobutyl, in this order, the change is : chloride to bromide 192, 191, 182, 167 ; bromide to iodide 106, 82, 67, 55.

In general longer and more complete series of homologues are required before the relations between the viscosity-energy term and chemical constitution can be systematically investigated. It is suggested that the comparison of the constant c is likely to be far more instructive than the old method of comparing viscosities at arbitrary temperatures, such as the boiling-point at atmospheric pressure, which implies that the magnitude of this pressure is significant for chemical structure.

9. *Variation of Viscosity with Pressure.*

In section 3 we derived the formula

$$\eta v^{1/6} = \frac{A'}{\sqrt{\kappa}} e^{c/vT}, \quad . \quad . \quad . \quad . \quad . \quad (4)$$

* It is not due to the exact type of formula used, for a fit with either $\eta = Ae^{c}{}^{T}$ or $\eta = Ae^{c/Tv^2}$ likewise shows the same alternating characters as expressed by the values of c.

which, although not so satisfactory as (2), gives, as there pointed out, a fair expression of the variation of η with T. We can use this formula to express the variation of viscosity with pressure, the frequency of vibration of the molecules increasing, inversely proportionally to $\sqrt{\kappa}$, with pressure. The question arises as to the value to be taken for c'. If there actually exists, as suggested by the analogy from specific heat, some mechanism that counterbalances the change of κ with temperature, so that A in formula (2) may be treated as constant with temperature, the value of c determined by the application of (2) is the appropriate value for c'. It may be added that the main part of the variation of η with pressure in (4) is given by the variation of κ, so that small changes in the value of c have comparatively little effect.

In this case, if η_1 is the viscosity at atmospheric pressure, and η_p the value at high pressure,

$$\frac{\eta_p}{\eta_1} = \left(\frac{v_1}{v_p}\right)^{1/6} \sqrt{\frac{\kappa_1}{\kappa_p}}\, e^{\frac{c}{T}\left(\frac{1}{v_p} - \frac{1}{v_1}\right)}.$$

There seem to be no data for adiabatic compressibility at low pressure for substances for which the viscosity data are available, although Bridgman gives sufficient data to enable them to be deduced at high pressure. The ratio of isothermal compressibility for liquids will not, however, be very different from the ratio of adiabatic compressibility, and accordingly, for the following, the isothermal values, which are available, have been used. The values calculated apply either to 40° or to 20°, since the compressibilities have been determined at these temperatures, while the viscosity data are available only at two temperatures, 75° and 30°. The values for both these temperatures are given, and that at 40° or 20°, as the case may be, obtained from the experimental figures by proportional interpolation or extrapolation, which over the small range in question is quite accurate enough for comparison purposes. The substances for which figures are given in Table VII. are all those for which all the necessary data have been found.

It will be seen that up to 2000 atmospheres the agreement is good, the difference between observed and calculated values not exceeding in general 10 per cent. This is satisfactory considering the sources of error already pointed out and the uncertainty of the experi-

mental data which are involved, especially of the compressibility, which is the first differential of the experimentally obtained relation between v and p. No fresh arbitrary constant has been introduced, c being determined by the temperature variation of viscosity.

TABLE VII.

Ether at 20°. $c=728$.

Pressure (in atms.).	$k\times10^4$.	Observed value of η_p/η_1. 75°.	30°.	20°.	Calculated η_p/η_1. 20°.
1	1·835	—	—	—	—
500	0·830	1·40	1·55	1·58	1·68
1000	0·605	1·87	2·11	2·15	2·11
2000	0·388	2·92	3·27	3·33	2·98
4000	0·220	5·28	6·19	6·39	4·65

Acetone at 40°. $c=720$.

		Observed value of η_p/η_1. 75°.	30°.	40°.	40°.
1	1·450	—	—	—	—
500	0·708	1·32	1·36	1·35	1·59
1000	0·564	1·65	1·68	1·67	1·90
2000	0·397	2·24	2·36	2·34	2·52
4000	0·225	3·55	4·03	3·93	3·90

Ethyl bromide at 40°. $c=378$.

1	1·476	—	—	—	—
500	0·806	1·43	1·32	1·34	1·49
1000	0·590	1·85	1·67	1·71	1·89
2000	0·364	2·70	2·44	2·50	2·66
4000	0·230	4·66	4·28	4·36	3·85

Ethyl iodide at 40°. $c=319$.

1	1·136	—	—	—	—
500	0·698	1·31	1·30	1·30	1·40
1000	0·546	1·60	1·65	1·66	1·70
2000	0·360	2·45	2·43	2·43	2·34
4000	0·210	4·27	4·53	4·48	3·56

Above 2000 atmospheres the experimental viscosity rapidly becomes greater than the calculated. Only the value at 4000 is given in the above tables; at higher pressures still the deviation increases progressively. This is only to be expected, and confirms rather than contradicts the views put forward. Bridgman's results

on the isothermal variation of p with v have shown that at very high pressure the intermolecular space is abolished and the molecules themselves heavily deformed *. The fact that $\left(\frac{\partial^2 v}{\partial T^2}\right)_p$ changes sign at a certain pressure is put down by Bridgman to the intermolecular forces becoming non-linear, owing to the very close approach of the molecules, and "the pressure of reversal is in almost all cases less than 4000, and is usually near 3000" †. Our formula, then, fails badly exactly where the conditions postulated in its deduction fail badly, and in the sense to be expected.

The increase of viscosity with pressure up to pressures of 3000 or so can therefore be attributed partly to the increase of natural frequency ν, and partly to an increase in the energy in the Boltzmann exponential incident on diminished v, the latter effect being numerically the less important. That the natural frequency increases with pressure has, quite apart from Einstein's formula, been recognized by other workers, *e. g.*, Bridgman ‡. When our formula is applied to the variation of viscosity with temperature at constant pressure this natural frequency is included in the constant A.

To account for the variation of viscosity with pressure at higher pressures than 3000 some special hypothesis is needed as to the behaviour of the molecules when forced into such close proximity that they are deformed. Little is known to guide us in the search for a plausible hypothesis here, and an attempt to cover this field is deferred to a future occasion.

10. *Summary.*

A liquid is regarded as consisting of molecules vibrating, under the influence of local forces, about equilibrium positions which, instead of being fixed as in a solid, are slowly displaced with time. The liquid state is, then, much closer to the solid state than to the gaseous state.

* See, *e. g.*, Bridgman, 'Physics of High Pressure,' p. 131 *et seq.* (London, 1931).

† *Loc. cit.* p. 137.

‡ For example, "On the other hand, there is the fact that the natural frequency of the molecules increases at high pressure" (Bridgman, *loc. cit.* p. 136).

At extreme libration a molecule of one layer may combine momentarily with one of an adjacent parallel layer, supposed moving past with a drift given by the bulk velocity gradient, the combination being of extremely short duration, but sufficing to ensure a sharing of momentum parallel to the drift. If the frequency of vibration of a liquid at the melting-point be taken as that of the solid form at the same temperature a coefficient of viscosity can be calculated for elementary substances in the liquid state which agrees closely with the experimental value. This calculation does not involve an arbitrary constant.

Communication of momentum takes place only if the mutual potential energy, probably determined by the relative orientation of the approaching molecules, is favourable. Under the influence of local intermolecular forces the molecules tend to be similarly oriented within very small groups, the boundary and molecular population of each group being in continual change. The tendency to orientation, which is favourable for interchange of momentum, is disturbed by the heat agitation. On this basis the formula

$$\eta v^{1/3} = \mathrm{A}\, e^{c/T}$$

is derived for the variation of viscosity with temperature, A and c being arbitrary constants. This formula agrees closely with experiment for all liquids except water and certain tertiary alcohols. It applies to ordinary associated liquids as well as to non-associated liquids, although the meaning to be attributed to the constant c is somewhat different in the two cases. The formula gives a good representation of the variation of viscosity with temperature even in extreme cases where the viscosity of the liquid goes from a given value to one hundred times that value in the experimental temperature range.

For a large class of substances c is proportional to (about one-tenth of) the total internal energy as derived from van der Waals' equation or from the latent heat. The question of associated liquids and the anomalous behaviour of certain alcohols and of water is discussed, as well as the special case of mercury.

The variation of viscosity with pressure can be expressed by considering the variation of fundamental frequency,

taken to be inversely proportional to $\sqrt{\kappa}$, where κ is the adiabatic compressibility. This leads to the formula

$$\frac{\eta_p}{\eta_1} = \left(\frac{v_1}{v_p}\right)^{1/6} \left(\frac{\kappa_1}{\kappa_p}\right)^{1/2} e^{\frac{c}{T}\left(\frac{1}{v_p} - \frac{1}{v_1}\right)},$$

which involves no fresh arbitrary constant. The agreement with experiment is satisfactory up to about 3000 atmospheres, above which pressures Bridgman's work indicates that the properties of liquids are complicated by fresh factors. The inclusion or omission of the compressibility factor in the temperature variation is discussed.

I owe my best thanks to Professor C. G. Darwin, who has read through the paper and made certain very pertinent suggestions, of which I have taken advantage. My thanks are also due to the Government Grant Committee of the Royal Society, which provided funds for the purchase of a calculating machine used in preliminary computations, and to the Imperial Chemical Industries, Ltd., for a grant from which expenses in connexion with the final computations were met.

LIX. *The Inner Potential of Semi-Conductors. A Correction.* *By* K. R. Dixit.*

IN the above paper I have given the value of Φ, the inner potential of zinc-blende, as negative. This, as already remarked, is unusual. Now I find that this was a numerical error in calculation, and my thanks are due to Mr. J. R. Tillman for pointing it out.

In an electron camera of the Thomson type there are two lengths, L_1 the distance from the crystal to the photographic plate, and L_2 the distance from the crystal to the willemite screen and $L_2 > L_1$. The error in question comes from using L_1 instead of L_2 in the case of ZnS. The correct values were used for all other substances.

Formula (5) gives

$$\Phi = \frac{150n^2}{4d^2}\left[1 - \frac{n'^2}{n^2}\right], \quad \text{where } n' = \frac{7{\cdot}64.x}{L.\lambda}.$$

* Communicated by Prof. G. P. Thomson, M.A., F.R.S.

If a smaller value of L is used n' would be larger than n instead of smaller, and give Φ a negative value. If, however, we use formula (6),

$$\Phi = P\frac{x_0^2 - x^2}{4L^2},$$

then for L 1 per cent. smaller, Φ would be 2 per cent. larger, while the sign of Φ would remain unaltered.

Thus it will be seen that the slightly smaller value L_1 combined with the formula (5) are responsible for the negative value. The value of Φ calculated, taking the correct length, comes out as $+2{\cdot}6 \pm 1$ volts. This also appears rather unusually low. ZnS includes Fe atoms as isomorphic inclusions, and it may be of interest to study the variation of Φ with the iron content, especially from the theoretical point of view considering the difference in their respective valencies.

LX. *Notices respecting New Books.*

A Text-book of Physics. By E. Grimsehl. Edited by R. Tomaschek. Translated from the VIIth German Edition by Winifred M. Deans. Vol. IV.—*Optics.* [Pp. 301.] (London & Glasgow: Blackie & Son, Ltd. Price 15*s.*)

PARTS I. to III. of this treatise on Physics have already been reviewed. The present part possesses the same excellence as its predecessors. The subject of optics gives greater opportunity for the use of diagrams, and these are undoubtedly exceedingly well conceived and executed.

It is somewhat difficult to place the book in regard to the text. The volume is far above the "Intermediate" standard (although many "Intermediate" problems are provided at the end). In many respects it is above the Final Pass standard. It is not sufficiently complete for an Honours Course, though in the hands of a good teacher who can supplement it where necessary it might form a good nucleus for the tuition in such a course.

The "local" character of the volume is indicated by the fact that there are only three references to Lord Rayleigh. One of these is a somewhat casual explanation of the use of wide angle beams for illuminating microscopic objects. The second gives (without proof) his formula for the resolving power of prisms. The third refers (again without proof) to the inverse fourth power wave-length law for the intensity of light scattered from small particles.

On the contrary, in the major part of the volume the information is very fully and satisfactorily given.

The historical and etymological footnotes form a very interesting feature. It appears that the word collimator (in connection with spectroscopes) is based on wrong etymology. "The word *collimare* was erroneously formed, in place of the correct term *collineare* (to bring into a straight line) owing to a wrong reading in Cicero; the tube should really be called a *collineator*."

On the whole the treatise is an excellent one and well up-to-date. It contains, for example, an excellent description of Michelson's interferometric methods for measuring the diameters of stars.

An Introduction to Thermodynamics for Chemists. By D. Johnston Martin. [Pp. vi + 343.] (London: Edward Arnold & Co. Price 16*s*.)

The aim of this book is to provide an introduction to thermodynamics, especially in regard to its applications to chemistry, including both constant volume and constant pressure reactions. The latter reactions are much more common than the former, yet have been to some extent neglected.

The author aims at stating the questions discussed in such a way that even a beginner cannot go wrong. This tends to make the discussion somewhat prolix, and the sharper student may therefore be set against it. It is difficult to draw the line between full detail and prolixity. A little extra revision would have eliminated the explanations of explanations which frequently occur. But the author usually gets home in the end, and the result is a treatise which will receive a good welcome.

We have noted a few points where the statements can be improved: "It follows from this theorem that the work done by any system working in a reversible cycle between the same temperature limits must perform the same amount of work" (p. 27). This statement is clearly not true.

Clapeyron's formula is always given in terms of $\left(\frac{\partial P}{\partial T}\right)_V$. It should be pointed out that for a saturated vapour $\frac{\partial P}{\partial T}$ is independent of V. The statements in the part-paragraph at the top of p. 32 provide a rather unsatisfactory basis for the Second Law. The statement near the bottom of p. 305, which implies that surface tension is the force tending to *separate* two portions of that surface is rather remarkable in view of the shrinkage of soap bubbles when open to the air, and in view of the fact that the surface tends to take the minimum area consistent with the constraints.

These are not very serious points, though they will tend to bother a student.

We regret that so much stress has been laid upon G. N. Lewis's Activity Coefficients. Their main function seems to be to blind one to the fact that Nature does not always act according to simply expressible laws.

Causality. By Ludwik Silberstein. [Pp. 159.] (Macmillan & Co., 1933. Price 4*s.* 6*d.*)

This essay, based on a lecture, is mainly concerned with an analysis of what is meant by "cause" in classical physics. The kind of relation which is regarded as causal is that between the sets of states of a system which is complete, or isolated, in the sense that its equations do not contain the time explicitly. The relation is discussed with reference to the pendulum, of which a state is specified by the deflexion and angular velocity, and to other examples. In Silberstein's view, the law of causality is to be regarded rather as a principle, or maxim, which, when a system appears incomplete, suggests a search for further systems, which, together with the first, shall form a complete system. Owing to difficulties such as those encountered in tracing backwards the history of the universe, it is suggested that the principle should be regarded as applicable only to "fragments of nature modestly sized." The general issue is certainly clarified by the change of attitude indicated by the suggested change of name from "law" to "maxim"; but old problems remain essentially unchanged though they may be reformulated.

The quantum indeterminacy principle is somewhat unsympathetically approached, towards the end of the essay, by a warning against premature acceptance of such a principle in view of the "handful of results" to which quantum mechanics has led, and to the fate of the Bohr theory. "Bohr's original quantum theory of line spectra .... has after a mere decade exhausted itself .... and has now been practically shelved." After this inauspicious opening, which surely gives a completely erroneous impression of the course of development, due recognition is given to the experimental facts which have led to the change of outlook, and the various statements about the situation, such as those in terms of indeterminacy and complementarity, are reviewed. The hope, however, is expressed that even in this domain, determinacy, as a heuristic maxim, may yet be "retained in its old glory." A number of mathematical notes are given in an appendix.

The book is pleasantly written, and should be appreciated by a wide circle of readers, particularly for its clear and fresh presentation of the classical position.

Elements of Coordinate Geometry. By J. M. Child, B.A., B.Sc. [Pp. xiii+458.] (Macmillan & Co., 1933. Price 12*s.* 6*d.*)

Thoroughness, maintained from beginning to end, is the most prominent quality in this book. The large amount of solid matter, all well arranged, that is provided at a relatively low price suggests almost a "bumper" book. The author deserves considerable praise for the manner in which he has attacked all the knotty points that normally occur in the presentation of the subject, and has at no stage imparted a specious simplicity to the subject by ignoring difficulties. It is emphasized that the work is not to be regarded as a treatise on conics, but of necessity conics occupies much of the space, and a student who worked carefully through this book would have a very thorough training in conics, besides being ready to attack the higher branches of geometry.

The preface suggests that the author is a man of strong views; but, quite apart from the fact that strong views are usually preferable to no views, a perusal of this volume shows that various innovations introduced have helped to clarify the subject considerably, notably in connexion with the gradient of a line, the length of the perpendicular from a point to a line, and with tangents. The author specifies a point, not merely by citing the Cartesian coordinates (a, b), but as the intersection of the two lines $x=a$ and $y=b$.

It is, perhaps, unlikely that many students will be permitted by the exigencies of school and university syllabuses to work right through the book; those who read only the more advanced parts will probably have learned the rudiments from some other (and perhaps less reliable) text-book, and many will perforce miss the interesting later chapters. This, however, is not a criticism of the book, but rather of the present educational system. The only serious criticism to be made here is of the presentation of the definition of irrationals by means of an R-class and an L-class. For one thing, the conditions laid down do not exclude rational numbers; the sequences $1+2^{-n}$ and $1-2^{-n}$, for instance, satisfy the author's four conditions, yet as n tends to infinity define the rational number 1. Further, the example given *seems* to suggest that it is *a priori* obvious that the ordinary square-root process, when applied to the integer 2, must give a never-ending decimal. Beginners would lose little if these paragraphs were omitted, and more advanced students are not likely to refer often to the first chapter.

In conclusion, mention must be made of the excellent discussion of the fitting of empirical formulæ to groups of observations by reducing the law to linear form.

[*The Editors do not hold themselves responsible for the views expressed by their correspondents.*]

Fig. 1.

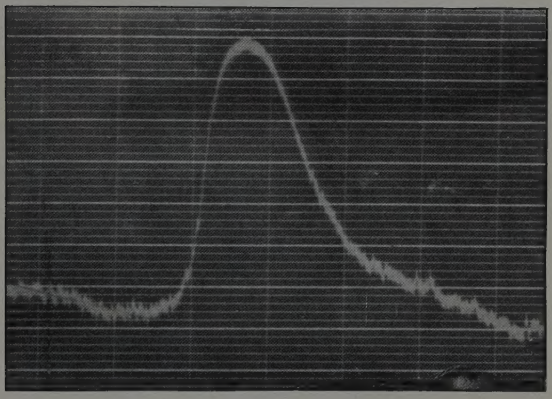

Carbon K_α-edge masked by the K line.

Fig. 2.

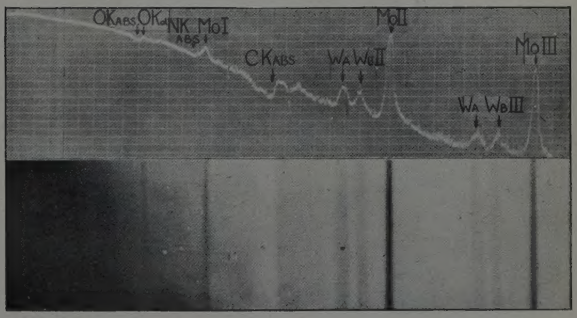

$\lambda \rightarrow$.

Absorption edges. K_χ lines absent.

Fig. 3.

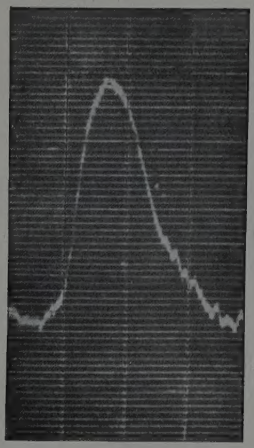

Carbon K_α (Order III.) 300 lines per mm. grating.

Fig. 4.